Exploring Folate Conjugated Liposomal Delivery Of Thymoquinone As A Novel Targeted Treatment For Human Papillomavirus Associated Cancers

A thesis submitted to Middlesex University in partial fulfilment of the requirements for the degree of Doctor of Philosophy

Poona Matin

M00623011

School of Science & Technology, Department of Natural Science, Middlesex University, The Burroughs, Hendon, London. NW4 4BT. UK

August 2021

Abstract

So far, systemic administration of free chemotherapeutic drugs has been the main delivery route in cancer patients despite its several drawbacks. Besides the adverse side effects, higher doses of these drugs are required for them to reach the tumour sites which eventually may lead to the development of drug resistance and limit the effectiveness of these drugs. Therefore, there is a need to develop drug delivery vesicles to overcome such problems and carry drugs to the desired sites and hence maximise their therapeutic index while reducing their cytotoxic effect.

Liposomes, as drug carriers have been used for delivering several chemotherapeutic drugs and have shown some success in treating certain cancers. By encapsulating anticancer drugs within lipid layers or aqueous core, liposomes offer a secure platform for targeted delivery. Thymoquinone (TQ), a component of *Nigella Sativa* has been shown to have anti-inflammatory, antioxidant and anticancer properties for different types of cancers. Although it has been shown to induce cell apoptosis for cervical cancer cells *in vitro*, its anti-HPV effect and the mechanism of its action has not been fully investigated.

In addition, its hydrophobic feature leads to its poor solubility, limited bioavailability and high lipophilicity which restrict it from reaching the cancer sites effectively.

Cervical cancer is one of the most common female malignancies worldwide and over 90% of cases are associated with high-risk HPV infection. Current treatment involves surgery, radiotherapy and chemotherapy depending on the stages and cisplatin is considered the most common drug choice despite its cytotoxicity.

In This study, unconjugated liposomal encapsulated thymoquinone (TQ) and folate conjugated liposomal encapsulated TQ were prepared and they were used to treat HPV16+ CaSki, HPV- C33A and normal human keratinocyte HK cell lines.

The anti-proliferative effect of TQ and cisplatin was compared by determining their half-maximal inhibitory concentration (IC_{50}) after 24 and 48 hours of drug exposure via performing MTT assay using HPV16+ CaSki, HPV- C33A and normal human keratinocyte (HK) cell lines. Results showed that TQ exhibited an anti-proliferative effect in a time and dose-dependent manner on the studied cancer cells but this effect was significantly reduced for the normal HK cells.

Liposomal encapsulated TQ (Lip-TQ) and folate-conjugated liposomal TQ (FA-Lip-TQ) were prepared and the encapsulation rates and physiochemical characteristics of prepared liposomal drugs were monitored over 17 weeks. Results showed that initial TQ encapsulation efficiency for both Lip-TQ and FA-Lip-TQ was 81% and 89% with their size ranging from 149.50nm±2.35 to 150.2nm±1.56 and 150.1nm±2.12 to 155.2nm±1.58 respectively. The zeta potential values demonstrated that both synthesised Lip-TQ and FA-Lip-TQ were neutral liposomes with PDI values lower than 0.2 indicating their homogeneity.

Furthermore, in order to enhance the specific targeting for cancer cells, a suitable surface tumour marker that is highly expressed on those cancer cells need to be identified. Folate receptors (FRs) have been well accepted as highly expressed receptors on cancer cells, therefore, they were evaluated on the three tested cell lines and the result showed that HPV positive CaSki cells expressed the highest levels of FRs among all three cell lines, followed by C33A cell line. FRs were scarcely expressed in HK cells.

The stability and TQ encapsulation efficiency from both Lip-TQ and FA-Lip-TQ were evaluated prior to their exposure to the cervical cancer cell lines. The anti-HPV effect of both free and liposomal encapsulated drugs (unconjugated and conjugated by FA) were investigated and results obtained demonstrated that FA-Lip-TQ was very effective in reducing the expression levels of HPV oncoproteins E6 and E7 in CaSki cells and in upregulating tumour suppressor proteins p53 and pRb comparing to free TQ and, Lip-TQ. For C33A cells Lip-TQ and FA-Lip-TQ were shown to be less effective in upregulating the tumour suppressor proteins compared to free TQ.

Also, FA-Lip-TQ showed more effectiveness in inducing cell apoptosis for CaSki cells than C33A cells. The proportion of early apoptotic CaSki cells after FA-Lip-TQ treatment was 37.7% which was significantly higher (p=0.0008) than the population of early apoptotic CaSki cells after Lip-TQ treatment (26.6%). However, the late apoptotic cells population did not follow the same trend. FA-Lip-TQ treated one was 7.18% which was less than those populations following Lip-TQ treatment (9.28%) (p=0.0005). As for the necrotic cell population, more was shown from Lip-TQ samples (4.82%) than FA-Lip-TQ treated one (2.98%) (p=0.002).

In the case of C33A cells, the population of early apoptotic cells (25.5%) after Lip-TQ treatment was higher than FA-Lip-TQ treated cells (22.7%) (p=0.0002), however, the late apoptotic cell population showed the opposite trend, in which more cells were shown from FA-Lip-TQ treated samples (17.7%) than Lip-TQ treated cells (13.5%) (p=0.0006). In addition, FA-Lip-TQ was shown to be more effective in upregulating both tumour suppressor proteins for both CaSki and C33A cell lines compared with free TQ and unconjugated Lip-TQ.

In conclusion, FA-Lip-TQ demonstrated a higher selectivity and efficiency in inducing apoptosis, downregulating HPV E6 and E7 oncoproteins and upregulating the tumour suppressor proteins p53 and pRb for HPV+ CaSki cancer cells than HPV- C33A cells. Therefore, using FA-conjugated liposomes to deliver TQ could play a crucial role in interfering with the life cycle of HPV viruses and the development of HPV associated cancers.

Acknowledgement

I would like to acknowledge and give my warmest thanks to my supervisors who have supported me throughout my PhD.

Initially, a big thanks to Dr.Xuesong Wen my director of study for having faith in me and for guiding me throughout the project.

I would also like to thank and acknowledge my supervisors Dr.Lucy Ghali and Prof.Hemda Garelick who made this work possible. Their guidance and advice carried me through all the stages of writing my project.

I would like to thank Middlesex University and all the laboratory technicians in the department of natural sciences for helping and allowing me to pursue my further education.

I would also like to give special thanks to my father Dr.Nematallah Matin, my mother Fataneh Karimi, my brother Dr.Pouyan Matin and my family as a whole for their continuous support and understanding when undertaking my research and writing my thesis. Their prayers for me was what sustained me this far.

Finally, I would like to thank my wife, Hanieh Baghbani for constantly supporting me to push through and finish my PhD.

Table Of Contents

List Of Figures

List Of Tables

List Of Abbreviations

Acronym / Symbols	Definition
%	Percentage
µl	Microliter
mL	Millilitre
µM	Micromolar
3T3	Mouse Embryonic Fibroblast Cell Line
4T1	Cell Derived from Mammary Gland Tissue Of Mouse (Breast Cancer Cell Line)
Ab	Antibody
ABC	Avidin-Biotin Complex Method
AIDS	Acquired Immunodeficiency Virus
AKT	Signal Transduction Pathway
AMP Kinase	Adenosine Monophosphate-Activated Protein Kinase
AP1	Activating Protein 1
ATCC	American Type Culture Collection
ATO	Arsenic Trioxide
BAX	Bcl-2 Associated X-Protein (Pro-Apoptotic Member)
Bcl-2A1	Bcl-2 Related Protein A1
BCL-XS	Pro-Apoptotic Gene Product
Bid	Pro-Apoptotic Protein
BIK	Pro-Apoptotic Protein
bp	Base Pair
Bp	Bandpass
BRD4	Bromodomain-Containing Protein 4
BSA	Bovine-Serum Albumin
C33A	Human Cervical Epithelial Cells (HPV Negative)

Ca^{2+}	Calcium
CaSki	Human Cervical Epithelial cell (HPV16+)
CD8+	Cytotoxic T-Cells
CDK	Cyclin-Dependent Kinase
CDKN2A	Cyclin-Dependent Kinase Inhibitor
Chol	Cholesterol
CIN	Cervical Intraepithelial Neoplasia
CL	Conventional Liposomes
cm	Centimetre
CO_2	Carbon Dioxide
COX-2	Cyclooxygenase 2
LOX	Lipoxygenase
Cys	Cysteine
Cy5	Cyanine 5 Reagent
DAPI	4’,6-Diamidino-2-Phenylindole
Dilc18(3)	1,1’-Dioctadecyl-3,3,3’,3;-Tetramethylindocarbocyanine Perchlorate
DL	Drug Loading
DLS	Dynamic Light Scattering
DM	Dichloromethane
DMSO	Dimethyl Sulfoxide
DNA	Deoxyribonucleic Acid
HC2	HPV DNA Test
DREAM Complex	Cell Cycle Regulator
DSPE	1,2-Distearoyl-sn-Glycerol-3-Phosphorylethanolamine
DSPE-PEG2000	Methoxypolyethyleneglycol-Disteroyl-Phosphatidylethanolamine With mPEG MW2000Da

E2F	Transcription Factor
ECL	Enhanced Chemiluminescence
EGF	Epidermal Growth Factor
EIS	Electrochemical Impedance Spectroscopy
EMT	Epithelial-Mesenchymal Transition
ELS	Electrophoretic Light Scattering
ENA78	Inflammatory Chemokine
EPR	Enhanced Permeability And Retention
ER	Endoplasmic Reticulum
FA	Folic Acid
FADD	FAS-Associated Death Domain Protein
FA-Lip-TQ	Folic Acid-Liposomal Encapsulating TQ
FAS	Type-II-Transmembrane Protein
FDA	Food And Drug Administration
TNF	Tumour Necrosis Factor
FBS	Fetal Bovine Serum
FCS	Fetal Calf Serum
FIGO	International Federation Of Gynecology And Obstetrics
FITC	Fluorescein Isothiocyanate
FRs	Folate Receptors
FRα	Folate Receptor 1 or Alpha
FRβ	Folate Receptor 2 or Beta
FRγ	Folate Receptor 3 or Gamma
FSC	Forward Scatter Signal
G0	Resting Phase Of The Cell Cycle
G1 Phase	Gap 1 phase Or Growth 1 Phase In Cell Cycle
G2 Phase	Gap 2 phase Or Growth 2 Phase In Cell Cycle
GPI	Glycosylphosphatidylinositol

HCL	Hydrochloric Acid
Hep3B	Human Liver Cancer Cell Line
HepG2	Human Liver Cancer Cell Line
HeLa	Human Cervical Epithelial Cells Of Adenocarcinoma (HPV 18+)
HGF	Hepatocyte Growth Factor
HGCIN	High-Grade Cervical Intraepithelial Neoplasia
HK	Primary Human Epidermal Keratinocyte Cell
HPLC	High-Performance Liquid Chromatography
HPV	Human Papillomavirus
HR-HPV	High-Risk Human Papillomavirus
HRP	Horseradish Peroxidase
HSIL	High-Grade Squamous Intraepithelial Lesion
HSPGs	Heparan Sulfate Proteoglycans
hTERT	Human Telomerase Reverse Transcriptase
IA1	Protein Tyrosine Phosphatase-Like A1
IA2	Protein Tyrosine Phosphatase-Like A2
IA3	Protein Tyrosine Phosphatase-Like A3
IB2	Islet-Brain-2 Protein
IC_{50}	Half-maximal Inhibitory Concentration
ICC	Immunocytochemistry
IgG	Immunoglobulin G
IL6	Interleukin 6
IL8	Interleukin 8
JNK	C-Jun N-Terminal Kinases
kDa	Kilodalton
KI-67	Cell Proliferation And Growth Biomarker
L1	Papillomavirus Major Caspid Protein 1
L2	Papillomavirus Major Caspid Protein 2

LCL	Long Circulating Liposomes
LCR	The Long Control Region
LGCIN	Low-Grade Cervical Intraepithelial Neoplasia
Lip-TQ	Liposomal Encapsulating TQ
LKB1/AMPK	Pathway Regulates Invasion And Metastasis
LUV	Unilamellar Vesicles
MCF-7	Michigan Cancer Foundation 7 (Breast Cancer Cell Line)
MCM2	DNA Replication Licensing Factor
MCP-1	Monocyte Chemoattractant Protein-1
Mg	Milligram
MLV	Multilamellar Vesicles
MMP-2	Matrix Metalloproteinase-2
MMP-9	Matrix Metalloproteinase-9
mol	Molarity
MPS	Mononuclear Phagocyte System
mRNA	Messenger Ribonucleic Acid
mTORC1	Mammalian Target Of Rapamycin Complex-1
MS	Mass Spectrometry
MTT	3-(4,5-Dimethylthiazol-2-yl)-2,5-diphenyltetrazolium Bromide
mV	Millivolt
MW	Molecular Weight
Na_2HPO_4	Disodium Phosphate
NaCl	Sodium Chloride
NaH_2PO_4	Monosodium Phosphate
NC	Nitrocellulose Membrane
NCR	Non-Coding Region

NF-κb	Nuclear Kappa-Light-Chain-Enhancer Of Activated B cells
nm	Nanometre
ORFS	Open Reading frames
P21	Cyclin-Dependent Kinase Inhibitor 1
P27	Cyclin-Dependent Kinase Inhibitor 1B
P53	Tumour Protein P53
P670	Promoter Of HPV-16
PAGE	Polyacrylamide Gel Electrophoresis
Pap test	Papanicolaou test
PBS	Phosphate Buffer Saline
PBST	Phosphate Buffer Saline And Tween-20
PC	Phosphatidylcholine
PCR	Polymerase Chain Reaction
PDI	Polydispersity Index
PDZ domain	Common Structure Domain Of 80-90 Amino Acids
PEG	Polyethylene Glycol
PFL	Human Periodontal Ligament Fibroblasts
pH	Potential Of Hydrogen
PI	Propidium Iodide
PIK1	Phosphatidylinositol 4-Kinase
PL6	Human Recombinant Protein
PML	Promyelocytic Leukemia
PMT	Photomultiplier Tube
pRb	Phosphorylated Retinoblastoma Protein
PS	Phosphatidylserine
RCC	Renal Cell Carcinoma
rclA	Probable Pyridine Nucleotide-Disulfide

	Oxidoreductase
REIB	Transcription Factor
RES	Reticuleondothelial System
RIPA Buffer	Radio-Immunoprecipitation Assay
RNS	Reactive Nitrogen Species
RNA	Ribonucleic Acid
ROS	Reactive Oxygen Species
RPM	Round Per Minute
RPMI	Roswell Park Memorial Institute Medium
S PHASE	Synthesis Phase Of Cell Cycle
SD	Standard Deviation
SDS	Sodium Dodecyl Sulfate
SF	Serum-Free Medium
SiHa	Cervical Cancer Cell Line (HPV16+)
SLNs	Solid Lipid Nano-Particles
SOP	Standard Operating Procedure
SPI-1	Transcription Factor-1
SSC	Side Scatter Signal
STD	Sexually Transmitted Disease
SUV	Small Unilamellar Vesicles
T-47D	Human Hormone-Dependent Breast Cancer Cell Line
TAMs	Tumour Associated Macrophages
TC	Transition Temperature
Tc	Total Cholesterol
TfR	Transferrin Receptor
TGF	Transforming Growth Factor
TNF-α	Tumour Necrosis Factor α
TQ	Thymoquinone

TSA	Tyramide Signal Amplification
TTDDSs	Tumour Targeted Drug Delivery Systems
TWIST1	Basic Helix-Loop-Helix Domain-Containing Transcription Factor
URR	The Upstream Regulatory Region
USA	United States Of America
UV	Ultraviolet
VEGF-2	Vascular Endothelial Growth Factor-2
V	Volts
VIA	Visual Inspection Of The Cervix With Acetic Acid
VILI	Visual Inspection Of The Cervix With Lugol's Iodine
VLPs	Virus-Like Particles
ZEB-1	Zinc Finger E-Box Binding Homeobox-1
ZEB2	Zinc Finger E-Box Binding Homeobox-2

1.0 Chapter 1

Introduction And Background

1.1 limitations Of Conventional Toxic Chemotherapy In Cancer Treatment

To date, cancer remained a disease with limited therapeutic options despite major improvements in medical science and technology (Falzone *et al.,* 2018). In 2018, there were an estimated 18.1 million new cancer cases reported along with 9.6 million deaths (Gallaher *et al.,* 2018). The Global Cancer Observatory (GCO) predicted that 30 million cancer patients will die each year by 2030. Therefore, prevention, early diagnosis and effective treatment of cancer are the important aspects that need to be considered (Ward *et al.,* 2021).

Imaging technologies, laboratory testing and morphological study of tissue and cells are all currently used in cancer diagnosis and are all considered reliable in the diagnosis of most cancer cases *(Z*hang *et al.,* 2019*)*. Alternative techniques such as immunohistochemical (IHC) study, histological changes, mutational and molecular genetics analysis can also be considered. Common treatments for cancers involve surgical resection, chemotherapy, radiotherapy and biological therapy (Cryer and Thorley, 2019). Surgery is an effective route to eliminate malignant solid tumours, especially when the cancer is still in its early stages whereas, combined therapy including chemotherapy, surgery and radiotherapy can be considered for severe cases at advanced stages. Chemotherapy is an effective treatment for various cancers such as acute lymphoblastic, Hodgkin's and non-Hodgkin's lymphoma, ovarian cancer, germ cell cancer, small cell lung cancer and acute myelogenous leukaemia (Arruebo *et al.,* 2011). However, its unwanted cytotoxicity causes undesirable side effects which could suppress the function of rapid-growing tissues and cells such as bone marrow,

gastrointestinal tract and hair follicles. Chemotherapy can potentially cause multi-drug resistance (MDR), which has a potential association with cancer stem cells (CSCs). The non-specificity and heterogeneity of distribution of cytotoxic chemical agents employed in chemotherapies could lead to MDR in the treatment process (Pérez-Herrero and Fernández-Medarde, 2015). This non-specificity reduces chemotherapeutic effectiveness which makes tumour development, metastasis and recurrence more difficult to control (Zhao *et al.,* 2018). Complex factors including ATP-binding cassette (ABC) transporters, multidrug resistance proteins (P-glycoprotein 1), MDR-associated proteins (MRPs), breast cancer resistance proteins (ABCG2), glutathione transferase, metallothionein, DNA topoisomerase II and catalytic enzymes can cause cancer MDR (Gottesman and Ling, 2005; Hui Wu, 2018). ATP-dependent efflux pumps and non-ATP-dependent efflux pumps are the two forms of cellular MDR. In the 'pump' type the energy released by ATP hydrolysis to efflux drugs through ATP-dependent transport proteins such as P-gp MRPs and BCRPs, lowering intracellular drug concentrations and resulting in drug resistance. While The 'non-pumps' do not rely on ATP hydrolysis for energy, instead activating anti-apoptotic proteins such as Bcl-2 and inducing efflux of the chemotherapeutic agents directly (Hu and Zhang, 2009). Drug absorption in tumour cells may be influenced by nanoparticle drug delivery systems. the method works by delivering chemotherapeutic drugs directly to tumour cells, thereby reversing MDR (Chidambaram *et al.,* 2011). As free drugs cross the cell membrane they can be easily identified via efflux pumps on the cell membrane or be captured by ABC transporter proteins, whereas drug encapsulated nanoparticles may avoid their recognition by ABC efflux pumps and endocytosis by ABC transporters, resulting in increased intracellular accumulation of chemotherapeutic drugs (Fig 1) (Kirtane *et al.,* 2013).

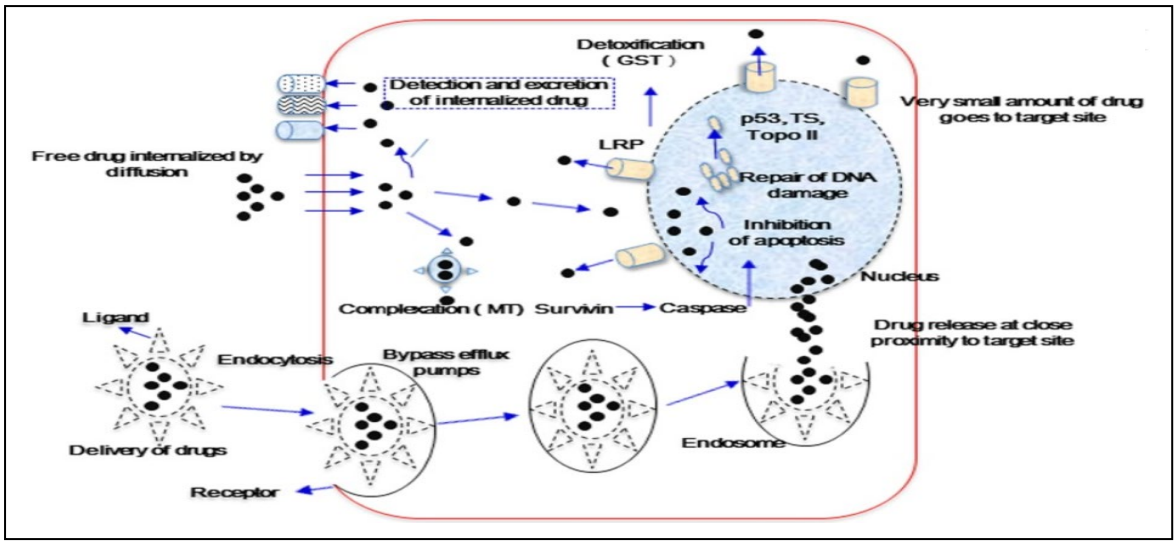

Fig 1: Demonstrating the main elements involved in drug excretion and the delivery of both free and encapsulated drugs to the tumour site and the possible influence of the nanoparticles in improving this mechanism (Huang *et al.,* 2016).

1.2 Nanotechnology

Treatment of cancers is currently limited to surgery, radiation and chemotherapy. Chemotherapy and radiotherapy treatments can cause damage to normal tissues or not completely eradicate cancer. Nanotechnology can facilitate the delivery of chemotherapeutic agents to neoplasm with reduced toxicity and increased bioavailability. It can also enhance the therapeutic efficacy of radiation-based treatment and other current treatment-induced modalities (Aliosmanoglu, 2012).

Nanotechnology is a field that has been introduced lately as one of the most favourable fields in cancer therapy. The medical applications of nanotechnology known as Nano-medicine have the potential in revolutionizing cancer therapeutics and diagnostics by developing inventive biocompatible nanomaterials for drug delivery which represent the most appropriate application of nanoparticles (Misra *et al.,* 2010).

Nanotechnology offers significant possible benefits compared to conventional anticancer drug construction that may change drug pharmacokinetics and distribution

improving anticancer drug's efficacy and reducing their side effects (McNeil, 2005). The size and surface characteristics linked with nanoparticles improve a few factors in drugs such as their portability, mobility, and detainment, increasing selective confinement in tumour tissue as well as making them potentially effective tumour delivery vectors (Sandanaraj *et al.*, 2010). Multiplex-nanoparticles comprising two or more mechanisms expand functional capabilities for concurrent imaging and drug delivery (Stern *et al.*, 2010). All nanoparticles contain macromolecular substances in which the reactionary drug (biologically active material or a pharmacologically active drug) is encapsulated, dissolved or entrapped or to which the active agent is attached or adsorbed (Narayana, 2014).

Due to their biological compatibility, lipids are one of the most promising agents that can be used to prepare a drug delivery system, like liposomes and solid lipid nanoparticles. Currently, liposomes encapsulating various chemotherapeutic drugs like Doxorubicin and Daunorubicin have been approved for the treatment of metastatic breast cancer and Kaposi's sarcoma (Bulbake *et al.*, 2014). Advantages of nanomaterials in drug delivery systems are their ability to pass through narrow capillaries and accessibility to remote areas, they can be easily consumed and they can be delivered at a specific site by passive or active targeting and also their ease in encapsulating drugs for protection or controlled release (Sci *et al.*, 2011).

1.3 Liposomes

Liposomes are amphipathic molecules composed of hydrophobic (tail) and hydrophilic (head) parts (Alavi *et al.,* 2017). They are spherical vesicles involving multiple phospholipid bilayers which can protect drugs from degradation by encapsulation of both hydrophilic and hydrophobic drugs (Pandey *et al.*, 2016). They are the most

common architectures for targeted drug delivery applications with their size ranging from 0.025μm to 0.25μm. Their size is an essential parameter determining their circulation half-life and the amount of encapsulated drug (Akbarzadeh *et al.,* 2013). Liposomes are classified into Multilamellar vesicles (MLV), Large unilamellar vesicles (LUV), and Small unilamellar vesicles (SUV) depending on their size or the number of lipid bilayers involved in their structure (Fig 2) (Sharma, 1997).

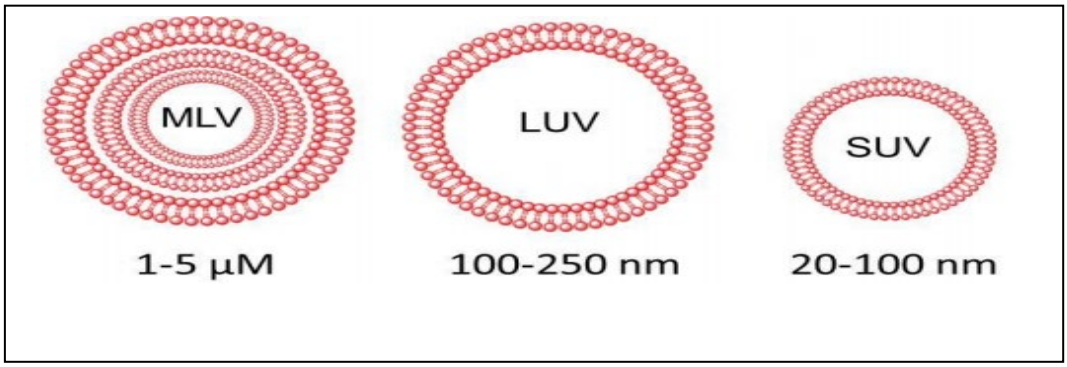

Fig 2: Based on lamellarity (number of phospholipid bilayers), liposomes can be classified as multilamellar vesicles (MLV), large unilamellar vesicles (LUV) and small unilamellar vesicles (SUV) (Emami *et al.,* 2016).

Liposomes main duty is to increase the accumulation of the anticancer drug in the solid tumour with longer circulation (Tran *et al.*, 2017). The application of liposomes to assist drug delivery has already had a major impact on many biomedical fields. They have been advantageous for stabilising therapeutic drugs, overcoming difficulties with cellular and tissue uptake, and increasing biodistribution of drugs to target cancer cells or tissue while reducing systematic toxicity of the agents (Sercombe *et al.*, 2015). There are four types of liposomes (Fig 3), Conventional liposomes, PEGylated liposomes, ligand targeted liposomes and multifunctional liposomes (Riaz *et al.*, 2018). Conventional liposomes are composed of phospholipid bilayers. This type of liposome has short circulation life due to the engulfment by phagocytes.

When they are administrated into the patient's body intravenously, they will be taken up by the reticuloendothelial system (RES) (Hatakeyama *et al.,* 2013). To increase the circulation time, the surface of the liposome will be coated with a hydrophilic polymer for example polyethylene glycol (PEG), which will lead to increasing repulsive forces between liposomes and serum components. These modified liposomes are named PEGylated (stealth) liposomes. PEG has often been used for its stealth functions in nanoparticles formulations because it is a hydrophilic and flexible polymer. The conjugation of PEG to the surface of the liposomal phospholipid bilayer leads to the reduction of the interaction between liposomes and plasma proteins through steric hindrance (Yingchoncharoen *et al.,* 2016).

Liposomes can be functionalised by binding to appropriate ligands like antibodies, peptides and aptamers for targeted therapy by anticancer drugs at cancer sites. For instance, tumours using overexpressed receptors as a docking site have given risen to the formation of ligand-targeted liposomes or targeted liposomes (Balazs and Godbey, 2011).

The use of targeted liposomes which are articulated by a variety of surface engineering techniques in cancer therapy has established minimum off-target effects on healthy tissues which ensure the healthy tissue or cells will be maintained intact after treatment. Another type of liposomes is known as immunoliposomes which have been formulated by the attachment of chemically coupling antibodies or their fragments to the liposomal surface resulting in high affinity for their targeted antigen (Khan *et al.*, 2015).

Multifunctional liposomes contain unique features to overwhelm the existing difficulties of liposomal formulations with a single functionality. Combinations of surface

functionalisation and modification practices have been utilized to convey a nanoscale liposomal formulation with a diversity of functionalities. For instance, liposomes that contain two ligands like two peptides or liposomes can carry two ligands and two anticancer drugs at the same time (Zhang *et al.*, 2017).

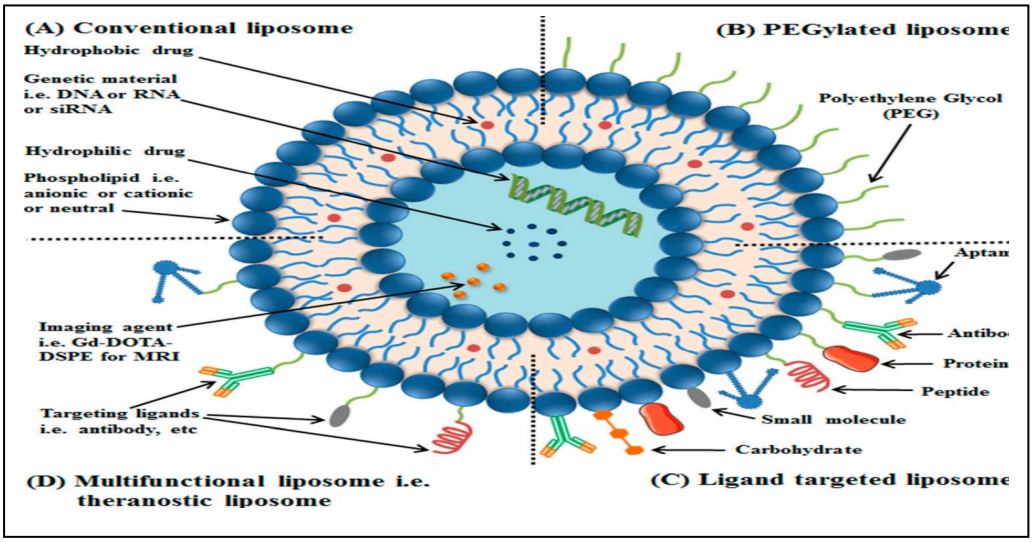

Fig 3: The image illustrates different types of liposomes. A) Those which are made of phospholipids and known as conventional liposomes. B) PEGylated liposomes which have a Polyethylene Glycol layer on their surface (also known as stealth liposomes), C) Targeted liposomes which target specific cancer site and D) Multifunctional liposomes which can be applied for solid tumour diagnosis and treatment (Riaz *et al.*, 2018).

1.4 Liposome Compositions

Glycerol encompassing phospholipids are the most corporate used components of liposomes formulation which signify greater than 50% of the weight of lipid in the biological membrane. These lipids are derived from phosphatidic acid and are known to be amphiphilic molecules (having a hydrophilic head and hydrophobic tail). There are few types of phospholipids that are being used to prepare liposomes such as phosphatidylcholine (Lecithin-PC) (Bailey and Cullis, 1997). Preferably for more

stabilised liposomes saturated fatty acids are used. The hydrophobic parts of the lipids are mostly phosphoric acid bound to a water-soluble molecule. On the other hand, the hydrophobic share involves two fatty acid chains with 10-24 carbon atoms and each chain contains 0-6 double bonds. When these phospholipids are disseminated in the aqueous medium formation of lamellar sheets will be resulted by organizing in such a mode that, the polar group will face outwards towards the aqueous region whereas the fatty acid groups will face each other and finally the formation of a spherical vesicle so-called liposomes will be achieved (KALEPU *et al.*, 2009).

Other main constituents of liposomes are sterols such as cholesterol and its derivatives that will decrease the fluidity or microviscosity of the lipids bilayer, reducing the permeability of the membrane to water-soluble molecules and stabilising the membrane in the presence of biological fluids such as plasma. The importance of cholesterol in liposome formation is because liposomes without cholesterol are known to interact rapidly with plasma protein (Albumin and Transferrin). These two proteins can extract the majority of phospholipids from liposomes and cause depletion of their outer monolayer of the vesicles and result in physical instability of the particles (Briuglia *et al.*, 2015).

1.5 Liposome Stability (Transition Temperature And Surface Charge)

Lipids all have a temperature at which their fluidity changes which is known as transition temperature (TC). The transition temperature is directly proportional to the length of the acyl chain so the longer the acyl chain the higher the transition temperature would be and also more rigidity of the membrane will be obtained. The rigidity of the membrane is an essential factor to be considered as it accounts for the superior stability of the liposomes. The greater the rigidity of the membrane causes

better entrapment of the encapsulated agents inside the liposomes. In other words, better rigidity prevents leakage of the drug from the liposomes. The transition temperature is highly essential as it can directly influence the way that the membrane reacts to fuse with other liposomes, aggregation stability, and permeability (Čeh and Lasic, 1995).

Liposomes could also be categorised according to their composition and their mechanism of intracellular delivery into 5 distinguished types which are known as conventional liposomes (CL), pH-sensitive liposomes, cationic liposomes, long circulation liposomes (LCL) and immunoliposomes (Sharma and Sharma, 1997).

One of the other factors that can be crucial in the classification of liposomes is liposome surface charges. The nature and density of charge on the liposome surface are essential parameters that influence the particles mechanism and extent of liposome-cell interaction. These two parameters can be changed by changing the lipid composition of the liposomes. Lack of surface charge can lead to a reduction of the physical stability of small unilamellar liposomes (SUV) hence increasing their aggregation (Zhao *et al.,* 2011). Moreover, in the case of neutral liposomes lack of significant interaction of liposomes with cancer cells will be resulted and in these cases, the drug may mainly enter cells after being released from liposomes extracellularly. Also, the presence of high electrostatic surface charge on the surface of the liposomes could increase liposome-cell interaction (Shah *et al.,* 2017). It has been shown that liposomes coated with negative surface charge are mostly coated-pit endocytosis. In addition, it has been shown that negatively charged density on liposomes could influence the extent of their interaction with cells. The negative surface charge may not only promote intracellularly uptake of liposomes by targeted cancer cells but through the same mechanism, it will increase their plasma clearance

after being administrated systematically (Fröhlich, 2012). Another feature linked with negatively charged liposomes is that they might release their contents in the circulation or extracellularly after they collaborate with blood constituents and tissue. Distinct positively charged liposomes, cationic liposomes have been suggested to deliver their drug load to cells by fusion with cell lipid membrane (membrane fusion) (Sharma and Sharma, 1997). Negatively charged liposomes have a shorter half-life in the blood in comparison to neutral liposomes and positively charged liposomes are toxic and thus will be rapidly removed from circulation (Immordino *et al.,* 2006).

1.6 Stealth Liposome Technology

A liposomal drug delivery system has been introduced to overcome the limitations associated with traditional chemotherapy as this system can increase the therapeutic outcome of anticancer drugs also to decrease their cytotoxic side effects. Liposomes have several advantages in comparison to other anticancer drug delivery systems such as their biocompatibility, their lack of immunogenicity, their ability to self-assemble, their ability to encapsulate both hydrophilic and hydrophobic agents or drugs and increase their characteristics features like their solubility, their ability to entrap and carry giant drug payloads and shield the encapsulated agents from the external media, ability to reduce the toxicity of the entrapped agent and the contact of sensitive tissues to toxic drugs together with the ability of site-specific targeting and improving penetration into tissues (Sercombe *et al.*, 2015).

Liposomal drug carriers have a robust impact on the pharmacokinetics and tissue distribution of integrated drugs. This may result in the enhancement of drug efficacy as well as in the reduction of toxic side effects of anti-tumour agents (Huwyler *et al.,* 2008).

Liposomes also improve the pharmacodynamics as well as pharmacokinetics of the encapsulated drugs. Numerous drugs need regular doses when administrated without a drug delivery system. Liposomes can be articulated to have a longer circulating time, thereby keeping anticancer drug dose constant for longer periods. The tactics in which circulation time of drugs can be increased is by creating Stealth liposomes which will be achieved by using phospholipid with great total cholesterol (Tc) value or by coating liposomes with polyethylene glycol (PEG) (Ernsting *et al.*, 2013).

Stealth technology helps to develop a liposomal drug delivery system that makes their elimination by the phagocytic system difficult. In this method, polymer strands will be attached to the dug molecules or the delivery vesicle that can enhance the safety and efficacy of the therapeutic drugs (Milla *et al.,* 2011). Generally, for the stealth technology polyethylene glycol (PEG) are used as a polymer through a process called PEGylation which is achieved by the incubation of the reactive derivative of PEG with the target moiety (Salmaso and Caliceti, 2013). The covalent bond between liposomes and PEG shield the active moiety from the immune system. It also facilitates few alterations in the physiochemical properties of the target moiety such as their hydrodynamic size and thus decrease the renal liposomal clearance rate and resulting in prolonged circulation time (Fig 4) (Bulbake *et al.,* 2017).

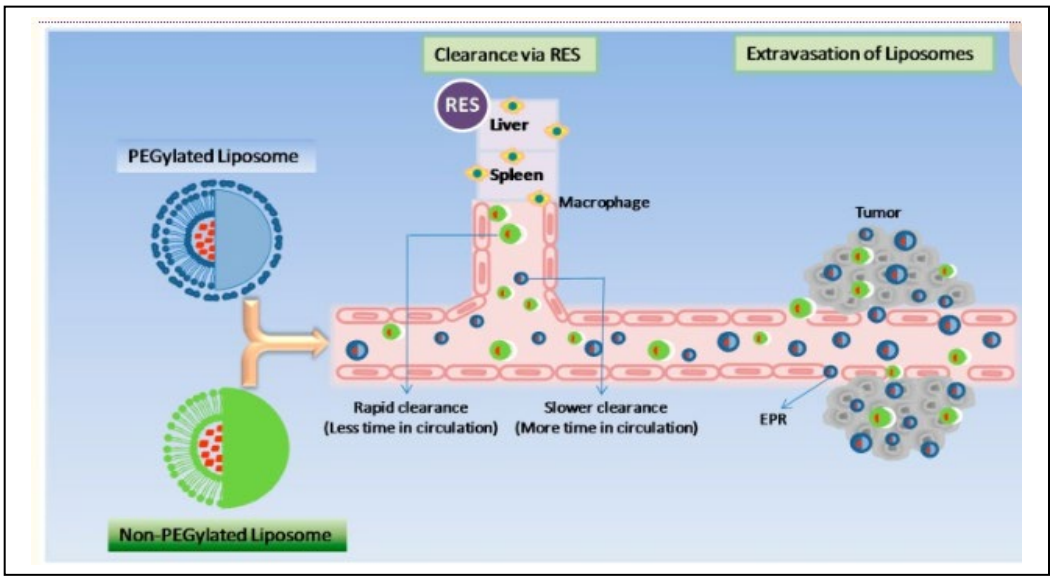

Fig 4: The differences between the pharmacokinetics (absorption, distribution, metabolism and excretion) of PEGylated and Non-PEGylated liposomes (Bulbake *et al.,* 2017).

Three main features of liposomes which are the fluidity of the lipid membrane, the size of the liposomes (smaller liposome circulates for a longer time), and the charge on the liposomes will have a direct influence on their circulation time. Furthermore, Liposomes can also avoid chemical and immunological breakdown of the drugs as well as shielding them against the effect of some of the enzymes (Bozzuto and Molinari, 2015).

1.7 Liposome Cellular Attachment And Targeting Strategies

Four strategies have been defined for liposomal cellular interaction and they are dependent on factors such as lipid composition, cell type and the presence of receptor or targeting vectors (Ducat *et al.,* 2011). These strategies are as follow; 1) Lipid or protein exchange with the cell membrane. As the liposomes and cells have a similar phospholipid monolayer of lipoproteins, the lipid transfer protein on the cell surface can recognise the liposomes, and thus lead to the lipid exchange mechanism (Kelly *et al.,* 2011). 2) Adsorption of liposomes to the cell surface is another mechanism that

arises as to the result of either a nonspecific weak hydrophobic or electrostatic force or through a specific interaction with the surface components of the target cells. 3) Endocytosis is the third strategy through which, initially liposomes will be adsorbed on the cell surface and engulfed by the endosome and transported to the lysosome. This will result in the digestion of the lipids and the release of the encapsulated drug into the cytoplasm (Mufamadi *et al.,* 2011). 4) The last strategy is the fusion of the encapsulated drugs directly into the cytoplasm. This process is regulated by cell membrane proteins and can be enhanced by adding fusogenic lipids to the liposome membranes. The fusion process occurs as the liposomes overcome the energy barriers which is because of the internal bilayer interaction (Goyal *et al.,* 2005).

There are two defined strategies for liposomes to target the tumour, which are known, as passive-targeting and active-targeting. The advantage of using nanocarriers including liposomes for delivering anticancer drugs to cancerous tissues has been broadly discussed. This approach for anticancer therapy involves passive-targeting of the drug-loaded liposomes because these particles are known to accumulate in the tumour area due to the leaky vasculature-enhanced-permeability and retention (EPR) effect (non-targeted liposomes) (Bozzuto and Molinari, 2015). This effect represents the anatomic differences between normal and cancerous tissues because capillaries in the tumour areas possess increased permeability (Bertrand *et al.*, 2014). The passive targeting effect is highly dependent on many characteristics, including the degree of tumour vascularisation and angiogenesis and the porosity and pore size of tumour vessels which vary with the type and status of the tumour. These factors contribute to the pharmacokinetics and biodistribution of the liposomes (Puri, 2014).

Liposomes are capable to encapsulate both hydrophilic and hydrophobic agents. Entrapment of hydrophilic drugs will lead to hydration of lipid hydrophilic drug mixture.

However, in such a method, anticancer drugs can enter the liposomes core and other materials remain in the outer part of the liposomes. Remained materials will remove drug entrapment in liposomes. In comparison to hydrophilic drugs, hydrophobic drugs will be encapsulated in the outer membrane of liposomes which are composed of phospholipid bilayers and are the appropriate site of encapsulation for hydrophobic molecules (Colletier *et al.*, 2002). By encapsulation of such hydrophobic drugs like Thymoquinone or verteporfin, the movement of these drugs will be reduced towards the outer aqueous and inner parts of liposomes. These drugs are encapsulated into the liposomes by solubilizing them in the organic solvent and phospholipids. The region of drug entrapment in liposomes is the hydrophobic part of liposomes (Schwendener and Schott, 2017)**.**

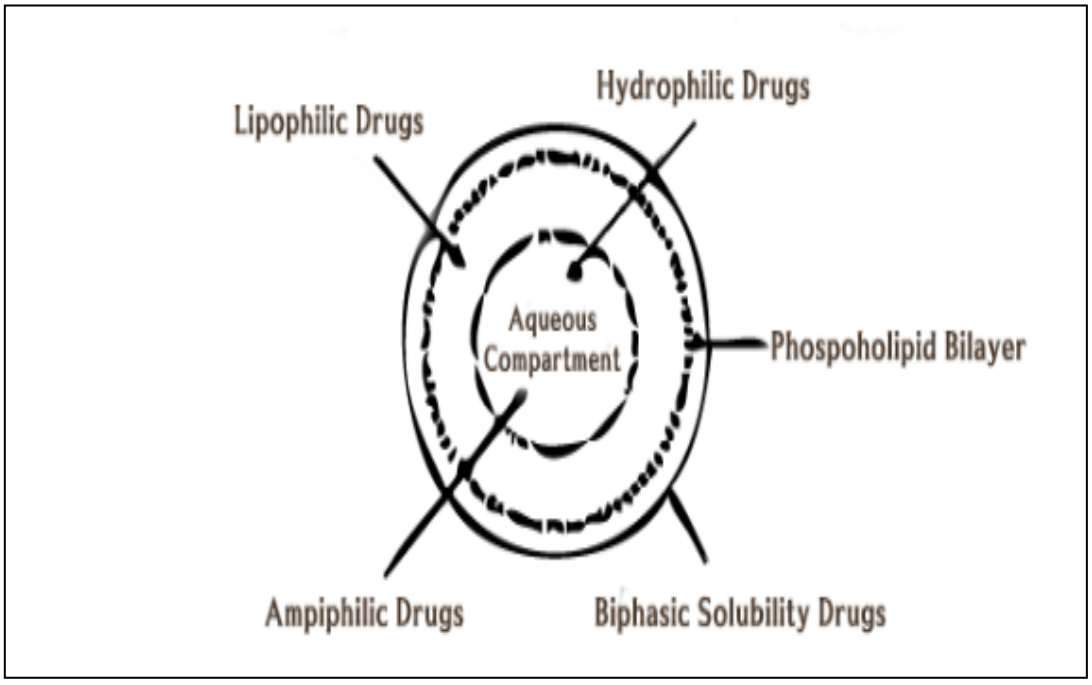

Fig 5: The interaction site of different drugs to liposomes (Malam *et al.,* 2009).

Currently, several liposomal based products are being used as therapeutic agents to treat various cancers, such as Doxorubicin (breast cancer, ovarian cancer and Kaposi's sarcoma), Daunorubicine (AIDS-related Kaposi's sarcoma), Mifamurtide (high grade, resectable and non-metastatic osteosarcoma), Vincristine (acute lymphoblastic leukaemia) and Irinotecan (adenocarcinoma of the pancreas) (Bulbake *et al.*, 2017).

1.8 Application Of Herbal Medicine In Cancer Treatment

Cancer remains a significant public health concern in most developing countries however due to early diagnosis and advances in medical procedures, there have been substantial changes in the survival rate of patients in the past three decades (DeSantis *et al.*, 2014). A large number of cancer patients receive either chemotherapy or chemoradiotherapy, however, they are associated with high toxic side effects on normal cells or normal tissue and compromising patients' quality of life, in some cases, these side effects make it difficult for the patients to continue with the treatments (Akin *et al.*, 2010).

Medicinal herbs and their derivative extracts are being progressively acknowledged as a useful complementary treatment for various cancers (Damery *et al.*, 2011). A large volume of clinical studies have stated the beneficial effect of herbal medicines on the survival, immunomodulation and quality of life of cancer patients when they are used in combination with common conventional therapeutics (Yin *et al.*, 2013). Herbal medicines are mostly being used as cancer treatment agents due to their unique characteristics such as their ability in primary prevention of cancer, which can be considered as an important factor for those who have a strong family history of malignancy. They are also capable of preventing a recurrence of cancer (Hsiao *et al.*,

2019). They can also be considered as important elements for the enhancement of the body's immune system. The mechanism of natural compounds in fighting cancer is governed by strengthening the immune system and stopping the cancer cells to spread by inhibiting angiogenesis, detoxifying the body and preventing further toxic accumulation in the body, quenching free radicals that cause mutational changes that lead to cancer formation and supporting all targeted organs, especially those affected directly by cancer (Treasure, 2005). Furthermore, another benefit of herbal medicines is that they can minimise the setting of a favourable environment for cancer growth by lacking conditions such as a high level of oxygen and temperature including increased metabolism rate, low sugar level, and a high alkalinity space (Tavakoli *et al.*, 2012).

Table 1: Some of the recent studies that investigated the application of herbal medicine for cancer treatment.

Herbal Drugs	Cell Lines/Mode of Study	Key Findings	References
Praeruptorin A	HeLa and SiHa cell lines, *in vitro*	Vanquishes expression of MMP-2 and resulting in cell growth inhibition.	(Wu *et al.*, 2018)
B-elemene	SiHa cell line, *in vitro*	Results in apoptosis induction via Increasing expression of p53 and Bax and decreasing expression of Bcl-2.	(Wang *et al.*, 2018)
Baicalein	HeLa cell line, *in vitro*	Downregulates expression level of MMP-2 and MMP-9.	(Ye *et al.*, 2017)
Elephantopus Mollis 23	HeLa and CaSKi cell lines, *in vitro*	Increases apoptosis and inducing cell cycle arrest.	(Shao *et al.*, 2016)
Artemisinin	MCF-7 cell line, *in vitro*	Decreases the proliferation of human breast cancer from expressing a high ERα:ERβ ratio.	(Sundar *et al.,* 2008)
Plumbagin	MCF-7 and MDA-MD-231 cell lines, *in vitro*	Induces G2-M arrest and autophagy by inhibiting the AKT/mammalian target of rapamycin pathway in breast cancer.	(Kuo *et al.,* 2006)
Baicalein	T24 cell line. *in vitro*	Inhibits growth and causes G1/S arrest of the cell cycle in the T24 bladder cancer cells.	(LI *et al.,* 2012)
Genistein	HT29 colon cancer cell line, *in vitro*	Induces apoptosis and inhibits proliferation of HT29 colon cancer cells.	(Shafiee *et al.* 2016)

1.9 Thymoquinone (TQ)

In recent years, interest in natural phytochemical compounds with anticancer potential has increased because they are non-toxic, relatively inexpensive, and available in an ingestive form. In the last 20 years, 25% of the medicines used derived directly from plants while the other 25% are chemically altered natural compounds (Amin *et al.*, 2009).

Nigella Sativa is an annual flowering plant referred to as black cumin, found in Mediterranean countries, India and, Pakistan. The oil extract of this plant was used in Arab countries as a traditional herbal medicine for the treatment of lung diseases, arthritis, and hypercholesterolemia (Salem, 2005). Several studies have reported that its biological activity is based on its oil extract which is predominantly composed of 30-40% thymoquinone (Burits and Bucar, 2000).

Thymoquinone (2-Isopropyl-5-methylbenzo-1,4-quinone) is a plant compound contained in black cumin and has a long history of medical use (Padhye *et al.*, 2008). TQ has a simple quinone structure in which a substituted dione is conjugated to a benzene ring with an additional isopropyl and methyl side-chain group in positions 5 and 2 (Fig 6) (Gali-Muhtasib *et al.,* 2006). TQ bears a chemical formula C10H12O2 with a molecular weight of 164.204g/mol and its concentration in seed oil varies between 18-25µg/mL (Glamočlija *et al.*, 2018).

TQ has shown antioxidative, anti-inflammatory and anti-neoplastic effects (Pagola *et al.*, 2004). The combination of TQ with various anticancer drugs such as cisplatin, ifosfamide and doxorubicin, was shown to have increased their therapeutic index and

also increased the protection of non-tumour tissue against therapeutic-induced damage (Tabasi *et al.*, 2015).

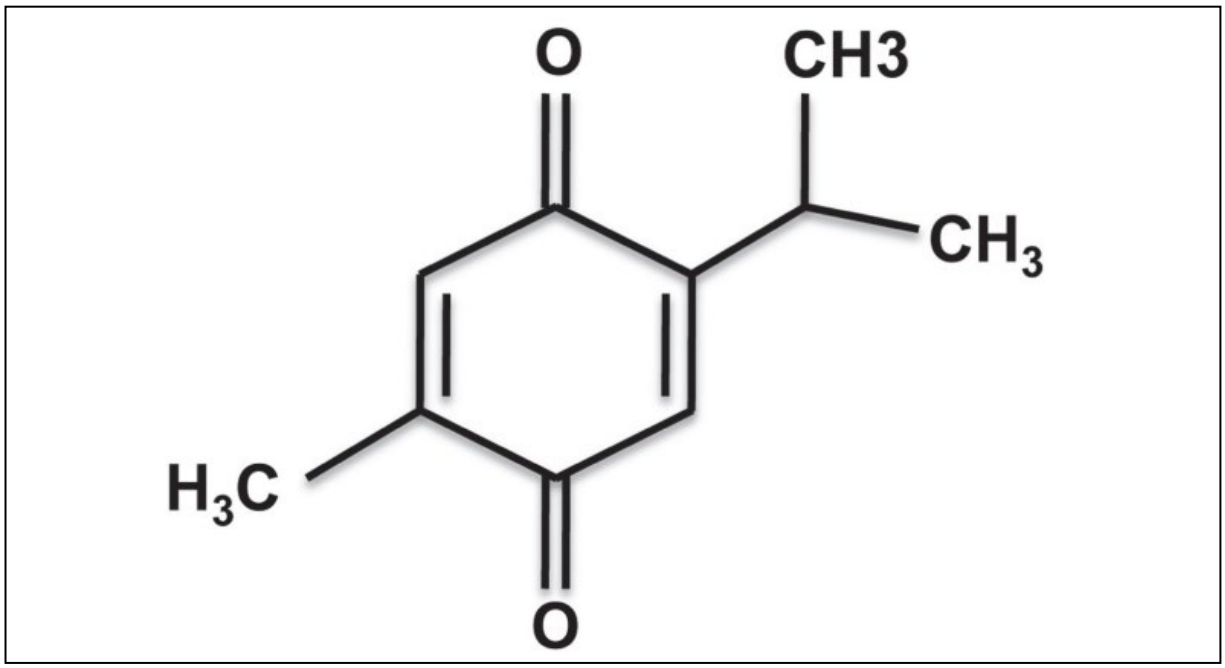

Fig 6: Schematic diagram of molecular structure of Thymoquinone (Asaduzzaman Khan *et al.,* 2017).

1.10 Anticancer Mechanism Of Thymoquinone

1.10.1 Anti-Oxidant And Anti-Inflammatory Effect

Inflammation is the first line of body immune response from noxious external stimuli and plays a key role in protecting the organ from early injury. If these immunity reactions are not controlled naturally by the physiological processes they might lead to inflammatory diseases (Ahmad *et al.*, 2019a). There are two types of medications for the treatment of these types of disorders which are Steroidal and non-steroidal anti-inflammatory medicines and their long term are associated with serious adverse effects. Therefore, to overcome these limitations phytochemical agent, such as TQ, has been justified to be a safer option (Shaterzadeh-Yazdi *et al.*, 2018).

TQ is reported to have a direct effect on the two main enzymes, COX and LOX involved in the inflammatory pathway, through inhibition of eicosanoids products thromboxane and leukotrienes B4. These two enzymes are responsible for the expressions of various inflammatory cytokines which cause oxidative stress and infiltration of neutrophils and macrophages leading to tissue damage. TQ is also very effective in preventing macrophages from producing nitric oxide (Pise and Padwal, 2017). It has also been suggested that TQ can function as free radical or superoxide radical scavengers by maintaining the activity of various antioxidant enzymes such as peroxidase, glutathione, catalase, and glutathione-S-transferase (Jain *et al.*, 2017).

TQ has also been reported to modulate the expression of cytokines such as TNF-α and IL-1 which are important for overexpression of pro-inflammatory cytokines such as IL-6, IL-8, ROS/RNS which can cause organ failure for instance in sepsis. Another inhibitory effect of TQ is the inhibition of NF-$_k$B in sepsis by inhibiting the production of the pro-inflammatory cytokine, hence decreasing the filtration of inflammatory cells (Alkharfy *et al.*, 2018).

1.10.2 Immunomodulatory Effect

Another important mechanism of TQ is its immunomodulatory activity. It is reported that TQ suppresses NF-$_k$B signalling pathway and also suppress IL-8 signal and induces extrinsic and intrinsic pathways of apoptosis in malignant brain tumour (Ashour *et al.*, 2016).

In pancreatic ductal adenocarcinoma, TQ functions as an inhibitor of the pro-inflammatory pathway by inhibition of MCP-1 protein, TNF-α, COX-2, and IL-1β resulting in the reduction of NF-$_k$B (Chehl *et al.*, 2009). Another important aspect of

TQ is its role in autophagy as it induces caspase-independent autophagic cell death by increasing the permeability of the mitochondrial outer membrane and activating JNK and p38 in colon cancer (Chen *et al.*, 2015).

TQ encourages the degradation of the α-tubulin and β-tubulin proteins in leukaemia cells (Jurkat) and astrocytoma cells (U87) without affecting the level of tubulin in normal fibroblast and thus exerting anticancer activity (Alhosin *et al.*, 2012).

TQ functions as an apoptosis stimulant in hepatic carcinoma cells (HepG2) by triggering the expression of mRNA of pro-apoptotic genes Bcl-xs and TRAIL death receptors, thus inhibiting the expression of Bcl-2 gene and preventing NF-$_k$B and IL-8 (Ashour *et al.*, 2014).

In the study by (Salem *et al.,* 2011), it was reported that TQ modulates T-cell (CD8+) for adaptive T-cell therapy against cancer, as it increases the survival and activity of these T cells.

1.10.3 Angiogenesis

Angiogenesis is referred to the process by which the development of new blood vessels from pre-existing ones occurs (Potente, Gerhardt and Carmeliet, 2011). This process is regulated by various growth factors such as fibroblast growth factor (TGF-α and β), hepatocytes (HGF), tumour necrosis factors (TNF-α), IL-8, angiogenin, and angiopoietins between all these growth factors the most important one is VEGF (Srivastava *et al.*, 2017).

TQ therapy reduces angiogenesis by controlling VEGF signals via Akt extracellular kinases pathway (Yi *et al.*, 2009). In human prostate cancer cells (PC3) and

osteosarcoma cells (SaOS-2), TQ decreases the formation of tumour blood vessels. In the case of osteosarcoma, TQ defeats angiogenesis markers (VEGF and CD34) and it also affects angiogenesis by targeting NF-kB (2-11). In addition, the combination of TQ with resveratrol compound was reported to cause inhibition of VEGF and hence necrosis in the specific area of tumour development (Alobaedi *et al.,* 2017).

Treatment of prostate cancer by TQ resulted in the inhibition of VEGF through AKT and ERK inhibitors deactivation. In both, *In vivo* and *in vitro* investigation, TQ was reported to block angiogenesis in xenograft human prostate cancer cell line (PC3) (Yi *et al.,* 2008).

Also, TQ was reported to be an appropriate regulator of two important cytokines (Gro-alpha and ENA-78) which plays a key role in neo-angiogenesis NSCLC and SCLC lung cancer cell lines (Jafri *et al.*, 2010)**.** These investigative findings indicate that TQ is capable of interfering with important stages of tumour survival and metastasis.

1.10.4 Apoptosis

Apoptosis is also known as programmed cell death that eliminates dead, mutated, or aged cells in response to pathological or physiological alteration. This mechanism is composed of two main pathways 1) intrinsic or mitochondrial-dependent pathway in which Bcl-2 family protein plays a crucial role in activating pro-apoptotic activators in response to various factors such as DNA-damaging agents, stresses and activations of oncogenes. 2) extrinsic pathway, which is a death receptor-mediated apoptosis in which death receptor ligands like FAS and TNF conjugated their receptor with the plasma membrane and activate caspase 8 (Baig *et al.*, 2016).

TQ has been shown to have the potential in activating apoptosis in various cancers. In brain cancer, TQ has been used to treat glioblastoma cells and was shown to induce apoptosis by increasing the expression levels of Bax and cytochrome-c proteins. In the same study, TQ showed the potential in activating apoptosis through p53 dependent pathway in which the concentration of TQ elevates the expression of p53 and downregulates Bcl-2 (Gurung *et al.,* 2010).

TQ was also found to be able to downregulate various proteins of Bcl-2 family proteins such as BAG-1, Bcl-2A1, Bcl-2, and BID in androgen receptor-independent prostate cancer as well as AR naive (PC-3) prostate cancer (Koka *et al.*, 2010).

In the bladder cancer cell lines (T24 and 253J), TQ has been shown to induce apoptosis via mitochondrial pathway mediation in which an elevated ratio of Bax/Bcl-2 and cytochrome-c was found (Zhang *et al.*, 2018). Another study also reported that TQ induced apoptosis in the prostate cancer cell line (DU-145) through ROS mediation (Dirican *et al.,* 2014).

1.10.5 Regulation Of Cell Cycle

The cell cycle is composed of two events S-phase (DNA replication) and M-phase (mitosis with G1 and G2). The deregulation of CDKs and cyclin in many cancers are associated with the induction of transcription of cell cycle regulating genes, avoiding checkpoints, and enabling mitosis. TQ was shown to be effective in interfering with the invasion of cancer cells from growth suppressor signals by acting on several CDKs inhibitors and cyclins (Schneider-Stock *et al.*, 2014).

It has been reported that in human colon cancer cells (HCT-116), TQ inhibits the expression level of p16 which is a CDK inhibitor, and thus downregulates cyclin D1 resulting in G1 cell cycle arrest (Gali-Muhtasib *et al.*, 2004).

TQ has also shown to be potential in inducing G0/G1 cell cycle arrest associated with the reduction level of D1 cyclin protein and upregulation of p16 protein level in Jurkat lymphoblastic leukaemia cell line (Alhosin *et al.,* 2010).

In the prostate cancer cell line (LNcaP), TQ increased the expression level of p21 and p27 proteins and caused G1/S cell cycle arrest. This resulted in the induction of cyclin A, E2, and androgen receptors which are essential for the process from G1 to S phase (Kaseb *et al.,* 2007).

The above studies concluded that TQ can cause cell cycle arrest at different phases and inhibit cell growth. They also stated that TQ interferes with cancer evasion from growth suppressors via increasing the expression level of p53 and p21 proteins.

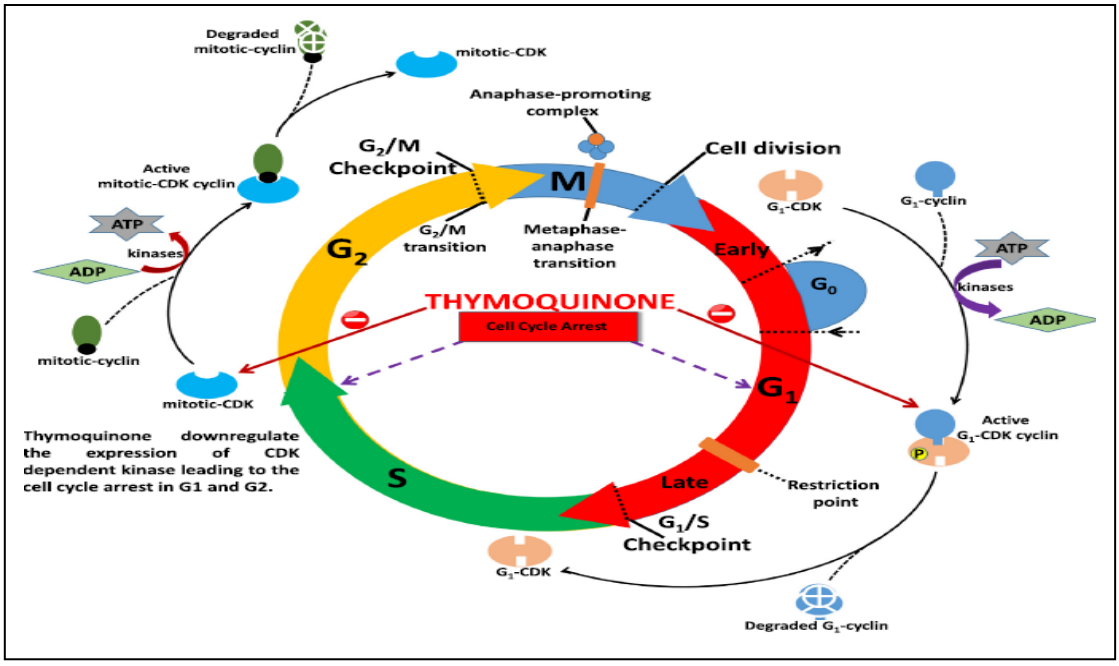

Fig 7: Role of Thymoquinone in the regulation of cell cycle (Ahmad *et al.*, 2019).

1.10.6 Migration And Invasion

Another important anticancer mechanism of TQ is reducing cancer metastasis which is known as the most deadly aspect of cancer due to the spread of cancer to distant sites in the body (Gali-Muhtasib *et al.*, 2008). It has been reported that in pancreatic cancer, two metastasis markers NF-$_k$B and MMP-9 were targeted by TQ and their expression levels have been downregulated (Wu *et al.*, 2011). In another study, TQ was reported to have similar anti-metastasis mechanisms by downregulating MMP-9 and MMP-2 metastasis markers in brain cancer glioblastoma cells (Kolli-Bouhafs *et al.*, 2012).

Epithelial-mesenchymal transition (EMT) is considered as another mechanism of TQ's action. It was reported that in breast cancer TQ inhibits the activity of Twist1 promoter and reduces its expression level which leads to inhibition of EMT (Khan *et al.*, 2015).

TQ was also reported to target and modulate EMT in CaSki and SiHa cervical cancer cell lines. TQ showed to have time and dose-dependent toxic effects in these cell lines and inhibit their migration and invasion. TQ reduces the expression of Zeb1 and Twist1 by targeting them directly and thus upregulates the expression level of E-Cadherin. Therefore it was suggested that metastasis inhibition of cervical cancer by TQ is caused by either Twist1/E-cadherin or Zeb/E-Cadherin signalling pathways (Li *et al.,* 2017).

In renal cell carcinoma cell lines RCC 769-P and 786-O, TQ has inhibited migration and invasion by upregulating E-cadherin expression level and downregulating the expression of both mRNA and protein level of Snail, Zeb1 and vimentin. TQ also targeted LKB1/AMPK signalling pathway in the same cell lines and caused an increase

in the phosphorylation level of liver kinase B1 (LKB1) and AMP protein kinase (Kou *et al.*, 2018).

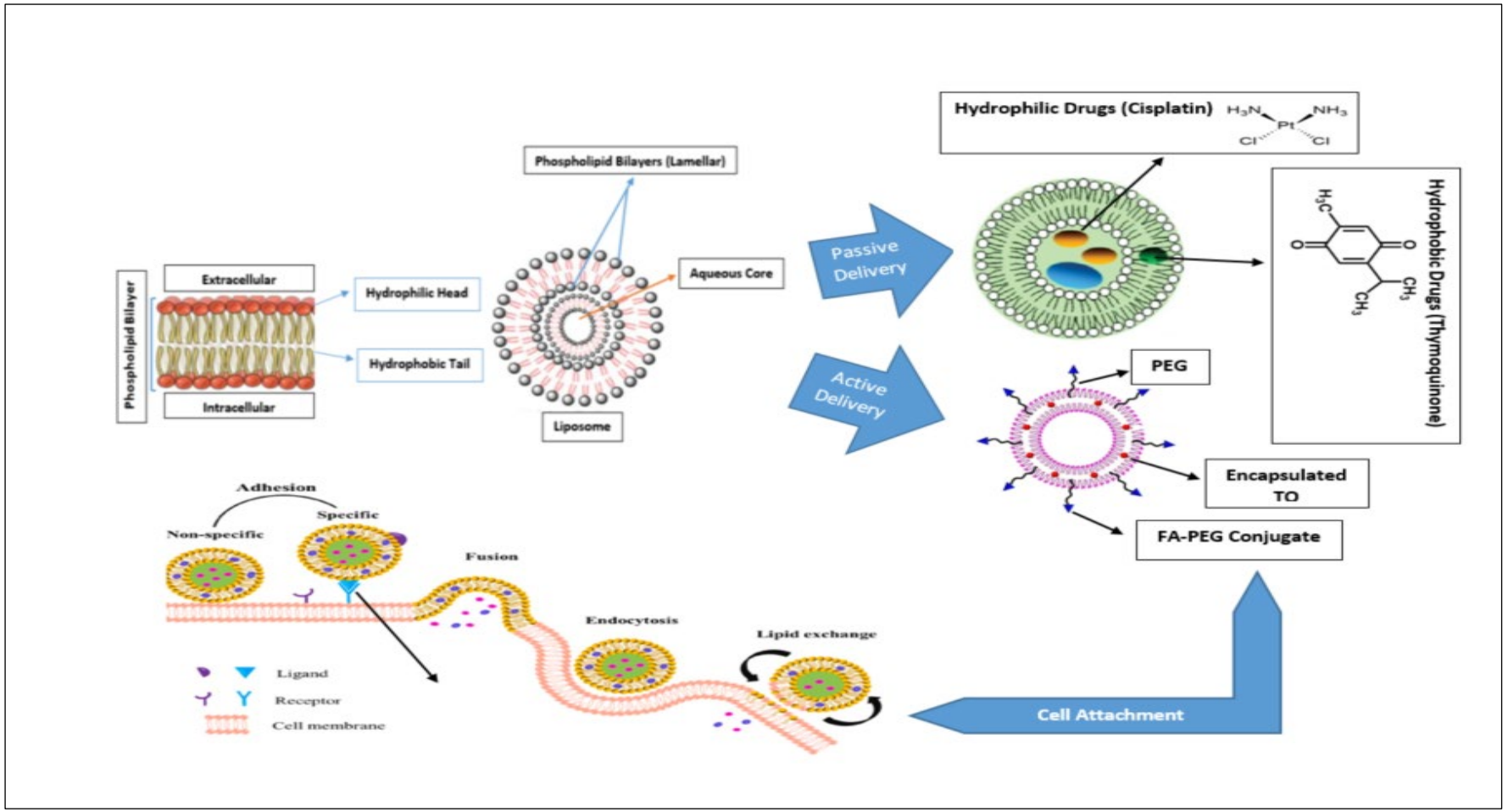

Fig 8: The Image shows the process of liposomes formation from phospholipid bilayers. It also illustatres the appropriate targeting sites for both hydrophobic, hydrphlic dugs and the process of liposomal PEGylation.

Table 2: The table below summarizes the latest research which have investigated the anticancer activity of TQ for cancer treatment.

Mode Of Study ***in vitro / in vivo***	**Cancer Type / Cell Line Used**	**Mechanism Of Action**	**References**
In vitro	Cervical Cancer / SiHa and CaSki	TQ inhibited migration and invasion of both cancer cells by targeting Twist/E-Cadherin/EMT or Zeb1/E-Cadherin/EMT.	(Li *et al.,* 2017)
In vitro	Cervical Cancer, HeLa	TQ showed a cytotoxic effect towards HeLa cells, it decreased cell population at G0/G1 phase whereas increased the cell population at the sub-G1 phase of the cell cycle. TQ also caused overexpression of p53 and thus apoptosis induction.	(Yazan *et al.,* 2009)
In vitro	Cervical Cancer, HeLa	TQ showed an anti-proliferative and dose-dependent cytotoxic effect towards HeLa cells.	(Butt *et al.,* 2019)
In vitro	Breast Cancer, MCF-7	TQ inhibited Akt and Bcl-2 phosphorylation and increased the expression of PTEN and apoptotic regulators such as Bax, p53 and p21in MC7-7 breast cancer cell line.	(Fatfat *et al.,* 2019)
In vitro	Colon Cancer, LoVo	TQ reduced proliferation by inhibiting p-PI3k, p-GSK3β, and β-catenin in LoVo colon cancer cell line.	(Hsu *et al.,* 2017)
In vitro	Head and Neck Cancer, UMSCC-14C	TQ increased the apoptosis in UMSCC-14C head and neck cancer cell line by inducing expression levels of p53 and caspase-9 proteins and inhibiting Bcl-2.	(Alaufi *et al.,* 2017)
In vitro	Gastric Cancer, HGC27 and BGC823	TQ inhibited JAK2 and c-SRc and induced apoptosis by inhibiting the phosphorylation of STAT3 and STAT-3 downstream genes such as Bcl-2 cyclin D, survivin and VEGF and upregulated caspase-3, 7 and 9 in HGC27 and BC823 cell lines.	(Zhu *et al.,* 2016)

1.10.7 TQ Limitations For Clinical Use

The main limitation associated with the clinical use of TQ is its poor bioavailability. Bioavailability is a term to describe the rate and extent of a drug that enters the systemic circulation from the site of administration (Beg *et al.*, 2011). One of the physiochemical parameters that influence the bioavailability and dosage of TQ is its poor solubility which is due to its hydrophobic characteristic (Kalam *et al.*, 2017). The calculated bioavailability of TQ was reported to be 58% with a lag time of 23 minutes and several pharmacokinetic investigations stated that the bioavailability of TQ is due to its rapid elimination and slow absorbance rate in the body (Alkharfy *et al.*, 2015). TQ can be administered in the body through four different routes including intravenous, oral subacute and subchronic, and intraperitoneal administration (Hosseinzadeh and Parvardeh, 2004). Once TQ is administered orally, it will be metabolized by DT-diaphorase which is a metabolic enzyme in the liver and results in its modification to thymohydroquinone (Jang *et al.*, 2008). The clearance of TQ directly relies on the route of administration. During intravenous administration, TQ elimination rate is 7.19mL/kg/min with the volume of distribution to a steady state of 700.90mL/kg in the animal model. In the case of oral administration, TQ clearance rate is 12.30 mL/min/kg with a distribution rate of 5109.46mL/kg and its elimination half-life is 217 minutes (Alkharfy *et al.*, 2015). Also, TQ protein binding in human and rabbit plasma was estimated at 98.99% and 98.19% which proves its rapid elimination and slow absorption (Lupidi *et al.*, 2010). Therefore various nanoformulations have been introduced such as solid lipid-nanoparticles (SLNs), liposomes, nanoemulsions, and nanostructured lipid carriers (NLCs) to improve the bioavailability and efficacy of TQ (Tubesha *et al.*, 2013).

A study done by (Surekha and Sumathi, 2016) reported that the bioavailability of TQ was increased by 3.87 fold when nanoemulsion delivery system was applied. Another study confirmed that solid lipid nanoparticles (SLNs) delivery of TQ enhanced its bioavailability 5 times compared to conventional formulations (Singh *et al.*, 2013). In an *in vivo* study on Wistar rats, TQ bioavailability was reported to increase by 3.97 folds by using nanostructured lipid carriers (NLCs) (Elmowafy *et al.*, 2016).

As mentioned above, poor solubility of TQ has a direct effect on its bioavailability but is not an important obstacle for the drug formulation. However, a study reported that water solubility of TQ (>5µg/mL) is enough to exert its pharmacologic effect. They reported that delivery of TQ by nanostructured lipid carriers (NLCs) improved its bioavailability with an elimination half-life of 5 hours which causes toxic effect against cancer cells and initiate apoptosis and cell cycle arrest (Abdelwahab *et al.*, 2013)

1.11 Liposomal TQ

As discussed previously, TQ has shown some therapeutic effects in treating various cancers including cervical cancers, however, due to its hydrophobic nature, the effectiveness was compromised. Many investigative studies have now been carried out to synthesize soluble TQ analogs or encapsulate TQ in Nano-particles. The purpose of entrapment or encapsulation of anticancer drugs into drug-loaded nanoparticles is to upsurge the therapeutic index of the anticancer drug by improving the drug delivery or uptake by the target cells and also reduce or minimize the cytotoxicity of free anticancer drugs to nano-targeted organs (Nallamuthu *et al.,* 2013). From all the nanomaterials, lipid-based nano-particles have several advantages over others such as their bioacceptable and biodegradable nature that make them being

less toxic to healthy cells and tissues compared to other nanoparticles. The nano-lipid carriers (NLCs) are characterised as a better-quality generation of lipid nanoparticles which are established from solid lipid particles (SLNs) with enhanced characteristics. The general idea behind the scheme is to mix solid lipid matrices with spatially incompatible liquid matrix, hence increasing the drug-loading (DL) capacity. Meanwhile, NLCs still maintain the advantages of solid lipid vesicles (SLVs) such as biocompatibility, controlling drug release and the possibility of production on a large industrial scale (Ong *et al.*, 2016).

Table 3: The table summarises published works that have used liposomal drugs for cancer treatment.

Nano-Particle Used	Cancer Type	*In vivo* / *In vitro*	Encapsulation Efficiency (%) and Particle Size (nm)	Results Obtained	References
Liposomes	Breast Cancer	*In vitro.* Breast cancer cells (T47D, MCF-7) and periodontal ligament fibroblasts cells (PLF)	90% Encapsulation Efficiency Size: 122 (nm)	Lip-TQ was effective in suppressing the proliferation of breast cancer cells and it showed less toxicity towards the normal periodontal ligament fibroblasts cells.	(Odeh *et al.*, 2012)
Liposomes	Breast Cancer and Cervical cancer	*In vitro* Breast cancer cell lines (MDA-MB-231 and MCF-7), cervical cancer cell lines (Hela and SiHa)	97% Encapsulation Efficiency Size: 35.66$\pm$0.1235 (nm)	TQ-NLC exhibited anti-proliferative activity towards all the cell lines in dose dependant manner but it was more cytotoxic towards MDA-MB-231 cells. In cell apoptosis, population and induction in cell cycle arrest were reported.	(Ng *et al.*, 2015a)
Nano-lipid carriers	Breast cancer	*In vitro* The mouse mammary breast cancer cell line (4T1)	Not Recorded Size: 46$\pm$0.17 (nm)	Free TQ and TQ-NLC inhibit lung metastasis by modulating the expression of MMP-2 and induction of the intrinsic apoptosis pathway in tumour cells with the involvement of Bcl-2 and caspase-8.	(Ong *et al.*, 2018)
Nano-lipid carriers	Liver Cancer	*In vitro* Human liver cancer cells with detected Hepatitis genome (Hep3B), Normal skin fibroblast cell lines (3T3)	Not Reported	TQ-NLC was reported to induce non-phase-specific cell cycle arrest. it also causes apoptosis induction via caspase-3 and caspase-7 activation.	(Haron *et al.*, 2018)

1.12 Anti-HPV Effect Of Thymoquinone In HPV Associated Cancer Treatment

Cancer development involves various stages such as transformation, dysregulation of apoptosis, proliferation, invasion, angiogenesis and metastasis (Gravante *et al.*, 2006). All cancers share a common trait in which cancer cells do not die and can produce new abnormal cells (Sudhakar, 2009). Approximately 14 million cancer cases were reported globally in 2012 and the figures are expected to rise by 70% within the next 20 years. 8.8 million death was recorded worldwide due to cancer in 2015 which accounts for, 1 in 6 deaths overall (WHO, 2018). In the UK, 163,444 deaths were recorded in 2014 with 50% survival rate and 980 new cancers are reported everyday which show the epidemic nature (Cancer research UK, 2018).

1.12.1 Epidemiology Of Cervical Cancer

Cervical cancer is known as one of the most mutual female cancers with high mortality rates worldwide but it becomes preventable cancer for women due to the significant role of HPV in its carcinogenesis. Cervical cancer is accountable for more than 275000 deaths per year, of which 88% arise in developing countries (Kashyap *et al.,* 2019). It was the 4th regularly diagnosed cancer in women in 2012, accounting for 6% of all malignancies in women with an estimated 527,600 new cases reported worldwide. The number of cases of cervical cancer begins to rise among females aged 20-29 and increased in females aged 55-64 and reduced among those aged over 65 years. With the rising population and ageing numbers of cervical cancer cases, is predicted to continue to increase 1.5-fold by 2030 (Kumar and Gupta, 2016).

Most cervical cancers originate from the transformation zone of the cervix and metastasises to regional lymph nodes. The parametrial invasion is furthermore mutual.

Clinical presentation of cervical cancer mainly depends on two key factors which are the location and the extent of the disease. Precancerous changes or primary stage of cervical cancer are generally asymptomatic and detectable via a cervical smear. Symptoms normally arise when the tumour causes continuous bleeding and pain in the case of lymph nodes involvement and also serosanguinous foul-smelling vaginal discharge or backache could also be considered as the main symptoms (Petignat and Roy, 2007a).

1.12.2 Cervical Cancer Risk Factors

In the development of cervical malignancy and precursor lesions, high-risk human papillomaviruses (HPVs) play an important role. HPVs are considered as the major factors causing sexually transmitted diseases in males and females worldwide (Burd, 2003). The susceptibility of women to this infection in the USA has been reported to be twice compared to men and the same situation was observed in other regions of the world with a much higher prevalence seen in women (17.9%) in comparison to men (8%). People with multiple sex partners during their lifetime were reported to be at higher risk of HPV infection (20.1%) than those individuals who had only one sexual partner in their entire life (7%) (Faridi *et al.*, 2011).

Although historically HPVs are known as the cause of anogenital warts and other disorders, but since 1980 extensive studies started to explore the role of HPVs in the development of cervical cancer and other tumours (Wang and Palefsky, 2016).

Infection of the uterine cervix which is caused by persistent high-risk HPVs (HRHPVs) is considered as a crucial factor that results in cervical cancer development. These high-risk infections are highly prevalent with approximately 80% of females being

infected at some time in their lives (Narisawa-Saito and Kiyono, 2007). HRHPVs infections usually start in early adulthood, soon after sexual initiation. However, the prevalence of the infection falls rapidly and it persists in only roughly 10% of females older than 30 years of age. Cervical cancer arises in a minor proportion of women (12%) who have been infected persistently via HPVs (Adebamowo *et al.*, 2017).

Although, only a smaller proportion of women infected with HPVs progress to cervical intraepithelial neoplasia (CIN) or high-grade squamous intraepithelial lesion (HSIL), persistent HPVs infections are essential risk factors for cervical cancer development (Iftner *et al.*, 2010).

HPV-16 and HPV-18 are considered as the most common subtypes of HRHPVs worldwide because they are mainly linked to carcinogenesis. However, both of these subtypes are preventable by HPV vaccination at an early age (Brianti *et al.,* 2017).

HPV infection can be transmitted initially by skin-to-skin contact such as sexual activity. HPV infection can be also transmitted through prolonged exposure to share contaminated clothing (Burd, 2003).

1.12.3 Human Papillomaviruses (HPVs)

More than 200 papillomaviruses have been identified and 150 HPVs have been completely sequenced to date. Based on the differences in DNA sequences, HPVs are divided into five classes with individual types with at least 10% dissimilarity in their nucleotide sequence from that of other papillomaviruses (Doorbar *et al.,* 2015). HPVs are small non-enveloped viruses of 50-60nm in virion size with double-stranded DNA which is approximately (6800-8000 bp in size). They have an icosahedral capsid that

replicates their genome within the nucleus of infected host cells (Aref-Adib and Freeman-Wang, 2016).

All types of HPVs have a similar viral genome structure that contains three main regions, early (E), late (L) and the genomic regulatory regions (Graham, 2010). In virions, the virus DNA is found allied with cellular histones which result in the formation of chromatin-like multiplexes. The viral genomes of the HPVs composed of 8 major open reading frames (ORFs), which are expressed by polycistronic mRNAs which are transcribed from a single DNA strand (Longworth and Laimins, 2004).

1.12.4 HPV Structure And Genome Organization

The HPV genome consists of eight open reading frames (ORFs) transcribed from a single DNA strand. (Verssimo and de Medeiros Fernandes, 2012). The viral genome of the HPVs can be divided into three major areas known as early, late and long control regions (LCR) which is also known as the noncoding region (NCR) (Zheng and Baker, 2006). The function and structure of these viruses are preserved throughout the papillomaviridae. The first element is the early gene region (denoted by E) which consists of six open reading frames (ORFs) known as E1, E2, E4, E5, E6 and E7 essential for viral infection. Some of the early genes (E1, E2, E6 and E7) are generated as a polycistronic transcript (mRNA that encodes for several proteins) (Fehrmann and Laimins, 2003). The second element is the late gene region which consists of L1 and L2 ORFs. L1 and L2 proteins are respectively responsible for encoding for the structural proteins and the major and minor capsid proteins of the virus. The difference between the two late gene regions are described as L2 ORF encodings for group-specific epitopes whereas the L1 ORF contains type-specific protein domains. The

final element of the viral genome of the HPVs is the upstream regulatory region known as URR which is responsible for the noncoding region between the end of the L1 ORF and the E6 start codon that compromises almost 10% of the genome of the virus. The URR encompasses DNA recognition sites for both viral and host transcription factors and it is capable of regulating three mechanisms which are early gene transcription, viral amplification and cellular tropism (Harari *et al.,* 2014).

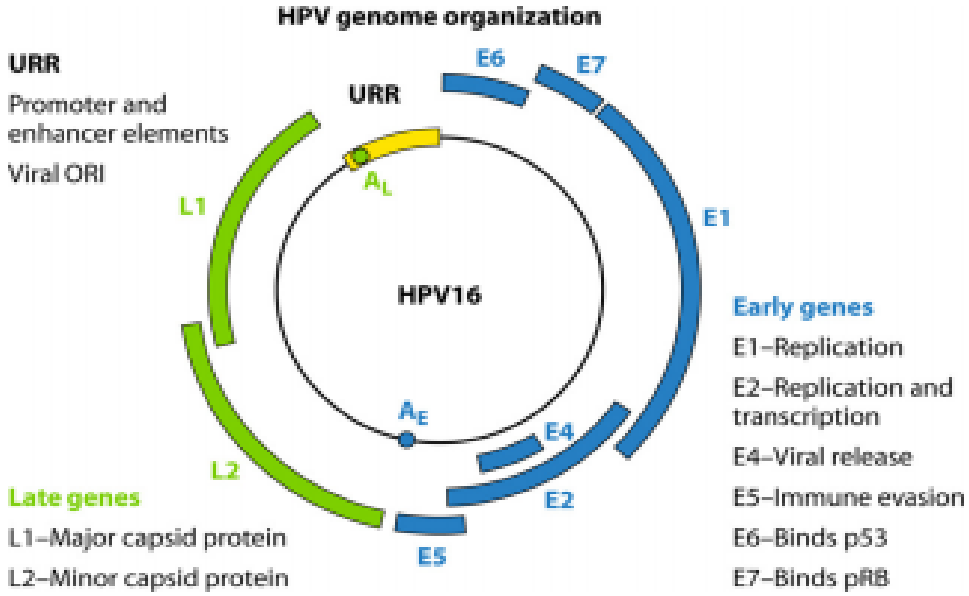

Fig 9: The image illustrates the genomic structure of HPV virus. The genome is composed of early, late and URR regions. Early region involves number of genes (E1, E2, E6 and E7) which play different role in viral replication and transcription. The late region encodes two viral structural proteins (L1 major capsid protein and L2 minor capsid protein. URR region is also responsible for controlling the early gene transcription and replication (Stanley, 2010).

1.12.5 Low-Risk And High-Risk HPVs

HPVs are categorized as Low-risk and High-risk viruses. Low-risk HPV viruses subtypes such as 6, 11, 42, 43, 44, 54, 61, 70, 72 and 80 are the subtypes that can cause disorders like genital lesions but they are considered as non-carcinogenic subtypes as they do not link with cancerous lesions and are very rarely associated

with precancerous conditions or lesions (Münger *et al.*, 2004). Low-risk subtypes are capable of causing benign tumours or leading to minor changes in cervical tissue and genital warts (condyloma acuminata), which can further grow on the cervix, vagina, vulva and anus in women and the penis, scrotum or anus in men. Low-risk HPVs infection can also cause further serious conditions such as epithelial overgrowths over the vocal cords of children and adults leading to conditions known as juvenile respiratory papillomatosis or recurrent respiratory papillomatosis (Cutts *et al.*, 2007).

Among all Low-risk HPV subtypes, subtypes 6 and 11 are considered as the most common subtypes that are allied with genital warts and account for up to 90% of these lesions (Braaten and Laufer, 2008a).

High-risk HPV subtypes include 16, 18, 31, 33, 35, 39, 45, 51, 52, 56, 58, 59 and 66. These subtypes can result in the development of various cancers such as cervical cancer and they are also linked with other types of cancers such as head and neck and mucosal anogenital cancers. From High-risk HPVs, subtypes 16 and 18 are known as the most oncogenic subtypes and approximately account for up to 70% of cervical cancer development (Braaten and Laufer, 2008b).

1.12.6 Entry Of HPV In Cervical Epithelial Cells

HPVs enter the epithelium through microabrasion or in cervical cancer, HR-HPVs infection occurs when the virus enters cells of the single-layered squamous cellular junction between the endocervix and ectocervix (Fig 10) (Herfs *et al.,* 2012). To develop infection effectively, HR-HPVs need to actively infect dividing cells including basal, stem, or epithelium cells (K. Egawa, 2003). Once the virus enters the cell, the capsid protein (L1) binds to the surface receptors known as Heparin sulphate

proteoglycans (HSPGs) on the basement membrane or the basal layer cells (Kines *et al.,* 2009). The binding of HPV to HSPGs receptors causes a conformational shift in the viral capsid protein that is mediated by cyclophilin B that exposes the N-terminus of the L2 part on the surface of the virion. Furin or PC5/6 cleave this N-terminus and this results in the clamping of the virus to the receptors on the plasma membrane of the destination cell (Woodham *et al.,* 2012).

Several recent studies have shown other targeting receptors for HPVs as entry receptors such as vimentin, syndecan-1, laminins, epidermal growth factor (EGF), tetraspanin-enriched membrane microdomains, integrins (α6) and the annexin-A2 heterotetramer (Zhang *et al.,* 2014).

HPV comes into cells through a process of endocytosis which has the most similarities to micropinocytosis. The virus passes across cytoplasmic components bound to the membrane and the trans-Golgi network, even though the endoplasmic reticulum (ER) might be involved in trafficking (Day *et al.,* 2004). Finally, the viral genome will be transported to the nucleus through a tubulin-mediated pathway where it can enter through nuclear pores during mitosis when the nuclear membrane breaks down. Approximately 24 hours after cellular attachment, HPV enters the nucleus where the capsid dissembles and incoming L2 and the viral genome are associated with promyelocytic leukaemia (PML) nuclear bodies. This nuclear site is widely used for DNA viral transcription, but HPV appears to need the completeness of PML to cause nuclear infection whereas other viruses disrupt PML upon infection (Day *et al.,* 2004).

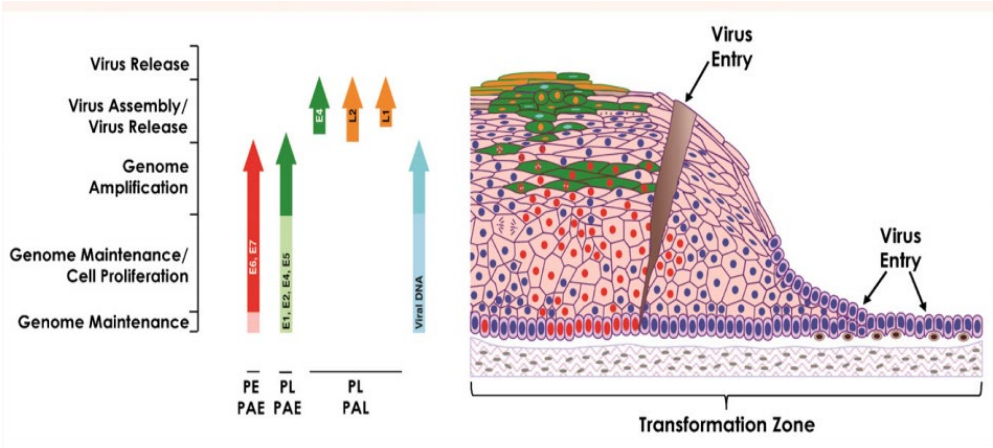

Fig 10: The image shows life cycle of High-Risk HPVs in cervical epithelium. In the case of ectocervix, infection requires the presence of a microwound to allow the virions to get access to the basal cells. Viral genome will be presented in the infected cells in a very low copy number of episomes. Once the infected cells start dividing, daughter cells will be produced which will be shifted outwards the epithelial surface. Cells present in the lower layers express E6 and E7. Proteins which are essential for genome amplification will be expressed by the cells. These cells express E4 and they are typically in S or G2 phase of the cell cycle. In the upper epithelial layer cells are ready to leave the cell cycle therefore L2 and L1 proteins are made which facilitate packaging of the amplified viral genomes (Doorbar *et al.*, 2012).

1.12.7 HPV Viral Infection (Early Phase)

Early transcription is initiated when nuclear reaches the dividing cells of the basal layer or ectocervix. A study showed that the replication/transcription factors E1 and E2 were the initial RNA species to be identified after nuclear infection via HPV31 (Ozbun, 2002). This is possible as the first goal of the incoming virus is to replicate its genome initially. In addition, early expression of E2 will facilitate correct regulation of the viral early promoters E6 and E7 proteins which ensures the continued survival of HPV-infected cells. E2 is composed of one DNA-binding domain and one protein-binding domain linked via a flexible hinge area forming a homodimer that can be connected to the palindromic site in the LCR. These sites are re-localised adjacent to the origin of

replication and are needed for viral infection triggered by E1 (Price, 2008). E2 protein binds to E1 which later binds as a dimer of hexamer to the viral origin of replication and recruits the cellular DNA replication machinery. Initial replication of the HPV genome produces roughly 50-100 episomal copies per nucleus. The viral genome amplification is regulated by E8/E2 protein by the cellular NCoR/SMRT complex. This is the first stage in the replication of the viral DNA and maintenance of the viral genome. Circularly viral genomes in the infected basal cells, are replicated alongside the cellular DNA replication and equally divided into daughter cells through binding virus genome to host cell chromosome by E2 linked to the viral LCR as well as chromatin-binding proteins Brd4 (Maglennon *et al.,* 2011). In infected basal cells, viral proteins are most likely expressed at low rates to prevent the activation of local immune responses. This is accomplished by E2 repressing the P97 promoter by stopping access of transcription factors to the promoter and by changing the conformation of chromatin (Wu *et al.,* 2006). HPV is thus able to sustain epithelial cell infection over a significant time. Division of infected cells may create a transit-amplifying cell that can differentiate and transfer into the upper epithelial cells and carry the viral genome as they move through the upper epithelial layers. HPV has developed to conduct its replication process with epithelial differentiation and during epithelial differentiation where viral genome expression is carried out (N. Egawa *et al.,* 2015).

1.12.8 HPV Viral Infection (Late Phase)

The viral DNA replication and subsequent formation of virions are parts of the late phase of the viral life cycle. To accomplish this stage, overexpression of E1 and E2

proteins are required (Van Doorslaer *et al.,* 2017). This stage is characterized by the activation of the viral late promoter such as P670 or P811 which are located in the E7 gene region. As a consequence, not only E1 and E2, but also E4 and E5 protein levels are increased (Graham, 2010). E8 is still active and E8/E2 can still suppress the amplification of the viral genome. The DNA replication of late-stage possibly produces several thousand viral genomes via a circular rolling process. The most abundant viral regulatory factors are HR-HPV E4 proteins, which play a key role in differentiated keratinocytes that enable the replication of the viral genome and supports late events in the life cycle. In contrast, the Low-risk HPV11 E4 is not essential for viral genome amplification (Lorenz *et al.,* 2013).

1.12.9 The Role Of E6 And E7 In Cervical Cancer Development

HPV E6 and E7 oncoproteins play a crucial role in promoting the cells towards oncogenesis. While they are processing their viral genome, they can encourage all the hallmarks of cancer cells such as uncontrolled cellular proliferation, angiogenesis, invasion metastasis and unrestricted telomerase activity together with the evasion of apoptosis a growth suppressor's activity (Yamato *et al.,* 2008). These two oncoproteins are polycistronially transcribed from a single promoter placed on the 3'end of the URR region and their transcription is regulated by various transcription factors such as AP1 and SP1. E7 was the first oncoprotein that was discovered among all HPVs oncogenes. It is an approximately 100 amino acids phosphoproteins containing three conserved regions CR1, CR2 and CR3. CR3 is responsible for the zinc-dependent dimerization and also for mediation of E7 interaction with cellular

proteins such as p21 and pRb which are responsible for the regulation of the cell cycle and apoptosis (Ohlenschläger *et al.,* 2006).

E6 is comparatively a larger protein (18 kDa) containing 150-160 amino acids. E6 is divided into two zinc finger binding domains by four Cys-X-X-Cys motifs found to be responsible for E6 oncogenicity. The carboxy-terminal domain of E6 contains a PDZ-binding motif which is responsible for the interaction of various cellular proteins (Zanier *et al.,* 2012).

1.13 Aims

The main aim of this study is to investigate the efficiency and efficacy of the use of liposomal drug delivery system to deliver thymoquinone (TQ) to treat HPV positive cervical cancer cells and its associated mechanism. In addition, to investigate whether this anticancer effect could be further enhanced by using targeted liposomal delivering TQ.

1.14 Objectives

I. To evaluate the IC_{50} of thymoquinone and cisplatin from two cervical cancer cell lines (CaSki and C33A cells) and normal control cell line human keratinocyte (HK) using MTT assay.

II. To prepare liposomal TQ (Lip-TQ) and to evaluate its encapsulation efficiency, stability and toxicity for the tested cell lines, CaSki and other two cell lines C33A (cervical cancer cells without HPV infection) and HK cells.

III. To examine HPV-16 oncogenes changes following Lip-TQ treatment using immunocytochemistry and western blotting.

IV. To prepare folate conjugated liposomal TQ (FA-Lip-TQ) and test the encapsulation efficiency and stability. The toxicity of the drug toward two cervical cancer cell lines will be evaluated.

V. To evaluate the drug effect on HPV oncoproteins, HPV-16 E6 and E7 and tumour suppressors p53 and pRb.

VI. To compare HPV-16 E6 and E7 oncoproteins and tumour suppressor changes following free TQ, Lip-TQ, and FA-Lip-TQ treatments for CaSki cells.

VII. To investigate protein expression for tumour suppressors p53 and pRb in C33A cells following free TQ, Lip-TQ and FA-Lip-TQ treatments.

Chapter 2

2 Materials and Methods

Table 4: Table of Major Equipment.

Equipment	Manufactured
Plate Reader	FLUOStar Omega BMG Plate Reader, BMG LABTECH Ltd, Bucks, UK
Flow Cytometry	BD FACSCalibur, BD Biosciences, Oxford UK
Flow Cytometer Software	Cell Quest Pro software, BD Biosciences, Oxford, UK
Western Blot Imaging System	LICOR Odyssey Fc Imaging system, LICOR Biosciences, Cambridge, UK
Western Blot Imaging Software	Image Studio Lit ever. 4.0, LICOR Biosciences Cambridge, Cambridge, UK
Western Blot Transfer Equipment	Trans-Blot Turbo ™ Transfer System, Bio-Rad Laboratories Ltd, Hertfordshire, UK
Gel Electrophoresis Tank	Mini-PROTEAN Tetra Vertical, Electrophoresis Cell, Bio-Rad Laboratories Ltd, Hertfordshire, UK

Gel Electrophoresis Tank Power Supply	Mini Trans-Blot Module and PowerPac™ HC Power Supply, Bio-Rad Laboratories Ltd, Hertfordshire, UK
Eppendorf Thermostat Heating Block	Eppendorf Thermostat plus, Fisher Scientific, Leicestershire, UK
Dynamic Light Scattering (DLS)	Zetasizer Nano ZS, Malvern Instrument Ltd, Malvern, UK
High-Pressure Liquid Chromatography (HPLC)	SHIMADZU, Shimadzu UK Limited
0.4µm Syringe Filters	Whatman Anotop Filters, Sigma-Aldrich Company Ltd, Dorset, UK
Dialysis Tubing	Dialysis Tubing (MW 20kDa), Sigma-Aldrich Company Ltd, Dorset, UK
Cell Culture Hoods	Mars Class 2 Cabinets, Labogene, Thistle Scientific Ltd, UK
CO_2 Incubator	Binder CO_2 Incubator, Series C, BINDER GmbH-Headquarters, Germany
Water Bath	Grant SUB Aqua 5 digital water bath, Laboratory Analysis Ltd, Exeter, UK
Deionized Water Purifier	Purite Select Fusion Water, Purification System, Camlab Limited, Cambridge, UK
ICE Machine	Scotsman AF200 Ice Flaker, Hubbard System, Suffolk, UK
Autoclave	BioCote, Coventry, UK
Balances	Acculab ALC-110.4, Fisher Scientific, Leicestershire, UK
Eppendorf Centrifuges	Eppendorf Centrifuge 5430 R, Fisher Scientific, UK

Falcon Tube Centrifuge	Sigma 4-16K Centrifuge, SciQuip Ltd, Shropshire
Heating Block	Techne Dir-Block DB.3, Cole-Parmer, Staffordshire, UK
Vortex	Vortex Genie-2T, Scientific Industries, New York, USA
Roller Mixers	Thermo Denley Spiramix 5, Thermo Scientific, Paisley PA4 9RF, UK
Roller Mixers	Roller Stuart roller mixer SRT6D, Cole-Parmer, Staffordshire, UK
Rocker	Rocker 35 EZ Large Capacity Lab Rocker, Labnet International Inc, Edison, NJ
Magnetic Stirrer	Hot Plate Magnetic Stirrer FB15001, Fisher Scientific, Leicestershire, UK
Cell Count Machine	LUNA-II Automated Cell Counter, Biocompare, UK
Confocal Microscope	A1 NIKON Confocal Microscope, Nikon Instrument Inc, USA
HPLC Column	Reversed-Phase HPLC Column, Agilent, USA

Table 5: Table of Minor Equipment.

Equipment	Manufactured
Pipettes, Pipette tips	Gilson Pipettes, Starlab UK Ltd, Milton Keynes, UK
Vortex Mixers	Stuart Vortex Mixers SA8, Cole-Parmer, Staffordshire, UK
Gas 95% O_2; 5% CO_2; Nitrogen	BOC Group Plc, Surrey, UK
Pipette Tips, 5000mL, 2000mL and 1000mL Graduated Beakers, Eppendorf Tubes, CorningTM FalconTM Round-Bottom Polymerase Tubes, Glassware, Sarstedt 96 and 6 well plates, Gloves, 1.5mL and 4mL Glass Vials, BD Plastipak Syringes, Wypall Absorbent Paper Towel, Menzel Glaser Coverslips, Cryovials	Fisher Scientific, Leicestershire, UK
Haemocytometer	Neubauer Haemocytometer, Paul Marienfeld GmbH & Co. KG, Germany
Microscopic Slides	Superfrost Microscopic Slides, VWR International Ltd, Leicestershire
Microscopes	

2.1 Cell Culture

2.1.1 Materials

Table 6: The table shows the list of cell lines used.

Cell Lines	Company
CaSki (HPV16+)	American Type Culture Collection (ATCC), UK
C33A (HPV-)	
HK (Normal Human Keratinocyte cell line)	

Table 7: The table shows the list of growth media used for cell culture.

Media	Company
RPMI 1640 (C33A and CaSki cell lines)	Gibco, Thermo Fisher Scientific, UK
Epilife (HK cell line)	

Table 8: The table shows the list of reagents used for cell culture.

Cell Culture Reagents	Company
Trypsin	Gibco, Thermo Fisher Scientific, UK
Penicillin Streptomycin	Sigma-Aldrich, UK
Fetal Bovine Serum (FBS)	
Dimethylsulfoxide (DMSO)	
Trypan Blue	
Ethanol	Fisher Scientific

2.1.2 Preparation Of Growth Media And Cell Growth Conditions

For the unconjugated liposomal study, CaSki and C33A cell lines were grown in RPMI media-1640 and HK cell was grown in Epilife® medium. Therefore a bottle of each media was placed in a water bath at 37˚C for 15 minutes.

Laminar Flow Cabinet (Hood) was sterilised by using 5% Decon and 70% Ethanol. Under a sterile condition, 55mL of the media was then transferred into a falcon tube and labelled as serum-free media (SF). 5mL of penicillin-streptomycin (1%) and 50mL (10%) of Fetal Bovine Serum (FBS) were added to RPMI-1640 media and HK's Epilife® media was supplemented with Human Keratinocyte Growth Supplement.

For the FA-conjugated liposomal study, CaSki and C33A cells were grown in folate free RPMI-1640 media for a minimum of three weeks before experiments.

Cells were obtained from the liquid nitrogen tank (-196˚C) and incubated in a water bath (37˚C) for 1 minute. 1mL of appropriate complete culture media depending on the cell line was added to the Cryotube containing cells and mixed gently. Cells were transferred into a 75cm^2 flask containing 15mL of growth medium. The flask was incubated at 37˚C with 5% CO_2 in a humidified incubator to allow cell attachment. The media was renewed 2-3 times per week.

2.1.3 Cell Passaging

The cells were incubated at 37˚C and allowed to reach around 70% confluence before dividing them in a 3:1 ratio. The cells were visualised under a light microscope to check their growth. The laminar flow cabinet was sterilised using 70% ethanol. The growth media in the flasks were discarded. 3mL of serum-free media was added to the flasks

to wash the cells briefly and was discarded. 3-4mL of trypsin was added to the flasks to detach the cells. The flasks were placed back in the incubator for 3-5 minutes until the cells were fully detached from the surface of the flasks. To stop trypsin action, 6mL of complete media was added to the flasks and were transferred to the falcon tube to be centrifuged (3 minutes, 1500RPM). After centrifugation, the supernatant was discarded and the cell pellet was resuspended in 1mL of complete media. Cells were then transferred into a new T25, T75, or T175 flask containing 15mL of complete media and incubated for future experiments.

2.1.4 Cell Counts

Cell count was performed by using the Haemocytometer. The haemocytometer was sterilised using 70% ethanol and a coverslip was placed in the central position of the chamber. 20µL of the cell suspension was mixed with 20µL of 0.4% trypan blue solution and 20µL of the obtained mixture was loaded on the haemocytometer. The chamber was placed under an inverted light microscope to be visualised under x100 magnification. The number of cells in all four outer squares were counted (The number of cells per square $x10^4$ = The number of cells/mL of cell suspension).

2.1.5 Freezing Cells

Cells were grown in T75 flasks and allowed to reach 60-70% confluence. The flasks containing cells were visualised under the inverted microscope to check the morphological appearance of the cells and to make sure they were not contaminated. The culture media in the flasks were discarded and washed briefly using 3mL of serum-free media. Cells were trypsinised by adding 3-4mL of trypsin and incubated for 3-5 minutes at 37˚C in a 5% CO_2 incubator. After the cell detachment, 6mL of

appropriate complete media was added to the flasks and mixed with the cells. Cell suspensions were transferred into a Falcon tube and centrifuged (3 minutes, 1500RPM). The supernatant was discarded and the cell pellet was collected.

The freezing media was freshly prepared in a falcon tube by adding 5mL of complete media containing 10% Dimethyl sulfoxide (DMSO).

Freezing media was added gently to the cell pellet and mixed. 1mL of cell suspension containing 2 million cells were transferred into a cryotube and labelled accordingly with passage number, cell name, and the date of freezing. Tubes were kept at -80˚C for 24 hours before they were transferred into the liquid nitrogen for long term maintenance.

2.2 Drug Preparation

2.2.1 Materials

Table 9: The table shows the list of anticancer drugs and the solvent used.

Drugs and Solvents	Molecular Weight	Company
Thymoquinone (TQ)	164.201g/mol	Sigma-Aldrich, UK
Cisplatin	300.01g/mol	
Dimethylsulfoxide (DMSO)	78.13g/mol	
Sodium Chloride (NaCl)	58.44g/mol	

2.2.2 Method

Thymoquinone (TQ) and cisplatin were the drugs investigated throughout this research project. TQ is hydrophobic therefore the stock solution was prepared in DMSO. Its molecular weight is 164g/mol, therefore to prepare a 10mM stock solution, 1.64mg of TQ was measured on the scale and dissolved in 1mL of DMSO.

1.64mg of TQ + 1mL of DMSO= 10mM TQ

Cisplatin is hydrophilic and its molecular weight is 300.01g/mol, therefore to prepare a 10mM stock solution, 6mg of cisplatin was dissolved in 2mL of saline solution.

2.3 MTT Assay (3-4,5-Dimethylthiazol-2-yl-2,5 Diphenyl Tetrazolium Bromide)

2.3.1 Instrument Specification (Microplate Reader)

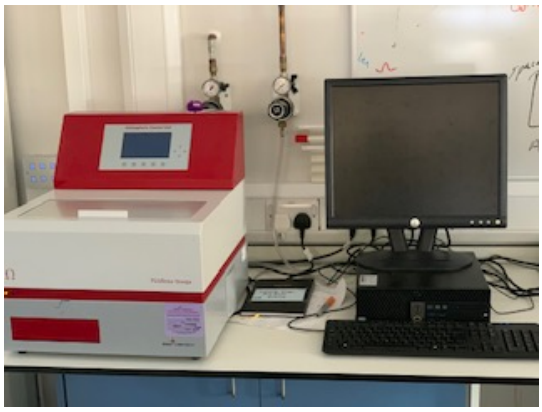

Fig 11: BMG LabTech (The FLUOstar Omega, UK) Microplate Reader.

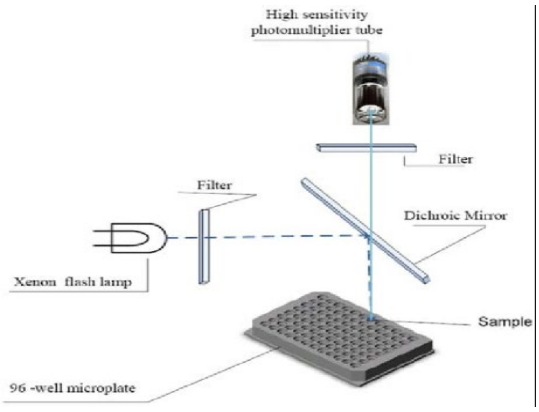

Fig 12: Schematic diagram of Microplate Reader (www.BMGLABTECH.com).

The microplate reader machine detects light signals produced from samples loaded in the 96 well plates. The optical properties of such samples are the results of factors such as their biological, chemical, biochemical, or physiological reactions. This machine detects the light signals which are generated by a sample, converted by a sample or transmitted through a sample. The signals detected, will be measured by a detector called photomultiplier tube (PMT). PMT converts photons into electricity that is then quantified by the machine. Initially, a primary optical system or the filter irradiates the sample using a specific range of wavelengths ranging from (100-1000nm) which is selected by an optical filter or a monochromator and a second optical system or light detector collects the emitted light. The amount of light being transmitted via the sample will be typically correlated to the amount of reagent present. Colourimetric assays such as (MTT) are designed to detect and quantify the amount of a specific reagent in an assay by detecting and measuring the amount of the light

absorbed by the reagent or chromogenic reaction product at a particular wavelength between (400-900nm). The high amount of the reagent present in the reaction results in a greater amount of light absorbed. These assays can be run in clear-bottom polystyrene plates as these plates do not absorb light in the visible range and this will minimise the risk of cross-talk or interference of the neighbouring wells with the measurement of the well of interest (bmglabtech.com). This experiment aimed to measure the cytotoxic effect of TQ and cisplatin on CaSki, C33A, and HK cell lines. MTT assay was used to determine the population of viable cells after drug treatment. Live cells with active metabolism transform MTT into a purple colour formazan product with an absorbance maximum near 570nm.

2.3.2 Materials

Table 10: The table shows the list of reagents used for the MTT assay.

Materials and Reagents	Company
Tetrazolium Bromide (MTT)	Sigma-Aldrich, UK
Phosphate Buffered Saline Tablets (PBS)	Thermo Fisher Scientific, UK
Isopropanol	
Hydrochloric Acid	

2.3.3 Method

Cells were cultured and seeded at different densities onto 96 well plates in duplicates CaSki ($5x10^4$), C33A ($5x10^4$), and HK ($1x10^5$) for 24 and 48 hours of treatment. The plates were incubated for 24 hours for cell attachment. Afterwards, cells were treated with different doses of TQ (Table 11) and cisplatin (Table 12). After 24-48 hours of

treatment, cells were initially visualised under the inverted microscope. The media in every well was aspirated and 10μL of MTT solution was added to each well. The plates were incubated for 3-4 hours at 37˚C with 5% CO_2. To stop the MTT reaction, 150μL of MTT solvent was added to each well and the plates were wrapped in foil and placed on an orbital shaker for 15 minutes at room temperature. Finally, the absorbance was read by using a spectrophotometer at OD= 570nm within 1 hour.

2.3.4 MTT Reagent Preparation

5mg of the Tetrazolium compound (MTT) was added to 1mL of phosphate buffer saline (PBS).

2.3.5 Preparation Of MTT Solvent (4mM HCL 0.1% In Isopropanol)

To make 40mL of stock solution, 200μL of 2N HCL was added to 39.2mL of Isopropanol.

Table 11: The table below demonstrates the MTT assay using different concentrations of TQ on 96 well plates.

100μL Media	**100μL Media**	**100μL Media**	**100μL Media**	**100μL Media**	**100μL Media**	**100μL Media**	**100μL Media**	**100μL Media**	**100μL Media**	**100μL Media**
100μL Media	Control (cells + media)	Cells+ Media+ 1%DMSO	Cells+ 1.25μM TQ in DMSO	Cells+ 2.5μM TQ in DMSO	Cells+ 5μM TQ in DMSO	Cells+ 10μM TQ in DMSO	Cells+ 20μM TQ in DMSO	Cells+ 40μM TQ in DMSO	Cells+ 80μM TQ in DMSO	**100μL Media**
100μL Media	Control (cells + media)	Cells+ Media+ 1%DMSO	Cells+ 1.25μM TQ in DMSO	Cells+ 2.5μM TQ in DMSO	Cells+ 5μM TQ in DMSO	Cells+ 10μM TQ in DMSO	Cells+ 20μM TQ in DMSO	Cells+ 40μM TQ in DMSO	Cells+ 80μM TQ in DMSO	**100μL Media**
100μL Media	Control (cells + media)	Cells+ Media+ 1%DMSO	Cells+ 1.25μM TQ in DMSO	Cells+ 2.5μM TQ in DMSO	Cells+ 5μM TQ in DMSO	Cells+ 10μM TQ in DMSO	Cells+ 20μM TQ in DMSO	Cells+ 40μM TQ in DMSO	Cells+ 80μM TQ in DMSO	**100μL Media**
100μL Media	Control (cells + media)	Cells+ Media+ 1%DMSO	Cells+ 1.25μM TQ in DMSO	Cells+ 2.5μM TQ in DMSO	Cells+ 5μM TQ in DMSO	Cells+ 10μM TQ in DMSO	Cells+ 20μM TQ in DMSO	Cells+ 40μM TQ in DMSO	Cells+ 80μM TQ in DMSO	**100μL Media**
100μL Media	**100μL Media**	**100μL Media**	**100μL Media**	**100μL Media**	**100μL Media**	**100μL Media**	**100μL Media**	**100μL Media**	**100μL Media**	**100μL Media**

Table 12: The table below demonstrates the MTT assay using different concentrations of cisplatin on 96 well plates.

100µL Media	**100µL Media**	**100µL Media**	**100µL Media**	**100µL Media**	**100µL Media**	**100µL Media**	**100µL Media**	**100µL Media**	**100µL Media**
100µL Media	Control (cells + media)	Cells+2.5µM Cisplatin	Cells+5µM Cisplatin	Cells+10µM Cisplatin	Cells+20µM Cisplatin	Cells+40µM Cisplatin	Cells+60µM Cisplatin	Cells+80µM Cisplatin	**100µL Media**
100µL Media	Control (cells + media)	Cells+2.5µM Cisplatin	Cells+5µM Cisplatin	Cells+10µM Cisplatin	Cells+20µM Cisplatin	Cells+40µM Cisplatin	Cells+60µM Cisplatin	Cells+80µM Cisplatin	**100µL Media**
100µL Media	Control (cells + media)	Cells+2.5µM Cisplatin	Cells+5µM Cisplatin	Cells+10µM Cisplatin	Cells+20µM Cisplatin	Cells+40µM Cisplatin	Cells+60µM Cisplatin	Cells+80µM Cisplatin	**100µL Media**
100µL Media	Control (cells + media)	Cells+2.5µM Cisplatin	Cells+5µM Cisplatin	Cells+10µM Cisplatin	Cells+20µM Cisplatin	Cells+40µM Cisplatin	Cells+60µM Cisplatin	Cells+80µM Cisplatin	**100µL Media**
100µL Media	**100µL Media**	**100µL Media**	**100µL Media**	**100µL Media**	**100µL Media**	**100µL Media**	**100µL Media**	**100µL Media**	**100µL Media**

2.4 Liposome Synthesis

2.4.1 Materials

Table 13: The table shows the reagents and solvents used for liposome preparation.

Materials and Reagents	Company
L-α-phosphatidylcholine (95%) Soy	Sigma-Aldrich, UK
Thymoquinone (TQ)	
Dialysis Tubing	
Cholesterol	
(DilC 18(3)-DS)	
DSPE-PEG2000 mw2805	Avanti, USA
DSPE-PEG (2000) Folate	
Disodium Phosphate (Na_2HPO_4)	VWR, Part of Avantor, UK
Monosodium Phosphate (NaH_2PO_4)	

Methanol	Thermo Fisher Scientific, UK
Dichloromethane	

2.4.2 Method

2.4.2.1 Preparation Of Stock Solutions

- PC 100mg/mL
- Chol 20mg/mL
- mPEG-DSPE10mg/mL
- TQ 20mg/mL

The total amounts of the reagents were measured in glass vials and labelled accordingly. The samples were prepared by dissolving in Dichloromethane/Methanol at a 2:1 ratio at room temperature.

Dichloromethane/Methanol was evaporated by using Nitrogen gas until the lipid became solid. After evaporation 1mL of 0.02M NaH_2PO_4/Na_2HPO_4 was added to each vial and mixed gently for 1 hour on the roller. Then they were vortexed for a few minutes to resuspend the lipid films completely. Liposome suspensions were extruded by passing through 0.1μm Whatman Anotop filter using a 1mL syringe.

2.4.2.2 Dialysis

Extruded liposomes were dialysed overnight against 10mM sodium phosphate buffer at pH 7. To prepare sodium phosphate buffer, 4 litters of 20mM NaH_2PO_4/Na_2HPO_4 (pH 7) was prepared by dissolving 1.2g of NaH_2PO_4 and 4.26g of Na_2HPO_4 in deionised water. Liposome suspensions were transferred into Dialysis tubes and placed in dialysis buffer overnight with stirring to remove the free drugs. The next day

the samples were transferred into autoclaved Eppendorf tubes and labelled accordingly. The concentration of TQ encapsulated in liposomes was measured using spectrophotometry. Liposomes were kept at 4˚C for long term storage.

2.5 Liposome Stability Test And Encapsulation Efficiency

2.5.1 Major Instrument Specifications (Microplate Reader)

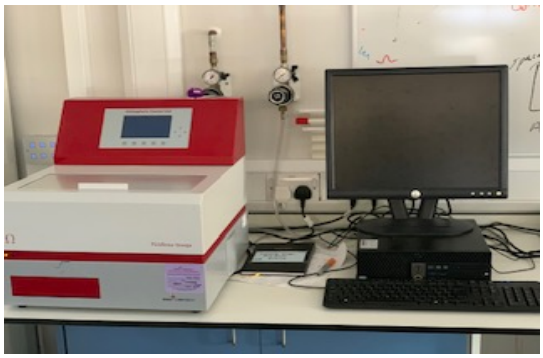

Fig 13: BMG LabTech (The FLUOstar Omega, UK) Microplate Reader.

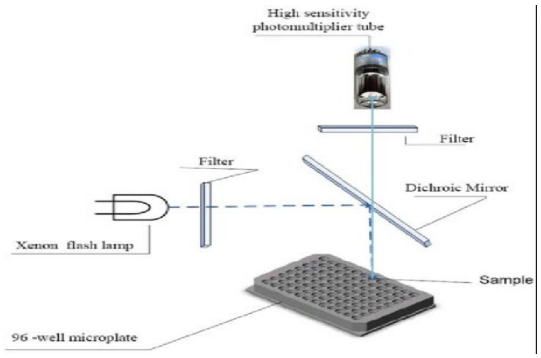

Fig 14: Schematic diagram of Microplate Reader (www.BMGLABTECH.com).

The concentration of TQ encapsulated in the liposomes was measured by using a plate reader. For that, a standard curve of TQ (2mg/mL) was prepared as well as a sample of TQ encapsulated liposomes (Table 15). The liposomal sample was dissolved in methanol to break liposomes phospholipid bilayers and release the encapsulated drug. The solutions were put in the 96 well plates and the absorbance was measured by selecting spectra and running a scan from 220-400nm. TQ has a maximum absorbance at 254nm therefore, this wavelength was selected for all the samples and the TQ concentration was calculated according to the standard curve.

2.5.2 Material

Table 14*:* The table shows the list of materials used for the stability study of liposomes.

Materials and Reagents	Company
TQ	Sigma-Aldrich, UK
96-Well UV Microplates	
Methanol	Thermo Fisher Scientific, UK

2.5.3 Method

Table 15: The table shows the preparation of standard samples for the stability study.

TQ was prepared by dissolving 2mg of TQ in 2mL of Methanol (2mg/mL).

Standard Solution (mg/mL)	2mg/mL TQ (µL)	Methanol (µL)
0	0	200
0.01	1	199
0.02	2	198
0.04	4	196
0.08	8	192
1.0	16	184
Control Liposome	10	190
Liposomal TQ	10	190

The samples were prepared accordingly and loaded onto 96 well plates in triplicate. Solutions were mixed gently by tapping on the solid surface. The plate was covered by foil to avoid light since TQ is very light sensitive. Finally, The absorbance of TQ was measured at 220-400nm by using a microplate reader.

2.6 High-Performance Liquid Chromatography (HPLC)

2.6.1 Major Instrument Specifications (HPLC)

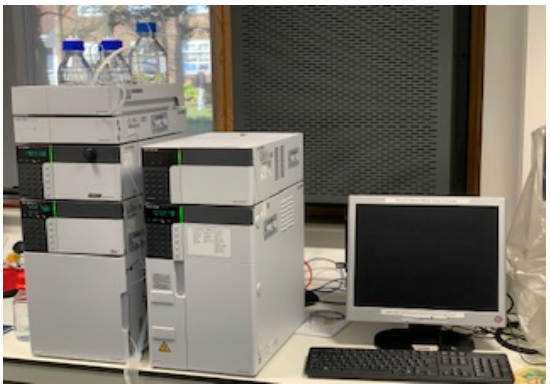

Fig 15: A HPLC system used for this study (Shimadzu, Japan).

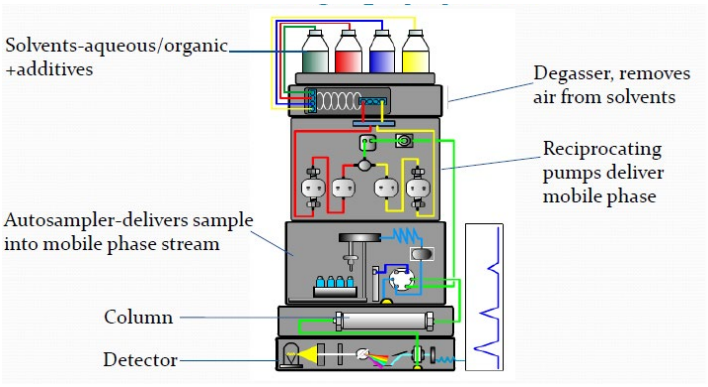

Fig 16: A schematic diagram of HPLC system.

High-performance liquid chromatography (HPLC) is a separation technique that can be used in a normal or reversed-phase mode (LaCourse, 2017). A complex mixture of compounds is dissolved and carried to the stationary phase by the mobile phase. Both of these phases are immiscible (Moldovenu and David, 2017). An HPLC system consists of a reservoir to hold the solvents (mobile phases) with a high-pressure pump solvent delivery system to generate a particular flow rate of the mobile phase (Fig 15). An injector (autosampler) introduces the sample into the continuously flowing mobile phase stream to carry it into the HPLC column (Sanchez *et al.,* 2018).

Analytes normally interact with mobile and stationary phases differently. If a solute has got strong interactions with the stationary phase then the solute will move slower. Alternatively, the solute with no interactions can move out faster. Chromatographic separations and peak broadening depend on the time an analyte takes to pass through the column. The time required for a compound to pass through the column in a chromatographic run until the compound reaches the detector is known as retention

time (t_R) (Moldovenu and David, 2017). Eluted compounds can be monitored through different detectors such as ultraviolet (UV) absorbance detectors, fluorescence detectors, and mass spectrometer detectors (MS) (Sanchez *et al.,* 2018; Waters, 2018).

2.6.2 Materials

Table 16: The table shows the list of reagents and materials used for HPLC analysis.

Materials and Reagents	Company
Thymoquinone (TQ)	Sigma-Aldrich, UK
Microsorb 100-C-18 column	
Acetonitrile	Thermo Fisher Scientific, UK

2.6.3 Method

HPLC was used to confirm the encapsulation efficiency of TQ in liposomes. A 25cm long with 5µm particle size varian microsorb 100-C-18 columns was used. The HPLC experiments were performed with a mobile phase of Acetonitrile: Water (80:20) with a flow rate of 1.0mL/min. Liposomes samples were initially destructed by using acetonitrile as follows: 800µL of acetonitrile were added to 200µL of dialysed liposomes and transferred into an Eppendorf tube. Samples were vortexed for (1 minute) and sonicated for (2 seconds) to generate a homogenous mixture. Afterwards, samples were centrifuged at (12000RPM for 10 minutes). The supernatant was then tested using HPLC to determine the encapsulated TQ in the liposomes.

2.7 Zetasizer

2.7.1 Major Instrument Specifications (Zetasizer Nano ZS Malvern)

Fig 17: The image of Zetasizer Nano ZS (Mlavern, UK).

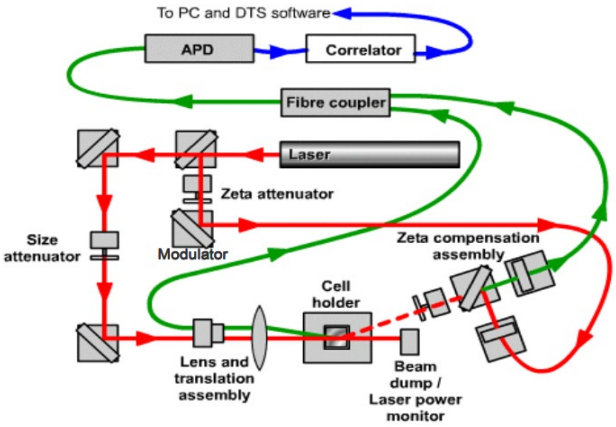

Fig 18: Schematic diagram of Zetasizer machine (www.malvernpanalytical.com)

Light scattering is used for the characterisation of particulate particles and is most commonly used for colloidal systems, nanoparticles and macromolecules in solution or dispersion for the determination of particle size, molecular weight or electrophoretic mobility. Different schemes of light scattering analysis offer a range of valuable information from tested samples which are as follow:

1- Dynamic light scattering (DLS) measures the size and size distribution of molecules and particles in the sample (Fig 17).
2- Electrophoretic light scattering (ELS) measures the electrophoretic mobility of particles or molecules in dispersion or solution-this is often converted to a zeta potential (Stetefeld *et al.,* 2016).

2.7.2 Size Determination

The size of the nanoparticles is one of the key factors that determine their mode of action and *in vivo* lifetime. The optimum size of nanoparticles for drug delivery is ranging between 10-1000nm. The smaller the nanoparticles in size, the easier they can fuse through the cell membranes and prevent detection by the reticuloendothelial system (RES) (Bertrand and Leroux, 2012). However, nanoparticles should not be too small in size to prevent them from being rapidly distributed into lymph nodes or being removed by fast renal clearance. In contrast, large nanoparticles are more likely to be accumulated at the site of injection or be trapped by different organs such as spleen, lung, and liver macrophages. Therefore, for using the nano-drug delivery system, the determination of the particle size is very important (Azhar Shekoufeh Bahari and Hamishehkar, 2016).

Zetasizer instrument operates by activating the laser light source and illuminating the sample in the cuvette. The scattered light generated by the laser is collected by one of the two detectors at two different angles, either at 90 degrees (Right Angle) or 173 degrees (Back Angle). There is a grey filter in between the laser and the cuvette containing the sample which is responsible to attenuate the incident laser light. Nanoparticles are considered as turbid samples hence the detector cannot process the amount of the photons so the filter attenuates the light generated by the laser to facilitate the detector to receive sufficient but processable signals. The movement of the nanoparticle in the sample is monitored depending on the amount of light detected over a specific time. The amount of the scattered light depends on the size of the nanoparticles, as the smaller particles move faster, therefore, show faster fluctuation

in the light intensity whereas the larger particles result in greater amplitudes between the maximum and minimum scattering intensities. The fluctuation in the scattered intensity depends on the diffusion coefficient of the nanoparticles undergoing Brownian motion which refers to the particle diffusion in the medium according to their size and their collision with the solvent molecule. There is also a correlator in the instrument which is essential for monitoring the changes in scattered intensity over time. To determine the size of the nanoparticles it is crucial to correlate intensity to the diffusion coefficient of the particles. The values obtained from the Zetasizer will be used in the Stoke-Einstine Equation to obtain particle size information (Carvalho *et al.,* 2018).

$$D = \frac{k_b T}{6\pi \eta R_h}$$

Fig 19: Stokes-Einstein equation; in which k_b is the Boltzmann constant, T is the absolute temperature and ɳ is the viscosity of the medium, and R_h is the hydrodynamic radius.

2.7.3 Zeta Potential

Another important parameter in the nanocarrier drug delivery system to be considered is zeta potential which is the electrical potential at the slipping plane. The surface charge of nanoparticles affects their physical state in liquids as well as their interaction with the biological system. Zeta potential value can also help to verify the nanoparticle tendency to aggregate in aqueous media and can be useful for correlating their physical-chemical properties to their *in vivo* and *in vitro* activity (Carvalho *et al.,* 2018). In the Zetasizer instrument, a micro-electrophoresis/electrophoretic light scattering

technology is used to measure zeta potential. Therefore to measure zeta potential, an electric field is applied to the sample which enhances the movement of the nanoparticles to the opposite electrodes. All dispersed nanoparticles have a thin layer of ions surrounding their surface which is called the stem layer (Montes Ruiz-Cabello *et al.,* 2014). Further from this layer is a layer of more loosely-associated ions that carry opposite charges to the stem layer that moves alongside the particles as they travel through a medium due to Brownian motion and is referred to as the double layer (Fig 20). The Zeta potential is the voltage at the edge of the slipping plane, where ions are no longer associated with the surface of the nanoparticles

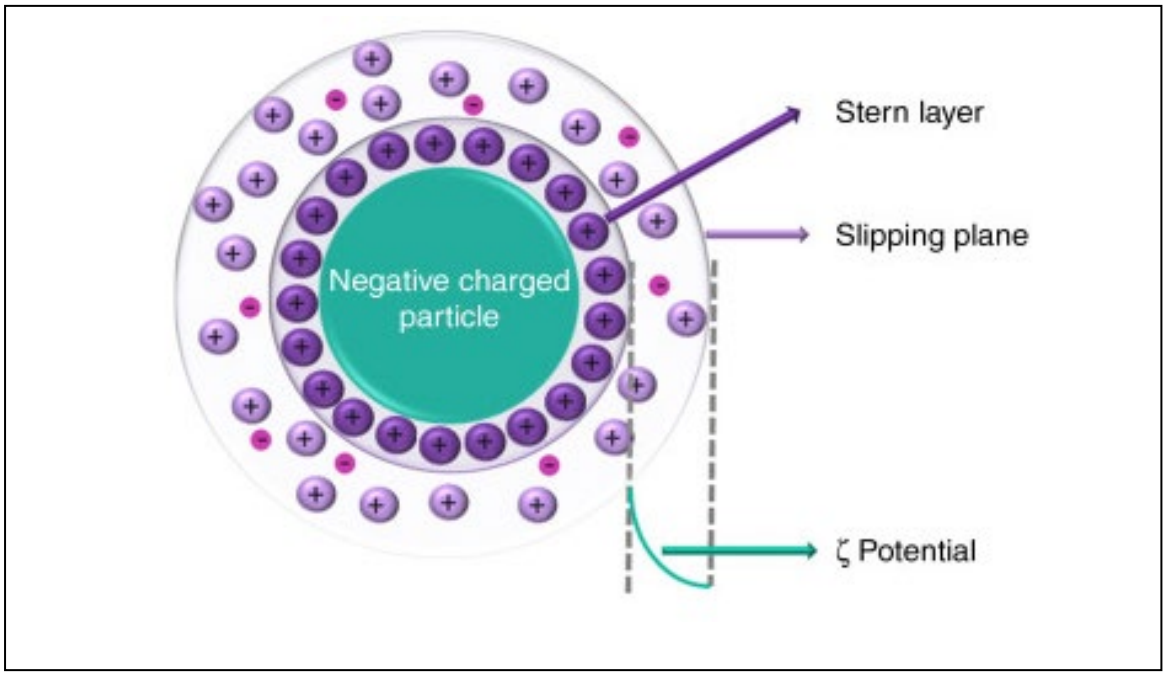

Fig 20: Zeta potential theory quantifies the repulsion between nanoparticles (Zeta potential measurement, 2020).

So if two adjacent nanoparticles have a high zeta potential of the same sign, they will not aggregate because of the repulsive electrostatic forces between particles with similar charges. Zeta potential values range from +100mV to -100mV and its magnitude is predictive of the colloidal stability which means nanoparticles with a zeta potential of >+25mV or <-25mV have a high degree of stability hence low zeta potential value compared to normal rage value results in aggregation of the particles due to Van Der Waal inter-particle attraction (Kaszuba *et al.,* 2010).

2.7.4 Materials

Table 17: The table shows the list of reagents and materials used for Zetasizer.

Materials and Reagents	Company
Phosphate Buffered Saline Tablets (PBS)	Thermo Fisher Scientific, UK
Disposable polystyrene cuvette (1mL)	Malvern Panalytical, UK
Folded Capillary Zeta Cell Cuvette	

2.7.5 Method

Liposomes size and zeta potential (charge) measurements were determined by the Malvern Zetasizer machine at 25˚C by running manual or standard operating procedure (SOP). For the size measurements, control liposomes and encapsulated liposomes were diluted in PBS (1 in 10 dilutions) in a clear cuvette with 1mL total volume and tested by the Zetasizer.

For zeta potential measurement, liposomal samples were diluted in the same ratio (1:10) in deionised water in a Folded Capillary Zeta Cell Cuvette and analysed by Zetasizer.

2.8 Apoptosis Detection

2.8.1 Instrument Specifications (Flow Cytometry)

Fig 21: Flow cytometer (BD FACSCalibur, Oxford, UK).

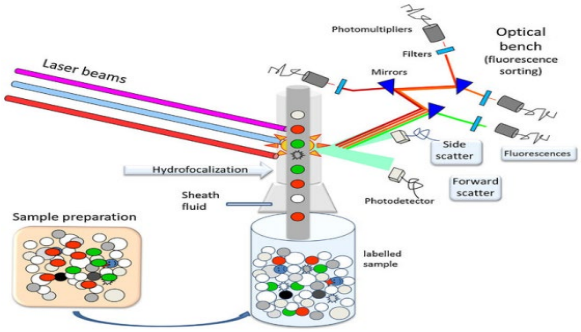

Fig 22: Schematic diagram of Flow Cytometer (www.bdbioscience.com).

Flow cytometry is a technique used to measure the physical and chemical characteristics of a specific population of cells. A sample of the cell population is suspended in a fluid, labelled with fluorochromes, and injected into the instrument. Cells are injected into a thin stream which is centralised hydrodynamically by the sheath fluid. Cells will be hit by the laser beam and the amount of the light scattered by the cells will be detected by forward (FSC) and side (SSC) photo-detectors. Fluorescence is sorted in the optical bench which holds the light source and the excitation and collection optics in a fixed position by providing a stable surface. Once cells go through the laser light, emitted SSC and fluorescence signals will be passed to the photomultiplier tubes (PMTs) and FSC signals will be collected via a photodiode. All the generated signals will be directed to their specific detectors by a system of mirrors and optical filters. The presence of a bandpass (BP) filter in front of the PMT specifies the signals to individual detectors as it only allows a narrow range of

wavelengths to reach the detectors. Generated signals by the cell samples will be converted to electronic signals and assigned to a channel number on a data plot (Depince-Berger *et al.,* 2016).

2.8.2 Annexin-V FITC And PI Staining For Apoptosis Detection

In this study, apoptotic cells were labelled with two fluorescent dyes (Annexin-V-FITC for early apoptotic cells and PI for late apoptotic or necrotic cells) which were detected by FL1 or FL2 respectively. Annexin-V is a single chain, a calcium-binding protein that has a high binding affinity to negatively charged phosphatidylserine (PS). Once cells undergo early events in apoptosis, they expose PS to their outer membrane. In normal cells, PS residues are in the cytoplasmic face which means they are hidden within the plasma membrane. In early apoptosis, PS molecules are translocated to the cell surface, and FITC conjugated Annexin-V that has a high Ca^{2+} dependent binding affinity to PS are bound to them to detect early apoptosis (Fig 23) (Demchenko, 2012).

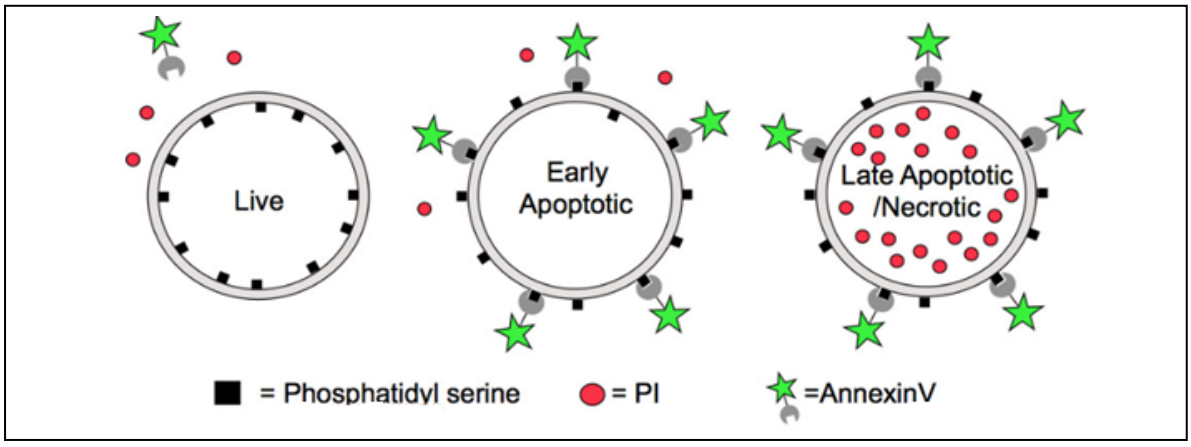

Fig 23: The mechanism of Annexin-V alone and conjugated with PI in apoptosis detection (Cell Death and Apoptosis, 2020).

Propidium iodide (PI) is a vital dye used to distinguish cells undergoing late apoptosis. In late apoptosis, PS translocation precedes the loss of cell membrane integrity resulting in late apoptosis or necrosis. Therefore conjugation of Annexin-V with PI is used for the identification of the cell population in the early or late phase of apoptosis. Dead cells contain damaged membrane which is permeable to PI. Therefore live cells are negative for both Annexin-V and PI, whereas cells in the early phase of apoptosis are Annexin-V positive and PI negative and cells that are undergoing late apoptosis or necrosis are both Annexin-V and PI-positive (Fig 24) (Riccardi and Nicoletti, 2006).

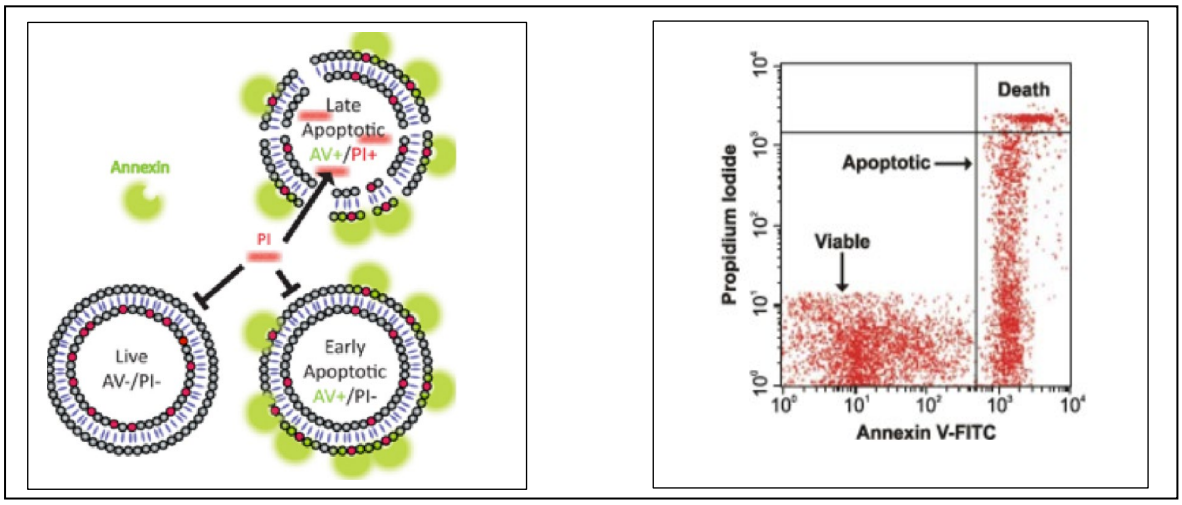

Fig 24: Cell distribution via CELLQest, according to stain intensity by Annexin-V and PI (Phosphatidylserine Externalization in Apoptosis, 2020).

2.8.3 Materials

Table 18: The table shows the list of reagents used for apoptosis analysis using flow cytometry.

Materials and Reagents	Company
Apoptosis Detection Kit (Annexin-V/PI)	Sigma-Aldrich, UK
Phosphate Buffered Saline Tablets (PBS)	Thermo Fisher Scientific, UK

2.8.4 Method

Cells were cultured and cell count was carried out. The cells were seeded at the required density ($5x10^5$) into T75 flasks. The flasks were incubated overnight in the incubator for cell attachment. On the second day, cells were treated with TQ and cisplatin as follow: (CaSki cells, 20μM of TQ and 14μM of cisplatin), (C33A cells, 17μM of TQ and 11μM of cisplatin). The arrangements for the sample treatment were as follow: media only (no treatment), 1% DMSO containing media, Liposome Control, Cisplatin, TQ, and Liposomal TQ. After 48 hours of treatment, cells were visualized under the inverted microscope. The culture media in every flask was collected and transferred into a falcon tube and labelled accordingly. The flasks were rinsed with a serum-free medium. 4mL of trypsin was added to each flask and incubated for 2 minutes until the cells were detached. 6mL of complete media was added to each flask and the total volumes of 10mL of cell suspension were transferred into the falcon tubes labelled previously. Cells were centrifuged for 3 minutes at 1500RPM. The supernatant was discarded and the pellets were washed in cold PBS and centrifuged again to recollect the pellet. 500μL of 1x binding buffer provided by the apoptosis

detection assay kit was added and re-suspended the cells for each sample. 5µL of FITC Annexin-V and 5µL of Propidium (PI) were also added to each sample. The tubes containing the samples were covered using foil to avoid light detection and were incubated at room temperature for 15 minutes with agitation every 2 minutes. Samples were analysed using Flow Cytometry via CellQuest Pro software to determine the number of events in each quadrant from the scatterplot to evaluate the population of cells undergoing early or late apoptosis.

2.9 Immunocytochemistry (ICC)

2.9.1 Major Instrument Specifications (Confocal Fluorescent Microscope)

Fig 25: Picture of confocal Fluorescent microscope (Leica, Germany).

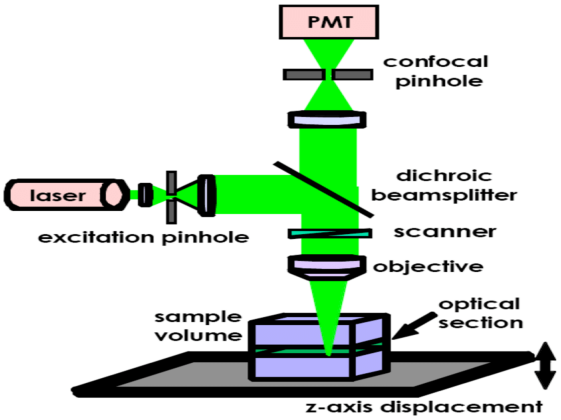

Fig 26: Schematic diagram of confocal Fluorescent microscope.

Confocal fluorescent microscopy was used in this experiment to detect the expression of HPV-E6, HPV-E7, p53, and pRb. A confocal microscope was used to detect the protein expression in the samples which were labelled by FITC. The principle of this machine is based on point excitation in the specimen and point detection of the resulting fluorescent signals.

Generally, immunocytochemistry (ICC) is used for the determination of specific protein localisation and distribution within the compartment of the cultured cells or cells with the extracellular matrix removed by using a biomolecule that is capable to bind to the protein of interest. Normally antibodies are used as biomolecules that can bind directly or indirectly to a reporter such as an enzyme, an isotope or a fluorescent dye. The reporter will give rise to detectable signals such as fluorescent signals which can be detected via using the fluorescent confocal microscope. The choice of whether to employ direct or indirect detection depends on the level of the antigen expression.

Normally direct detection is used for highly expressed epitopes in which a primary antibody is used alone which is conjugated to a fluorescence dye or an enzyme. In contrast, indirect detection is highly sensitive and generates very intense signals and more than one secondary antibody can bind to a single primary antibody (Fig 27).

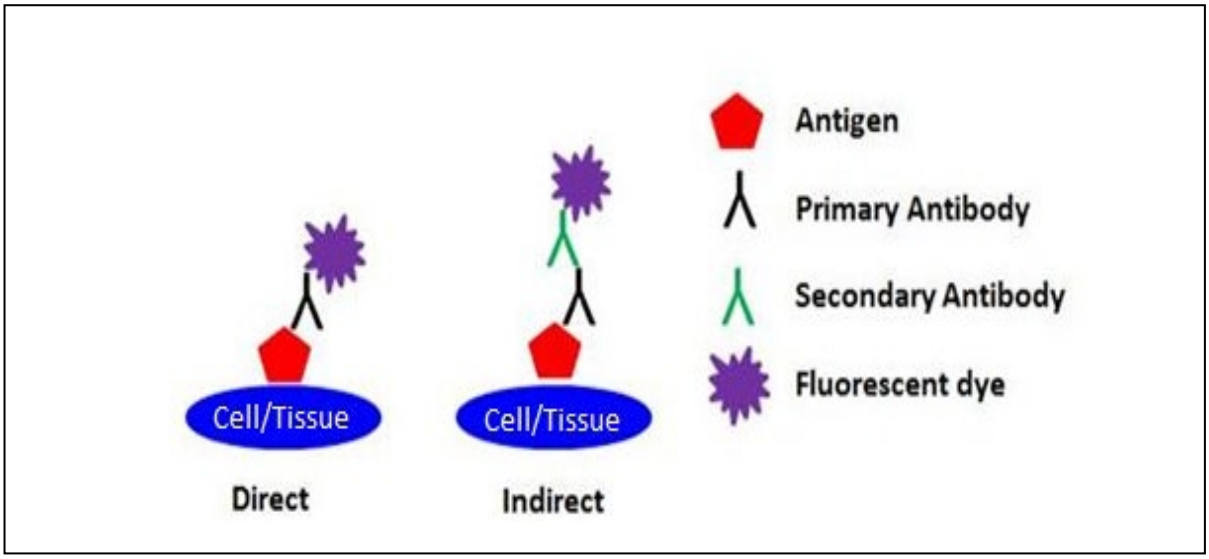

Fig 27: Direct and indirect detection methods in multicolour ICC. Antibodies are conjugated to fluorochromes which emit light upon excitation with light at a shorter wavelength. (BioLegend, 2020).

The signal generated throughout the indirect detection method can further be amplified by using ABC universal Kit which takes advantage of the strong binding affinity of Avidin to Biotin. If the secondary antibody is biotinylated, the signal generated can be amplified by subsequent incubation with an Avidin-Biotin complex. Avidin can be conjugated to a detection enzyme such as peroxidase or fluorochrome for fluorescence detection. The fluorescence detection method is based on the direct conjugation of fluorochrome to either primary or secondary antibodies and it will emit light when excited by light of a shorter wavelength. In this study two fluorochromes were employed as follows; 1) Fluorescein isothiocyanate (FITC, Green in colour,

excitation/emission 495nm/519nm), and 4',6-diamidino-2-phenylindole (DAPI, Blue in colour, excitation/emission 359nm/457nm) were used. To enhance the detection of low abundance targets such as protein, the Tyramide signal amplification (TSA) reagent can be used which integrates into any application that utilises horseradish peroxidase (HRP) (Fig 28).

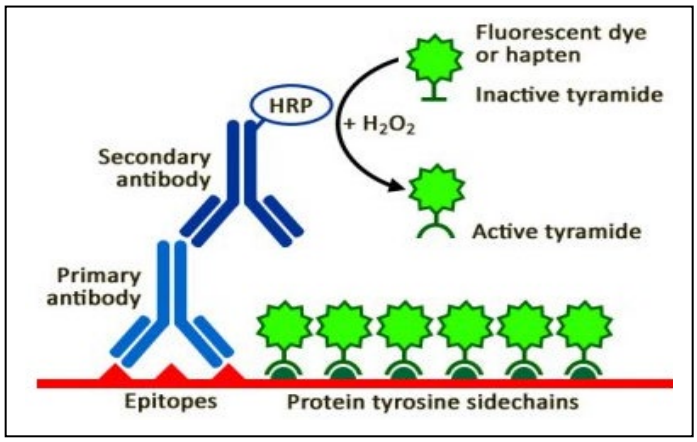

Fig 28: Illustration of TSA signal amplification system. A cell or tissue sample is labelled with primary and secondary antibody using conventional methods. The horseradish peroxidase, conjugated to the secondary antibody, catalyses the conversion of labelled tyramide into a reactive radical. The tyramide radical then covalently binds to nearby tyrosine residues, providing high-density labelling (Biotium, 2020).

2.9.2 Materials

Table 19: The table shows the list of antibodies and reagents used for immunocytochemical staining.

Material and Reagents	Company
Mouse anti-human HPV16-E6 antibody	Santa Cruz Biotechnology, UK
Mouse anti-human HPV16-E7 antibody	
Mouse anti-human Retino Blastoma (pRb) antibody	
Mouse anti-human p53 antibody	

Triton-x100	Sigma-Aldrich, UK
Paraformaldehyde	
DAPI containing Mounting Media	
Horse Serum	
Phosphate Buffered Saline Tablets (PBS)	Thermo Fisher Scientific, UK
TSA signal amplification system (FITC)	Perkin Elmer, UK
Vectastain ABC kit	Vectastain, UK

2.9.3 Method

Cells were cultured, counted and $1x10^5$ were seeded on each sterile coverslip in six-well plates. Plates were incubated overnight in the incubator for cell attachment on the coverslips. After incubation, cells were treated with three controls (media only, DMSO, and liposomes) and three drugs (cisplatin, TQ, and Lip-TQ) then incubated for 48 hours. After the treatment, cells were washed with 1mL of PBS 3 times for 1 minute each time. Cells were then fixed with 4% Paraformaldehyde for 8 minutes. After the fixation, cells were washed with PBS then 0.1% of Triton-100 in PBS was added to each well, and plates were incubated at room temperature for 7 minutes. Cells were washed again with PBS and then 100µL of 50% Horse serum was added on the top of each coverslip for 8 minutes at room temperature. The excess of horse serum was aspirated and 1^{st} antibodies were applied (HPV16-E6, HPV16-E7, pRb, and p53) which were diluted in 1:100 dilutions by PBS. Plates incubated for 2 hours at room temperature. After that, cells were washed again before 100µl of secondary antibody was applied from the ABC universal Kit (prepared according to Table 20) and plates were incubated for 30 minutes at room temperature. Thereafter 100µl of tertiary

antibody was applied from ABC universal kit (prepared according to Table 21) and the cells were incubated for 20 minutes at room temperature after cells were washed. The cells were washed again and 100µL of TSA-FITC reagent was applied to the coverslips with foil covering to avoid light and incubated for 5 minutes. After a final three times PBS washes, cells on coverslips were mounted on microscope slides by using DAPI (4′,6-diamidino-2-phenylindole) contained mounting media and the slides were properly labelled. Slides were viewed and analysed under a fluorescent confocal microscope.

Table 20: The table below demonstrates the preparation of reagents and antibodies used for immunocytochemistry.

Preparation of Antibodies	E6, E7, pRb, and p53 10µL + 100µL of PBS
Preparation of 50% Horse Serum:	500µL of Horse Serum + 500µL of PBS
Preparation of 0.1% Triton-100	50µL of Triton-100 + 50mL of PBS
Preparation of TSA-FITC	27µL of TSA-FITC Stock Solution + 2mL of DMSO
Preparation of Secondary and Tertiary Antibodies	Vectastain ABC kit (50µL of each antibody)

2.10 Western Blotting

2.10.1 Major Instrument Specifications (Li-Cor Machine):

Fig 29: LI-COR (ODYSSEY) Imaging System (LI-COR Bioscience, UK).

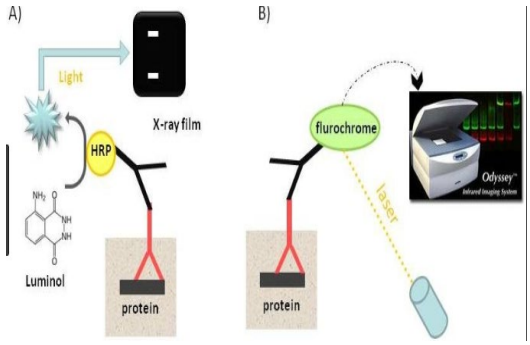

Fig 30: Schematic diagram of LI-COR machine (www.licor.com)

The western blotting technique is carried out to analyse the protein expression level of HPV oncoproteins (HPV-E6 and HPV-E7) and tumour suppressor proteins (p53 and pRb). Western blotting is a well-established method of the protein detection technique. Western blotting is often referred to as immunoblotting because an antibody will be used to specifically detect its antigen.

Western blotting can generate qualitative and semi-quantitative results about the protein of interest. Western blotting involves several stages as follows;

2.10.2 SDS-Polyacrylamide Electrophoresis (SDS-PAGE)

Electrophoresis defines a phase in which charged particles travel to the opposite electrode under the influence of an electric field. Throughout this technique, proteins can be separated according to their electrophoretic mobility which depends on several factors such as charge, molecule size, and protein structure. Polyacrylamide gel (PAG) is a three-dimensional polymer composed of acrylamide and methylene bisacrylamide under the catalysation of ammonium persulfate. PAG is referred to as

a versatile supporting matrix because of its stable hydrophily, little adsorption, and electroosmosis effect due to its neutrally charged nature. In the presence of SDS, migration and separation of charged particles are mainly based on the weight of the molecule rather than the charge or size. SDS is an anionic denaturing agent that can disrupt the hydrogen bond between the molecules to unfold proteins and break up secondary and tertiary structures. Mercaptoethanol is another strong reducing agent which can also break the disulfide bond between cysteine residues. SDS and mercaptoethanol work together to linearize protein as well as to impart a negative charge to linearized proteins. The binding of SDS creates electrostatic repulsion that results in the separation of proteins into rod-like shapes which have a length proportional to their molecular weight. For further denaturation and depolymerisation of the proteins, samples are heated to at least 60^{o}C which helps SDS to bind and enables the rod-shaped formation and negative charge adherence. A bromophenol blue dye can also be used to track the progress of the protein solution throughout the gel during the experiment. To run the electrophoresis a tris-glycin buffer system is used and as a voltage is applied the negatively charged samples move towards the positive electrodes in the lower chamber. High negatively charged proteins or those with higher molecular weight move faster than those with a less negative charge and lower molecular weight (Bass *et al.,* 2016).

2.10.3 Transfer (Protein Blotting)

The gel is removed and proteins are transferred to a nitrocellulose (NC) membrane. The combination of the proteins to the NC membrane is based on the hydrophobic interaction which can slightly affect the protein activities as well as producing minor

non-specific staining. The selection of an appropriate NC membrane depends on the molecular weight of the protein of interest. The small pores of the membrane result in a tighter combination of membrane and small molecular-weight proteins. The most used NC membranes are 0.2μm (for proteins below 20kDa) and 0.4μm (for proteins over 20kDa) (Yang and Mahmood, 2012).

2.10.4 Immunoblotting

It is very essential to block the unreacted site on the membrane with an insert protein or nonionic detergent as this can reduce the amount of non-specific binding of protein during subsequent steps in the assay. The blocking buffers should only block unreacted sites but should not bind to the epitopes of the target protein or should not cross-react with antibodies. The most commonly used blocking buffer are BSA, tween-20-PBS, and non-fat dry milk. Tween-20-PBS can decrease breakup to original interaction between proteins while it is used for protein emulsification. After blocking the primary antibody is applied which is selected depending on the target antigen to be detected. Both monoclonal and polyclonal antibodies can be used however, monoclonal antibodies are capable of recognising specific antigenic epitopes and thus having higher sensitivity and less background. After the primary antibody, the membrane is rinsed and the enzyme-conjugated secondary antibody is applied. The choice of the secondary antibody is highly dependent upon the species of the primary antibody. i.e., if the primary antibody is a rabbit monoclonal antibody, the secondary antibody should be an anti-rabbit antibody (Gallagher *et al.,* 2004).

2.10.5 ECL Signal Detection

To detect the signals, an ECL substrate kit is used which can react with the enzyme that is conjugated to the secondary antibody to produce a visible protein band (Fig 31). An ECL kit contains either horseradish peroxidase (HRP) or alkaline phosphatase (AP). HRP can act as a catalyser on the reaction among a hydrogen acceptor (oxidizing agent such as hydrogen peroxide) and hydrogen donor (chemiluminescence such as luminol). The presence of an enhancer in the luminescence system is essential as it can improve the luminescent intensity (Yang *et al.,* 2015).

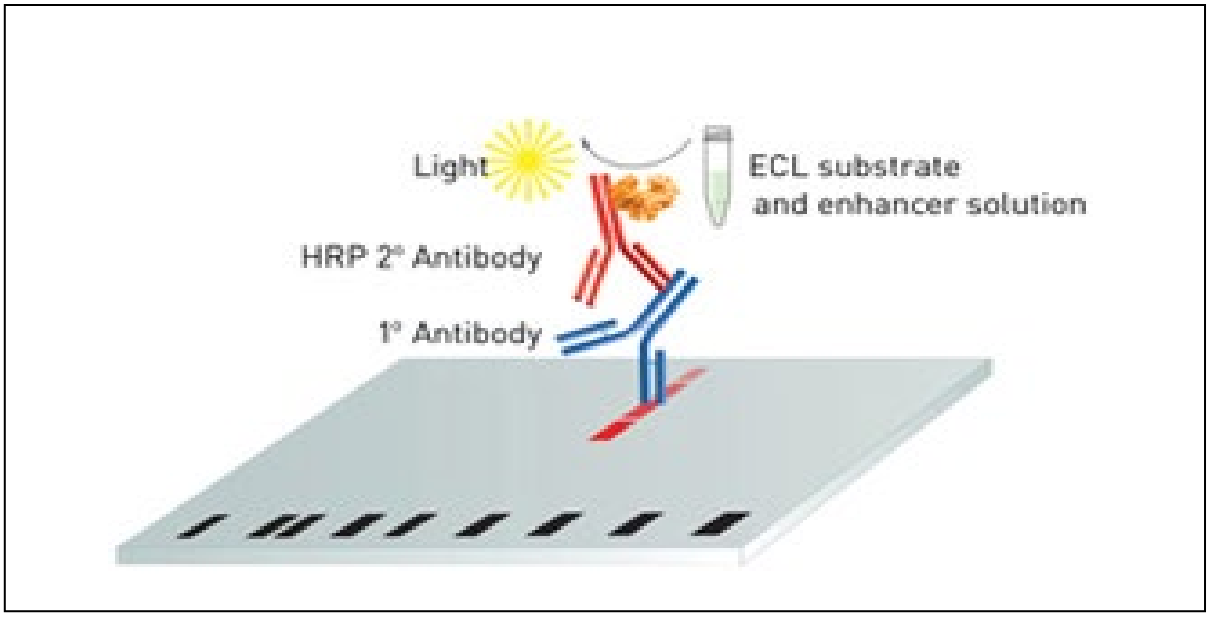

Fig 31: The principle of Enhanced Chemiluminescent (ECL) reagent in western blotting detection (ABP Biosciences, 2020).

2.10.6 Materials

Table 21: The table shows the list of reagents used for western blotting.

Material and Reagents	Company
10x Tris/Glycine Buffer	Thermo Fisher Scientific, UK
Phosphate Buffered Saline Tablets (PBS)	
ECL Western Blotting	
Bradford reagent	Sigma-Aldrich, UK
Bovine Serum Albumin (BSA)	
β-Mercaptoethanol	
Tween-20	
Mouse anti-human HPV-E6	Santa Cruz Biotechnology, UK
Mouse anti-human HPV-E7	
Mouse anti-human Retino Blastoma (Rb)	
Mouse anti-human p53	
Rabbit anti-human βactin	Abcam, UK
Anti-mouse IgG	Bio-Rad, UK
Anti-Rabbit IgG	
Mini-Protean TGX Precast Gels	
Trans-Blot TupRbo Transfer system	
Laemmli Loading Dye	

2.10.7 Method

Cells were grown until they are 80-90% confluence then they were trypsinised, counted then seeded ($5x10^5$) into 6 T75 flasks. Flasks were incubated overnight for cell attachment. Cells were treated (as described previously) and incubated for 48 hours. After the incubation, culture media from each flask were aspirated and transferred into individual falcon tubes and labelled accordingly. Cells were trypsinised by adding 4mL of trypsin for 1-3 minutes till they were detached from the surface of the flasks. 6mL of complete media was added to each flask and mixed gently with cell suspension and then transferred to the same falcon tubes which were labelled previously. Samples were centrifuged at 1500RPM for 3 minutes at 4˚C. The supernatant of each sample was discarded and the pellets were washed twice with cold PBS and incubated at room temperature on ice. 50µL of RIPA buffer was added to each sample and they were placed on ice for 15 minutes with gentle shaking every 5 minutes. The cell lysates were sonicated at 50% amplitude three times for 2 seconds each time and were placed on ice in between each two-second pulse. After sonication samples were incubated on ice for further 15 minutes. Samples were transferred into Eppendorf tubes and centrifuged at 4˚C at 13000RPM for 5 minutes. The supernatant from each sample was collected carefully and transferred into a new Eppendorf tube.

2.10.8 Bradford Protein Assay

The protein concentration of each sample was determined by performing the Bradford protein assay using Bradford reagent and BSA.

Table 22: The table below demonstrates the preparation of BSA standard dilutions.

Tubes	Volume of BSA 2mg/mL (µL)	Volume of H_2O (µL)	Final BSA concentration mg/mL
A	150	50	1.5
B	140	60	1.4
C	120	80	1.2
D	100	100	1.0
E	80	120	0.8
F	40	160	0.4
G	20	180	0.2
H	10	190	0.1
I	0	200	0

100µL of each known standard and unknown sample were pipetted out and 5µL of each was added to 95µL of PBS and loaded into 96 well plates in triplicate. 150µL of Bradford reagent was also added to each well. The plate was incubated for 10 minutes at room temperature and the absorbance was measured at 595nm by using a spectrophotometer. The protein concentration of each sample was calculated by plotting the final BSA concentration from the above table against average absorbance values obtained from the spectrophotometer. The amount of protein required was calculated for each sample and 12.5µL of loading dye was added to each sample. The total volume of each sample was 25µL.

The samples were prepared in Eppendorf tubes and labelled accordingly. The tubes were vortexed and heated up to 95˚C by using a heating block for 5 minutes to denature the proteins.

2.10.9 Sodium Dodecyl Sulphate-Polyacrylamide Gel Electrophoresis (SDS-PAGE)

Pre-packed gels (Bio-Rad, UK) were placed in the electrophoresis apparatus. The gel was assembled in the apparatus and was washed by a 1x running buffer to make sure there is no leakage. Then running buffer was then filled up to the required level depending on the number of gels. 25µL from each prepared sample was loaded into the gels wells as well as 8µL of the molecular ladder. The electrophoresis unit was connected to the power supply for 1 hour at 100 volts.

2.10.10 Membrane Transfer

After SDS-PAGE finishes, gel cassettes were removed from the tank and the gel was separated from the slides of the cassette using a spatula. The gel was placed on the membrane from a pre-prepared transfer pack (Bio-Rad, UK) and a roller was used to remove any bubbles within the membrane and gel sandwich. The Trans-Blot turbo machine was used to transfer the proteins from the gel to the membrane. The condition applied for the protein transfer was as follows: (Biorads, 2mini gels, 7 minutes, 25V).

2.10.11 Immunoblotting

When the protein transfer process finishes, membranes were removed carefully from the cassettes and were placed in flat-surfaced containers. They were rinsed 5 times with PBST and left on the plate shaker for a few minutes. After agitation, the excess of PBST was removed and the membrane was blocked using 10mL of BSA solution. The membranes were incubated at room temperature on the plate shaker. The blocking solution (BSA) was decanted and the membranes were washed 5 times with TBST for 5 minutes each time with gentle agitation. The primary antibodies (Mouse

anti-human E6, E7, pRb, and p53) were prepared in 1:500 dilutions in BSA. The membranes were incubated overnight at 4˚C with gentle shaking. The next day the membranes were placed on the shaker for 1 hour at room temperature. The primary antibody was removed and the membranes were washed 5 times with TBST for 10 minutes each time on the agitator. The secondary antibodies (Goat anti-mouse IgG) were prepared in 1:1000 dilution using BSA and they were incubated at room temperature for 1 hour. Finally, the secondary antibody was removed and the membranes were washed 5 times with 20mL of PBST for 10 minutes each time.

2.10.12 Detection (Signal Development By Electrochemiluminescence ECL)

The ECL kit was used and equal volumes of the two solutions (Luminol Enhancer and Peroxide Solution) were mixed in the ratio of 1:1 to prepare 3mL for each membrane. The excess PBST was drained off from the membrane and the ECL reagent was added. The membranes were incubated for 3 minutes in the darkness with an ECL solution. After incubation, the ECL solution was decanted carefully using a pipette and some tissue. The membranes were developed immediately on a Li-Cor imaging system to be visualised.

Table 23: The table demonstrates the preparations of antibodies and reagents used for western blotting.

Preparation of Primary Antibodies Dilutions 1:1000 or 1:500	Example 1:500: 10mL for each membrane (10mL of BSA + 20µL of each Antibody)
Preparation of Secondary Antibodies Dilutions 1:1000	5mL for each membrane (5mL of BSA + 5µL of each antibody)
Perpetration of Running Buffer	10x stock = for 500mL (15.15g of Tris + 72g Glycine + 5g of SDS) 1x= for 1 Littre (100mL of 10x Running buffer + 900mL of Deionised water.
Preparation of 5% Bovine Serum Albumin (BSA):	100mL (5g of BSA + 100mL of PBST)
Preparation of Phosphate-Buffered Saline (PBS)	10 tablets in 1 Littre of deionized water
Preparation of PBST (PBS Buffer Saline with 0.1% Tween-20)	1 Littre of PBS + 1mL of Tween 20
Preparation of Electrochemiluminescence ECL	1.5mL of Luminol Enhancer + 1.5mL of Peroxide solution (for each membrane)

2.11 Statistical Analysis

The data obtained were expressed by calculating the mean and standard deviation (SD) and interpreted using Microsoft Office Excel®. The significance of differences was analysed using Minitab®18 (Progress Way, Coventry, UK) and GraphPad Prism 9 (San Diego, California, USA). Statistical significance was determined by a paired two-sample t-test. A value of $p \leq 0.05$ was considered as a statistically significant difference.

For the liposomal stability study (size and charge), statistical analysis was determined by an unpaired t-test using GraphPad Prism 9 (San Diego, California, USA). A value of $p \leq 0.05$ was considered as a statistically significant difference.

For flow cytometry, statistical analysis was carried out via BD Calibur software provided with the instrument. For western blotting studies, the signals were normalised using Image J software and mean and SD was calculated accordingly.

Chapter 3

Preparation And Synthesis Of Unconjugated Liposomal TQ (Lip-TQ)

3.0 Introduction

Cisplatin is the most powerful chemotherapeutic treatment for advanced cervical cancer (Lorusso *et al.,* 2014). Cisplatin functions by inducing oxidative stress and apoptosis in cancerous cells via its direct interaction with DNA forming adducts, which inhibits gene transcription (Oz, Nurullahoglu Atalik *et al.,* 2015). However, its therapeutic application is limited because of its association with tumour resistance and serious side effects such as thrombocytopenia and anaemia due to haematological toxicity, bone marrow depression and nephrotoxicity (De Freitas *et al.,* 2014; Das *et al.,* 2014).

Present investigations aim to overcome these limitations by searching for potent, safe and effective anticancer agents. Currently, many herbal therapeutics such as Thymoquinone (TQ) is being investigated for cancer treatment which has a less cytotoxic side effect and is relatively less costly compared to conventional therapeutic procedures (Chehl *et al.,* 2009; Deng and Cassileth, 2005).

Researchers have conducted some studies investigating the anticancer potential of TQ in cervical cancer and reported its cytotoxic effect on HeLa and SiHa cells (Alobaedi *et al.,* 2017). It was also shown that it could induce cell apoptosis through p53 dependent pathway, elevating the level of p53-mediated apoptosis and activating caspase-3 levels in SiHa cells (Ichwan, 2014). TQ was also reported to be effective in regulating the expression level of BIK, BCL2L10 and CASP1 genes, mediating the

expression of transcription factors RELB, RELA and, tumour necrosis factors TNFRSF10B and TNFRSF10B, reducing the expression of anti-apoptotic gene and suppression of NF-$_K$B signalling (Hasan *et al.,* 2013). TQ has also been shown to inhibit the proliferation of SiHa cells via the enhancement of expression of caspase-3, 8 and 9 and inducing apoptotic cell death through p53 and caspases activation (Sakalar *et al.,* 2013).

Various drug delivery technologies have been developed to address these inconveniences and limitations associated with conventional therapy. Liposomes and lipid-based nanocarriers have shown great potential in enhancing the efficacy of hydrophobic drugs and the reduction of toxicity in cancer therapy (Pinzon-Daza *et al.,* 2013). In addition, the adaption of nanocarriers has also shown great potential in the treatment of cervical cancer compared to conventional chemotherapy due to their unique characteristics such as high biocompatibility, little toxicity, low clearance rate, controlled release of the chemotherapeutic agents and their ability in targeting specific site or tissue (Ordikhani *et al.,* 2016). Therefore, the entrapment of chemotherapeutic drugs in nanocarriers such as liposomes, micelles, dendrimers has attracted considerable attention for cancer treatment (Kijanka *et al.,* 2015). In addition, the encapsulation of chemotherapeutic agents in nanocarriers inhibits their degradation in the bloodstream, enhance their stability, minimise their toxicity, improves their bioavailability and thus equips them as suitable candidates as drug delivery vesicles (Ye *et al.,* 2014; Parveen *et al.,* 2012). In general, the use of nanocarriers as drug delivery vesicles have been shown to increase drug specificity, minimise systematic drug toxicity, increase the drug absorption rate and also prevents the active

encapsulated drug from biological and chemical degradation (Ma *et al.,* 2010; Sun *et al.,* 2015). Also, they can be modified in a way to act as a controlled or sustained drug release system for delivering therapeutic agents at a scheduled rate for a particular period of time (Akbarzadeh *et al.,* 2013).

Liposomes are one of the most studied nanocarriers which are spherical shaped particles composed of lipid bilayers and an aqueous core (Chen *et al.,* 2015).

In order to use liposomes for cancer treatment, various parameters need to be considered such as surface charge, membrane lipid packing, shape, steric stabilization and polyethylene glycol fluidity (Yeh *et al.,* 2011). These features have a direct impact on the pharmacokinetic properties of liposomes by regulating the clearance process, minimising surface toxicity, controlling mononuclear phagocytic system (MPS) recognition and enhancing permeability and retention effect (EPR) (Zamboni *et al.,* 2012). From these physicochemical characteristics, size and the surface charge are the most important factors to be deliberated because they affect EPR, cellular adhesion, cellular uptake and immune clearance of the liposomes. The size of liposomes usually ranges from 10nm to 150nm, to allow their improved accumulation in the tumour with extensive circulation time. Carriers smaller than 10nm can be rapidly eliminated and cleared by the kidneys while, those particles larger than 150nm would be at risk of being recognised and eliminated by the macrophages cells (Kijanka *et al.,* 2015). Regarding the surface charge, liposomes containing cationic lipids are more likely to bind target cells than those with anionic lipids because of the electrostatic interaction with the negatively charged cell membrane (Abu Lila *et al.,* 2009). It has also been reported that negative charge liposomes exhibit faster and

superior endocytosis compared to neutral liposomes (Miller *et al.,* 1998; Lee, Hong and Papahadjopoulos, 1992). Alongside the surface charge, other factors such as lipid composition and the cell type also play a crucial role in the cellular uptake of liposomes (Dan, 2002).

However, the only study that attempts to form TQ encapsulated liposomes to treat cervical cancer was studied by (Ng *et al.,* 2015). TQ-NLC was synthesised through lipid and aqueous matrices formulation via the hot high-pressure homogenization technique. They have synthesised TQ-NLC with an average diameter of 35.66nm with PDI value of less than 0.177 indicating that all the TQ-NLC particles were almost monodispersed and homogenous. They have also evaluated the stability of the particle by monitoring electrostatic charges on the surface of the particles which were 16.72mV. The synthesised particles were found to be stable over 24 weeks as the average diameter remained lower than 100nm and ranged from 35.66nm to 37.05nm. The initial TQ encapsulation efficiency of the particles was 97.83% which showed that TQ has perfect solubility in surfactants. TQ-NLC showed to be cytotoxic towards HeLa (HPV 18+) and SiHa (HPV 16+) in a time-dependent manner.

To the best of our knowledge, the anti-HPV activity of TQ has not been yet investigated therefore the main aim of this chapter is to synthesise liposomes with appropriate size and surface charge to encapsulate TQ to see if liposomal TQ can treat HPV infected cervical cancer cells and the expression of HPV oncoproteins could decrease following the treatment. Furthermore, cellular toxicity induced by liposomal encapsulated TQ will be compared with free TQ and cisplatin treatments.

3.1 Aim

The aim of this chapter was to prepare the unconjugated TQ liposomes and evaluate their size, charge and stability and their encapsulation efficiency for free TQ.

3.2 Objective

- To perform MTT assay to determine the IC_{50} value of TQ and cisplatin.
- To prepare liposomal TQ (Lip-TQ).
- To evaluate the stability of liposomal drugs by measuring the size, the charge of liposomal drugs and encapsulation efficiency.

3.3 Results

3.3.1 MTT Assay To Determine The Half-Maximal Inhibitory Concentration (IC_{50})

The half-maximal inhibitory concentration (IC_{50}) of cisplatin and TQ for both control cell line (HK) and two cervical cancer cell lines (CaSki HPV16+) and (C33A HPV-) were measured according to the dose-response curve obtained using MTT assay after 24 and 48 hours of drug exposure (Fig 32). The IC_{50} of HK cells after 24 hours of drug exposure were 38μM for TQ and 17μM for cisplatin; as for 48 hours of drug exposure, these values were 32μM for TQ and 10μM for cisplatin. The IC_{50} of CaSki after 24 hours of drug exposure were 31μM for TQ and 19μM for cisplatin. After 48 hours of treatment, the values were 20μM and 14μM for TQ and cisplatin respectively. For the C33A cell line, the IC_{50} values after 24 hours of drug exposure were 26μM for TQ and 15μM for cisplatin and after 48 hours were 17μM for TQ and 11μM for cisplatin. The IC_{50} values obtained indicate that C33A cells were more sensitive to both TQ and cisplatin than CaSKi cells although this was not statistically significant.

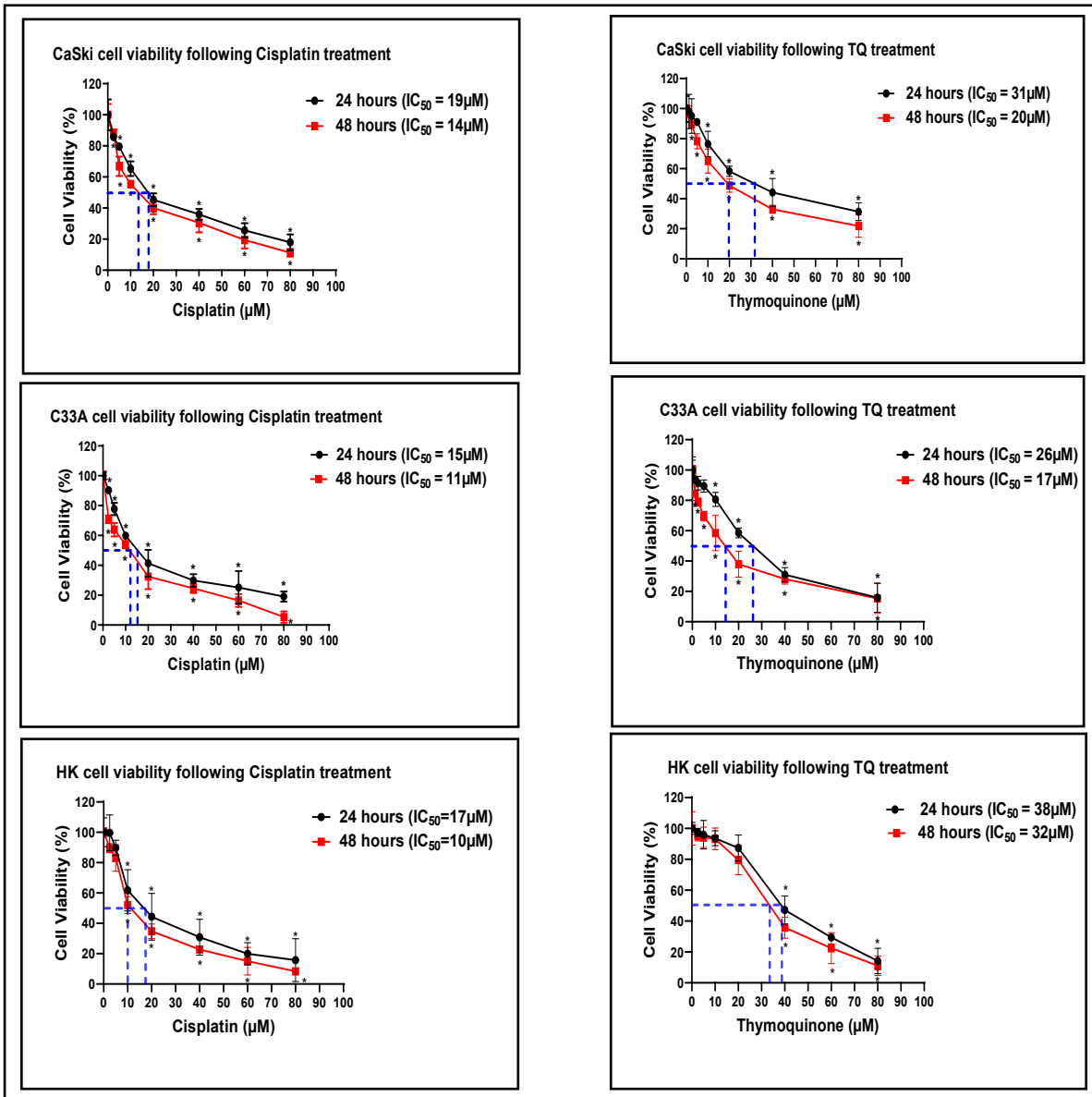

Fig 32: MTT assay showed viable cell population percentage changes following 24h and 48 hours cisplatin and TQ exposure. Both drugs decreased the number of viable cervical cancer cell lines CaSki and C33A and control cell line HK in a concentration-dependant manner. HK cell line was shown to be more sensitive towards cisplatin comparing with TQ. Dose-response curves on the effect of cisplatin and TQ in three cell lines have been analysed by MTT assay following 24 and 48 hours drug exposure. Data shown were the Mean ± SD of three independent experiments with each performed in triplicate. "*" indicates $p \leq 0.05$. The crossing points from broken lines in blue with x-axis indicated the corresponding values of IC_{50}.

3.3.2 Unconjugated Liposomal TQ (Lip-TQ) Preparation And Characterisation

Liposomes were composed of soy PC, cholesterol and distearoylp-phosphatidylethanolamine (DSPE-PEG2000). Firstly lipids were dissolved in methanol:dichloromethane and the mixture was dried by nitrogen gas. The dried lipid films were dissolved in NH_2PO_4/NA_2HPO_4. The samples were extruded through a 0.2μm filter and dialysed in sodium phosphate buffer to remove the free drugs. The initial encapsulation of liposomal-TQ (week 0) was measured via HPLC using the dialysis solution. HPLC was used for indirect quantification to measure the amount of TQ leaked out from the liposomes in comparison to the result from the microplate reader, which was used to measure TQ level directly from the sample. Initially, 2mg of TQ was used to prepare the liposomes. Liposomes were stored at 4˚C for over 17 weeks. The encapsulation efficiency, zeta potential and size of liposomes were monitored (Fig 35) every week to check the stability of liposomal encapsulated TQ by checking the TQ encapsulating percentage.

The calibration standards at five concertation points were prepared from 0 to 1mg/mL to perform external standard quantitation of TQ by HPLC. The known concentration of calibration standards of TQ was injected with an unknown sample. Table 25 showed all HPLC peak area readings from the known concentration of calibration standards.

Table 24: The table shows the readings of HPLC peak areas from calibration standards.

Concentration of TQ (1mg/mL)	HPLC peak area
0	0
0.1	65185
0.25	148440
0.5	283021
0.75	360337
1	621999

A calibration curve was generated as shown in (Fig 33) and the mathematical relationship (Y=mX+c; Y=dependent variable; m=slope; X=concentration of unknown sample; C=intercept) between the HPLC peak area against the unknown sample was used to quantify the TQ present in the sample. Y is the HPLC peak area obtained from the independent variables (concentrations). The data points were plotted using Microsoft excel® and the lines of best fit also known as regression line was added. R-squared (R^2) value was 0.9883 which indicated a good linear correlation.

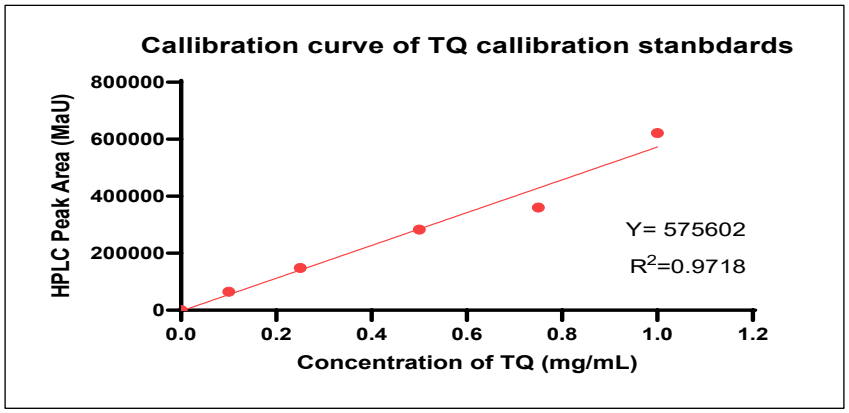

Fig 33: Callibration standard curve of TQ from 0-1µg/mL to quantify the amount of TQ by HPLC measurement.

The liposomes were dialysed in 4000mL of Buffer over 24 hours to find out the amount of TQ leaked out in the buffer; = 0.097µg/mL x 4000mL=390.4 µg/mL or 0.39mg/mL.

Since the starting concentration of TQ was 2mg/mL therefore the amount of the drug leaked out (0.39mg/mL) was deducted from the initial concentration to obtain the liposomes encapsulation efficiency of TQ (2mg/mL - 0.39mg/mL = 1.61mg/mL ≈ 80.5%).

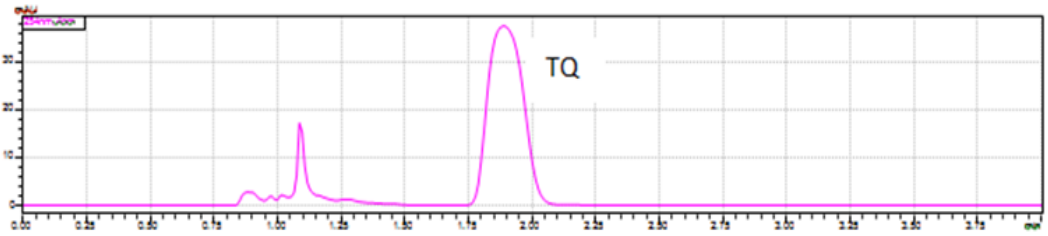

Fig 34: Chromatogram obtained from HPLC machine showed two peaks which represent the solvent and TQ retention time. The retention time of TQ was 1.85 minutes.

Physiochemical characteristics (size and charge) of the unconjugated liposomal drug was analysed over 17 weeks of storage (4˚C) by using zetasizer. The control liposomes (Lip-Control) size ranged from 130.24nm±2.55 to 135.50nm±1.86 and liposomal TQ (Lip-TQ) ranged from 149.50nm±2.35 to 150.2nm±1.56 in size over 17 weeks (Fig 35, A). The overall results showed a significant difference (p=0.0001) between the Lip-Control and Lip-TQ over 17 weeks of storage.

The membrane surface charges of nanoparticles were also monitored using zetasizer. The surface charge of liposomes is an important factor to be considered in the liposomal drug delivery system as it plays a crucial role in the interaction of liposomal membranes with peripheral membrane proteins and the immune system. Results

showed that all nanoparticles prepared in this study were neutral over the 17 weeks storage period (Fig 35, B). The liposomes were efficiently loaded with TQ and their loading efficiency and stability was analysed over 17 weeks of storage at 4˚C (Fig 35, C).

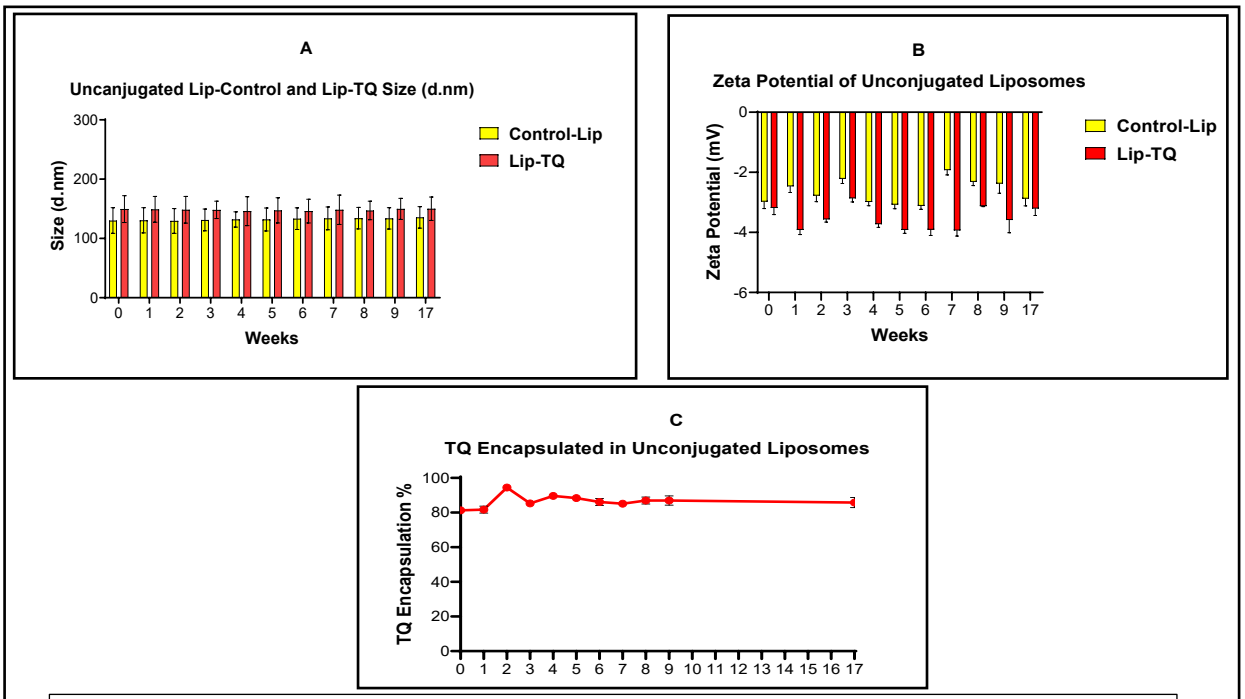

Number of weeks	Diameter (nm)	Zeta potential (mV)	PDI	Loading Efficiency %
0	149.5±2.35	-3.19±0.35	0.126	81.27±1.25
1	149.0±2.05	-3.91±1.54	0.101	81.71±1.18
2	148.4±1.75	-3.57±2.02	0.180	94.41±1.21
3	148.2±1.30	-2.87±1.61	0.123	85.26±1.23
4	146.0±2.21	-3.73±1.25	0.128	89.59±1.56
5	147.3±1.37	-3.92±3.25	0.119	88.34±1.02
6	146.1±3.35	-3.91±0.33	0.147	86.10±1.48
7	148.3±1.35	-3.93±1.24	0.139	85.10±2.08
8	147.2±2.41	-3.13±2.25	0.181	86.96±1.56
9	149.9±2.38	-3.59±1.92	0.196	86.96±0.47
17	150.2±1.56	-3.21±1.49	0.218	85.75±1.84

Fig 35: Diameter (A), Zeta potential (B) of unconjugated liposomes were measured via Zetasizer with a polydispersity index of less than 0.25. The encapsulation efficiency (C) of tested liposomes were also analysed using UV-vis spectrophotometry using TQ's λ_{max} at 220-400nm over 17 weeks of storage (4˚C). The above table shows the physiochemical properties of Lip-TQ prepared over 17 weeks storage. No significant difference was observed between encapsulation efficiency over the storage time. Data are mean ± SD of three replicate measurements of three independent experiments.

3.4 Discussion

Pharmacokinetics studies on the effectiveness of TQ as an anticancer drug showed that TQ was rapidly eliminated and had a low absorbance rate which resulted in its low bioavailability (Alkharfy *et al.,* 2014). Therefore, improving TQ interaction with cancer cells/tissue by introducing nanoparticles such as liposomes as drug carriers could provide a remarkable approach to improve TQ pharmacokinetic behaviour and increase its bioavailability (Odeh *et al.,* 2012). Furthermore, liposomes as a drug delivery system offer beneficial advantages such as their biocompatibility, low toxicity, biodegradability and targeting capability (Voinea and Simionescu, 2002).

One of the main characteristics of liposomes is their tiny size which makes it possible for them to penetrate through the leaky blood vessels of tumour cells through passive targeting while those conjugated with antibodies, peptides or sugars components are considered to function through active targeting (Dicheva and Koning, 2013). Furthermore, to increase the prolonged half-life of liposomes they can be coated with polymers such as polyethene glycol (PEG) which helps to mask their detection and destruction by the mononuclear phagocyte system (MPS) (Suk *et al.,* 2016).

As the first step of our study we have investigated and compared the cytotoxic effect of TQ and cisplatin and also determined their half-maximal inhibitory concentration (IC_{50}) after 24 and 48 hours of drug exposure via performing MTT assay using HPV 16+ CaSki cells, HPV- C33A cells and normal human keratinocyte HK cells. Results showed that TQ had a more anti-proliferative effect which is time and dose-dependent on cervical cancer cells but this effect was significantly reduced for the normal HK cells. The IC_{50} of HK cells after 24 hours of TQ and cisplatin exposure were 38μM and

17μM; 31μM and 19μM for CaSki cells and 26μM and 15μM for C33A cells respectively. After 48 hours of treatment, the IC_{50} of HK cells were 32μM for TQ and 10μM for cisplatin, these values were 20μM and 14μM for CaSki cells and 17μM and 11μM for C33A cells (Fig 32). Overall results showed that cisplatin and TQ exert a cytotoxic effect towards both HPV+ and HPV- cell lines after 24 and 48 hours of drug exposure which was shown by a significant ($p \leq 0.05$) decrease in viable cell population compared to the control sa159mple. However, the HK cell line showed to be more sensitive towards cisplatin than TQ treatments. The effect of TQ on the proliferation rate of SiHa (a HPV16+ cervical cancer cell line), C33A (HPV-) and HeLa (a HPV18+ cervical cancer cell line) were reported previously (Ichwan, 2014; Yazan *et al.,* 2009). Their studies showed that TQ treated cervical cancer cells have reduced their viability rates following TQ treatment in a dose and time-dependent manner. The results obtained from the current study is in agreement with another study by (Ng *et al.,* 2015). They have evaluated the cytotoxic effect of TQ and cisplatin on HeLa and SiHa cells and used two other cell lines 3T3 and Vero cells as controls. Results showed that cisplatin was more toxic towards normal cells than to cervical cancer cells. Therefore, our work supported by other studies demonstrated that TQ could be a suitable candidate to treat cervical cancers and it has a low cytotoxic effect on normal cells.

Although a few *in vivo* studies for TQ which was administered via an intraperitoneal mode showed its promising anticancer effect, however, this drug administration mode would cause discomfort and it was not cost-effective due to the aseptic techniques used (Ansar *et al.,* 2020). Therefore a non-invasive oral administration route is preferred as an attentive for TQ delivery however this can be largely restricted by the

poor solubility of TQ in water and also its poor bioavailability (Khader *et al.,* 2009). As TQ is a hydrophobic molecule thus lipid base drug carriers such as liposomes can be good biodegradable and bio-acceptable drug carrier candidates to encapsulate TQ and minimise its toxicity, control its release rate and prolong its circulation in the blood (Ng *et al.,* 2015).

In the present study, control liposomes (Control-Lip) and liposomal TQ (Lip-TQ) carriers were formulated via the lipid film hydration method. This has been described in detail in Chapter 2. When the samples were prepared, the loading efficiency and stability of the liposomal drug were measured from week 0 (the day that samples were initially synthesised) to week 17 (Fig 35, C). TQ encapsulation and drug loading capacity of Lip-TQ synthesized in this study were found to be relatively high (81% in week 0 and 85% in week 17). The result obtained suggest that TQ has good solubility in the surfactant (soy PC). The advantage of the high encapsulation efficiency is that it prevents the wastage of the compound (TQ) as the majority of them are encapsulated within the liposomes hence lowering the production cost. In addition, the size of the synthesised liposomes was monitored over 17 weeks (Fig 35, A) in which an average diameter of 130.24nm±2.56 to 135.5nm±1.86 for the Control-Lip and 149.50nm±2.35 to 150.2nm±1.56 for Lip-TQ were observed. The liposomes synthesised in the current study were stealth nanoparticles due to having a polyethylene glycol (PEG) layer grafted on their surface. This layer facilitates the liposomes to evade the immune response generated by macrophages (Danhier *et al.,* 2010). In addition, PEGylation helps to hinder the adsorption of protein opsonins onto particles surface which can cause increased elimination of liposomes by mononuclear

phagocytic cells in the liver and spleen hence resulting in prolonged circulation of the liposome in the blood (Mohamed *et al.,* 2019). Ideally, a solid tumour that undergoes angiogenesis generate discontinuous endothelium with a large fenestration meaning that molecules up to 4000kDa size or 500nm can enter the interstitial space (Bozzuto and Molinari, 2015). Liposomes within the range of 20-200nm in size can extravasate through the gaps in the leaky vasculature of the tumour into the interstitial space (Golombek *et al.,* 2018). Therefore PEGylated liposomes can remain in blood circulation for a much longer time leading to their accumulation in the interstitial space of the tumour via the enhanced permeability and retention process (EPR) effect and avoiding their removal (Zein *e al.,* 2020).

Furthermore, the polydispersity index (PDI) of the liposomes was measured which was less than 0.25 (Fig 35) indicated the homogeneity of the samples meaning that all particles were almost in monodispersity and homogenous with narrow size distribution. The closer the PDI value to 0, the higher the homology between the liposomes. PDI is an important factor as a value greater than 0.5 can be a sign of aggregation. During liposomal delivery, the aggregation can impede the targeting efficiency to cells and tissue. Also, the rate of the cellular uptake and cytotoxic effect of the liposomal drug might be reduced and there is a possibility that aggregated particles can remain out of the suspension and be no longer bioavailable (Kvítek *et al.,* 2008).

Zeta potential is considered as another essential factor in the stability of liposomal drugs. The zeta potential values obtained in the current study for Control-Lip was -2.98 mV±1.35 at week 0 and -2.88mV±1.29 at week 17 and for Lip-TQ these values were -3.19mV±0.35 at week 0 and -3.21mV±1.49 at week 17. Zeta potential refers to

the electrostatic charge on the surface of the nanoparticles in the suspension which can help to predict the fate of the liposomes *in vivo* (How *et al.,* 2013). The results obtained indicates a significant difference (p=0.0001) between the zeta potential of the Control-Lip and Lip-TQ over 17 weeks.

The toxicity level of the nanoparticles is highly dependent on their zeta potential and size. In general, zeta potential is an essential factor for adsorption of the nanoparticles such as liposomes onto the cell membrane and size is another important feature highly associated with their endocytic uptake (Schwegmann *et al.,* 2010). The high value of zeta potential >+30mV indicates the stability of the nanoparticles which means they are less likely to develop aggregation or increase in size. However, this parameter is not an absolute measurement of particle stability meaning that positively charged particles have a long-circulating half-life due to the adsorption of protein components of the blood while those with negative charge can be eliminated by the reticuloendothelial system (Honary and Zahir, 2013).

It has been stated that liposomes with zeta potential >+10mV are positively charged, those having zeta potential of <-10mV are referred to as negatively charged particles and any ZP value between -10 to +10mV is considered as neutral liposomes (Smith *et al*., 2017). The zeta potential values for the Lip-TQ liposomes synthesised in this study were ranging from -3.19mV±0.35 at week 0 and -3.21mV±1.49 at week17 which indicates they are neutral liposomes. However, there was no sign of aggregation as there was not any significant change in the size over long storage time and all PDIs were lower than 0.25. The result was confirmed by another study by (Ong *et al.,* 2018)

where nano-lipid carriers (NLC) encapsulating TQ was shown low zeta potential values ranging from (-4.38mV to -6.03mV).

The overall results from this chapter provide evidence that TQ can be considered as a suitable anticancer drug against cervical cancer with higher anti-proliferation rates towards both HPV-positive and HPV-negative cervical cancer cell lines than the normal control cell line. In addition, liposomal encapsulated TQ was successfully synthesised and it was stable for 17 weeks without significant changes in the sizes and encapsulation rate for TQ.

Chapter 4

Folate Receptor (FR) Screening

4.0 Introduction

4.1 Folate Receptors (FRs)

In recent years folic acid has been used as a ligand for targeting FRs which are often over-expressed on the surface of the cancer cells. This mechanism is called “tumour-targeted drug delivery systems” (TTDDSs). The use of folic acid as the targeting ligand is due to the ease of its conjugation to nanocarriers, high affinity for FRs and its relatively low expression. in normal cells as opposed to its excessive expression on activated macrophages and cancer cells (Low *et al.,* 2008).

Although various factors should be taken into consideration when choosing an effective drug administration target, the most important factor among them is that the chosen target needs to have a significantly high expression on the cancer cells compared to normal cells (Seitz *et al.*, 2015). Furthermore, in a receiver-mediated internalisation pathway, the receptor will ideally recycle back to the cell surface and/or be increased after interaction with the TTDDS to allow maximised delivery of targeted drugs. Besides, to guarantee the delivery of the drug to the appropriate cancer cells, the receptor must be ideally enriched on its surface and not released into circulation (Zhang *et al.*, 2017). Amongst all cell surface receptors, folate receptors fulfil most criteria. They are membrane glycoprotein family receptors (35-45kDa) which can be classified as three different isoforms known as FRα, FRβ, and FRγ (Srinivasarao *et al.,* 2015). The isoforms FRα and FRβ are bound to the cell membrane via glycosylphosphatidylinositol (GPI) anchors while FRγ can only be found in

hematopoietic cells lacking the GPI portion and hence free solubility (Ledermann *et al.,* 2015).

The FRβ isoforms have about 70% of FRα homology, they both have a compatible affinity for folate (Fernández *et al.,* 2018). The FRβ is mainly upregulated in monocytes and macrophages which are myeloid activated cells and they play a crucial role in inflammatory responses and autoimmune diseases (Xia *et al.*, 2009). The FRβ isoform has also been identified in tumour-associated macrophages (TAMs) for several cancers such as kidney, liver, heart, skin, hair, and soft tissues. Such macrophages may infiltrate solid tumours and facilitate their metastasis and development through the inhibition of $CD8^{+}$T cells and the secretion of proangiogenic factors. The FRβ isoform may also be potentially considered as a possible target for cytotoxic drugs in cancer treatment (Tie *et al.*, 2020).

Despite the expression of FRβ in certain non-epithelial originating cancers such as sarcoma and acute myeloid leukaemia, the FRα can be considered as the most suitable target for targeted therapy because this isoform is the most highly expressed FR isoforms in numerous epithelial originated cancers such as ovarian, kidney, lung, endometrial, colorectal, breast, renal, head and neck, brain and cervical cancer (Byrne *et al.,* 2008; Chenug *et al.,* 2016). The FRα expression in mentioned cancers is 100-300 times greater compared to its expression in healthy cells with 1-10 million copies of FRα isoform per cell (Vlahov and Leamon, 2012). The majority of healthy cells use reduced folate receptors for their folate uptake, therefore FRα is mainly restricted to cells that are important for embryonic development, choroid plexus in the brain, and kidney in which folates are transferred through the glomeruli and successively

reabsorbed into the proximal tubule cells via FR binding. Additionally, FRα is only expressed on the apical surface of these healthy cells hence the exposure of these receptors to the folates found in the circulation and cytotoxic agents are prohibited as intercellular junction stops small molecules from passing through the epithelium (Turk *et al.,* 2004). However, after tumourigenesis the entire cell composition changes, the vasculature becomes unstable, and the disorganised intracellular junction vanishes. This event results in FRα losing its polarised cell position and overexpressed on the whole cell surface and causes the FRα isoforms to become an appropriate site for conjugated drugs in the blood circulation (Azzi *et al.,* 2013).

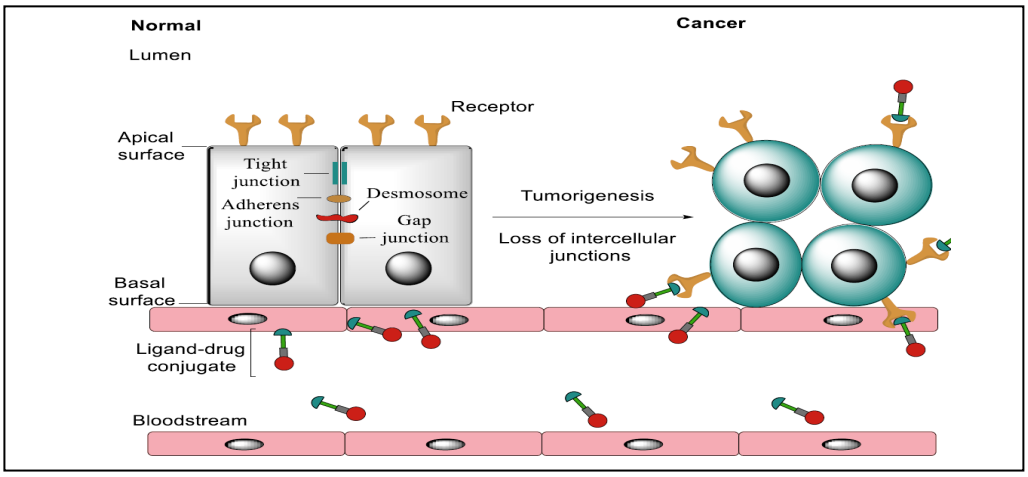

Fig 36: The process that leads to transformation of healthy epithelial cells to tumour cells. This event effects the re-positioning of the receptors such as FR which were only found on the apical surface to be localised on the tumour cells (Fernández *et al*., 2018).

The loss of receptors polarisation coupled with FRα strong binding affinity for oxidised folates (Folic Acid) results in the conjugation of drugs with Folic acid as a suitable targeting object. In addition, there are several other advantages in the use of folic acid

which include their non-immunogenicity, cost efficiency, high stability, tissue permeability, low molecular weight and easily be conjugated to different types of organic molecules, antibodies and nanoparticles (Cho *et al.,* 2015).

Folate is important for one-carbon methylation reaction as well as de novo synthesis of purines and thymidine within the cells which are essentially required for DNA synthesis and repair. This makes FA necessary for the survival of normal cells but particularly essential for tumour tissue as it helps them to sustain their rapid proliferation (Vineberg *et al.*, 2014). Ordinarily, folates are taken up via receptor-mediated endocytosis by both FRα and FRβ and the folate component of the conjugated drug will be bound to these two isoforms on the surface of the cancer cells which leads to the internalisation of folate conjugated drug inside the cell. Once the conjugated drug enters the cells inside an endosome, the pH level will be decreased in response to the proton pump which alters the conformation of the FR and hence allows the conjugates to detach from the receptor (Vlahov *et al.*, 2006). At this stage release of the free drug will be facilitated as late endosome and intracellular thiols such as glutathione (GluSH) fuse within the lysosome resulting in degradation of the conjugate by cleaving a self-immolative linker. Furthermore, the payload will diffuse into the cytosol where it causes induction of cell death. Meanwhile, the FR will be recycled back to the surface of the cell to be engaged in a further round of drug internalisation. Unoccupied surface receptors availability for further drug internalisation depends on the recycling rate of the empty receptors from the endosome which is around 8-12 hours (Vlahov and Leamon, 2012).

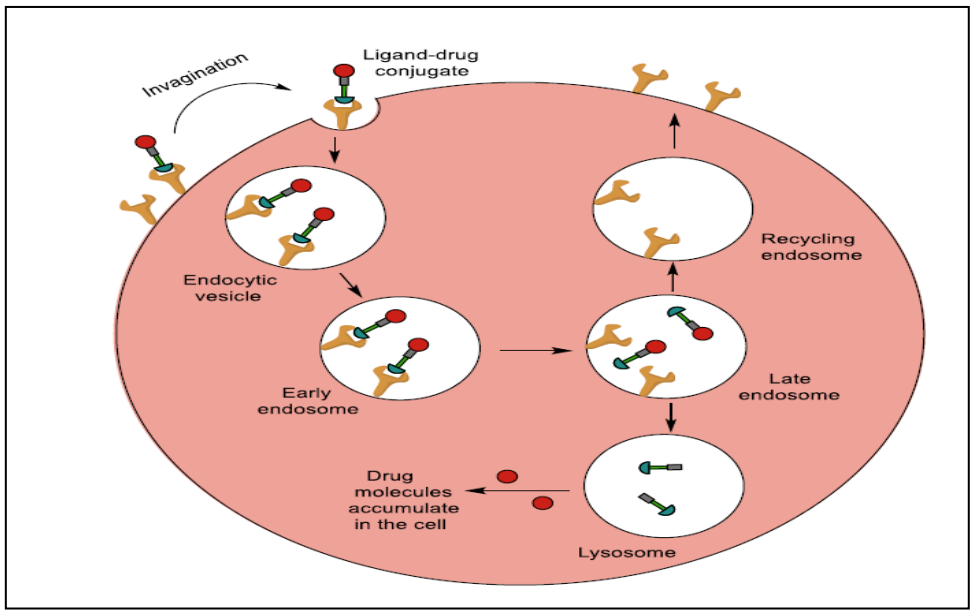

Fig 37: FA-conjugated liposomal drug enters the cell through receptor-mediated folate endocytosis. Through this event liposomal drug binds to both FRα and FRβ creating an invagination and leads to enclosing of conjugates in early endosome. A minor decrease in the pH level changes the conformation of FA receptors and results in detachment of the drug. Fusion of late endosome and lysosome contribute to conjugate degradation and hence release of the cytotoxic drug with the cell. Eventually endosome delivers the FA receptors back to the cell surface (Srinivasarao *et al.,* 2015).

Table 25: An overview of a few FA-conjugated liposomal drugs formulated and developed in recent years.

Targeted Receptors	Cytotoxic Drugs	Liposome Compositions	Nano-particle Size (nm)	Findings	References
Folate Receptors (FR)	Bleomycin	- CHOL - DOPE	100-150	A significant increase in the cellular uptake of FA-conjugate liposomes was observed in human cervical and breast cancer cell lines compared to those treated with FA-free-liposomes (*in vitro*).	(Chiani *et al.*, 2018)
	5-Fluorouracil	- PC - CHOL - DSPE	100-150	The 5-Fliorouracil FA-conjugated liposomes were used to treat human colon cancer. The result showed a significant increase in ROS level and resulted in a higher cytotoxic effect of the drug (*in vitro*).	(Handali *et al.*, 2018)
	Doxorubicin	- DSPE-PEG2000 - DPPC - CHOL	150-200	Nanorods and folic acid were used to coat liposomes to promote the combined use of photothermal and chemotherapy. The result showed an improved anticancer effect in breast cancer xenograft-bearing mice (*in vivo*).	(Nguyen *et al.*, 2019)
	Arsenic Trioxide (ATO)	- DSPE-PEG2000 - DSPE-PEG2000 - CHOL - PC	140-145	Liposomes with longer FA-PEG spacer showed greater efficiency in targeting FA receptors in HPV+ cervical cancer. The study also showed liposomal delivery of ATO indicated higher selectivity and efficiency in apoptosis induction in HPV+ cervical cancer compared to HPV- cervical cancer (*in vitro*).	(Akhtar *et al.*, 2019)
	N.A.	- DSPE-PEG2000 - DDCTMA - DSPC - CHOL	100-150	It is shown that the efficiency of DDCTMA/Chol cationic liposome transfection could be improved by FA. The study concluded that the liposomal delivery system can be considered as an appropriate candidate for gene delivery.	(Cui *et al.*, 2016)

4.2 Aim

This chapter aims to screen folate receptor expression from three investigated cell lines including HK, CaSki and C33A using two techniques, fluorescent immunocytochemical staining and western blotting.

4.3 Method

4.3.1 Cell Culture

The same cell culture procedure as detailed in Chapter 2.

Two cervical cancer cell lines CaSki (HPV16+) and C33A (HPV-) and a control cell line HK cells were employed in this research. For screening of folate receptors, CaSki and C33A cell lines were cultured in RPMI-1640 media with no folic acid and supplemented with 10% fetal bovine serum and 1% penicillin-streptomycin (100mg/mL). The HK cells were grown in Epilife® medium and supplemented with Human Keratinocyte Growth Supplement.

For the folate receptors screening study, CaSki and C33A cells were grown in folate free RPMI-1640 media for a minimum of three weeks before experiments, while HK cells were grown in Epilife® medium. Cells were grown in T75 flasks for further experiments.

4.3.2 Western Blotting To Screen FR Expression

The expression of folate receptors on the CaSki, C33A and HK cell lines was determined by western blotting. General procedures were described in Chapter 2. The primary antibody used was the rabbit-anti human FOLR1 polyclonal antibody in 1:1000 dilution. The secondary antibody used was anti-rabbit IgG. The mouse anti-β-actin antibody was used as the housekeeping gene for normalization in 1:1000 dilution and

mouse IgG was used as the secondary antibody. Finally, the protein quantification was done by using the Licor Odyssey imaging system.

4.3.3 Immunocytochemistry (ICC) To Screen FR Expression

Immunocytochemistry was carried out according to the protocol described in Chapter 2. The cells were grown in relevant culture media to 80-90% confluence then were seeded ($1x10^5$/well) on the sterile coverslips pre-placed in the wells of each 6 well plate. The primary antibody used was the rabbit-anti FOLR1 polyclonal antibody in 1:1000 dilution. 2^{nd} and 3^{rd} antibodies were from a universal ABC kit (VectaStain ABC kit, Vector Laboratories). They were then labelled using TSA-Cys5 reagents and mounted by DAPI containing mounting media on a microscope slide. Folate receptors will be labelled by TSA-Cys5 in red and nuclei will be showing blue from DAPI. All prepared slides will be further captured using a confocal microscope.

4.4 Results

4.4.1 Western Blot Analysis Of Folate Receptor (FR) Expression

The expression of folate receptors (FR) was examined for CaSki HPV (16+), C33A (HPV-), and control cell line HK respectively via western blotting (Fig 38). The signal intensity for the obtained bands was normalized with β-actin. Results obtained showed a very faint band for HK cells indicating low expression of FRs while the band detected for CaSki and C33A cell lines was very clear and distinct at around 38kDa. The overall result shows higher expression of FRs from the two cervical cancer cell lines (C33A and CaSki) which show 6 and 15 times more receptor expression respectively than the control cell line HK does.

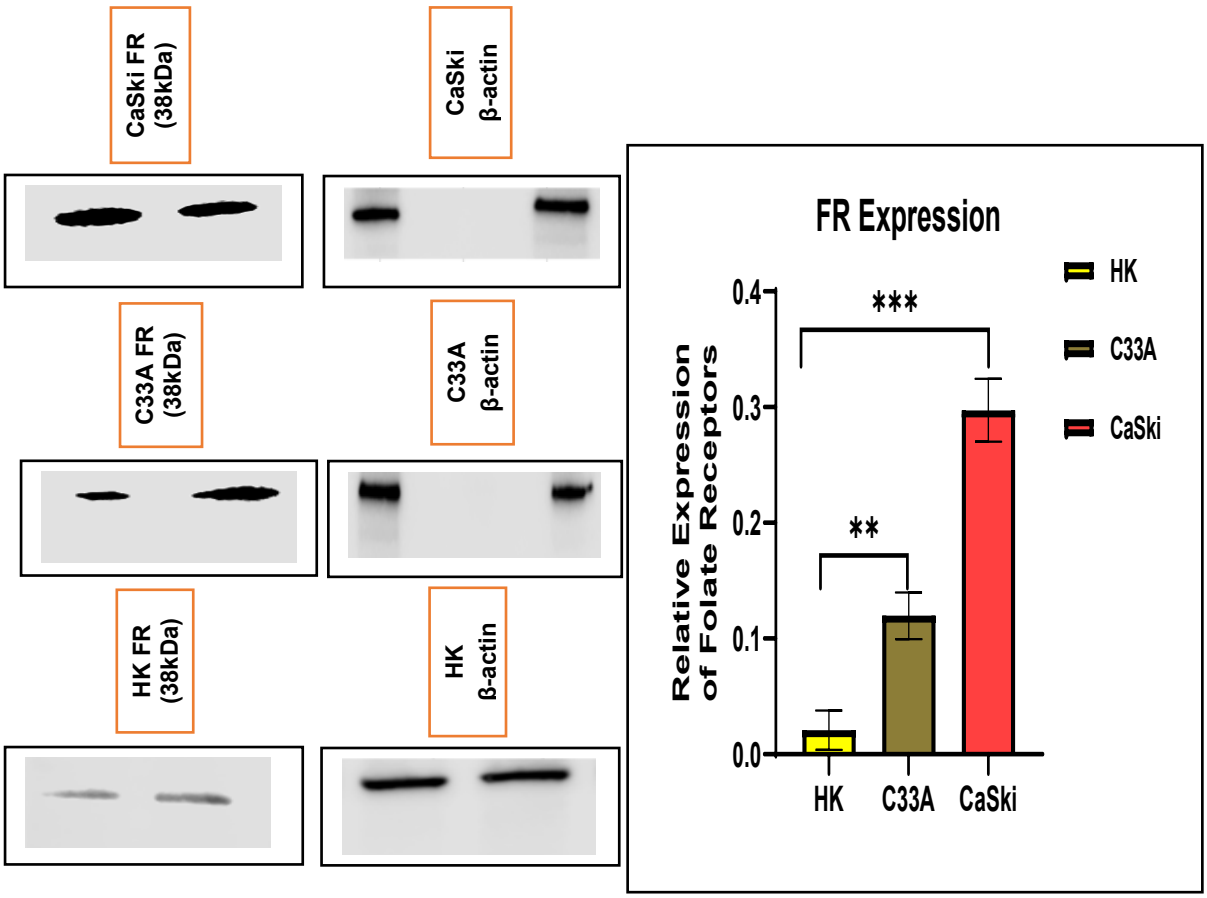

Fig 38: Comparative western blot analysis of Folate receptors (FR) in CaSki, C33A and HK cell lines. Relative protein expression were normalized with β-actin. Data shown were expressed as mean ± SD from 3 independent experiments. ** indicates $p \leq 0.01$ and *** indicates $p \leq 0.001$. The above images have been captured from three diffrenet fields of the same slide.

4.4.2 Immunocytochemical Staining To Analyse Folate Receptor (FR) Expression

Immunocytochemical staining followed by confocal microscopic analysis was employed to further confirm the result obtained from western blotting (Fig 39). A high percentage of FR positively stained cells was observed in CaSki and C33A cells which is confirmed by the western blot results. Normal HK cells did not show significant staining for FR which is also consistent with the results obtained previously from western blotting.

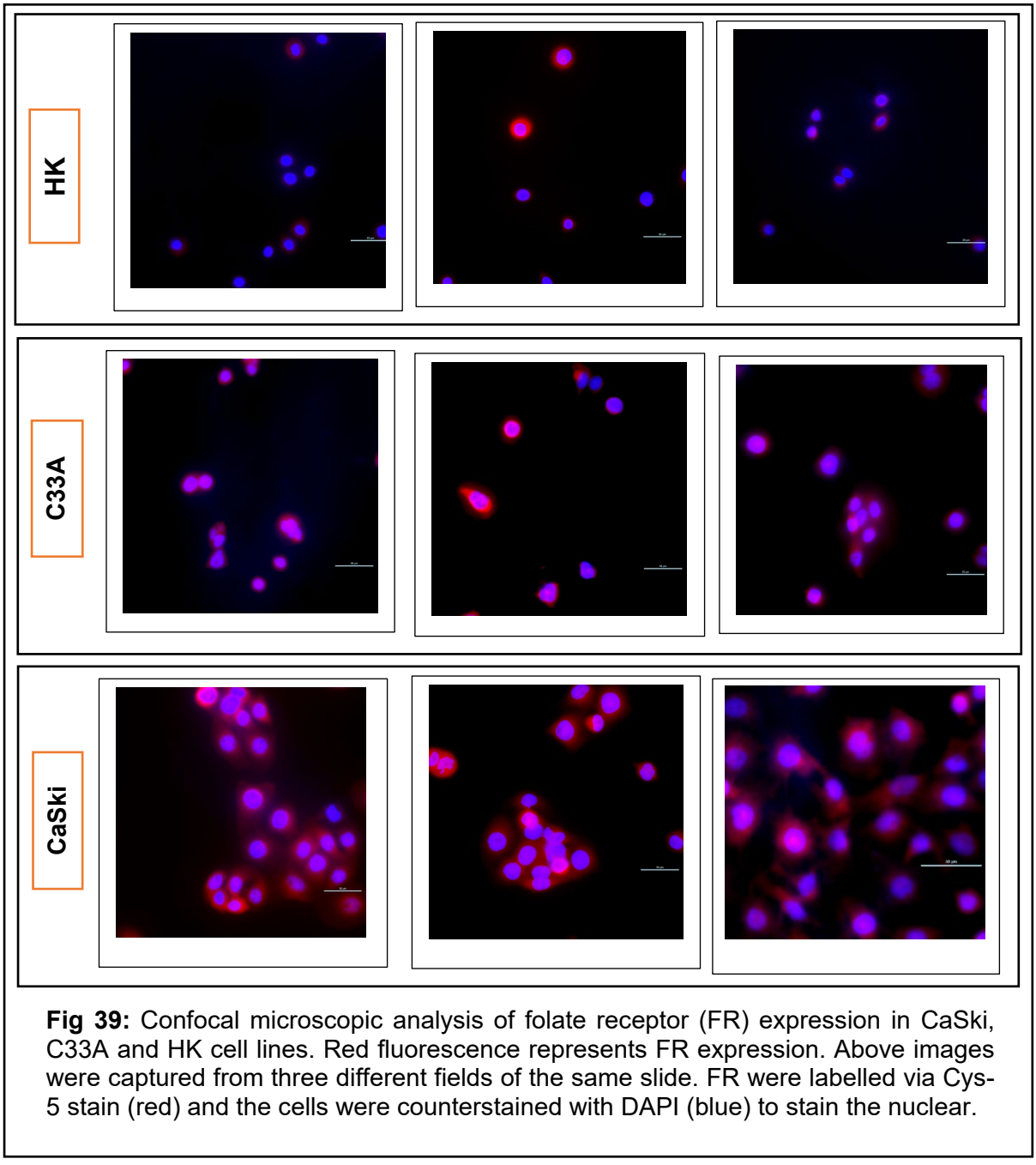

Fig 39: Confocal microscopic analysis of folate receptor (FR) expression in CaSki, C33A and HK cell lines. Red fluorescence represents FR expression. Above images were captured from three different fields of the same slide. FR were labelled via Cys-5 stain (red) and the cells were counterstained with DAPI (blue) to stain the nuclear.

4.5 Discussion

Passive targeting of liposomal delivered drugs takes advantage of two distinct differences between cancer cells and tissues. EPR is one of them which was discussed earlier (Chapter 1) and the second one is the microenvironment of the tumour. The cytosol within the cancer cells tends to be very acidic with a low pH (Deshpande *et al.,* 2013). Hence these low pH can be exploited by employing pH-sensitive drug conjugates which can be degraded after entering the cancer cells (Sinha *et al.,* 2006). This feature leads to an increased concentration of the drug being applied and released in cancer cells with minor toxicity (Heneweer *et al.,* 2012). Furthermore, active targeting can help to further improve affinities of the liposomal drugs surfaces with specific ligands binding to the tumour markers which were expressed on the surface of the cancer cells (Yoo *et al.,* 2019). Folate receptors (FRs) are one of the surface receptors overexpressed in the vast majority of epithelial cancer cells such as cervical, colorectal, renal and breast cancers (Yoo and Park, 2004). The interaction of liposomes to the cell surface and their penetration into the cells is highly dependent on the overexpression of suitable target sites or receptors on the cancer cells at the high density (Kim *et al.,* 2017). Other benefits associated with FRs as a ligand are their small size, low immunogenicity and easy conjugation to the liposome surface (Low, 2004; Doucette and Stevens, 2001). In several studies, FA-conjugated liposomes were tested for efficient and stable drug encapsulation and effective drug delivery to the tumour site. In a study conducted by (Wang *et al.,* 2019), novel FA–modified curcumin liposomes were developed with a high encapsulation efficiency of 87.6%. The result showed the formation of spherical shaped liposomes of 112.34nm in size with a PDI of 0.19 and zeta potential of -15.3mV. It appeared that the liposomal formulation had excellent stability during 3 months of storage at 4^{o}C and no sign of

aggregation or drug precipitation was observed. These liposomes showed a superior antiproliferative effect on HeLa cells (HPV 18+). Another study by (Sriraman *et al.,* 2016) tested the effect of FA-conjugated liposomes encapsulating doxorubicin on HeLa cervical cancer cells. The synthesised liposomes were 152nm in size with a PDI of 0.1, a zeta potential of -21mV to -27mV and an encapsulation efficiency of 98%. The overall result showed that FA-conjugated liposomes were able to inhibit tumour growth. Another study by (Akhtar *et al.,* 2019) examined the FA-conjugated liposomal encapsulated arsenic trioxide (ATO) on HeLa cells. The FA-conjugated liposomal ATO was stable over one month observation period with high drug encapsulation rates.

In this study, folate receptor expression was considered as the appropriate binding site on the cancer cell to be targeted. The expression of folate receptors was evaluated via western blot (Fig 38) and ICC (Fig 39).

Results from western blot analysis of the FRs expression (Fig 38) showed a clear and distinct band at around 38kDa for CaSki cells, and a less intense band was observed from C33A cells. For HK cells, the band was very faint. When the relative expression of FR was corrected for beta-actin, it was shown that significantly higher levels of FRs expression were observed from cervical cancer cell lines ($p \leq 0.05$) than in HK cells. In addition, a higher level of FR was from HPV+ CaSki cells than HPV- C33A cells.

Furthermore, fluorescent ICC was performed to evaluate FR's expression to validate the results obtained from western blot. Red fluorescence showed the expression of the FRs on the cell surface. Cells were counterstained with DAPI (blue) to reveal the nucleus. The CaSki and C33A cells showed clear cell membrane stain (red) which demonstrates FRs' expression in the cervical cancer cells (Fig 39). The staining result

for HK cells from ICC confirmed the western blot results which showed much less expression of FRs in comparison to the other two cervical cancer cell lines.

Overexpression of biomarkers such as FRs on the cancer cells facilitates the selective delivery of the therapeutic drug to the tumour site hence minimising the cytotoxic side effect and increasing the therapeutic index in the patients (Fernández *et al.,* 2018). FRs are composed of three isoforms including FRα, FRβ, and FRγ (Elnakat, 2006). Folates are usually absorbed into the cells with the help of FRα and FRβ via receptor-mediated endocytosis (Lynn *et al.,* 2015). The folate portion of the FA-conjugated liposomes can act as the tumour targeting ligand and binds firmly to FRα or/and FRβ on cancer cells leading to the subsequent internalisation of the conjugated drugs (Kularatne *et al.,* 2009). Once the FA-conjugated particles enter the endosome they will experience a decrease in the pH which is caused by the resident protons being pumped within the endosome. This will result in the detachment of the conjugates from the receptors (Lee, Wang and Low, 1996). At this stage, the late endosome fuses with the lysosome and intracellular thiols and degrade the conjugated drug via cleavage of a self-immolative linker resulting in the release of the free drug from the nanoparticles (Vlahov *et al.,* 2006). The free drug can later diffuse out of the endosome into the cytosol to induce cell death and the folate receptors will be recycled back to the cell surface for further drug internalization (Vlahov and Leamon, 2012).

The overall result showed that FRs are highly expressed on HPV positive CaSki cells and HPV negative C33A cells compared to normal HK cell lines. Therefore active targeting could further enhance the specificity of the FA-conjugated liposomes, modifying them for an effective anticancer response towards cervical cancer. As more FRs are expressed on CaSki cells which are HPV+ cells than HPV- C33A cells, further investigation on the effectiveness of FR-conjugated liposomal TQ on HPV

oncoproteins and their associated tumour suppressors, p53 and pRb will be carried out and discussed in Chapter 5 and 6.

Chapter 5

5.0 Preparation And Synthesis Of FA-Conjugated Liposomes Encapsulating TQ

5.1 Introduction

Since it was first discovered, liposomes have become more and more popular as drug carriers due to their unique characteristics such as their efficiency, biocompatibility, nonimmunogenicity, enhanced solubility of chemotherapeutic drugs and their ability in encapsulating a wide range of drugs (Deshpande *et al.,* 2013). In recent years, liposomal delivery of drugs has been significantly improved and has been used wider in cancer therapy. Liposomes have presented themselves as suitable drug carriers to deliver chemotherapeutic drugs to targeted sites following the optimisation of liposomal formulations (Voinea and Simionescu, 2002). In particular by conjugating a suitable ligand for the tumour biomarkers expressed from the surface of cancer cells using a liposomal drug delivery system could boost therapeutic drugs pharmacokinetic and pharmacodynamic profiles, facilitate regulated and sustained release of drugs and reduce systemic toxicity in comparison to free drugs (Strebhardt and Ullrich, 2008). The external membrane of liposomes can be modified by different strategies to provide them with numerous functionalities, including systemic circulation, increased drug build-up in the targeted tissue, increase cell internalisation and organ-specific drug delivery (Torchilin, 2011).

5.1.2 Passive Targeting:

Due to the leaky features of the tumour-associated blood vessels, biomacromolecules and nanosized drug delivery vehicle systems translocate readily through the capillary endothelium and move into interstitial space. Depending on the type of cancer, the size of the gaps between the endothelial cells covering the tumour capillaries varies

from 100-780nm, compared to that of typical normal endothelium of 5-10nm (Haley and Frenkel, 2008). Solid tumours do not have adequate lymphatic drainage. Therefore the extravasated molecules are limited in the cancerous region, resulting in the accumulation of macromolecules and nanoparticles in the microenvironment of the tumour which has been referred to as enhanced permeability and retention (EPR) (Lammers *et al.*, 2012). Therefore, the use of the EPR effect is a very beneficial element for targeting nanoparticles such as liposomes at the tumour site. This factor helps, low molecular weight drugs not be retained at the tumour site for a longer time as they re-enter the circulation primarily through diffusion (Frank *et al.*, 2010).

Prolonged systemic circulation enables longer interaction between liposomes with the target site because the increased number of blood vessels in the tumour area increases the EPR effect. The retention of liposomal drugs in the blood circulation is accomplished by covering the liposomes with polymers such as PEG, which essentially prevents their uptake by the reticuloendothelial system (RES) (Santos, 2015). To create a steric stabilisation effect PEG is normally inserted on the liposome surface. PEG molecules form a hydrophilic protective layer on the liposome surface which inhibits their aggregation and contact with blood components (Rovira-Bru *et al.,* 2002). PEG molecules also prevent opsonisation through various mechanisms such as surface charge shielding, increasing the repulsive interface between polymer-coated liposomes and blood components, the surface hydrophilicity, and the creation of a polymeric coating over the liposome surface to make them impermeable even at relatively low concentrations to large molecules or opsonins. This decreases the absorption by macrophages of the mononuclear phagocytic system of PEG-like polymers on the surface of the liposomes and increases its flow through the blood (Wen *et al.*, 2007).

The size of the liposomes is another key element that affects passive targeting by the EPR effect. The build-up of liposomes in the tumour depends heavily on the size of the endothelial gaps for certain cancer in the capillary vasculature (Danhier *et al.,* 2010). The liposomes should normally be smaller than 400nm in size to use the EPR effect. For extravasation into the tumour, the threshold vesicle size is approximately 400nm. However, more successful extravasation was reported from those particles larger than 200nm (Sawant and Torchilin, 2012).

Other factors that affect passive targeting are the composition and charge on the liposome surface. Anionic or neutral liposomes avoid renal clearance (Danhier *et al .,* 2010). While cationic liposomes appear to locate in newly developed tumours vessels, their positive surface load contributes to non-specific interactions with the anionic species in the blood, resulting in the rapid RES clearance from circulation, reducing the impact of EPR. Aggregation of liposomes however increases in the liposomal membrane with high levels of cationic lipids. Even optimal surface modification with cationic lipids may considerably increase the penetration of tumours (Zhao *et al.,* 2011).

5.1.3 Active Targeting

Specifically targeted liposomes are typically designed to reduce the off-target effect of the anticancer drugs (Byrne *et al.,* 2008). Targeted liposomes are formed as a result of conjugating their surface with targeting molecules such as small molecule ligands, peptides, and monoclonal antibodies. For instance, various receptors such as folate receptors (FRs) and transferrin receptors (TfRs) are highly expressed on many cancer cells, therefore, they have been used as a target to increase the specificity of liposome tumour cells (Egusquiaguirre *et al.*, 2012). Via association with different surface cell

receptors, the liposomes that accumulate in the tumour microenvironment can then be endocytosed into cells. To target cancer cells effectively using the liposomal drug, the targeted moiety must be related in adequate amounts to have an optimal affinity for the cell surface receptors (Wu and Chang, 2010).

The use of ligands on liposomes to target cancer cells is important because they can intensify therapeutic response manifold through their participation in the cellular uptake mechanism. The relation of liposomes to vascular cells via non-internalising epitopes which are uniquely expressed on tumour endothelial cells increase the concentration of the extracellular drug, thus increasing the amount of drugs provided to target cells (Byrne *et al.,* 2008).

The use of receptor-specific ligands and antibodies are the common techniques for targeting cell surface receptors overexpressed on cancer cells (Allen, 2002). Active targeting by modulation of cell surface receptors has been widely explored in cancers as the upregulation of specific tumour markers is expressed in many cancer types. Cell surface receptors such as FRs and TfRs are highly expressed on different types of tumour cells in response to their increased metabolic demand (Wu and Chang, 2010). Several studies evaluated the folate targeting particles in preclinical settings and demonstrated promising results confirming that FRs can be considered as both therapeutic and diagnostic agents (Zhao, 2004; Sudimack and Lee, 2000; Akhtar *et al.,* 2019).

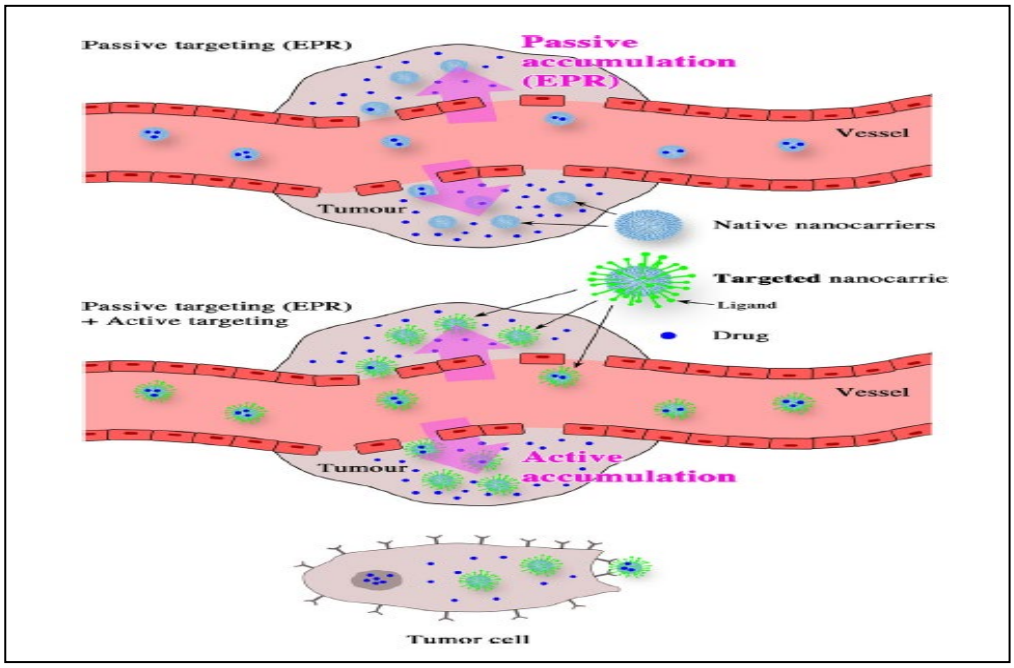

Fig 40: The differences between the passive and active targeting processes of nanoparticles in the tumour area (Attia *et al.*, 2019).

5.2 Aim

The aim of this chapter was to prepare FA-conjugated liposomal TQ (FA-lip-TQ) for actively targeting cervical cancer cells which express high levels of FRs then characterise the synthesised drug and its stability.

5.3 Objectives

- To prepare the FA-conjugated Liposomal TQ.
- To evaluate drug encapsulation efficiency and the stability of FA-conjugated liposomal TQ.
- To evaluate the size and the charge of FA-conjugated liposomal TQ.

5.4 Method

5.4.1 Liposome Preparation

The folate conjugated TQ encapsulating liposomes were prepared and synthesised with a similar procedure as unconjugated liposomal TQ as detailed in Chapter 2. The only difference is that DSPE-PEG2000-FA 10mg/mL was included.

For FA-conjugated liposomes the initial stock solutions were prepared as described below:

- PC 100mg/mL
- Cholesterol 20mg/mL
- mPEG-DSPE10mg/mL
- DSPE-PEG_{2000}-FA 10mg/mL
- TQ 20mg/mL

1. Control Liposome: 25mg of PC, 3.3mg of mPEG-DSPE, 0.2mg of DSPE-PEG_{2000}-FA, 11mg of Cholesterol in 1mL of Dichloromethane and Methanol (2:1) at room temperature.
2. Liposome encapsulated TQ: 25mg of PC, 3.3mg of mPEG-DSPE, 0.2mg of DSPE-PEG_{2000}-FA, 11mg of Cholesterol and 2mg of TQ in 1mL of Dichloromethane and Methanol (2:1) at room temperature.

5.4.2 Liposome Characterization

Liposomes stability over 17 weeks was assessed by analysing their encapsulation efficiency, size, and charge by using a plate reader and a Zetasizer as described in Chapter 2. liposomes were stored at 4^{o}C in buffers of pH 7.4.

5.4.3 Cell Culture

Cell culture protocol was carried out as described in detail in Chapter 2. Two cervical cancer cell lines CaSki (HPV16+) and C33A (HPV-) and a control cell line HK cells were employed in this research. For screening of folate receptors, CaSki and C33A cell lines were cultured in RPMI-1640 media with no folic acid and supplemented with 10% fetal bovine serum and 1% penicillin-streptomycin (100mg/mL). The HK cells were grown in Epilife® medium and supplemented with Human Keratinocyte Growth Supplement.

Cellular uptake of FA-conjugated TQ liposomes was investigated following liposomal TQ exposure by using a plate reader and ICC using a confocal microscope. The cellular toxicity of FA-conjugated liposomes were determined using MTT assay. Finally, the anti-HPV effect of FA-conjugated liposomes was investigated using Flow cytometry, western blotting, and ICC.

5.4.4 Cellular Uptake Analysis By Confocal Microscope

Cells were counted and seeded at $1x10^5$ per well in 6 well plates on the pre-inserted coverslips and incubated at 37^{o}C overnight for cell attachment. After cell settlement, cells were treated with DILC-TQ-unconjugated liposomes, FA-DILC-conjugated liposomes, and FA-DILC-TQ-conjugated liposomes respectively for 24 and 48 hours and kept in the humidified 5% CO_2 incubator at 37^{o}C. Following the treatment, the cells were washed 3 times with PBS and fixed with 4% paraformaldehyde at room temperature for 8 minutes. The coverslips were washed again 3 times by PBS then mounted on a microscope slide using DAPI containing mounting media (staining nuclei in blue). The fluorescence of DILC (staining red, excitation/emission 549nm/565nm) was measured under the confocal fluorescent microscope.

5.4.5 Cellular Uptake Analysis Using A Plate Reader

Cells were counted and seeded at $1x10^5$ per well in 96 well plates in triplicates and incubated at 37°C overnight for cell attachment. Cells were then treated with (DILC-unconjugated liposomes, DILC-FA-conjugated liposomes) for 24 and 48 hours at 37°C in the incubator as mentioned previously. Following the treatment, the cells were washed 3 times with PBS and the fluorescence of the DILC stain was measured (excitation/emission 549nm/565nm) via the plate reader.

5.4.6 MTT Assay To Evaluate Cellular Cytotoxicity Of Unconjugated and FA-Conjugated Liposomes

Cytotoxicity of the FA-Lip-TQ liposomes was determined by MTT assay as detailed in Chapter 2. Briefly, cells were counted and seeded $5x10^4$ per well for both CaSki and C33A cells on 96 well plates. The cells were treated with Lip-TQ and FA-Lip-TQ with TQ concentrations ranging from 10μM to 100μM. The cells were prepared as triplicates then were exposed to the drugs for 24 and 48 hours respectively. The plates were incubated at 37°C in the humidified incubator. After the incubation, the MTT assay was performed as described in Chapter 2 and the absorbance was measured at 570nm via the plate reader.

5.5 Results

Physiochemical characteristics (size and charge) of the FA-conjugated liposomal drug was analysed over 17 weeks of storage (4˚C) by using zetasizer. The FA-control liposome's (FA-Control-Lip) size ranges from 141.5nm±1.35 to 143.5nm±1.15 and FA-liposomal-TQ (FA-Lip-TQ) ranged from 150.10nm±2.12 to 155.13nm±1.58 in size over 17 weeks (Fig 41, A), which showed that FA-Lip-TQ were significantly (p=0.0001) larger in size compared to FA-Control-Lip.

The membrane surface charges of nanoparticles were also monitored by using zetasizer. The surface charge of liposomes is an important factor to be considered in the liposomal drug delivery system as it plays a crucial role in the interaction of liposomal membranes with peripheral membrane proteins and the immune system. Results showed that all FA-conjugated nanoparticles prepared in this study were negatively charged over the 17 weeks storage period and had a polydispersity index value of less than 0.2 confirming their homogeneity (Fig 41, B). The liposomes were efficiently loaded with TQ and their loading efficiency and stability was analysed over 17 weeks of storage at 4˚C (Fig 41, C).

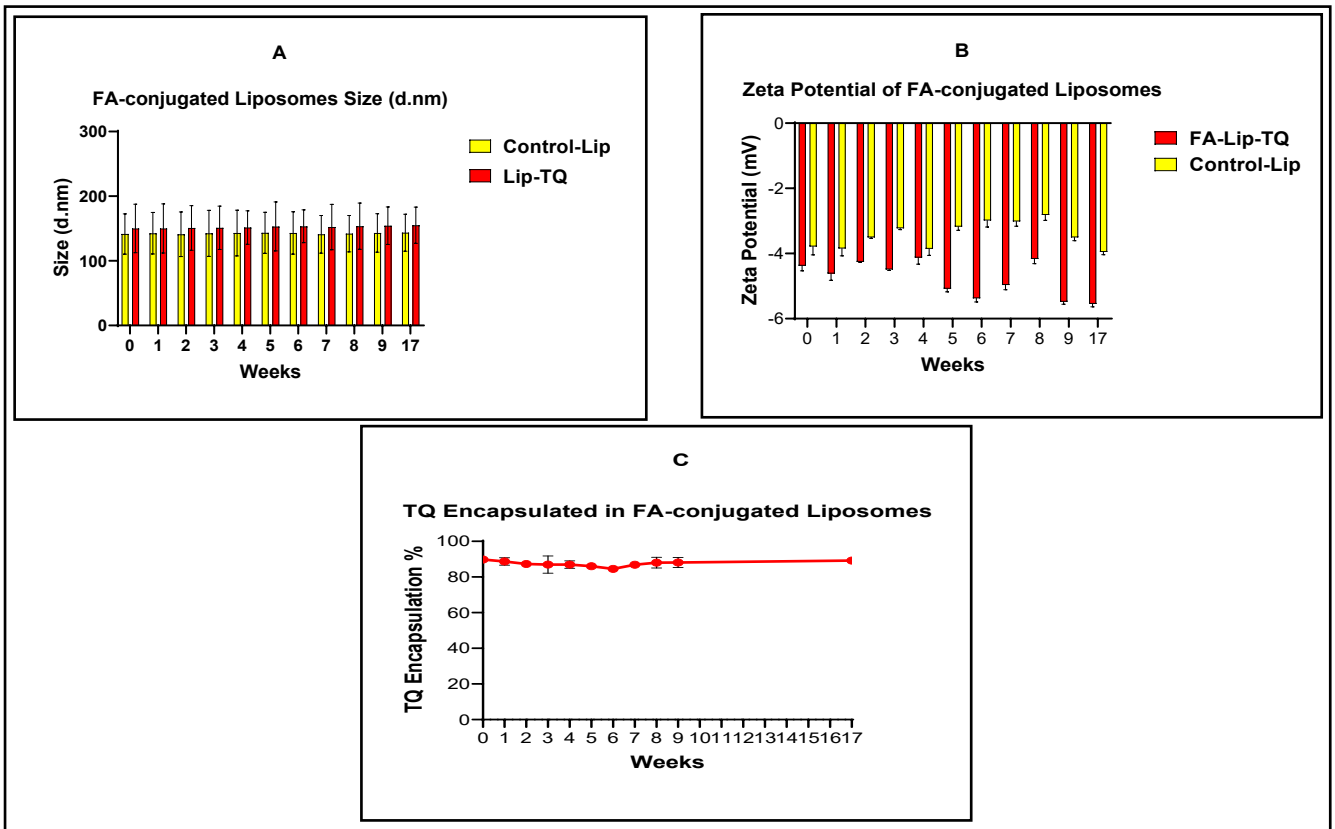

Number of weeks	Diameter (nm)	Zeta potential (mV)	PDI	Loading Efficiency %
1	150.10±2.12	-4.38±1.35	0.095	89.80±1.35
2	150.14±1.25	-4.62±2.54	0.118	88.69±1.28
3	150.86±1.55	-4.26±2.02	0.112	87.25±2.21
4	151.10±2.60	-4.49±1.31	0.107	86.93±2.23
5	151.60±2.81	-4.13±1.55	0.132	86.93±2.56
6	153.21±1.07	-5.08±1.25	0.107	86.20±1.12
7	153.46±2.25	-5.38±3.33	0.106	84.57±1.48
8	152.25±3.35	-4.97±1.30	0.146	86.85±2.98
9	153.62±1.41	-4.17±2.85	0.121	88.50±2.56
10	154.30±2.28	-5.48±2.92	0.188	88.08±2.47
17	155.13±1.58	-5.55±1.29	0.158	89.21±1.24

Fig 41: Diameter (A), Zeta potential (B) of FA-conjugated liposomes were measured via zetasizer with a polydispersity index of less than 0.2. The encapsulation efficiency (C) of tested liposomes were also analysed via UV-vis spectrophotometry using TQ's λ_{max} at 220-400nm over 17 weeks of storage (4°C). No significant difference was observed between encapsulation efficiency over the storage time. Table above summarises the physiochemical properties of FA-Lip-TQ over 17 weeks. Data are mean ± SD of three replicate measurements of three independent experiments.

5.5.2 Confocal Microscopy To Analyse Cellular Uptake Of Liposomal Drugs

Confocal microscopy was employed to analyse the cellular uptake of DilC18(3) labelled conjugated and unconjugated liposomes. From the previous finding, CaSki and C33A cells showed very high expression of FRs compared to the HK negative control cells. Due to the high FR expression on CaSki and C33A cells, they showed to have higher cellular uptake of DilC18(3)-DS labelled conjugated and unconjugated liposomes (Fig 42) as the high intensity of red fluorescence observed around the cell surface from the Dil18(3)-DS stain. The extensive internalisation and accumulation of conjugated and unconjugated liposomes in the cytosol of CaSki and C33A cells were indicated by the red fluorescence around the nuclei. However, the red fluorescence was not seen in HK cells which could be due to a lack of FR expression on their surface.

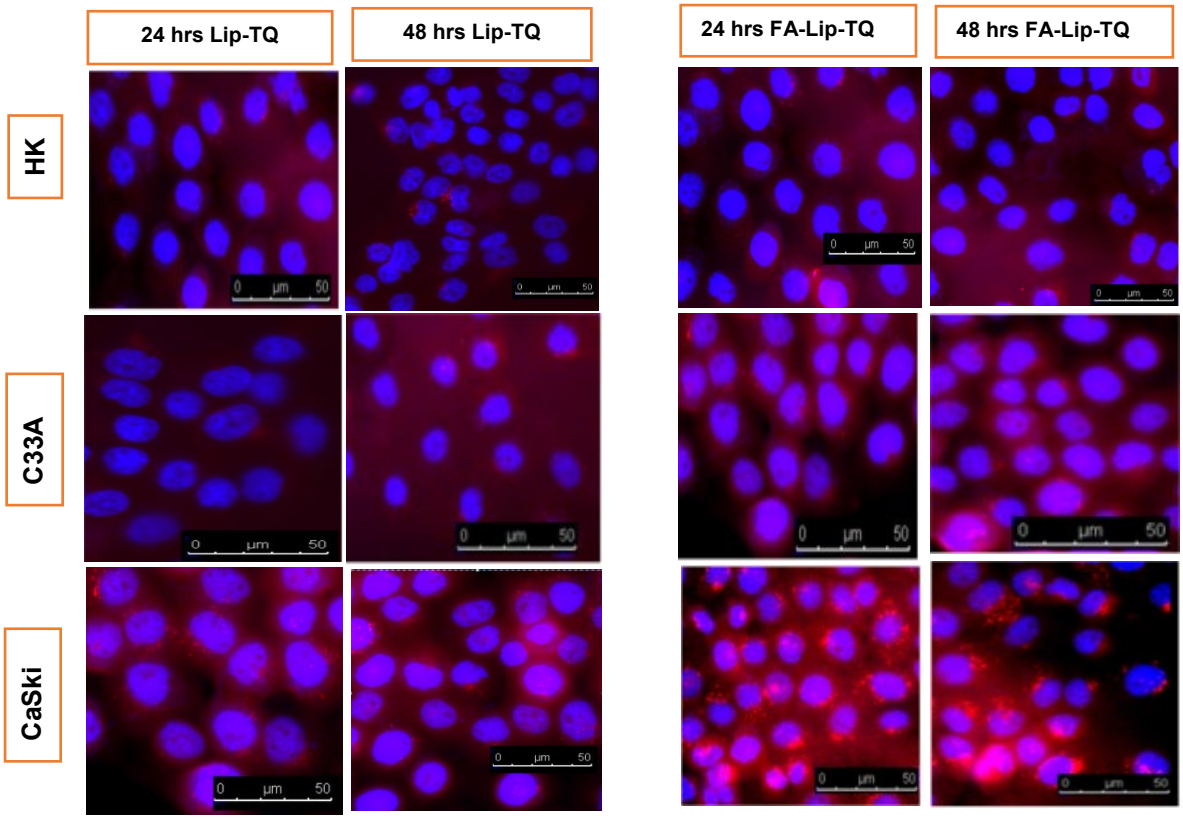

Fig 42: Confocal microscopic images showing cellular uptake of DilC18(3) labelled unconjugated and conjugated liposomes by CaSki, C33A and HK cells at 24 and 48 hours. Cells were counterstained with DAPI to stain the nuclear in blue. FA-conjugated and unconjugated liposomes labelled by red DilC 18(3) are shown in most CaSki cells and some C33A cells which are consistent with the amount of FR expression on their surfaces.

5.5.3 Plate Reader Analysis Of Liposomal Cellular Uptake

The cellular uptake of conjugated and unconjugated liposomes was also analysed via the microplate reader after 24 and 48 hours of treatment. CaSki and C33A cells were seeded on 96 well plates and treated with DILC18(3) labelled conjugated and unconjugated liposomes for 24 and 48 hours. The data obtained (Fig 43) showed the difference between liposomal cellular uptake by analysing the ratio of DILC18(3) fluorescent cells. CaSki and C33A cells displayed a significant difference after 24 and 48 hours compared to HK cells. This is expected as the higher expression of folate receptors on their surface might have resulted in more uptake of the liposomal drug. on their surface.

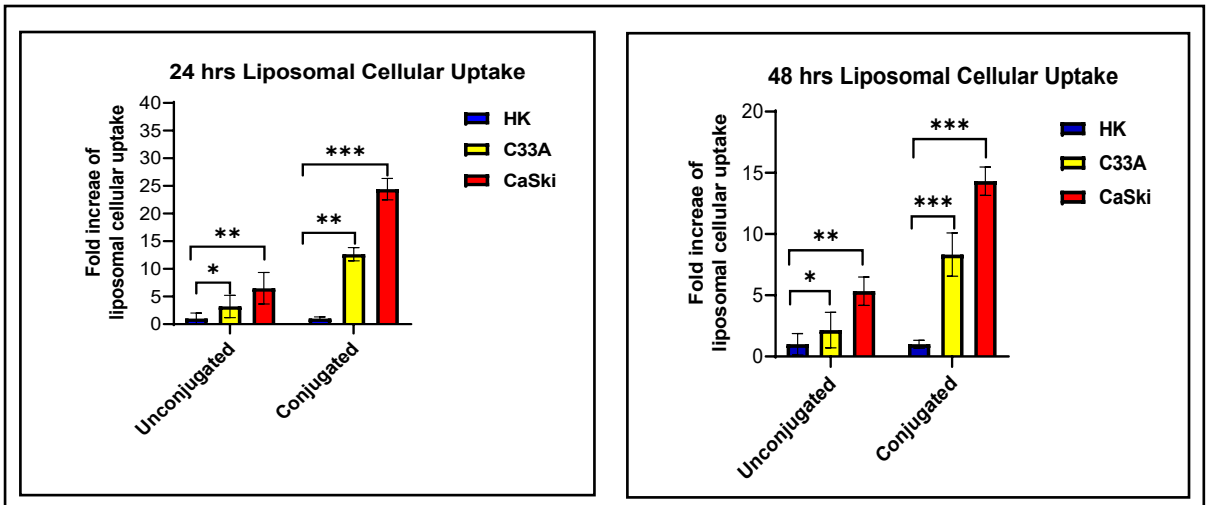

Fig 43: Comparison of liposomal uptake by CaSki, C33A and HK cell lines after 24 and 48 hours treatment. CaSki and C33A cells displayed significant enhancement in liposomal uptake after folate conjugation, corresponding with the high expression of folate receptors on their surface. On the contrary, HK cells did not show much increase. Data are shown as means ± SD of duplicate measurement of three independent experiments. . "*" indicates $p \leq 0.05$, ** $p \leq 0.01$ and *** $p \leq 0.001$.

5.5.4 MTT To Analyse The Toxicity Of Lip-TQ And FA-Lip-TQ

To evaluate and compare the toxicity of unconjugated and FA-conjugated liposomes the MTT assay was performed (Fig 44). The dose-response curve obtained from the MTT assay after 24 and 48 hours of drug treatments, revealed that FA-Lip-TQ showed more toxicity towards both CaSki and C33A cells compared to their Lip-TQ counterpart by showing lower IC_{50} values. However, in CaSki cells FA-Lip-TQ showed to be more effective after 48 hours of drug treatment in inducing cell death compared to C33A.

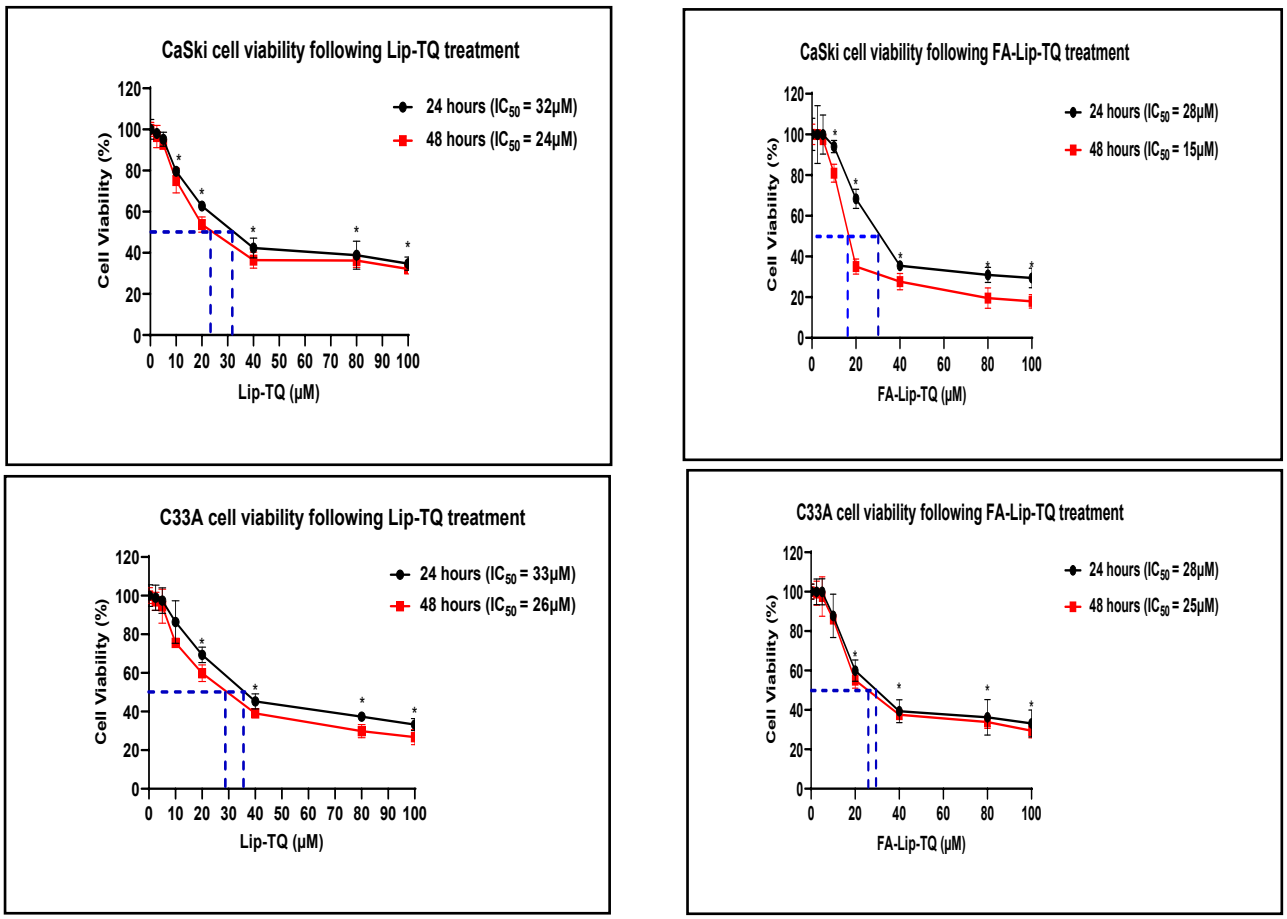

Fig 44: MTT assay to compare toxicity of unconjugated and FA-conjugated liposomes on CaSki and C33A cells after 24 and 48 hours of drug treatments. The data shown are the Means ± SD from three independent experiments. "*" indicates $p \leq 0.05$.

5.6 Discussion

As mentioned earlier FRs are tumour associated antigens that can bind to FA conjugated nanoparticles with high affinity and the encapsulated molecules can get inside the cell through the endocytosis mechanism (Reddy and Low, 2000). Therefore, in the current study FA-conjugated liposomes were synthesised by using FA-conjugated lipids (DSPE-PEG_{2000}-FA). As seen in Fig 41, the physicochemical properties of the synthesized liposomes (size, charge and encapsulation efficiency) were monitored over 17 weeks of storage at 4^{o}C. The mean diameter of FA-Control-Lip prepared ranged from 141.5nm±1.35 at week 0 and 143.50nm±1.15 at week 17 and the mean diameter for FA-Lip-TQ ranged from 150.1nm±2.12 at week 0 and 155.13nm±1.58 at week 17. The polydispersity index value was less than 0.2 stating the homogeneity of the nanoparticles. Zeta potential values obtained for FA-Lip-Control were in the range between -3.79mV and -3.95mV and for FA-Lip-TQ these values were -4.38mV±1.35 and -5.55mV±1.29 over 17 weeks of storage which showed a significant difference between the zeta potential of the control and encapsulating liposomes (p=0.0001). Additionally, the encapsulation efficiency of the TQ was also measured and the result showed that 89.8% of TQ was encapsulated within the liposomes at week 0 and 89.2% at week 17.

The size of the liposomes synthesised in this study satisfies the size condition (<500nm) required to pass through tumour vessels and accumulate in the target site (Hashizume *et al.,* 2000). However previously researchers observed that small liposomes (<100nm) interact less with the plasma protein, therefore, their detection by the RES can be avoided and their half-life can be longer in the blood circulation. It was also found that larger liposomes can be eliminated more rapidly from blood however they can have better drug encapsulation efficiency due to their bigger size compared

to the smaller liposomes (Hoshyar *et al.,* 2016). Usually, liposomes greater than 150nm can be eliminated through phagocytosis via specialised cells of the immune system such as macrophages, monocytes and Kupffer cells (Fanciullino *et al.,* 2005). The zeta potential of the FA-conjugated liposomes in this study was ranging from -4.38mV to -5.55mV which means that all the nanoparticles were neutral as nanoparticles with zeta potential ranging from -10 to +10mV are considered to be neutral (Qi *et al.,* 2011). The lack of surface charge on the liposome is associated with the high possibility of aggregation. On the other hand, charged liposomes (negative or positive) increase the electrostatic repulsion among the nanoparticles and prevent their aggregation, therefore, could introduce better cell interaction (Yingchoncharoen *et al.,* 2016). However, in this study, the low zeta potential did not show any sign of aggregation on the liposomes as the size of the particles over 17 weeks of storage remained unchanged. Literature evidence shows that negatively charged liposomes can be less stable when injected into the blood circulation compared to positive and neutral liposomes due to their electrostatic properties. Negatively charged liposomes rapidly bind to the biological proteins in the plasma and lead to two adverse consequences including rapid uptake by RES and high cytotoxic effects such as pseudoallergy, dyspnea and pulmonary hypertension (Inglut *et al.,* 2020).

Furthermore, in the current study, the cellular uptake of unconjugated and FA-conjugated liposomes (both no drug and drug-loaded ones) by CaSki, C33A and HK cells were evaluated after 24 and 48 hours of exposure to fluorescently labelled liposomes with DILC 18(3) using the confocal microscope (Fig 42). From our previous finding in this study about the expression of FRs, much higher FRs were expressed on the surface of CaSki and C33A cells in comparison to HK cells. Following 24 and 48 hours of drug exposure, FA-conjugated liposomal TQ treated CaSki cells showed

a visible more intense staining which was located around the cell surface and cytoplasm followed by C33A with less intense red fluorescence observed around the cell surface from the DILC 18(3) label of the liposomes. The intensity of the fluorescence observed from both stained CasKi and C33A cells after 48 hours of treatment by FA-conjugated liposomal TQ were higher than those observed in non-FA-conjugated liposomal drug-treated cells. A widespread internalisation and accumulation of FA-conjugated liposomes were seen in CaSki cells and also C33A cells with less intensity and coverage (Fig 42). To validate these findings the cellular uptake of the DILC 18(3) labelled unconjugated and FA-conjugated liposomes were also analysed using a microplate reader by evaluating the fluorescence of cells (Fig 43). As expected FR highly expressed CaSki cells displayed the maximum fluorescent signals among all three cell lines from both FA-conjugated and unconjugated ones. The signal difference observed in CaSki cells after 24 hours was 5.3±1.65 fold for unconjugated and 13.3±1.21 fold for FA-conjugated and after 48 hours these have increased to 8.8±0.86 fold and 24.4±1.47 fold respectively compared to the control cell line HK. For C33A cells the fold difference of fluorescent signals observed after 24 hours of drug treatment by unconjugated liposomes was 2.16±1.11 fold and 5.33±0.84 from FA-conjugated ones. After 48 hours these fold values have raised to 3.60±1.21 fold and 12.63±1.32 fold respectively.

Next, the anti-proliferation effect of Lip-TQ (unconjugated) and FA-Lip-TQ (conjugated) liposomes on CaSki and C33A were evaluated by performing MTT assay (Fig 44). The result showed that the cell population decreased for both tested cell lines. In CaSki cells, IC_{50} values obtained after 24 and 48 hours of Lip-TQ treatment (unconjugated) were 32μM and 24μM however, when the same cells were treated with FA-Lip-TQ the IC_{50} values decreased to 24μM and 15μM. This could be caused by an

increased drug uptake into CaSki cells due to the high expression of folate receptors on their surface compared with C33A cells. This result was supported by another research (Zhao *et al.,* 2013) and indicated that increased expression of folate receptors could lead to more drug uptake through FR-mediated endocytosis within the early endosomes.

The results obtained in this chapter showed that FA conjugated liposomes are suitable drug carrier candidates for delivering TQ with high encapsulation efficiency and stability. In addition, the conjugation of liposomes with folic acid enhances the cellular uptake of targeted liposomes by the HPV positive cervical cancer CaSki cells.

Chapter 6

6.0 Evaluating The Expression Of Oncoproteins (E6 and E7) And Tumour suppressor Proteins (p53 and pRb) In CaSki And C33A Cells Following Lip-TQ And FA-Lip-TQ Treatments

6.1 Introduction

HPVs-induced cervical cancers are the main health issue among women worldwide and account for a high mortality rate due to the late diagnosis and poor prognosis. Cervical cancer development initially relies on two major oncogenes E6 and E7 which are overexpressed continuously resulting in tumorigenesis.

6.1.1 Evasion Of Growth Suppressors

Both E6 and E7 enable unregulated proliferation through the degradation of suppressor proteins. E6 targets p53 while E7 targets pRb. E6 mediates inhibition of p53 and causes numerous cellular modifications to transform a healthy cell into an oncogenic cell. One of the important pathways of this process is the activation of uncontrolled cell proliferation by avoiding the cellular checkpoint. The P53 tumour suppressor protein (53KDa) is also called the guardian of the genome as it determines the fate of a cell under stressful conditions by acting as a transcription factor, transcribing genes needed for either cell cycle arrest or apoptosis. On the other hand, an E3 ubiquitin ligase known as MDM2 helps to hold E6 at the basal level in healthy cells. Therefore, p53 degradation by E6 is required to ensure continuous cellular proliferation (Pflaum *et al.,* 2014). Also, E6 was found to degrade p53 via ubiquitination with the aid of E6AP. The HPV-E6 forms a heterotrimeric complex (E6/E6AP/p53) through binding to LXXLL sequence in the E6AP which ultimately leads to the degradation of p53 resulting in the cell being forced to uncontrolled cellular division and avoiding preventive checkpoint in the cell cycle (Martinez-Zapien *et al.,* 2016).

Likewise, mediation of retinoblastoma protein (pRb) by E7 oncoprotein is also an essential step towards achieving unregulated cell proliferation. The pRb-E2F interaction facilitates the movement of the cells to an essential checkpoint G1-S phase transition. In cases where cells are not ready to enter the S-phase, pRb stays bound to E2F transcription factor preventing them from transcribing genes required for S-phase (Nguyen *et al.,* 2002). In HPV infection, ubiquitination of pRb via E7 results in the release of E2F which transcribes cyclin E, A and p16INK4A, an inhibitor of CDK4/6 leading to the cell entry into the premature S-phase. The tumour suppressor protein P16INK4A, is a CDK inhibitor that is an essential target for HPV-E7 to control the cell cycle. The E7 protein activates P16INK4A expression not only through pRb decay but also through epigenetic depression through KDM6B (McLaughlin-Drubin *et al.,* 2013). The E7 protein can also interact with DREAM complex functioning downstream of the p53 pathway. This complex suppresses the activity of cell cycle associate genes when not required. For the cell cycle progression in cervical cancer, the E7 motif (LxCxE) binds to p130 of the DREAM complex to induce its proteasomal degradation. The overexpression of E6 and E7 in HPV infected cells provides an appropriate environment for sustained proliferative signalling (Rashid *et al.,* 2011). Another target for E6 and E7 could be the c-myc which is known as a marker protein for various cancers such as cervical cancer. Once c-myc is disrupted via E6/E7, as consequence cell proliferation, cellular apoptosis and transformation will also be disrupted. The HPV genome integrates within MYC locus therefore, c-myc expression in HPV infected cervical cancer cells is altered. The change in expression of c-myc results in disruption of Cdks, cyclins and E2F because Myc is proficient in inducing cyclin/Cdk complexes with the assistance of Cdk activating kinase and Cdc25 phosphatase. Also, Cdk inhibitory activity of p21 and p27 inhibitors are further demonstrated by Myc. In

addition, the interaction of both E6 and E7 to Myc causes hTERT promoter to be activated and contributes to the immortality of cancer cells (Liu *et al.,* 2007). The HPV-infected cells have to bypass the mitotic spindle checkpoint, which is also performed by E6 and E7 together, to ensure continuous cell proliferation. E6 is p53 dependent while E7 relies on pRb to evade the spindle checkpoint in p53 dependent manner. The Cyclin-CDK complexes are the main players of the cell cycle, which is transformed drastically into HPV-infected cervical cancer cells, due to the alteration of many cell cycle regulators. In the cells expressing E6 protein, the cell cycle regulators D1-CDK4 and D1-CDK2 are decreased or get removed in those expressing both E6 and E7 resulting in a reduced level of p21 and activated level of p16 (Veldman *et al.,* 2003).

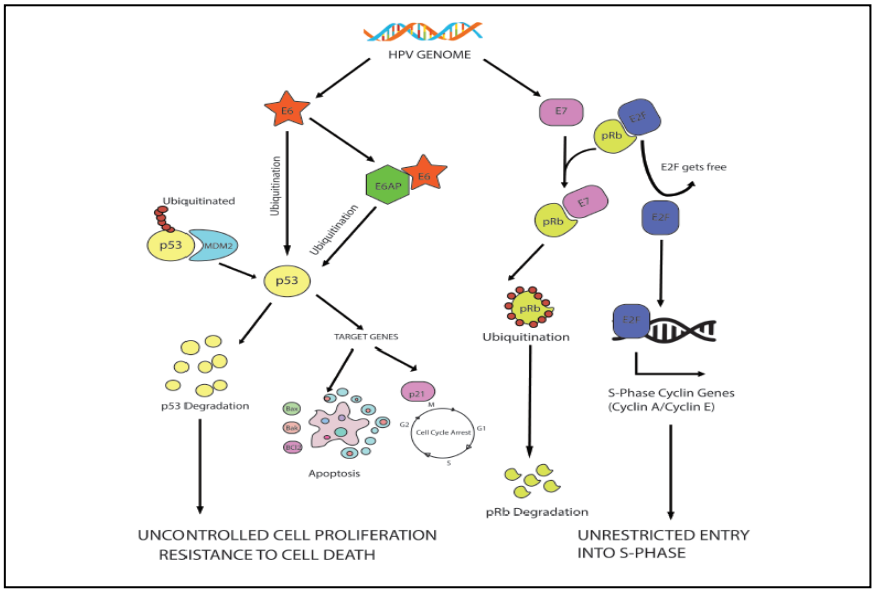

Fig 45: The role of E6 and E7 oncoproteins in the development of HPV-associated cervical carcinogenesis. HPV-E6 and E7 both interfere with normal function of the tumour suppressors (p53 and pRb). E6 protein binds to p53 and E7 protein binds to pRb (Pal and Kundu, 2020).

6.1.2 Apoptosis

To assess malignancy, HPV-infected cells rely on E6 together with E7 to escape the apoptotic defence system. The HPV-E6 and HPV-E7 disrupt both extrinsic and

intrinsic pathways of apoptosis to help HPV-infected cells to escape the innate immune protection. E6 is capable of blocking apoptosis through both p53-dependent and independent manners. E6 can also block the BAK-mediated intrinsic mode of apoptosis via p53-E6AP interaction (Gravante *et al.,* 2006). Another function of E6 is independent of p53, where it impedes the TNF-mediated extrinsic pathways of apoptosis via its PDZ domain, which may bind to TNF1 and inhibit TRADD from interacting with it. E6 can interfere in apoptosis with several alternative targets including FADD and caspase-8. The activation of the survivor promoter is another striking operation of E6 oncoprotein which can also avoid apoptosis (Gyöngyösi *et al.,* 2012).

In contrast, E7 functions differently and eliminates less pro-apoptotic activities compared to E6. A study by Shankar *et al.,* 2017 reported TALENT-based editing of HPV-E7 caused induction in necrosis in cervical cancer cells.

6.1.3 Sustained Proliferative Signalling Pathways

Normal cells enter the cell cycle in response to many growths and promoted signals that are generated or released in a regulated manner. The receptor kinases present on the surface of the cells sense these signals and transmit them inside the cell through various pathways. Deregulation of these signalling pathways in the cancer cells leads to unregulated cell proliferation. The oncogenic Ras is one of these important signals for cell survival and proliferation. When Ras becomes mutated it helps the cells to migrate to tumour progression via downstream effector pathways such as PI3K-PKB/AKT and MAPK (Chakrabarti *et al.,* 2004). Both E6 and E7 affect the regulation of cell proliferation through the mTOR pathway. The HPV16 infected cells expressing E7 undergo autophagy even in a nutrient-rich state however even if the nutrients are restricted to these cells, they would continue dividing and result in

caspase-independent cell death which is different from the normal cells (Zhou and Münger, 2009). When E6 is present, this mechanism can be inhibited because E6 activates mTORC1 signalling via upstream kinase PDK1 and mTORC2 which leads to induction of protein synthesis even in the lack of growth factors. A study done by (Spangle and Munger, 2013) showed that even in the lack of nutritional factors, expression of E6 in the HPV infected cells caused the internalisation of phosphorylated PRTKs resulting in an increase in Mtorc1-dependant cellular proliferation which helps in the tumour progression.

6.1.4 Enabling Replicative Immortality

Through every round of cellular replication, the telomeres will shorten their length as part of cellular ageing, however, in cancer cells, telomeres length should stay stable to help sustain the tumour progression. As telomeres are responsible for chromosomal end replication therefore it is overexpressed in cancer cells compared to healthy cells. In cervical cancer, the role of E6 and E7 oncoproteins in HPV infected cells are defined by managing the expression of hTERT to launch replicative immortality. E6 is found to activate hTERT promoter via ubiquitin-ligase-E6AP together with c-myc, Sp1 and NFX1 (Liu *et al.,* 2009). In the later stage, the NFX1 becomes degraded via E6AP and activates hTERT, whereas the other two promoters c-myc and Sp1 will be activated by E6 and function as positive regulators (Gewin *et al.,* 2004).

6.1.5 Angiogenesis

Angiogenesis is the recruitment of blood circulation to the transformed cells from the current vasculature which is a significant prerequisite for tumorigenesis. In the HPV infected cells, E6 and E7 assist them to obtain essential nutrition and oxygen from the

surrounding tissues via angiogenesis through the regulation of activities and expression of the inhibitors and inducers (Toussaint-Smith *et al.,* 2004). The change in the expression level of p53 by E6 and pRb by E7 is associated with the angiogenesis modulators In HPV infected cells expressing E6 and E7, the p53 regulates three genes which are thrombospondin-1, mspin and VEGF. As the p53 becomes degraded by E6 the angiogenesis inhibitors (thrombospondin-1 and mspin) lose their functionality hence the angiogenesis inducer (VEGF) become activated through the HIF-1α in the lack of p53 and helps the angiogenesis process (López-Ocejo *et al.,* 2000). E7 also play a key role in angiogenesis by activating AP1 binding site on VEGF promoter. A study by (Wang *et al.,* 2014) reported that PRM2 is upregulated by E7 oncoprotein, and induces angiogenesis through ROS-ERK1/2-HIF-1α-VEGF in cervical cancer.

6.1.6 Invasion And Metastasis

Another important function of E6 and E7 is the induction of the EMT, a process needed for cellular invasion into the bloodstream and metastasis (Kim *et al.,* 2013). The overexpression of E6 and E7 results in the induction of EMT-inducing transcriptional factors including Slug, Twist, ZEB1and ZEB2 increasing the migratory and invasive potential of the cells (D'Costa *et al.,* 2012). In the epithelial cells, the overexpression of E6 and E7 leads to the reduced level of epithelial markers such as E-cadherin whereas, mesenchymal markers like vimentin, fibronectin, N-cadherin will be increased (Hellner *et al.,* 2009).

6.2 Aim

This chapter aims to evaluate and compare the anti-HPV effect of unconjugated liposomal TQ with targeted FA-conjugated liposomal TQ and their mechanism of action.

6.3 Objectives

- To evaluate the anti-HPV effect of unconjugated liposomal TQ on E6 and E7 oncogenes
- To evaluate the anti-HPV effect of FA-conjugated liposomal TQ on E6 and E7 oncogenes
- To compare and investigate the mechanism of action of unconjugated and FA-conjugated liposomal drug in CaSki (HPV 16+) cells line by evaluating the protein level of tumour suppressor p53 and pRb.

6.4 Method

6.4.1 Immunocytochemical Staining For HPV Oncogenes And Tumour Suppressor Proteins (ICC)

To evaluate and compare the anti-HPV effect of conjugated and unconjugated liposomal drugs ICC was employed. Cells were cultured, counted and $1x10^5$ were seeded on each sterile coverslip inserted in six-well plates. Plates were incubated overnight in the incubator for cell attachment on the coverslips. For the unconjugated liposomal study, cells were treated with three controls (media only, DMSO, and liposomes) and three drugs (cisplatin, TQ, and Lip-TQ) then incubated for 48 hours. In FA-conjugated liposomes, cells were treated with two control samples (media only, FA-Lip-control) and two drugs (Lip-TQ and FA-Lip-TQ). As DMSO control from the previous study did not show any significant toxic effect on the cells. The expression of E6, E7, p53 and pRb proteins were amplified using FITC fluorescent reagent and a fluorescent confocal microscope was used to capture images which were described in full detail in Chapter 2.

6.4.2 Western Blotting To Detect HPV Oncoproteins And Tumour Suppressors

Expression of E6, E7, p53 and pRb were also determined in the two cervical cancer cell lines (CaSki and C33A). Cells were grown until they were 80-90% confluence then they were trypsinised, counted then seeded ($5x10^5$) into six T75 flasks. Flasks were incubated overnight for cell attachment. On the second day, media were replaced by different treatments (as described in ICC protocol) and incubated for 48 hours. Then cells were lysed and the total protein concentration was measured via Bradford assay. The primary antibodies used were (Mouse anti-human E6, E7, p53, and pRb) which were prepared in 1:500 dilutions in BSA. The secondary antibodies (Goat anti-mouse IgG) were prepared in 1:1000 dilution using BSA. Protein quantification was done

using the primary antibody, Rabbit anti-β-actin housekeeping gene for normalisation in 1:1000 dilution. Finally, the ECL kit was applied to detect the band signals developed as described in full detail in Chapter 2.

6.4.3 Apoptosis

Cells were cultured and cell count was carried out. The cells were seeded at the required density ($5x10^5$) into T75 flasks. The flasks were incubated overnight in the incubator for cell attachment. On the second day, for unconjugated liposomal study, cells were treated with three controls (media only, 1% DMSO, and control liposomes) and three drugs; TQ, Lip-TQ and cisplatin as the following concentrations: For CaSki cells: 20μM of TQ, Lip-TQ and 14μM of cisplatin, for C33A cells: 17μM of TQ, Lip-TQ and 11μM of cisplatin. In the case of FA-conjugated liposomal study, cells were treated with two controls (medial only and FA-Lip-Control) and two drugs, Lip-TQ and FA-Lip-TQ as following concentrations, for CaSki cells: 20μM of Lip-TQ and FA-Lip-TQ and for C33A cells: 17μM of Lip-TQ and FA-Lip-TQ. Annexin V-FITC/PI kit was used to evaluate the apoptosis process using BD Calibur flow cytometer via CellQuest Pro software as described in full detail in Chapter 2.

6.5 Results

6.5.1 Investigating Liposomal Encapsulated TQ On HPV Oncoproteins And Tumour Suppressors Using Immunocytochemical Staining

The expressions of HPV oncoproteins (HPV-E6 and HPV-E7) were investigated in CaSki cells and the expressions of tumour suppressor proteins p53 and pRb were investigated in both CaSki and C33A cells using fluorescent immunocytochemical staining. TSA-FITC reagents were used to amplify the fluorescent signal. Both E6 and E7 oncoproteins were expressed in CaSki control samples and significantly reduced after 48 hours of cisplatin, TQ and Lip-TQ treatments (Fig 46 and Fig 47). In addition, HPV-E7 expression was reduced more from TQ treated cells than cisplatin and Lip-TQ treated ones. On the other hand, the expressions of tumour suppressor proteins (p53 and pRb) were increased following all drug-treated samples in comparison to the control samples (Fig 46 and Fig 47).

For C33A Cells, both p53 and pRb were not shown from control samples, but a slight increase in the expression of p53 was shown in both TQ and Lip-TQ treated cells but not from cisplatin-treated cells. However, a significant increase in expression of pRb was seen from both TQ and cisplatin-treated samples and some increase was seen from Lip-TQ treated cells (Fig 48).

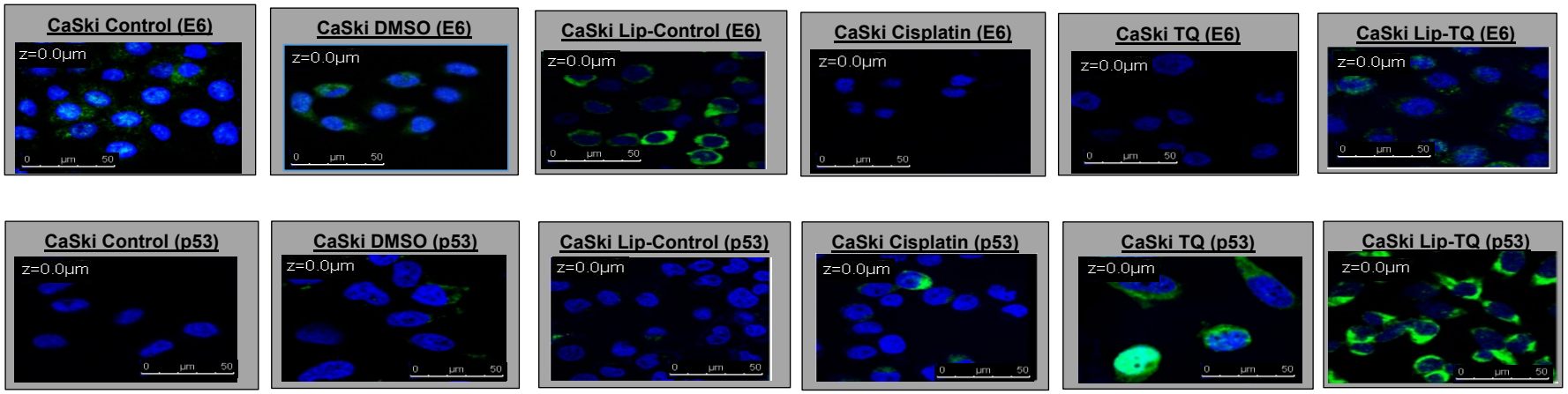

Fig 46: Confocal fluorescent immunocytochemical staining images for HPV-E6 and p53 expression of CaSki (HPV16+) cells following 48 hours drug treatment (cisplatin, TQ and Lip-TQ). The top row presented E6 expression and the bottom row presented the p53 expression. Nuclei were labelled by DAPI in blue and E6 and p53 were shown in green by FITC. Magnification X400.

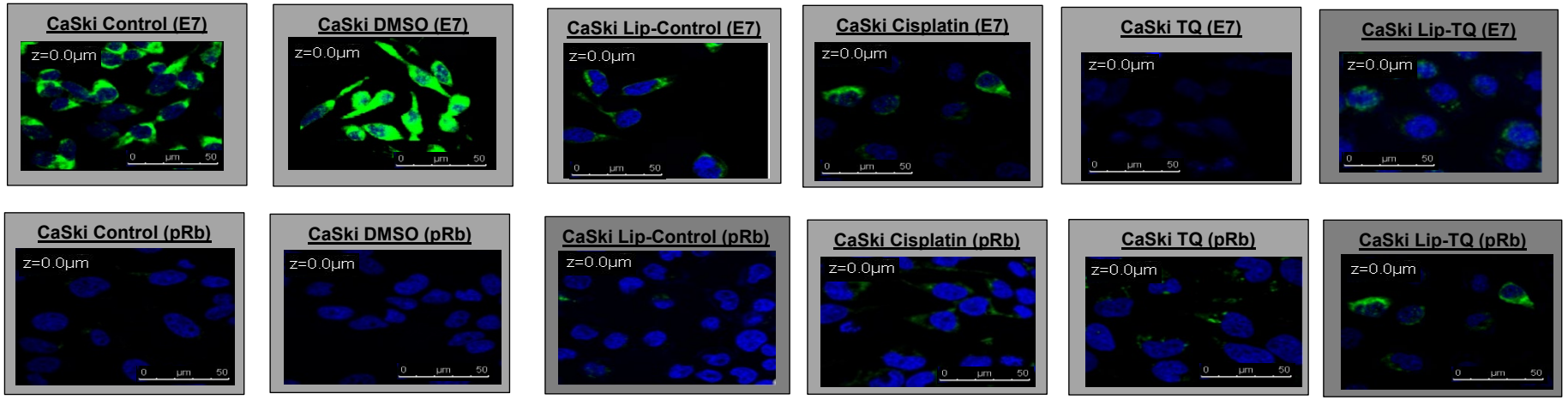

Fig 47: Confocal fluorescent immunocytochemical staining images for HPV-E7 and pRb expression of CaSki cells following 48 hours drug treatment (cisplatin, TQ and Lip-TQ). The top row presented E7 expression and the bottom row presented the pRb expression. Nuclei were labelled by DAPI in blue and E7 and pRb were shown in green by FITC. Magnification X400.

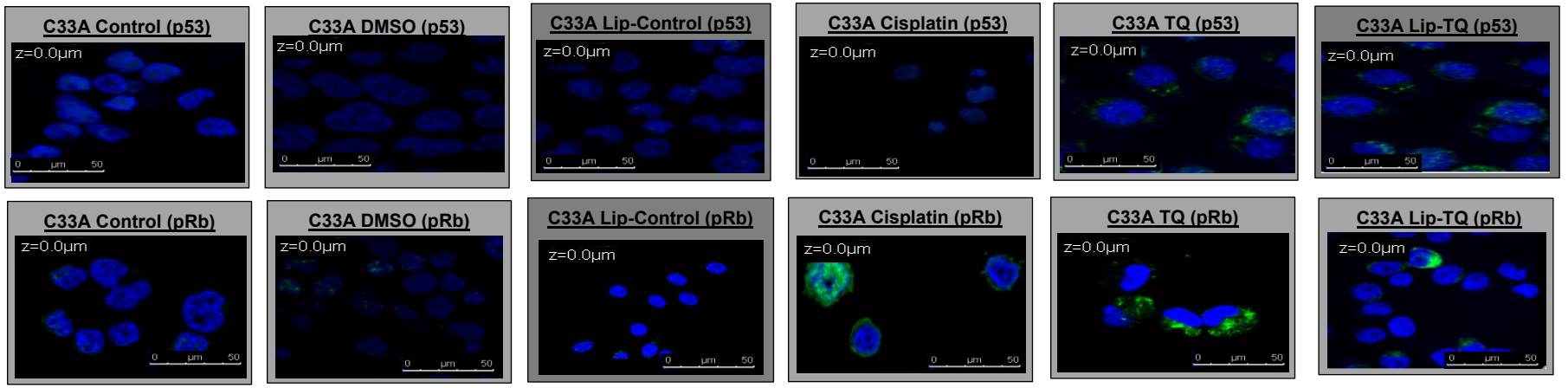

Fig 48: Confocal fluorescent immunocytochemical staining images for p53 and pRb expression of C33A (HPV-) cells following 48 hours drug treatment (cisplatin, TQ and Lip-TQ). The top row presented p53 expression and the bottom row presented the pRb expression. Nuclei were labelled by DAPI in blue and p53 and pRb were shown in green by FITC. Magnification X400.

6.5.2 Investigating The Expressions Of HPV Oncoproteins And Tumour Suppressors Using Western Blotting

The western blotting technique was used to investigate the expressions of HPV oncoproteins (E6 and E7) and tumour suppressor proteins (p53 and pRb) from CaSki and C33A cells following cisplatin, TQ and Lip-TQ treatments and compare with three controls (Control, DMSO and Lip-control).

For CaSki cells, results showed that the expressions of both oncoproteins E6 and E7 were reduced by cisplatin and TQ and Lip-TQ treatments. In addition, cisplatin seemed to be slightly more effective than TQ in reducing the expression levels of both E6 and E7 and free TQ and Lip-TQ showed to be more effective in boosting the expression level of p53 than cisplatin. Surprisingly, no significant effects from both drugs were identified concerning pRb levels compared with the controls although pRb levels were higher in TQ and Lip-TQ treated cells than in cisplatin-treated ones (Fig 49 and Fig 50).

As for C33A cells, pRb expression levels were higher in TQ and cisplatin-treated cells than in two control samples but a similar trend was not seen for p53. On the contrary, the levels of p53 were lower in all drug-treated ones than in control samples (Fig 51).

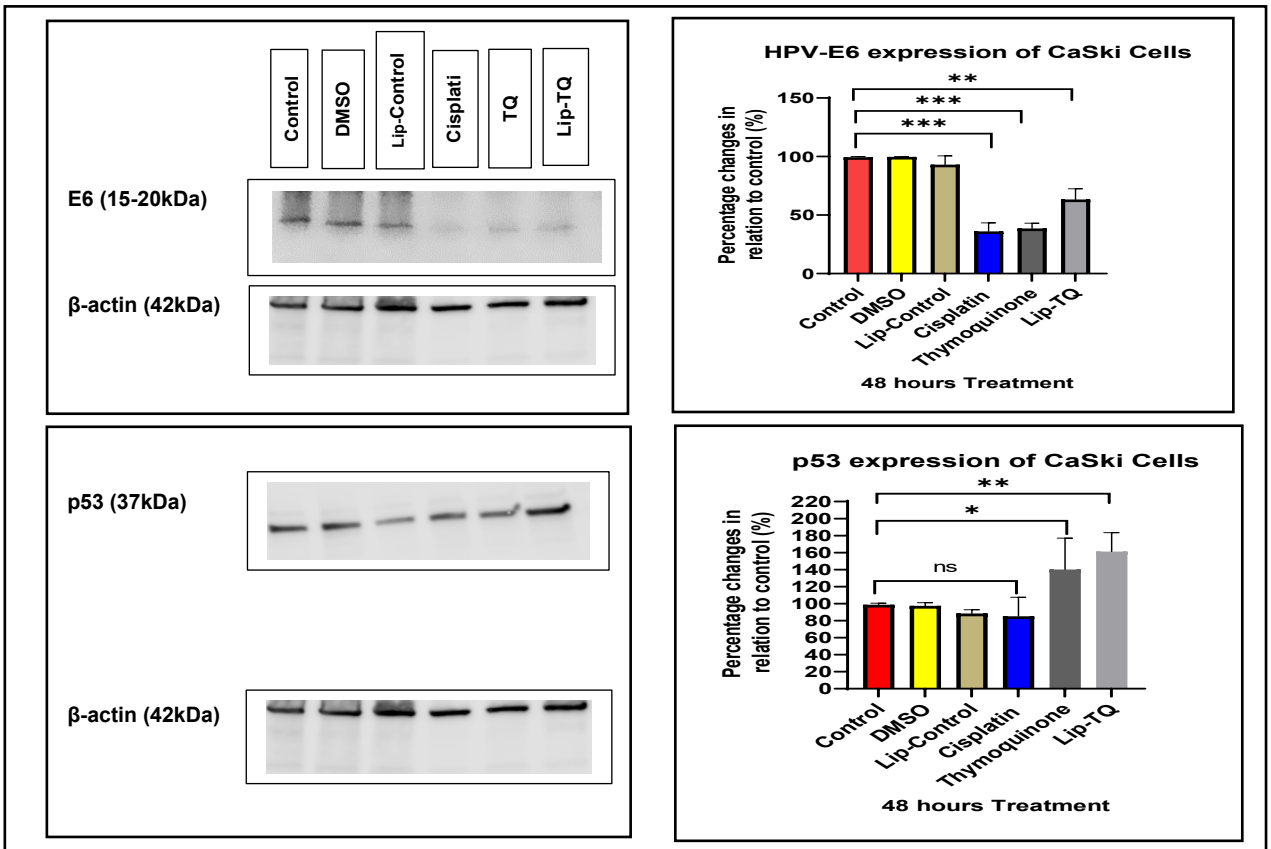

Fig 49: HPV-E6 and p53 expressions in CaSki cells treated with cisplatin, TQ and Lip-TQ for 48 hours were determined by western blotting. Relative protein levels of E6 and p53 were normalised against the loading control, β-actin. The data shown are the Means ± SD from three independent experiments. "*" indicates $p \leq 0.05$, ** $p \leq 0.01$ and *** $p \leq 0.001$.

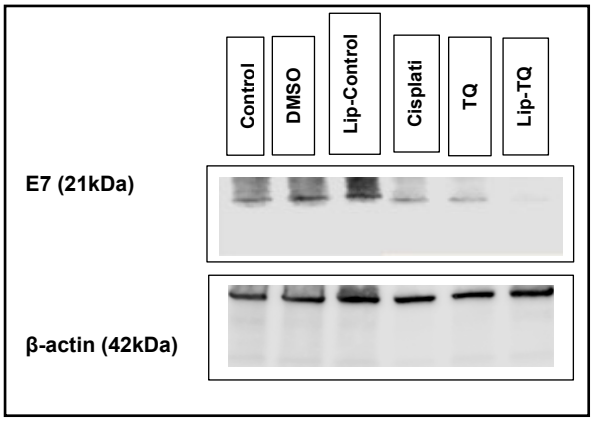

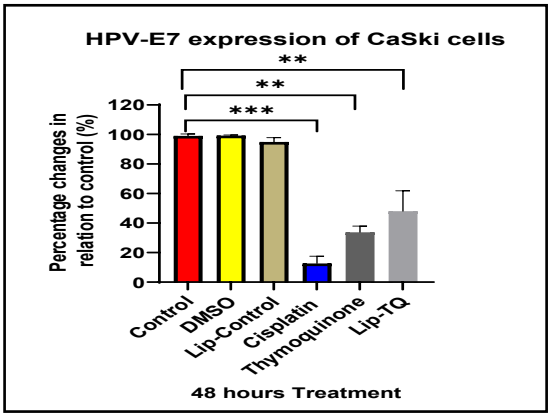

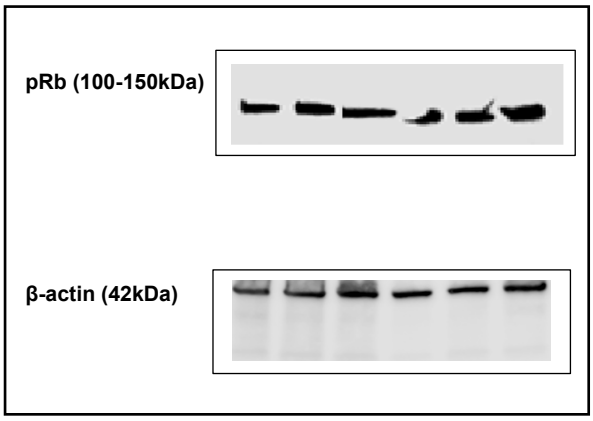

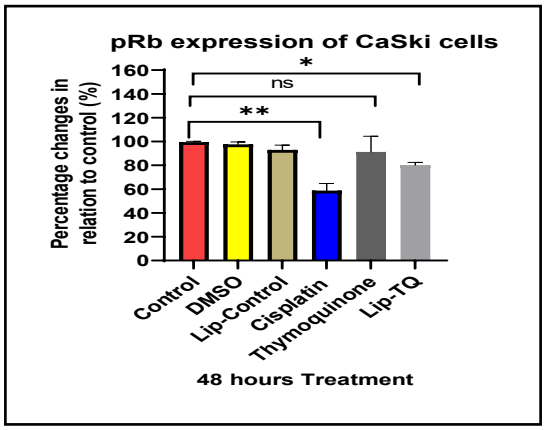

Fig 50: HPV-E7 and pRb expressions in CaSki cells treated with cisplatin, TQ and Lip-TQ for 48 hours were determined by western blotting. Relative protein levels of E7 and pRb were normalised against the loading control, β-actin. The data shown are the Means ± SD from three independent experiments. "*" indicates $p \leq 0.05$, ** $p \leq 0.01$ and *** $p \leq 0.001$.

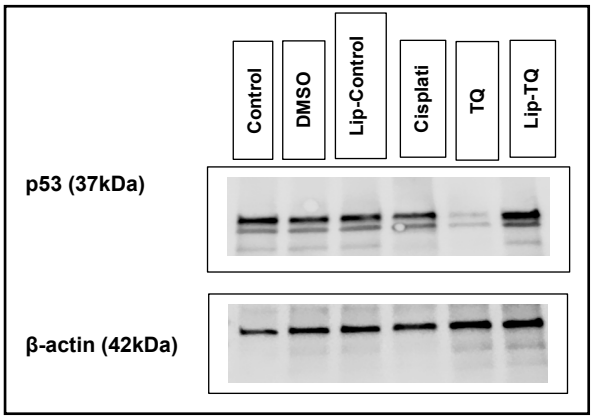

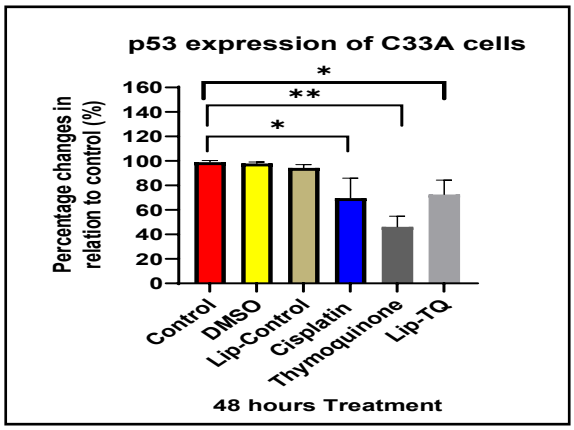

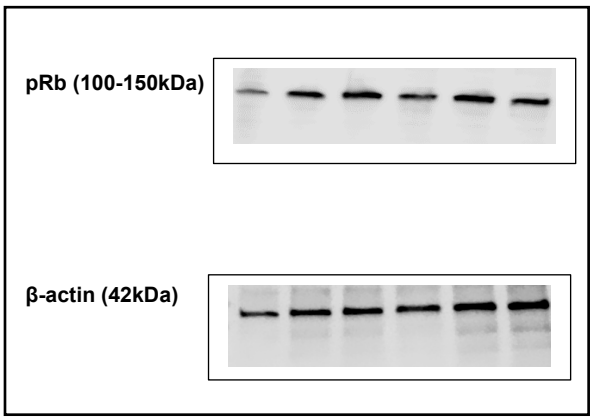

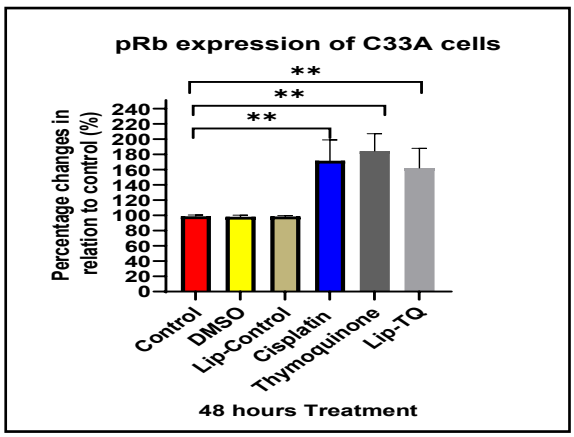

Fig 51: p53 and pRb expressions from C33A cells treated with cisplatin, TQ and Lip-TQ for 48 hours were determined by western blotting. Relative levels of p53 and pRb were normalised against the loading control, β-actin. The data shown are the Means ± SD from three independent experiments. "*" indicates $p \leq 0.05$, ** $p \leq 0.01$ and *** $p \leq 0.001$.

6.5.3 Apoptosis Analysis Using Flow Cytometry

The apoptotic effect of cisplatin, TQ and Lip-TQ were analysed using Annexin V-FITC/PI Apoptosis Kit. The result showed that the percentage of early and late apoptotic cells were significantly increased after 48 hours of drug treatments compared with the control samples for both cell lines (Fig 52).

The proportion of early apoptotic CaSki cells after cisplatin treatment was 22.7% which was less than the population of early apoptotic CaSki cells after TQ treatment (30.8%) (p=0.03) and Lip-TQ (34.80%) (p=0.01). However, in the case of late apoptosis, TQ showed to be more effective in increasing the late apoptotic cell population (16%) than Lip-TQ (9.9%) (p=0.01) and cisplatin (4.2%) (p=0.002). As for the necrotic cell population, more was shown from cisplatin-treated samples (11%) than TQ treated ones (8.3%) (p=0.01) and even more than Lip-TQ treated samples (2.15%) (p=0.005).

In the case of C33A cells, the population of both early and late apoptotic cells after cisplatin treatment was significantly lower than TQ (p=0.005*;* p=0.01) and Lip-TQ (p=0.0006*;* p=0.02) treated cells (cisplatin: 10.7% and 2.7%; TQ: 33.2% and 39.0%; Lip-TQ 25.8% and 18.6%) however, necrotic cell population showed the opposite trend, which could indicate higher cell toxicity generated from cisplatin-treated cells than those from TQ and Lip-TQ treated cells.

In general, the results indicated that two free drugs and encapsulated TQ (Lip-TQ) induced cell apoptosis, however, TQ and Lip-TQ were more effective in inducing cell apoptosis for both cell lines and was less toxic towards cells as demonstrated by the reduced necrotic percentages than cisplatin-treated samples.

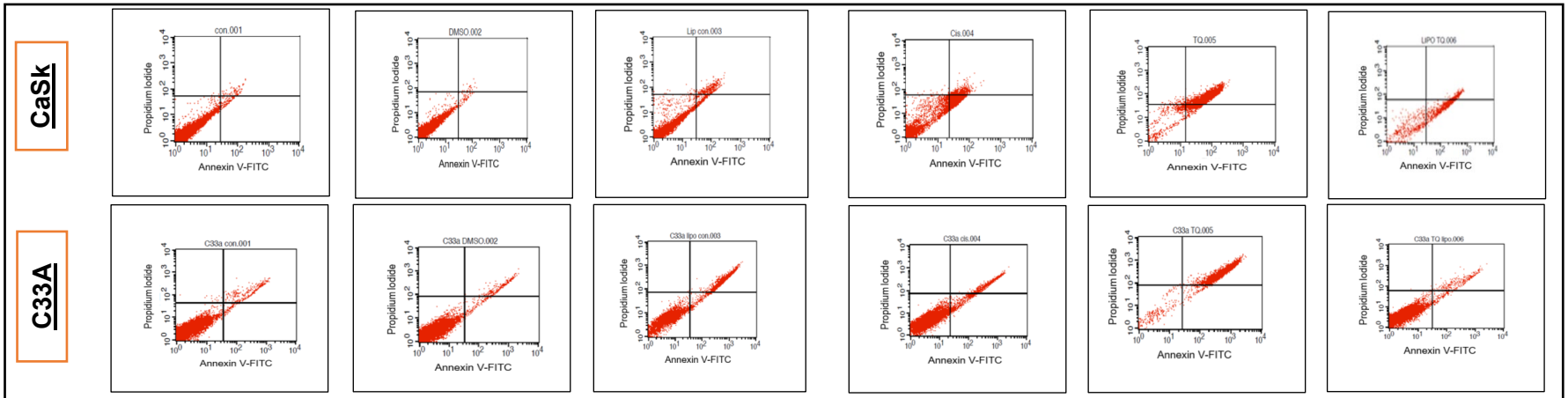

Sample	Cell Population (%) (Mean ± SD)							
	Live Cells		Early Apoptosis		Late Apoptosis		Necrosis	
	CaSki	C33A	CaSki	C33A	CaSki	C33A	CaSki	C33A
Control	98.44±0.24	97.50±1.46	0.55±0.55	1±0.24	0.27±0.14	0.59±0.32	0.74±0.17	1.29±0.91
DMSO	97.96±1.03	92.67±2.62	1±0.24	2.31±1.03	0.25±0.20	0.93±0.39	0.79±0.59	4.08±1.99
Lip-Control	97.31±1.6	97.85±1.1	1.62±0.54	1.53±0.5	0.68±1.02	0.52±1.26	0.39±0.5	0.1±0.85
Cisplatin	62.13±2.06	62.78±0.22	22.71±0.36	10.72±2.54	4.19±0.07	2.72±0.49	10.98±3.66	14.78±2.72
TQ	45.64±0.34	41.73±0.82	30.08±1.61	23.21±2.48	16.04±1.03	29.02±2.31	8.26±2.96	6.04±0.99
Lip-TQ	53.2±1.15	57.68±2.48	34.80±0.85	25.81±0.98	9.85±0.65	18.63±0.6	2.15±1.25	2.36±0.75

Fig 52: Flow cytometry analysis of apoptotic effect of cisplatin, TQ and Lip-TQ on CaSki and C33A cells following 48 hours drug exposure. Apoptosis was examined using flow cytometry analysis by Annexin V-FITC/PI apoptosis detection assay. The data shown are the Mean ± SD of three independent experiments. $p \leq 0.05$ indicates the significant differtence.

6.5.4 Immunocytochemical Staining To Evaluate The Anti-HPV Effect Of FA-Conjugated Liposomes On The Expression Of E6 and E7 And The Tumour Suppressor Protein (p53 and pRb)

CaSki cells were stained by the following antibodies: E6, E7, p53 and pRb. C33A cells were stained by p53 and pRb antibodies. TSA-FITC was used to amplify the signals detected by the relevant antibodies and fluorescent confocal microscopy was used to capture the images.

For CaSki cells (Fig 54) and (Fig 55), E6 and E7 oncoproteins were extensively expressed in all control samples however the expression of E6 and E7 oncoproteins were reduced after drug treatment. As for the expressions of tumour suppressor proteins (p53 and pRb) in CaSki cells shown in (Fig 54) and (Fig 55) both of them were increased following Lip-TQ and FA-Lip-TQ treatment in comparison to the control samples.

With regards to C33A, HPV negative cells (Fig 53), although both drug-treated samples (Lip-TQ and FA-Lip-TQ) showed an increased expression of both tumour suppressor proteins (p53 and pRb) the p53 expression was significantly higher than pRb.

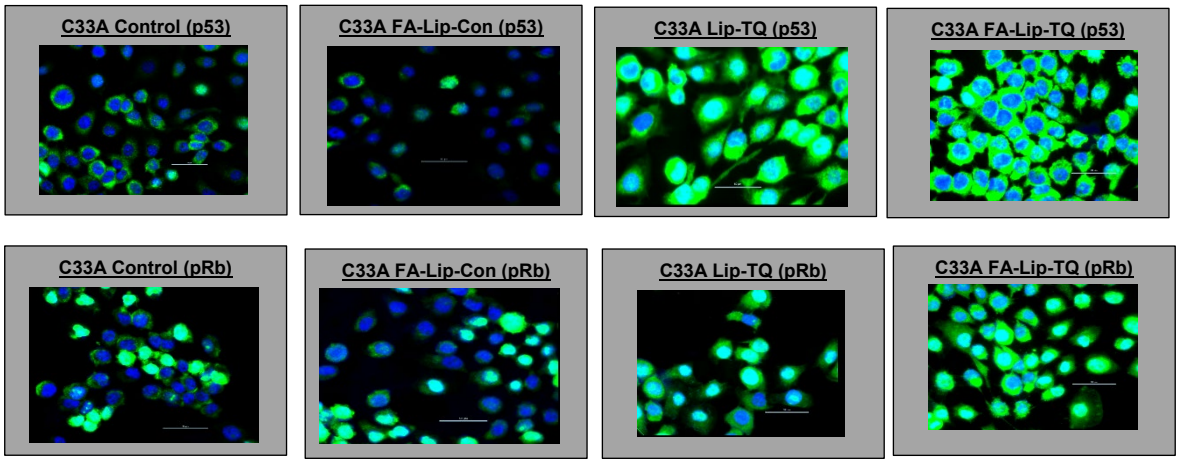

Fig 53: Confocal microscopy images for p53 and pRb expression of C33A cells following drug Lip-TQ and FA-Lip-TQ treatments. The top row presented p53 expression and the bottom row presented pRb expression in C33A treated cells. Nuclei were labelled by DAPI in blue and p53 and pRb were shown in green by FITC.

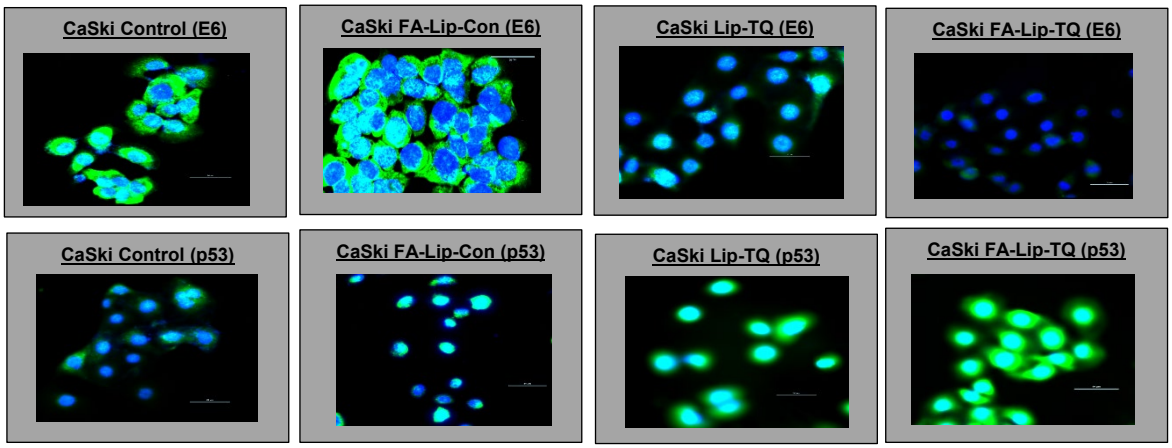

Fig 54: Confocal microscopy images for HPV-E6 expression of CaSki cells following Lip-TQ and FA-Lip-TQ drug treatments. The top row presented E6 expression and the bottom row presented the p53 expression in the cells. Nuclei were labelled by DAPI in blue and E6 was shown in green by FITC.

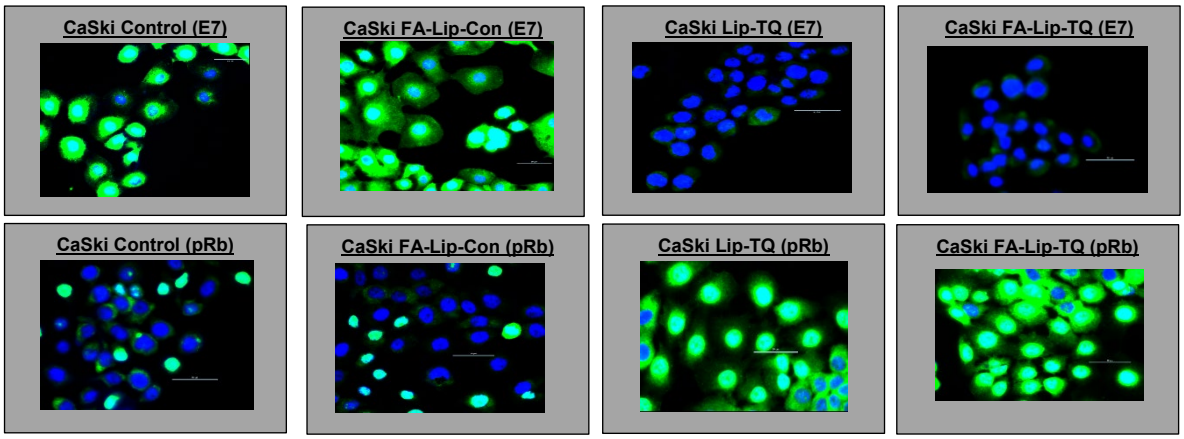

Fig 55: Confocal microscopy images for HPV-E7 expression of CaSki cells following Lip-TQ and FA-Lip-TQ drug treatments. The top row presented E7 expression and the bottom row presented the pRb expression in the cells. Nuclei were labelled by DAPI in blue and E6 was shown in green by FITC.

6.5.5 Western Blot To Analyse The Effect Of UnConjugated And FA-Conjugated Liposomal TQ On HPV Oncoproteins (E6/E7) And Tumour Suppressor Proteins (p53/pRb)

Further to confirm the result obtained from immunocytochemical staining, western blot was performed to evaluate the expression of E6/p53 and E7/pRb in CaSki cells (Fig 56 and Fig 57), and p53/pRb in C33A cells (Fig 58) following 48 hours Lip-TQ and FA-Lip-TQ treatments.

For CaSki cells, results showed that the expressions of both oncoproteins E6 and E7 were significantly reduced by Lip-TQ and FA-Lip-TQ treatment. In addition, FA-Lip-TQ seemed to be slightly more effective than Lip-TQ in reducing the expression levels of both E6 and E7. Furthermore, both drugs showed to be effective in boosting the expression level of p53 and pRb. Although, FA-Lip-TQ seem to be slightly more effective in boosting the expression levels of both p53 and pRb compared to Lip-TQ (Fig 56 and Fig 57).

As for C33A cells, both drugs showed to be significantly effective in increasing p53 and pRb expression levels, however, FA-Lip-TQ seemed to be slightly more effective in enhancing the expression level of pRb than p53 compared with compared to Lip-TQ (Fig 58).

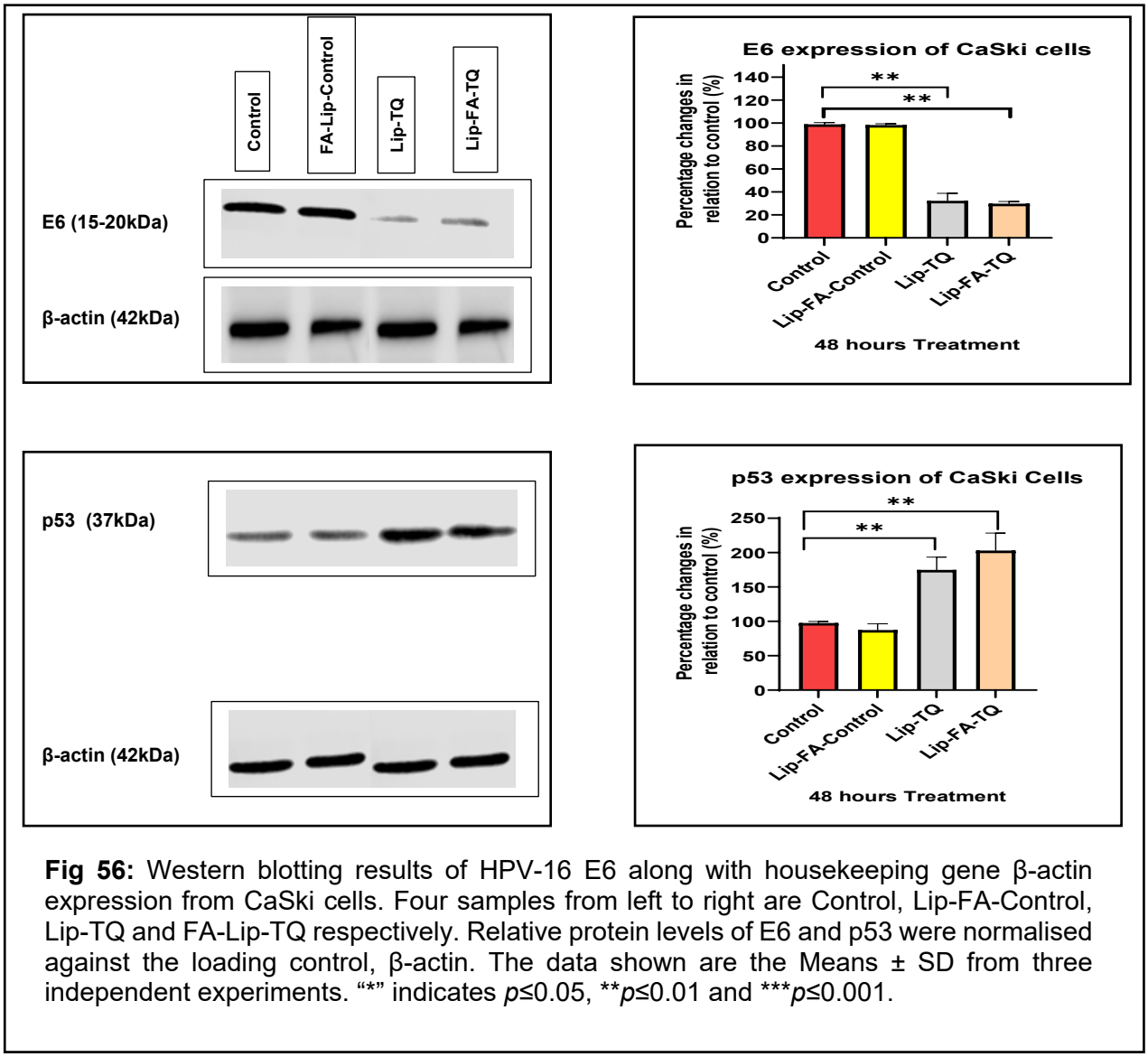

Fig 56: Western blotting results of HPV-16 E6 along with housekeeping gene β-actin expression from CaSki cells. Four samples from left to right are Control, Lip-FA-Control, Lip-TQ and FA-Lip-TQ respectively. Relative protein levels of E6 and p53 were normalised against the loading control, β-actin. The data shown are the Means ± SD from three independent experiments. "*" indicates $p \leq 0.05$, ** $p \leq 0.01$ and *** $p \leq 0.001$.

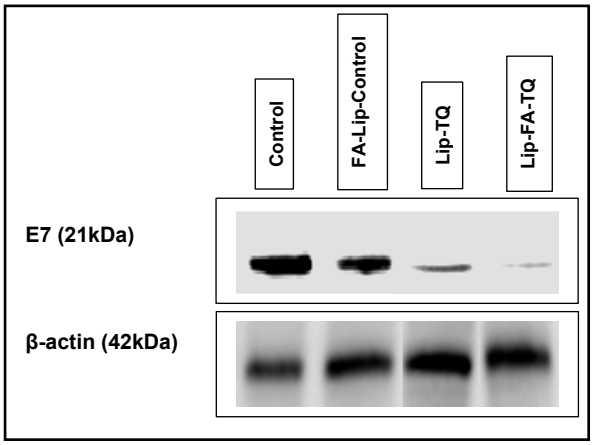

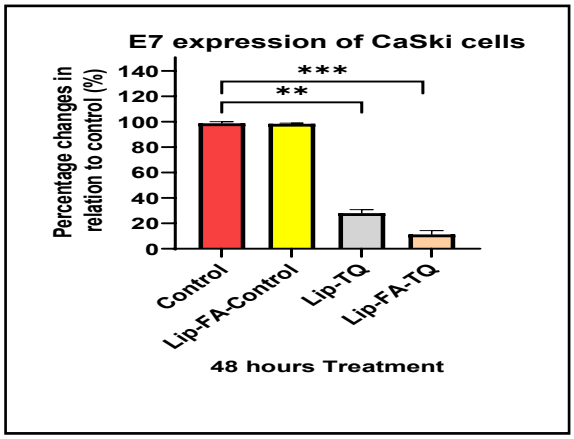

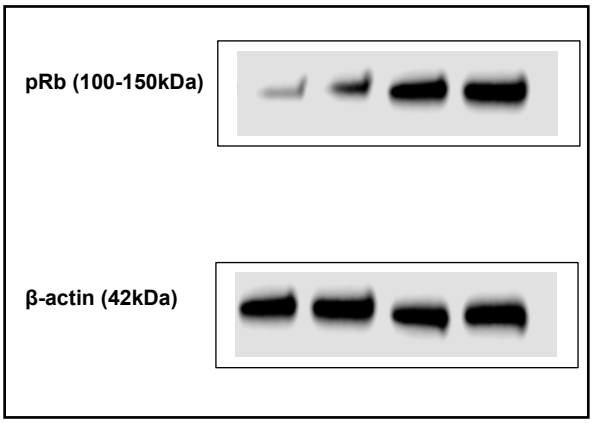

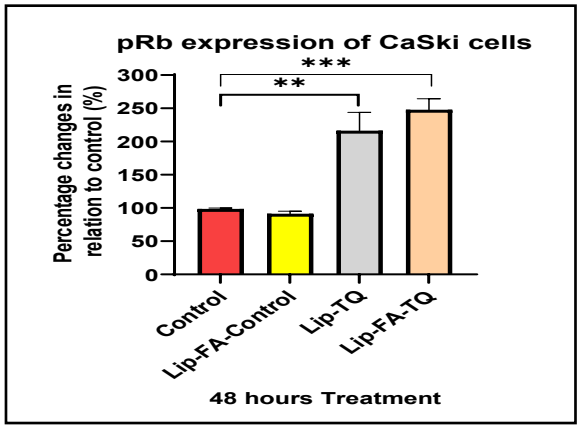

Fig 57: Western blotting results of HPV-16 E7 along with the housekeeping gene β-actin expression from CaSki cells. Four samples from left to right are Control, Lip-FA-Control, Lip-TQ and FA-Lip-TQ respectively. Relative protein levels of E7 and pRb were normalised against the loading control, β-actin. The data shown are the Means ± SD from three independent experiments. "*" indicates $p \leq 0.05$, ** $p \leq 0.01$ and *** $p \leq 0.001$.

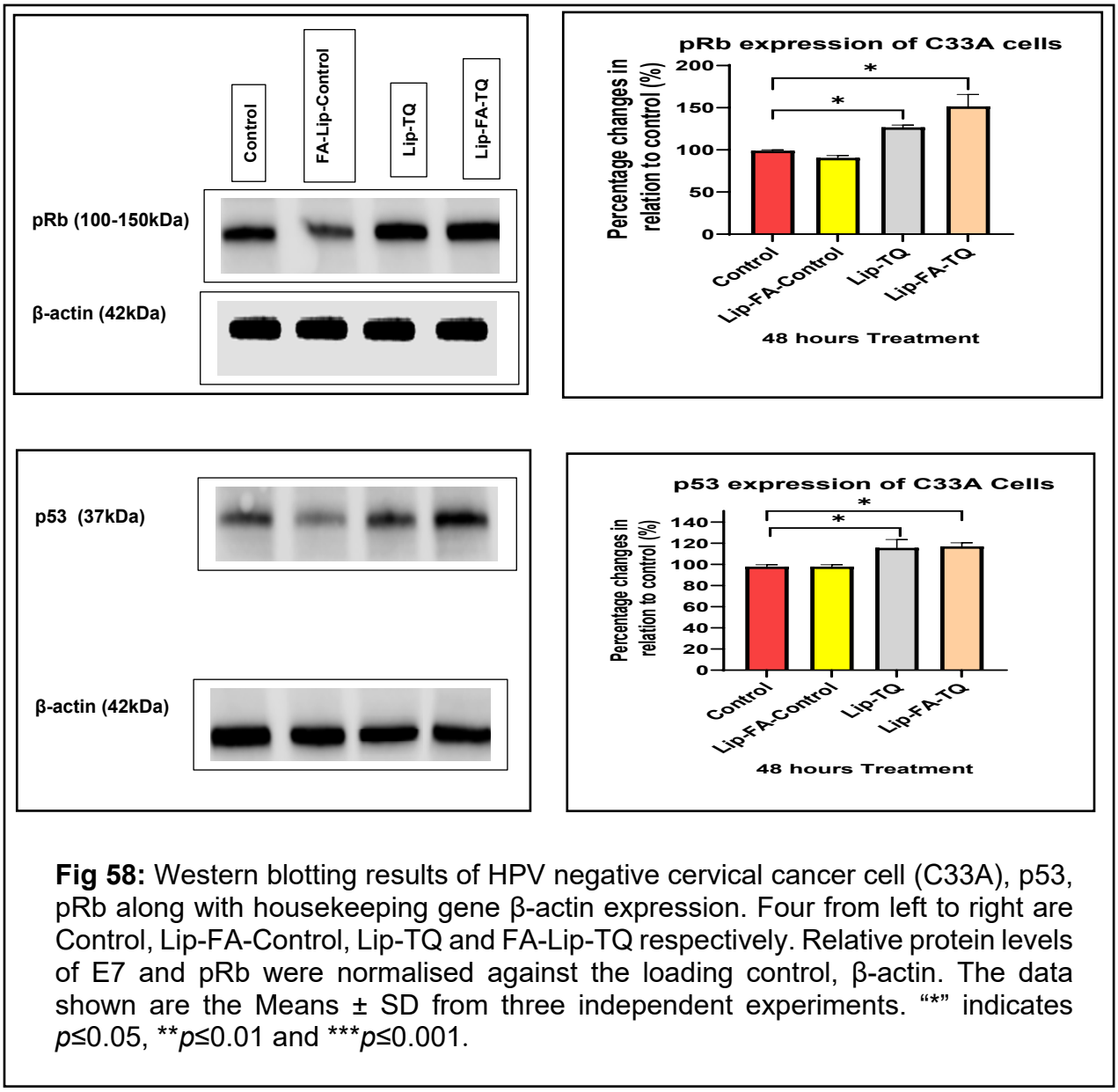

Fig 58: Western blotting results of HPV negative cervical cancer cell (C33A), p53, pRb along with housekeeping gene β-actin expression. Four from left to right are Control, Lip-FA-Control, Lip-TQ and FA-Lip-TQ respectively. Relative protein levels of E7 and pRb were normalised against the loading control, β-actin. The data shown are the Means ± SD from three independent experiments. "*" indicates $p \leq 0.05$, ** $p \leq 0.01$ and *** $p \leq 0.001$.

6.5.6 Apoptosis Analysis Using Flow Cytometry

The apoptotic effect of Lip-TQ and FA-Lip-TQ were detected using Annexin V-FITC/PI Apoptosis Kit. The result showed that the percentage of early and late apoptotic cells were significantly increased after 48 hours of drug treatments compared with the control samples for both cell lines (Fig 59).

The proportion of early apoptotic CaSki cells after FA-Lip-TQ treatment was 37.7% which was significantly higher (p=0.0008) than the population of early apoptotic CaSki cells after Lip-TQ treatment (26.6%). However, the late apoptotic cells population did not follow the same trend. FA-Lip-TQ treated one was 7.18%, which was less than those populations following Lip-TQ treatment (9.28%) (p=0.0005). As for the necrotic cell population, more was shown from Lip-TQ samples (4.82%) than FA-Lip-TQ treated one (2.98%) (p=0.002).

In the case of C33A cells, the population of early apoptotic cells (25.5%) after Lip-TQ treatment was higher than FA-Lip-TQ treated cells (22.7%) (p=0.0002), however, the late apoptotic cell population showed the opposite trend, in which more cells were shown from FA-Lip-TQ treated samples (17.7%) than Lip-TQ treated cells (13.5%) (p=0.0006).

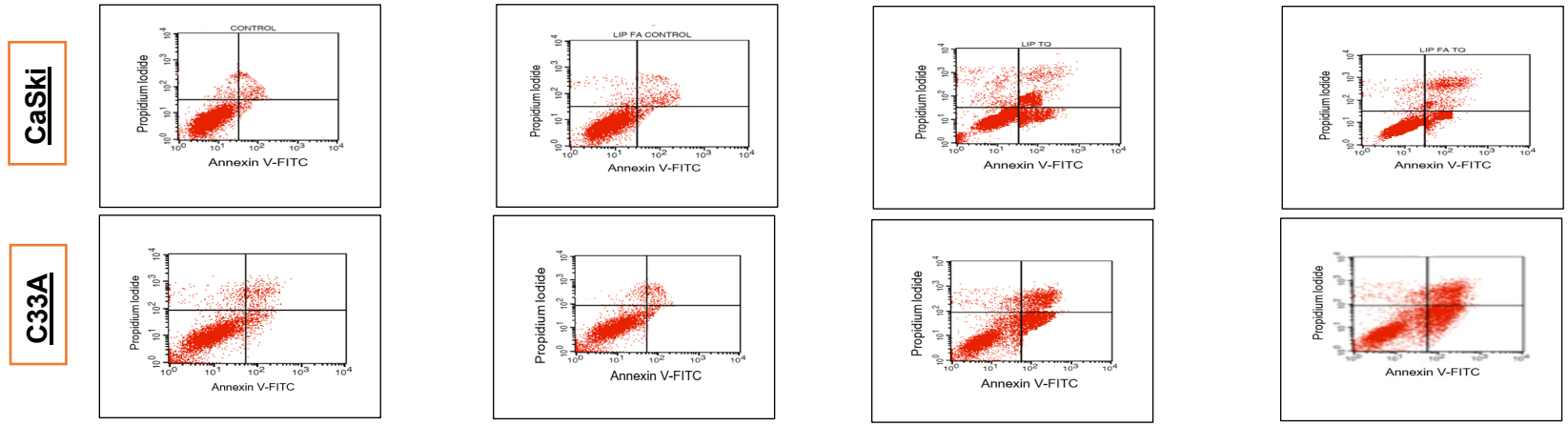

Sample	Cell Population (%) (Mean ± SD)							
	Live Cells		Early Apoptosis		Late Apoptosis		Necrosis	
	CaSki	C33A	CaSki	C33A	CaSki	C33A	CaSki	C33A
Control	96.70±0.85	97.50±1.16	0.49±0.5	0.3±0.64	1.93±1.4	1.6±0.32	0.88±0.95	0.6±0.91
FA-Lip-Control	97.15±1.5	96.77±1.62	1.87±1	2.01±1.23	0.86±0.80	1.03±2.39	0.12±0.59	0.19±1.59
Lip-TQ	59.30±1.12	54.85±1.1	26.6±0.54	25.53±0.5	9.28±1.02	13.52±1.26	4.82±0.5	6.1±0.85
FA-Lip-TQ	52.13±4.06	56.78±0.22	37.71±0.36	22.72±3.04	7.18±1.07	17.72±2.49	2.98±3.66	2.78±2.12

Fig 59: Flow cytometry analysis of apoptotic effect of Lip-TQ and FA-Lip-TQ on CaSki and C33A cells following 48 hours drug exposure. Apoptosis was examined using flow cytometry analysis by Annexin V-FITC/PI apoptosis detection assay. The data shown are the Mean ± SD of three independent experiments. $p \leq 0.05$ indicates the significant differtence.

6.6 Discussion

The result obtained from the previous chapters of this study showed that encapsulated TQ in FA-conjugated liposomes could enhance the drug's internalisation in FA highly expressed cervical cancer cells, especially CaSki cells, which are HPV16+. Therefore, the anti-HPV effect of FA-conjugated liposomal TQ on HPV-E6 and E7 oncoproteins and its effect on tumour suppressors, p53 and pRb were investigated. Both E6 and E7 are essential early oncoproteins involved in uncontrolled cell proliferation via degrading growth suppressor proteins p53 and pRb (Yeo-Teh *et al.,* 2018). Degradation of p53 and pRb results in continuous cell proliferation and allows the amplification of HPV leading to HPV-induced malignancy (Tomaić, 2016). Additionally, the complementary action of both E6 and E7 are necessary to immortalise primary human keratinocyte meaning that E6 interferes with the cellular survival pathway and E7 induce cellular proliferation (McMurray and McCance, 2004). E6 protein induces cell proliferation by degrading p53 protein and formation of a trimeric complex with ubiquitination enzyme E6-AP leading to an increase in tumour cell growth (Awad *et al.,* 2016). On the other hand, the E7 oncoprotein encoded by high-risk type HPV 16 such as CaSki (HPV16+) has a higher affinity compared to those encoded by the low-risk HPV type in binding to Rb (Abulfadl *et al.,* 2018). E7 disrupts the interaction of E2F transcription factor resulting in cell replication and division (Helt and Galloway, 2001).

Initially, the anti-HPV effect of the unconjugated liposomal drug (Lip-TQ) was evaluated for CaSki cells and C33A cells were used as a control cell line. The cells were treated with free TQ and Lip-TQ for 48 hours. At the same time, media and 1% DMSO were used as negative control and cisplatin as a positive control drug. Oncoprotein expression levels of HPV-E6 and E7 were evaluated via fluorescent

immunocytochemical staining. Fig 46 showed results for CaSki cells which demonstrates that E6 oncoprotein was effectively downregulated following cisplatin, free TQ and Lip-TQ treatments. However, free TQ and Lip-TQ were more potent in increasing the expression level of p53 protein compared to cisplatin. In the case of HPV-E7 oncoprotein, a similar trend from CaSki cells was observed as HPV-E6. The expression level of E7 (Fig 47) was downregulated following all three drug treatments, however, free TQ and Lip-TQ treatment were more effective in comparison to cisplatin. For C33A cells, HPV negative cervical cell line (Fig 48), both p53 and pRb were not observed in the negative control samples (medial and DMSO treated cells) but an increase in the expression level of p53 was seen in both TQ and Lip-TQ treated cells but this was not observed from cisplatin-treated ones. However, pRb expression was significantly increased following TQ and cisplatin treatment but only a slight increase was seen for Lip-TQ treated C33A cells. To further validate these results, the relative expression level of E6 and E7 was also evaluated via western blot.

The western blotting results obtained for HPV-E6, E7 and p53 for Caski cells showed similar findings as shown from the ICC results. The relative expression level of E6 and E7 from CaSKi cells was significantly decreased for all three drug-treated samples however, more reduction for E6 expression was seen from cisplatin and free TQ treated cells than Lip-TQ treated ones. In addition, p53 expression was significantly increased by free TQ and Lip-TQ compared with cisplatin-treated ones (Fig 49).

Interestingly, protein levels of pRB following drug treatments did not increase as expected and this is similar to the result obtained from the ICC study (Fig 47) and (Fig 50). pRb protein expression levels were different from C33A cells from the western blot result. They were higher in TQ, Lip-TQ and cisplatin-treated cells than in two no drug-treated control samples.

Our results agree with another study which was carried out by Ichwan *et al* (2014) but they used a different cervical cancer cell line SiHa, not CaSki, however, both cell lines are HPV16+. C33A was also used in their study. They proposed that TQ caused apoptosis in SiHa cells through the activation of p53 dependent pathway and via the caspase-3 pathway in C33A cells. Furthermore, p53 upregulation by TQ was also reported from a few breast cancer studies (Ng *et al.,* 2011; Arafa *et al.,* 2011; Ebrahimi *et al.,* 2017).

The effect of free TQ and Lip-TQ in inducing apoptosis was evaluated by Annexin V-FITC/PI apoptosis detection kit (Fig 52). Result obtained showed that all three treatments (cisplatin, free TQ and Lip-TQ) induced cell apoptosis, however, TQ and Lip-TQ were more effective in inducing cellular apoptosis for both CaSki and C33A cell lines but was less toxic towards these cells than cisplatin was, which demonstrated by the higher percentages of both early and late apoptotic cell population and lower necrotic cell population percentages.

The findings from apoptosis studies and upregulated p53 expression from the results of ICC and western blot for CaSki cells indicate that the cell apoptosis induction in CaSki cells could occur through a p53-dependent pathway was not seen from C33A cells. C33A cells have mutant p53 gene therefore caspase-3, caspase 8 or caspase 9 can be the right candidate to be considered (Ledgerwood and Morison, 2009). The anticancer mechanism of TQ was investigated by another study (Gali-Muhtasib *et al.,* 2004) and it was reported that TQ induced growth inhibition by inducing G2/M cell cycle-arrest which was associated with the p53 tumour suppressor protein and decrease in cyclin B1 protein.

Ichwan *et al.,* 2014 also reported that TQ induces apoptosis through the p53-mediated pathway in HPV- positive SiHa cells, but for HPV negative C33A cells were reported to be due to caspase proteases such as caspase-3 which is responsible for orchestrating DNA fragmentation. In general, p53 protein is degraded in the cells with E6 oncoprotein integration which results in their escape from the G1 checkpoint in the cell cycle at a very early stage. On the other hand, the interaction of E7 protein with pRb results in degradation and phosphorylation of the pRb and transition of G1/S to G2/M and further cell proliferation (Yim and Park, 2005). The anticancer activity of TQ-NLC was also investigated in breast cancer in the study by (Ng *et al.,* 2015) and they reported that TQ-NLC induced cell cycle arrest at G2/M and S phase after 24 and 48 hours of treatment.

After establishing the effectiveness of Lip-TQ in reducing the HPV-E6 and HPV-E7, the next step was to compare the anticancer effect of FA-Lip-TQ and to see if it can further increase the specificity of treatments by Lip-TQ and therefore reduce the adverse effect of toxicity toward the surrounding healthy tissues and cells. The results obtained from ICC demonstrated that FA-Lip-TQ has significantly reduced the expression level of both E6 (Fig 54) and E7 (Fig 55) oncoproteins in CaSki cells compared to Lip-TQ and a corresponding increase in expression of p53 and pRb tumour suppressor protein were also observed.

Surprisingly, FA-Lip-TQ has also resulted in a significant increase in p53 and pRb levels in C33A HPV negative cells compared to control samples. This result was inconsistent with the findings observed when C33A was treated with unconjugated liposomal TQ.

The results obtained from the western blot experiment (Fig 56 and Fig 57) validates ICC findings. Results revealed that FA-Lip-TQ was more efficient in reducing both E6 and E7 oncoproteins and increasing the expression level of p53 and pRb compared to Lip-TQ. Moreover, even the downregulation of E7 after FA-Lip-TQ treatment was slightly more than what was observed in ICC. In the case of C33A cells, both Lip-TQ and FA-Lip-TQ treatments were shown to be very effective in increasing p53 and pRb expression levels compared to the control samples.

Apoptosis evaluation of Lip-TQ and FA-Lip-TQ on CaSki and C33A cells (Fig 59) showed that FA-Lip-TQ significantly increased the population of early apoptotic CaSki cells compared to Lip-TQ. However, this enhancement was not observed in C33A cells as the population of late apoptotic cells and early apoptotic cells tend to be roughly the same. FA-Lip-TQ showed to be slightly more effective in reducing the population of necrotic cells in both cell lines compared to Lip-TQ which indicates that it could be less toxic due to the targeted treatment.

In summary, the current study demonstrates that TQ is a suitable drug candidate for treating HPV-associated cancer with a low cytotoxicity effect compared to the positive chemotherapeutic drug cisplatin. It was also shown that liposomes can be considered as promising drug delivery vesicles for delivering TQ. Physiochemical properties of liposomal TQ synthesised confirmed the stability of the drug carriers over 17 weeks period. Free TQ and liposomal TQ showed to be very effective in reducing the expression of E6 and E7 oncoprotein and increasing the expression of tumour suppressor proteins p53 and pRb. Conjugation of Liposomal TQ with folic acid increased the affinity of liposomes to bind to FRs on the cancer cells which increases cellular uptake of liposomes and hence increasing the effectiveness in reducing E6 and E7 oncoprotein and inducing apoptosis in both cells lines.

This suggests that FA-conjugated liposomal encapsulated TQ could be used as a suitable cancer treatment and highly expressed folate receptors on cancer cells with high-risk HPV integration could be a better target in particular.

Chapter 7

7.0 General Discussion

Among all types of HPV, HPV-16 is the most identified type of HR-HPVs which was detected in 90% of squamous cell carcinoma cases (Harper and Demars, 2014; Vaccarella *et al.,* 2013). Almost 61% of Individuals infected with HPV-16 and 10% of those infected with HPV-18 were shown to have a 200 fold higher risk for the development of cervical cancer (Bosch *et al.,* 2002). The HPV oncoproteins E6 and E7 play a crucial role in the pathogenesis of HPV associated cervical cancer (Münger and Howley, 2002). It was also reported that the expression level of these two viral proteins increased from cervical intraepithelial neoplasia grade 1 to 3 (CIN1 to CIN3) (Soutter *et al.,* 2005). Therefore the interaction of E6 and E7 oncoproteins with the cellular pathway of the host cells makes them potential targets for new HPV associated cancer treatment strategies (Tulay and Serakinci, 2016).

Regarding the potential anticancer drugs, previous studies have demonstrated that TQ could target numerous signalling pathways involved in the carcinogenesis of various cancers and hence it is regarded as a promising anticancer drug (Imani *et al.,* 2017; Khan *et al.,* 2015; Asaduzzaman Khan *et al.,* 2017). TQ has been reported as a potent phytochemical drug for the treatment of leukaemia, breast, colon and lung cancer via inhibiting cancer cell proliferation (Pang *et al.,* 2017; Barkat *et al.,* 2018; Zhang et al., 2016; Samarghandian *et al.,* 2018). The bioavailability and the drug formation of TQ are limited because of its hydrophobic feature and also its solubility. Depending on the duration of drug administration, effective TQ concentration was shown ranging from 549µg/mL to 669µg/mL in aqueous solution at 24 hours, to 665µg/mL to 740µg/mL at 72 hours (Salmani *et al.,* 2014). Therefore, scientists have

attempted to employ TQ-based nanotechnology to overcome these barriers and synthesis new TQ analogues with higher efficiency and bioavailability which have been successful (Darakhshan *et al.,* 2015).

Previously liposomal TQ formulation was found to be effective in treating breast cancer by inhibiting the proliferation of breast cancer cells *in vitro* (Odeh *et al.,* 2012). TQ-NLC was also reported to exhibit anti-proliferative activity and induce cell apoptosis towards cervical cancer and liver cell lines (Ng *et al.,* 2015; Haron *et al*., 2018).

In this study, we encapsulated TQ in liposomes and investigated their anticancer and anti-HPV activity for HPV positive cervical cancer cells. As the first step, the cytotoxicity of TQ was compared to cisplatin (a standard chemotherapeutic drug). Results showed that both cisplatin and TQ exerted an anti-proliferation effect towards CaSki and C33A cell lines after 24 and 48 hours of drug treatment and significantly ($p \leq 0.05$) decreased viable cell population compared to no drug treatment control samples. More promisingly, the normal control HK cells were shown to be less affected by TQ than cisplatin treatment.

After PEGlayted liposomal TQ was synthesised, their physical parameters such as encapsulation efficiency, surface charge and size were monitored over 17 weeks of storage at 4^{o}C, as these parameters play a crucial role in stability, loading efficiency and cellular uptake of the liposomes (Bozzuto and Molinari, 2015). TQ encapsulation efficiency was found to be as high as 81% in week 0 and 85% at week 17 and liposomes size were ranging from 149.50nm±2.35 to 150.2nm±1.56 with zeta potential values between -2.98 mV±1.35 at week 0 and -2.88mV±1.29 with polydispersity index ranging from 0.126 to 0.218. Relatively consistent values from liposome size, surface charges and PDI over 17 weeks storage period indicate that the current synthesised

Lip-TQ tend to be stable and had no sign of aggregation, therefore, it is worth further investigating its bioavailability to the cells and the anticancer effects. The advantages of PEG on the surface of the liposomes is linked to the improvement of their stability, increasing their long circulation in the blood and boosting their intracellular uptake also protecting them from being metabolically degraded or eliminated by plasma proteins (Hoang Thi *et al.,* 2020). These stable PEGylated liposomes can take advantage of the EPR effect in the tumour microenvironment to accumulate in the tumour interstitium (Danhier *et al.,* 2010). However, for the chemotherapeutic drug to reach its target site, which is cancer tissue for the purpose of this study, identifying a highly and specifically expressed target present on the surface of cancer cells will be the first approach. Folate was known to have a high affinity with specific ligands such as FRs on the surface of the cancer cells (Reddy *et al.,* 2002). Therefore, screening for the expression of FRs from the studied cell lines (CaSki and C33A) along with the normal control cell line HK was carried out.

The results obtained demonstrated that FRs are highly expressed on HPV positive CaSki cells and their expression level was 15 times more than that of the normal HK cell line. This was followed by HPV negative C33A cells which showed 6 times higher expression levels than Hk cells. Therefore, active targeting approach by preparing FA-conjugated liposomal encapsulated TQ was used to target FR highly expressed cervical cancer cells. This method was tested to see if actively delivering TQ to cancer cells with highly expressed FRs could further enhance the specificity of TQ treatment for cancer cells and then reduce the unwanted adverse effect of exposing them to normal healthy tissue and cells.

FA-conjugated liposomes encapsulating TQ was then synthesised. The encapsulation efficiency of the TQ was ranging from 89.8% at week 0 to 89.2% at week 17 of storage

at 4°C. The physiochemical parameters of the liposomes stated the homogeneity (PDI<0.25) and stability of the liposomal drugs over 17 weeks of storage. The size of the liposomes was ranging from 150.1nm±2.12 at week 0 and 155.13nm±1.58 at week 17 with the zeta potential of -4.38mV to -5.55mV. Liposomes with zeta potential values from -10mV to +10mV were considered to be neutral (Qi, Zhao and Zhuang, 2011). Zeta potential is an important factor in liposomal drug delivery and the lack of surface charge on the liposome might result in particle aggregation, however, in this study no sign of aggregation was observed over the storage time, as the size of liposomes did not change.

Furthermore, the cellular uptake of unconjugated liposomal TQ and FA-conjugated liposomal TQ were evaluated to find out whether FR's conjugation could improve the cellular uptake of the liposomes by the target cells. Unsurprisingly, the results showed that FR positive CaSki cells with the highest expression of FRs on their surface among three analysed cell lines displayed the highest uptake of liposomal drugs compared to HPV negative C33A cells and HK cells.

Further comparison of the cytotoxicity of Lip-TQ and FA-Lip-TQ on CaSki and C33A cell lines was also carried out. The result demonstrated that as the time of incubation increased, the live cell population decreased for both tested cell lines also the IC_{50} values obtained showed that FA-Lip-TQ was more effective towards both cell lines in a time-dependent manner with lower IC_{50} values after 48 hours of treatment compared to 24 hours. The differences in the release rate of the drug can be due to the size of the liposomes and the number of phospholipid bilayers involved in the compartment of the liposomes (Bozzuto and Molinari, 2015). Moreover, the increased cellular uptake of TQ following FA conjugated liposomal encapsulated TQ treatment could be

due to the high expression of folate receptors which leads to more drug uptake through FR-mediated endocytosis within the early endosomes (Zhao *et al.,* 2013).

As a final part of this study, the mode of action of liposomal TQ and its anti-HPV effect was evaluated on the HPV positive CaSki and HPV negative C33A cells *in vitro*. As mentioned earlier the replication of E6 and E7 viral genes leads to the overproduction of E6 and E7 oncoproteins which affects the cell cycle (Gupta *et al.,* 2003). The E6 oncoprotein interacts with the E6-AP complex and selectively binds to p53 resulting in its proteolytic degradation (Li *et al.,* 2019). p53 is responsible for inducing cell cycle arrest and apoptosis in case of any DNA damage and when it becomes degraded it will be unable to fulfil its task (Tang *et al.,* 2002). The other tumour suppressor protein affected by HPV oncoprotein E7 is the retinoblastoma protein (Rb) which is responsible for blocking the cell cycle progression from G1 to S phase by interacting with transcription factors E2F (Kim *et al.,* 2014). Furthermore, overexpression of E7 leads to phosphorylation of Rb and only a small proportion of pRb can bind to E2F, hence the E2F-Rb interaction is disrupted which results in the inactivation of the E2F transcription factor (Yim and Park, 2005). The overall results demonstrated that TQ, Lip-TQ and FA-Lip-TQ were all very effective in reducing the expression levels of E6 and E7 in CaSki cells and therefore in upregulating tumour suppressor proteins p53 and pRb. For C33A cells Lip-TQ and FA-Lip-TQ were shown to be less effective in upregulating the tumour suppressor proteins compared to free TQ. Also, FA-Lip-TQ induced significantly higher apoptosis in CaSki cells than C33A cells but in general, FA-conjugated liposomal TQ was more effective in upregulating both tumour suppressor proteins in both HPV cell lines. These findings supported our hypothesis that Lip-TQ and in particular FA-Lip-TQ have an advantage as a therapeutic drug delivery system for treating HPV positive cancer such as cervical cancer.

8.0 Future Studies

In the current study, we have demonstrated a suitable strategy for targeting TQ to HPV positive cervical cancer cells using FA-conjugated encapsulating liposomes. These conjugated liposomes were shown to be more effective than unconjugated liposomes in downregulating expression levels of HPV-E6 and HPV-E7 oncoproteins and upregulating expression levels of tumour suppressor proteins p53 and pRb. Additionally, they were shown to have higher selectivity in targeting HPV positive cervical cancer cells than free TQ and unconjugated liposomal TQ due to the high expression of folate receptors. This was supported by the results obtained from the evaluation of FR receptors on the tested cells and their role in increasing the cellular uptake of liposomal drugs. Future investigations on the mechanism of action of Lip-TQ, FA-Lip-TQ and TQ is required via cell cycle analysis which can give a better understanding of the molecular pathways involved in the apoptotic effect of these drugs. Cyclin-dependent kinase (CDK) and cyclins could be a potential targets to investigate. TQ has previously been reported to induce G1 cell cycle arrest which corresponds with reduced expression levels of CDK inhibitors p16 and downregulation of cyclin D1 (Shoieb *et al.,* 2003). In addition, various signalling pathways such as NF-$_K$B, STAT3, MAPK and PI3/AKT could also be targeted among the most significant pathways through which TQ mediates its anticancer activity (Majdalawieh *et al.,* 2017).

In the current *in vitro* study, we have investigated the therapeutic effect of free TQ and liposomal encapsulation TQ on CaSki (HPV16+) and C33A (HPV negative) cell lines. *In Vitro,* studies are important tools in cancer research, as they enable the scientist to identify carcinogens, investigate the development of cancer therapies, evaluate drug screening and provide insight into the molecular mechanism of tumour growth and

metastasis. Therefore it would beneficial to include many other cervical cancer cell lines such as HeLa (HPV 18 positive), SiHa (HPV 16 positive), HT-3 (HPV negative) and HCK1T (human cervical keratinocytes) in future research.

In the current study, the 2D cell culture technique was used which is associated with many limitations such as changes in cell morphology, disruption of the interaction between the cellular and extracellular environment and changes in cellular polarity. Therefore, the 3D cell culture method can be employed for further studies which are more closely able to mimic conditions of *in vivo* study (Kapałczyńska et al., 2016).

9.0 Conclusion

This study has evaluated the anticancer effects of TQ in treating cervical cancer cells *in vitro*. Two different liposomal delivered TQ samples (non-FA-conjugated liposomal TQ and FA-conjugated liposomal TQ) were prepared, their toxicity, TQ encapsulation efficiency and stability were evaluated. Two cervical cancer cell lines, one HPV negative C33A cell line and one HPV positive CaSki cell line, along with normal keratinocytes as a control cell line, were used in the study. Results have shown that FA-conjugated liposomal encapsulated TQ is more potent than free TQ and non-FA-conjugated liposomal TQ, which was demonstrated by an enhanced apoptosis effect, more reduction in HPV oncoprotein E6/E7 and increased expression for tumour suppressors proteins (p53/pRb) for CaSki cells. These results indicated that FA targeted liposomal encapsulated TQ could enhance both controlled drug release and targeted drug delivery for folate receptor highly expressed cancer cells, in this study, HPV+ CaSki cells. This could minimise the normal cell uptake of the drug and thus improve the therapeutic index. However, further study is warranted to confirm the current findings by including different subtypes of HPV positive and HPV negative cell lines from other cancer types which are associated with HPV infection such as head and neck cancers.

10.0 References

Abdelfadil, E., Cheng, Y., Bau, D., Ting, W., Chen, L., Hsu, H., Lin, Y., Chen, R., Tsai, F., Tsai, C. and Huang, C., (2013). Thymoquinone Induces Apoptosis in Oral Cancer Cells Through P38β Inhibition. *The American Journal of Chinese Medicine*, 41(03), pp.683-696.

Abdelwahab, S., Taha, Sheikh, How, El-Sunousi, Abdullah, Eid and Umar Yagoub, (2013). Thymoquinone-loaded nanostructured lipid carriers: preparation, gastroprotection, in vitro toxicity, and pharmacokinetic properties after extravascular administration. *International Journal of Nanomedicine*, pp.2163-2172.

Abusnina, A., Alhosin, M., Keravis, T., Muller, C., Fuhrmann, G., Bronner, C. and Lugnier, C., (2011). Down-regulation of cyclic nucleotide phosphodiesterase PDE1A is the key event of p73 and UHRF1 deregulation in thymoquinone-induced acute lymphoblastic leukemia cell apoptosis. *Cellular Signalling*, 23(1), pp.152-160.

Adebamowo, S., Dareng, E., Famooto, A., Offiong, R., Olaniyan, O., Obende, K., Adebayo, A., Ologun, S., Alabi, B., Achara, P., Bakare, R., Odutola, M., Olawande, O., Okuma, J., Odonye, G., Adebiyi, R., Dakum, P. and Adebamowo, C., (2017). Cohort Profile: African Collaborative Center for Microbiome and Genomics Research's (ACCME's) Human Papillomavirus (HPV) and Cervical Cancer Study. *International Journal of Epidemiology*, 46(6), pp. 1745-1745.

Aggarwal, P., (2014). Cervical cancer: Can it be prevented?, *World Journal of Clinical Oncology*, 5(4), pp.775–780.

Aharon, D., Weitman, H. and Ehrenberg, B., (2011). The effect of liposomes' surface electric potential on the uptake of hematoporphyrin. *Biochimica et Biophysica Acta (BBA) - Biomembranes*, 1808(8), pp.2031-2035.

Ahmad, A., Mishra, R., Vyawahare, A., Kumar, A., Rehman, M., Qamar, W., Khan, A. and Khan, R., (2019). Thymoquinone (2-Isopropyl-5-methyl-1, 4-benzoquinone) as a chemopreventive/anticancer agent: Chemistry and biological effects. *Saudi Pharmaceutical Journal*, 27(8), pp.1113-1126.

Akbarzadeh, A., Rezaei-Sadabady, R., Davaran, S., Joo, S., Zarghami, N., Hanifehpour, Y., Samiei, M., Kouhi, M. and Nejati-Koshki, K., (2013). Liposome: classification, preparation, and applications. *Nanoscale Research Letters*, 8(1), pp.2-9.

Akhtar, M., Ghali, L., Wang, S., Bell, C., Li, D. and Wen, S., (2019). Optimisation of Folate-Mediated Liposomal Encapsulated Arsenic Trioxide for Treating HPV-Positive Cervical Cancer Cells In Vitro. *International Journal of Molecular Sciences*, 20(9), pp.1-20.

Akin, S., Can, G., Aydiner, A., Ozdilli, K. and Durna, Z., (2010). Quality of life, symptom experience and distress of lung cancer patients undergoing chemotherapy. *European Journal of Oncology Nursing*, 14(5), pp.400-409.

Alaufi, O., Noorwali, A., Zahran, F., Al-Abd, A. and Al-Attas, S., (2017). Cytotoxicity of thymoquinone alone or in combination with cisplatin (CDDP) against oral squamous cell carcinoma in vitro. *Scientific Reports*, 7(1), 1-12.

Alhosin, M., Abusnina, A., Achour, M., Sharif, T., Muller, C., Peluso, J., Chataigneau, T., Lugnier, C., Schini-Kerth, V., Bronner, C. and Fuhrmann, G., (2010). Induction of apoptosis by thymoquinone in lymphoblastic leukemia Jurkat cells is mediated by a p73-dependent pathway which targets the epigenetic integrator UHRF1. *Biochemical Pharmacology*, 79(9), pp.1251-1260.

Alhosin, M., Ibrahim, A., Boukhari, A., Sharif, T., Gies, J., Auger, C. and Schini-Kerth, V., (2011). Anti-neoplastic agent thymoquinone induces degradation of α and β tubulin proteins in human cancer cells without affecting their level in normal human fibroblasts. *Investigational New Drugs*, 30(5), pp.1813-1819.

Aliosmanoglu, A., (2012). Nanotechnology in Cancer Treatment, *Journal of Nanomedicine & Biotherapeutic Discovery*, 2(4), pp.1–3.

Alkharfy, K., Ahmad, A., Jan, B. and Raish, M., (2018). Thymoquinone reduces mortality and suppresses early acute inflammatory markers of sepsis in a mouse model. *Biomedicine & Pharmacotherapy*, 98, pp.801-805.

Alkharfy, K., Ahmad, A., Khan, R. and Al-Shagha, W., (2014). Pharmacokinetic plasma behaviors of intravenous and oral bioavailability of thymoquinone in a rabbit model. *European Journal of Drug Metabolism and Pharmacokinetics*, 40(3), pp.319-323.

Allen, T. and Cullis, P., (2013). Liposomal drug delivery systems: From concept to clinical applications. *Advanced Drug Delivery Reviews*, 65(1), pp.36-48.

Allen, T. M., (2002). Ligand-targeted therapeutics in anticancer therapy, *Nature Reviews Cancer*, 2(10), pp. 750–763.

Alobaedi, O., Talib, W. and Basheti, I., (2017). Antitumor effect of thymoquinone combined with resveratrol on mice transplanted with breast cancer. *Asian Pacific Journal of Tropical Medicine*, 10(4), pp.400-408.

Amin, A., Gali-Muhtasib, H., Ocker, M. and Schneider-Stock, R. (2009). Overview of major classes of plant-derived anticancer drugs, *International Journal of Biomedical Science*, 5(1), pp.1–11.

Amin, B. and Hosseinzadeh, H., (2016). Black Cumin (Nigella sativa) and Its Active Constituent, Thymoquinone: An Overview on the Analgesic and Anti-inflammatory Effects, *Planta Medica*, pp. 8–16.

Ansar, F., Latifah, S., Kamal, W., Khong, K., Ng, Y., Foong, J., Gopalsamy, B., Ng, W., How, C., Ong, Y., Abdullah, R. and Aziz, M., (2020). Pharmacokinetics and biodistribution of thymoquinone-loaded nanostructured lipid carrier after oral and intravenous administration into rats, *International Journal of Nanomedicine*, 15, pp. 7703–7717.

Arafa, E., Zhu, Q., Shah, Z., Wani, G., Barakat, B., Racoma, I., El-Mahdy, M. and Wani, A., (2011). Thymoquinone up-regulates PTEN expression and induces apoptosis in doxorubicin-resistant human breast cancer cells. *Mutation*

Research/Fundamental and Molecular Mechanisms of Mutagenesis, 706(1-2), pp.28-35.
Arbyn, M., Ronco, G., Anttila, A., Meijer, C., Poljak, M., Ogilvie, G., Koliopoulos, G., Naucler, P., Sankaranarayanan, R. and Peto, J., (2012). Evidence Regarding Human Papillomavirus Testing in Secondary Prevention of Cervical Cancer. *Vaccine*, 30, pp.F88-F99.
Aref-Adib, M. and Freeman-Wang, T., (2016). Cervical cancer prevention and screening: the role of human papillomavirus testing., *Obstetrician & Gynaecologist*, 18(4), pp. 251–263.

Arruebo, M., Vilaboa, N., Sáez-Gutierrez, B., Lambea, J., Tres, A., Valladares, M. and González-Fernández, Á., (2011). Assessment of the Evolution of Cancer Treatment Therapies. *Cancers*, 3(3), pp.3279-3330.

Asaduzzaman Khan, M., Tania, M., Fu, S. and Fu, J., (2017). Thymoquinone, as an anticancer molecule: from basic research to clinical investigation. *Oncotarget*, 8(31), pp.51907-51919.

Ashour, A., Abd-Allah, A., Korashy, H., Attia, S., Alzahrani, A., Saquib, Q., Bakheet, S., Abdel-Hamied, H., Jamal, S. and Rishi, A., (2014). Thymoquinone suppression of the human hepatocellular carcinoma cell growth involves inhibition of IL-8 expression, elevated levels of TRAIL receptors, oxidative stress and apoptosis. *Molecular and Cellular Biochemistry*, 389(1-2), pp.85-98.

Ashour, A., Ahmed, A., Kumar, A., Zoheir, K., Aboul-Soud, M., Ahmad, S., Attia, S., Abd-Allah, A., Cheryan, V. and Rishi, A., (2016). Thymoquinone inhibits growth of human medulloblastoma cells by inducing oxidative stress and caspase-dependent apoptosis while suppressing NF-κB signaling and IL-8 expression. *Molecular and Cellular Biochemistry*, 416(1-2), pp.141-155.

Aslani, F., Safaei, A., Pourjabali, M. and Momtahan, M., (2013). Evaluation of Ki67, p16 and CK17 markers in differentiating cervical intraepithelial Neoplasia and benign lesions, *Iranian Journal of Medical Sciences*, 38(1), pp.15–21.

Attia, M., Anton, N., Wallyn, J., Omran, Z. and Vandamme, T., (2019). An overview of active and passive targeting strategies to improve the nanocarriers efficiency to tumour sites. *Journal of Pharmacy and Pharmacology*, 71(8), pp.1185-1198.

Badr, G., Mohany, M. and Abu-Tarboush, F., (2011). Thymoquinone decreases F-actin polymerization and the proliferation of human multiple myeloma cells by suppressing STAT3 phosphorylation and Bcl2/Bcl-XL expression. *Lipids in Health and Disease*, 10(1), p.236.

Baig, S., Seevasant, I., Mohamad, J., Mukheem, A., Huri, H. and Kamarul, T., (2016). Potential of apoptotic pathway-targeted cancer therapeutic research: Where do we stand?. *Cell Death & Disease*, 7(1), pp.e2058-e2058.

Bailey, A. L. and Cullis, P. R., (1997). Liposome Fusion, in *Current Topics in Membranes (Lipid polymorphism and membrane properties)*, 44, pp.359–373.

Balasubramaniam, S., Balakrishnan, V., Oon, C. and Kaur, G., (2019). Key Molecular Events in Cervical Cancer Development. *Medicina*, 55(7), pp.1-13.

Balazs, D. and Godbey, W., (2011). Liposomes for Use in Gene Delivery. *Journal of Drug Delivery*, 2011, pp.1-12.

Ballout, F., Habli, Z., Rahal, O., Fatfat, M. and Gali-Muhtasib, H., (2018). Thymoquinone-based nanotechnology for cancer therapy: promises and challenges. *Drug Discovery Today*, 23(5), pp.1089-1098.

Banerjee, R. and Kamrava, M., (2014). Brachytherapy in the treatment of cervical cancer: A review, *International Journal of Women's Health*, 6(1), pp. 555–564

Banerjee, S., Azmi, A., Padhye, S., Singh, M., Baruah, J., Philip, P., Sarkar, F. and Mohammad, R., (2010). Structure-Activity Studies on Therapeutic Potential of Thymoquinone Analogs in Pancreatic Cancer. *Pharmaceutical Research*, 27(6), pp.1146-1158.

Banerjee, S., Padhye, S., Azmi, A., Wang, Z., Philip, P., Kucuk, O., Sarkar, F. and Mohammad, R., (2010). Review on Molecular and Therapeutic Potential of Thymoquinone in Cancer. *Nutrition and Cancer*, 62(7), pp.938-946.

Bashmail, H., Alamoudi, A., Noorwali, A., Hegazy, G., AJabnoor, G., Choudhry, H. and Al-Abd, A., (2018). Thymoquinone synergizes gemcitabine anti-breast cancer activity via modulating its apoptotic and autophagic activities. *Scientific Reports*, 8(1), pp.1-11

Beg, S., Swain, S., Rizwan, M., Irfanuddin, M. and Shobha Malini, D., (2011). Bioavailability Enhancement Strategies: Basics, Formulation Approaches and Regulatory Considerations. *Current Drug Delivery*, 8(6), pp.691-702.

Bekkers, R., Keyser, K., Bulten, J., Hanselaar, A., Schijf, C., Boonstra, H. and Massuger, L., (2002). The value of loop electrosurgical conization in the treatment of stage IA1 microinvasive carcinoma of the uterine cervix. *International Journal of Gynecologic Cancer*, 12(5), pp.485-489.

Bertrand, N., Wu, J., Xu, X., Kamaly, N. and Farokhzad, O., (2014). Cancer nanotechnology: The impact of passive and active targeting in the era of modern cancer biology. *Advanced Drug Delivery Reviews*, 66, pp.2-25.

Bhattacharya, S., Ahir, M., Patra, P., Mukherjee, S., Ghosh, S., Mazumdar, M., Chattopadhyay, S., Das, T., Chattopadhyay, D. and Adhikary, A., (2015). PEGylated-thymoquinone-nanoparticle mediated retardation of breast cancer cell migration by deregulation of cytoskeletal actin polymerization through miR-34a. *Biomaterials*, 51, pp.91-107.

Bodily, J. M. and Meyers, C., (2005). Genetic Analysis of the Human Papillomavirus Type 31 Differentiation-Dependent Late Promoter, *Journal of Virology*, 79(6), pp. 3309–3321.

Braaten, K. P. and Laufer, M. R., (2008). Human Papillomavirus (HPV), HPV-Related Disease, and the HPV Vaccine.," *Reviews in obstetrics & gynecology*, 1(1), pp.2–10.

Briuglia, M., Rotella, C., McFarlane, A. and Lamprou, D., (2015). Influence of cholesterol on liposome stability and on in vitro drug release. *Drug Delivery and Translational Research*, 5(3), pp.231-242.

Buchanan, F. G. and DuBois, R. N., (2006). Connecting COX-2 and Wnt in cancer, *Cancer Cell*, 9(1), pp.6–8.

Bulbake, U., Doppalapudi, S., Kommineni, N. and Khan, W., (2017). Liposomal Formulations in Clinical Use: An Updated Review. *Pharmaceutics*, 9(4), pp.2-33.

Burd, E. M., (2003). Human papillomavirus and cervical cancer., *Clinical microbiology reviews*, 16(1), pp.1–17.

Burits, M. and Bucar, F., (2000). Antioxidant activity of Nigella sativa essential oil, *Phytotherapy Research*, 14(5), pp.323–328.

Butt, A. S., Nisar, N., Ghani, N., Altaf, I. and Mughal, T. (2019). Isolation of thymoquinone from nigella sativa L. And thymus vulgaris L., and its anti-proliferative effect on HeLa cancer cell lines, *Tropical Journal of Pharmaceutical Research*, 18(1), pp.37-42.

Byrne, J., Betancourt, T. and Brannon-Peppas, L., (2008). Active targeting schemes for nanoparticle systems in cancer therapeutics. *Advanced Drug Delivery Reviews*, 60(15), pp.1615-1626.

Byun, J., Jeong, D., Kim, Y., Jung, E., Lee, K., Sung, M. and Kim, K., (2018). Persistent HPV-16 infection leads to recurrence of high-grade cervical intraepithelial neoplasia. *Medicine*, 97(51), pp.1-6.

Castle, P., Schiffman, M., Wheeler, C. and Solomon, D., (2009). Evidence for Frequent Regression of Cervical Intraepithelial Neoplasia–Grade 2. *Obstetrics & Gynecology*, 113(1), pp.18-25.

Cecarini, V., Quassinti, L., Di Blasio, A., Bonfili, L., Bramucci, M., Lupidi, G., Cuccioloni, M., Mozzicafreddo, M., Angeletti, M. and Eleuteri, A., (2010). Effects of thymoquinone on isolated and cellular proteasomes. *FEBS Journal*, 277(9), pp.2128-2141.

Čeh, B. and Lasic, D. D., (1995). A Rigorous Theory of Remote Loading of Drugs into Liposomes, *Langmuir*, 11(9), pp.3356–3368.

Chakrabarti, O., Veeraraghavalu, K., Tergaonkar, V., Liu, Y., Androphy, E., Stanley, M. and Krishna, S., (2004). Human Papillomavirus Type 16 E6 Amino Acid 83 Variants Enhance E6-Mediated MAPK Signaling and Differentially Regulate Tumorigenesis by Notch Signaling and Oncogenic Ras. *Journal of Virology*, 78(11), pp.5934-5945.

Chehl, N., Chipitsyna, G., Gong, Q., Yeo, C. and Arafat, H., (2009). Anti-inflammatory effects of the Nigella sativa seed extract, thymoquinone, in pancreatic cancer cells. *HPB*, 11(5), pp.373-381.

Chen, M., Lee, N., Hsu, H., Ho, T., Tu, C., Hsieh, D., Lin, Y., Chen, L., Kuo, W. and Huang, C., (2015). Thymoquinone Induces Caspase-Independent, Autophagic Cell Death in CPT-11-Resistant LoVo Colon Cancer via Mitochondrial Dysfunction and Activation of JNK and p38. *Journal of Agricultural and Food Chemistry*, 63(5), pp.1540-1546.

Cheung, A., Bax, H., Josephs, D., Ilieva, K., Pellizzari, G., Opzoomer, J., Bloomfield, J., Fittall, M., Grigoriadis, A., Figini, M., Canevari, S., Spicer, J., Tutt, A. and

Karagiannis, S., (2016). Targeting folate receptor alpha for cancer treatment. *Oncotarget*, 7(32), pp.52553-52574.

Chiani, M., Norouzian, D., Shokrgozar, M., Azadmanesh, K., Najmafshar, A., Mehrabi, M. and Akbarzadeh, A., (2017). Folic acid conjugated nanoliposomes as promising carriers for targeted delivery of bleomycin. *Artificial Cells, Nanomedicine, and Biotechnology*, 46(4), pp.757-763.

Chidambaram, M., Manavalan, R. and Kathiresan, K., (2011). Nanotherapeutics to Overcome Conventional Cancer Chemotherapy Limitations. *Journal of Pharmacy & Pharmaceutical Sciences*, 14(1), pp.60-66.

Cho, H., Lee, C. and Lee, Y., (2015). Preparation and Evaluation of PEGylated and Folate-PEGylated Liposomes Containing Paclitaxel for Lymphatic Delivery. *Journal of Nanomaterials*, 2015, pp.1-10.

Chou, R., Hsieh, S., Yu, Y., Huang, M., Huang, Y. and Hsieh, Y., (2013). Fisetin Inhibits Migration and Invasion of Human Cervical Cancer Cells by Down-Regulating Urokinase Plasminogen Activator Expression through Suppressing the p38 MAPK-Dependent NF-κB Signaling Pathway. *PLoS ONE*, 8(8), pp.1-12.

Chowdhury, R., Singhvi, A., Bagul, N., Bhatia, S., Singh, G. and Goswami, S., (2018). Sex determination by amplification of amelogenin gene from dental pulp tissue by polymerase Chain Reaction. *Indian Journal of Dental Research*, 29(4), pp.470-476.

Chrysostomou, A., Stylianou, D., Constantinidou, A. and Kostrikis, L., (2018). Cervical Cancer Screening Programs in Europe: The Transition Towards HPV Vaccination and Population-Based HPV Testing. *Viruses*, 10(12), pp.1-35.

Chung, K., Choi, J., Back, N., Choi, M., Kang, E., Chung, H., Jeong, T. and Lee, K., (2010). Eupafolin, a flavonoid isolated from Artemisia Princeps, induced apoptosis in human cervical adenocarcinoma HeLa cells. *Molecular Nutrition & Food Research*, 54(9), pp.1318-1328.

Ciavattini, A., Sopracordevole, F., Di Giuseppe, J., Moriconi, L., Lucarini, G., Mancioli, F., Zizzi, A. and Goteri, G., (2016). Cervical intraepithelial neoplasia in pregnancy: Interference of pregnancy status with p16 and Ki-67 protein expression. *Oncology Letters*, 13(1), pp.301-306.

Cryer, A. and Thorley, A., (2019). Nanotechnology in the diagnosis and treatment of lung cancer. *Pharmacology & Therapeutics*, 198, pp.189-205.

Cui, S., Zhi, D., Zhao, Y., Chen, H., Meng, Y., Zhang, C. and Zhang, S., (2016). Cationic liposomes with folic acid as targeting ligand for gene delivery. *Bioorganic & Medicinal Chemistry Letters*, 26(16), pp.4025-4029.

Cutts, F., (2007). Human papillomavirus and HPV vaccines: a review. *Bulletin of the World Health Organization*, 85(09), pp.719-726.

Damery, S., Gratus, C., Grieve, R., Warmington, S., Jones, J., Routledge, P., Greenfield, S., Dowswell, G., Sherriff, J. and Wilson, S., (2011). The use of herbal medicines by people with cancer: a cross-sectional survey. *British Journal of Cancer*, 104(6), pp.927-933.

Danhier, F., Feron, O. and Préat, V., (2010). To exploit the tumor microenvironment: Passive and active tumor targeting of nanocarriers for anti-cancer drug delivery. *Journal of Controlled Release*, 148(2), pp.135-146.

Dasari, S. and Tchounwou, P. B., (2014). Cisplatin in cancer therapy: molecular mechanisms of action.," *European journal of pharmacology*, 740, pp.364–78.

Dastjerdi, M., Mehdiabady, E., Iranpour, F. and Bahramian, H., (2016). Effect of thymoquinone on P53 gene expression and consequence apoptosis in breast cancer cell line. *International Journal of Preventive Medicine*, 7(1), pp.1-6.

Day, P., Baker, C., Lowy, D. and Schiller, J., (2004). Establishment of papillomavirus infection is enhanced by promyelocytic leukemia protein (PML) expression. *Proceedings of the National Academy of Sciences*, 101(39), pp.14252-14257.

Day, P., Lowy, D. and Schiller, J., (2008). Heparan Sulfate-Independent Cell Binding and Infection with Furin-Precleaved Papillomavirus Capsids. *Journal of Virology*, 82(24), pp.12565-12568.

D'Costa, Z., Jolly, C., Androphy, E., Mercer, A., Matthews, C. and Hibma, M., (2012). Transcriptional Repression of E-Cadherin by Human Papillomavirus Type 16 E6. *PLoS ONE*, 7(11), p.e48954. D'Costa, Z., Jolly, C., Androphy, E., Mercer, A., Matthews, C. and Hibma, M., 2012. Transcriptional Repression of E-Cadherin by Human Papillomavirus Type 16 E6. *PLoS ONE*, 7(11), p.1-10.

De Marco, F., (2013). Oxidative stress and HPV carcinogenesis, *Viruses*, pp.708–731.

DeSantis, C., Lin, C., Mariotto, A., Siegel, R., Stein, K., Kramer, J., Alteri, R., Robbins, A. and Jemal, A., (2014). Cancer treatment and survivorship statistics, 2014. *CA: A Cancer Journal for Clinicians*, 64(4), pp.252-271.

Deshpande, P., Biswas, S. and Torchilin, V., (2013). Current trends in the use of liposomes for tumor targeting. *Nanomedicine*, 8(9), pp.1509-1528.

Diaz, J., Yu, D., Micaily, B., Ferriss, J. and Hernandez, E., (2014). Radiation Therapy with Concurrent Chemotherapy for Locally Advanced Cervical Carcinoma: Outcome Analysis with Emphasis on the Impact of Treatment Duration on Outcome. *Obstetrics and Gynecology International*, 2014, pp.1-6.

Dine, J., GordoN, R., Shames, Y., Kasler, M., Barton-Burke, M., (2017). Immune Checkpoint Inhibitors: An Innovation in Immunotherapy, *Asia Pac J Oncol Nurs*, 4(2), pp.127–135.

Doorbar, J., Quint, W., Banks, L., Bravo, I., Stoler, M., Broker, T. and Stanley, M., (2012). The Biology and Life-Cycle of Human Papillomaviruses. *Vaccine*, 30, pp.F55-F70.

Drulis-Kawa, Z. and Dorotkiewicz-Jach, A., (2010). Liposomes as delivery systems for antibiotics, *International Journal of Pharmaceutics*, pp.187–198.

Duarte-Franco, E. and Franco, E. L., (2004). Cancer of the Uterine Cervix, *BMC Women's Health*, 4(1), pp.S1-S10.

Ducat, E., Evrard, B., Peulen, O. and Piel, G., (2011). Cellular uptake of liposomes monitored by confocal microscopy and flow cytometry. *Journal of Drug Delivery Science and Technology*, 21(6), pp.469-477.

Dunton, C., (2008). A review of topotecan in combination chemotherapy for advanced cervical cancer. *Therapeutics and Clinical Risk Management*, Volume 4, pp.213-218.

Egawa, K., (2003). Do human papillomaviruses target epidermal stem cells?, *Dermatology*, 207(3), pp.251–254.

Egawa, N., Egawa, K., Griffin, H. and Doorbar, J., (2015). Human Papillomaviruses; Epithelial Tropisms, and the Development of Neoplasia. *Viruses*, 7(7), pp.3863-3890.

Egusquiaguirre, S., Igartua, M., Hernández, R. and Pedraz, J., (2012). Nanoparticle delivery systems for cancer therapy: advances in clinical and preclinical research. *Clinical and Translational Oncology*, 14(2), pp.83-93.

El-Far, A. H., (2015).Thymoquinone Anticancer Discovery: Possible Mechanisms., *Current drug discovery technologies*, 12(2), pp.80-89.

Ellis, B. R. and Barret D. T., (2009). The enigma of yellow fever in East Africa, *Reviews in medical virology*, 19(1), pp.57-64.

Elmowafy, M., Samy, A., Raslan, M., Salama, A., Said, R., Abdelaziz, A., El-Eraky, W., El Awdan, S. and Viitala, T., (2015). Enhancement of Bioavailability and Pharmacodynamic Effects of Thymoquinone Via Nanostructured Lipid Carrier (NLC) Formulation. *AAPS PharmSciTech*, 17(3), pp.663-672.

Elst, P., Ahankour, F. and Tjalma., (2007). Management of recurrent cervical cancer. Review of the literature and case report, *European Journal of Gynaecological Oncology*, 28(6), pp.435-441.

Ernsting, M., Murakami, M., Roy, A. and Li, S., (2013). Factors controlling the pharmacokinetics, biodistribution and intratumoral penetration of nanoparticles. *Journal of Controlled Release*, 172(3), pp.782-794.

Faridi, R., Zahra, A., Khan, K. and Idrees, M., (2011). Oncogenic potential of Human Papillomavirus (HPV) and its relation with cervical cancer. *Virology Journal*, 8(1), pp.2-8.

Fatfat, M., Fakhoury, I., Habli, Z., Mismar, R. and Gali-Muhtasib, H., (2019). Thymoquinone enhances the anticancer activity of doxorubicin against adult T-cell leukemia in vitro and in vivo through ROS-dependent mechanisms. *Life Sciences*, 232, pp.1-19.

Fernández, M., Javaid, F. and Chudasama, V., (2018). Advances in targeting the folate receptor in the treatment/imaging of cancers. *Chemical Science*, 9(4), pp.790-810.

Ferrigno, R., Santos, A., Martins, L., Weltman, E., Chen, M., Sakuraba, R., Lopes, C. and Cruz, J., (2010). Comparison of conformal and intensity modulated radiation therapy techniques for treatment of pelvic tumors. Analysis of acute toxicity. *Radiation Oncology*, 5(1), pp.1-7.

Finocchario-Kessler, S., Wexler, C., Maloba, M., Mabachi, N., Ndikum-Moffor, F. and Bukusi, E., (2016). Cervical cancer prevention and treatment research in Africa: a systematic review from a public health perspective. *BMC Women's Health*, 16(1), pp.1-25.

Fogleman, C. and Leaman, L., (2019). Prophylactic vaccination against human papillomavirus to prevent cervical cancer and its precursors, *American Family Physician*, 99(1), pp.15-17.

Fridman, J. S. and Lowe, S. W., (2003). Control of apoptosis by p53," *Oncogene*. Nature Publishing Group, 8(22), pp.9030-9040.

Fröhlich, E., (2012). The role of surface charge in cellular uptake and cytotoxicity of medical nanoparticles. *International Journal of Nanomedicine*, 7, pp.5577-5591.

Gali-Muhtasib, H., Diab-Assaf., Boltze, C., Al-Hamira, J., Harting, R., Roessner, A. and Schneider-Stock, R., (2004). Thymoquinone extracted from black seed triggers apoptotic cell death in human colorectal cancer cells via a p53-dependent mechanism., *International journal of oncology*, 25(4), pp. 857-866.

Gali-Muhtasib, H., Ocker, M., Kuester, D., Krueger, S., El-Hajj, Z., Diestel, A., Evert, M., El-Najjar, N., Peters, B., Jurjus, A., Roessner, A. and Schneider-Stock, R., (2007). Thymoquinone reduces mouse colon tumor cell invasion and inhibits tumor growth in murine colon cancer models. *Journal of Cellular and Molecular Medicine*, 12(1), pp.330-342.

Gali-Muhtasib, H., Roessner, A. and Schneider-Stock, R., (2006). Thymoquinone: A promising anti-cancer drug from natural sources. *The International Journal of Biochemistry & Cell Biology*, 38(8), pp.1249-1253.

Gallaher, J., Enriquez-Navas, P., Luddy, K., Gatenby, R. and Anderson, A., (2018). Spatial Heterogeneity and Evolutionary Dynamics Modulate Time to Recurrence in Continuous and Adaptive Cancer Therapies. *Cancer Research*, 78(8), pp.2127-2139.

García, C., Hernández-García, D., Valencia, C., Rojo-León, V., Pérez-Estrada, J., Werner, M. and Covarrubias, L., (2017). E6/E7 oncogenes in epithelial suprabasal layers and estradiol promote cervical growth and ear regeneration. *Oncogenesis*, 6(8), pp.e374-e374.

Gariglio, P. and Organista Nava, J., (2016). Role of HR-HPVs E6 and E7 Oncoproteins in Cervical Carcinogenesis. *Journal of Molecular and Genetic Medicine*, 10(2), pp.1-11.

Garnett, T. O. and Duerksen-Hughes, P. J., (2006). Modulation of apoptosis by human papillomavirus (HPV) oncoproteins, *Archives of Virology*, 151(12), pp.2321-2335.

Gewin, L., Myers, H., Kiyono, T. and Galloway, D., (2004). Identification of a novel telomerase repressor that interacts with the human papillomavirus type-16 E6/E6-AP complex. *Genes & Development*, 18(18), pp.2269-2282.

Ghaem-Maghami, S., Sagi, S., Majeed, G. and Soutter, W., (2007). Incomplete excision of cervical intraepithelial neoplasia and risk of treatment failure: a meta-analysis. *The Lancet Oncology*, 8(11), pp.985-993.

Ghosheh, O., Houdi, A. and Crooks, P., (1999). High performance liquid chromatographic analysis of the pharmacologically active quinones and related compounds in the oil of the black seed (Nigella sativa L.). *Journal of Pharmaceutical and Biomedical Analysis*, 19(5), pp.757-762.

Gius, D., Funk, M., Chuang, E., Feng, S., Huettner, P., Nguyen, L., Bradbury, C., Mishra, M., Gao, S., Buttin, B., Cohn, D., Powell, M., Horowitz, N., Whitcomb, B. and Rader, J., (2007). Profiling Microdissected Epithelium and Stroma to Model Genomic Signatures for Cervical Carcinogenesis Accommodating for Covariates. *Cancer Research*, 67(15), pp.7113-7123.

Gizzo, S., Ancona, E., Saccardi, C., Patrell, T., Berretta, R., Anis, O., Noventa, M., Bertocco, A., Fagherazi, S., Longone, M., Vendemiati, L., Dantona, D. and Nardel, G., (2013). Radical trachelectomy: The first step of fertility preservation in young women with cervical cancer (Review). *Oncology Reports*, 30(6), pp.2545-2554.

Glamočlija, U., Padhye, S., Špirtović-Halilović, S., Osmanović, A., Veljović, E., Roca, S., Novaković, I., Mandić, B., Turel, I., Kljun, J., Trifunović, S., Kahrović, E., Kraljević Pavelić, S., Harej, A., Klobučar, M. and Završnik, D., (2018). Synthesis, Biological Evaluation and Docking Studies of Benzoxazoles Derived from Thymoquinone. *Molecules*, 23(12), pp.1-17.

Goel, S. and Mishra, P., (2019). Thymoquinone loaded mesoporous silica nanoparticles retard cell invasion and enhance in vitro cytotoxicity due to ROS mediated apoptosis in HeLa and MCF-7 cell lines, *Materials Science and Engineering C*, 104(1), pp.1-36.

Gottesman, M. and Ling, V., (2005). The molecular basis of multidrug resistance in cancer: The early years of P-glycoprotein research. *FEBS Letters*, 580(4), pp.998-1009.

Goyal, P., Goyal, K., Kumar, V, G, S., Singh, A., Katare, P, O. and Mishra, N, D., (2005). Liposomal drug delivery systems - Clinical applications, *Acta Pharmaceutica*, 55(1), pp.1-25.

Goyal, S., Prajapati, C., Gore, P., Patil, C., Mahajan, U., Sharma, C., Talla, S. and Ojha, S., (2017). Therapeutic Potential and Pharmaceutical Development of Thymoquinone: A Multitargeted Molecule of Natural Origin. *Frontiers in Pharmacology*, 8, pp.1-19.

Graham, S., (2010). Human papillomavirus: gene expression, regulation and prospects for novel diagnostic methods and antiviral therapies. *Future Microbiology*, 5(10), pp.1493-1506.

Gravante, G., Filingeri, V., Delogu, D., Santeusanio, G., Palmieri, M., Esposito, G., Montone, A. and Sconoccia, G., (2006). Apoptotic cell death in deep partial thickness burns by coexpression analysis of TUNEL and Fas. *Surgery*, 139(6), pp.854-855.

Gurung, R., Lim, S., Khaw, A., Soon, J., Shenoy, K., Mohamed Ali, S., Jayapal, M., Sethu, S., Baskar, R. and Hande, M., (2010). Thymoquinone Induces Telomere Shortening, DNA Damage and Apoptosis in Human Glioblastoma Cells. *PLoS ONE*, 5(8), pp.1-11.

Gyöngyösi, E., Szalmás, A., Ferenczi, A., Kónya, J., Gergely, L. and Veress, G., (2012). Effects of human papillomavirus (HPV) type 16 oncoproteins on the expression of involucrin in human keratinocytes. *Virology Journal*, 9(1), pp.1-12.

Haley, B. and Frenkel, E.. (2008) Nanoparticles for drug delivery in cancer treatment," *Urologic Oncology: Seminars and Original Investigations*, 26(1), pp.57-64.

Handali, S., Moghimipour, E., Rezaei, M., Ramezani, Z., Kouchak, M., Amini, M., Angali, K., Saremy, S. and Dorkoosh, F., (2018). A novel 5-Fluorouracil targeted delivery to colon cancer using folic acid conjugated liposomes. *Biomedicine & Pharmacotherapy*, 108, pp.1259-1273.

Harari, A., Chen, Z. and Burk, D, R., (2014) Human papillomavirus genomics: Past, present and future," *Current Problems in Dermatology (Switzerland)*. NIH Public Access, pp.1-21.

Haron, A., Syed Alwi, S., Saiful Yazan, L., Abd Razak, R., Ong, Y., Zakarial Ansar, F. and Roshini Alexander, H., (2018). Cytotoxic Effect of Thymoquinone-Loaded Nanostructured Lipid Carrier (TQ-NLC) on Liver Cancer Cell Integrated with Hepatitis B Genome, Hep3B. *Evidence-Based Complementary and Alternative Medicine*, 2018, pp.1-13.

Hatakeyama, H., Akita, H. and Harashima, H., (2013). The Polyethyleneglycol Dilemma: Advantage and Disadvantage of PEGylation of Liposomes for Systemic Genes and Nucleic Acids Delivery to Tumors. *Biological and Pharmaceutical Bulletin*, 36(6), pp.892-899.

He, W., Staples, D., Smith, C. and Fisher, C., (2003). Direct Activation of Cyclin-Dependent Kinase 2 by Human Papillomavirus E7. *Journal of Virology*, 77(19), pp.10566-10574.

Hellner, K., Mar, J., Fang, F., Quackenbush, J. and Münger, K., (2009). HPV16 E7 oncogene expression in normal human epithelial cells causes molecular changes indicative of an epithelial to mesenchymal transition. *Virology*, 391(1), pp.57-63.

Herfs, M., Yamamoto, Y., Laury, A., Wang, X., Nucci, M., McLaughlin-Drubin, M., Munger, K., Feldman, S., McKeon, F., Xian, W. and Crum, C., (2012). A discrete population of squamocolumnar junction cells implicated in the pathogenesis of cervical cancer. *Proceedings of the National Academy of Sciences*, 109(26), pp.10516-10521.

Herrero, R., González, P. and Markowitz, L., (2015). Present status of human papillomavirus vaccine development and implementation. *The Lancet Oncology*, 16(5), pp.e206-e216.

Hosseinzadeh, H. and Parvardeh, S. (2004) "Anticonvulsant effects of thymoquinone, the major constituent of," *Control*, 11(1), pp.56-64.

Hsiao, Y., Lin, C., Wang, P., Hsin, M. and Yang, S., (2019). The Potential of Chinese Herbal Medicines in the Treatment of Cervical Cancer. *Integrative Cancer Therapies*, 18, pp.1-9.

Hsu, H., Chen, M., Day, C., Lin, Y., Li, S., Tu, C., Padma, V., Shih, H., Kuo, W. and Huang, C., (2017). Thymoquinone suppresses migration of LoVo human colon cancer

cells by reducing prostaglandin E2 induced COX-2 activation. *World Journal of Gastroenterology*, 23(7), pp.1171-1170.

Hu, C. and Zhang, L., (2009). Therapeutic Nanoparticles to Combat Cancer Drug Resistance. *Current Drug Metabolism*, 10(8), pp.836-841.

HUANG, Y., COLE, S., CAI, T. and CAI, Y., (2016). Applications of nanoparticle drug delivery systems for the reversal of multidrug resistance in cancer. *Oncology Letters*, 12(1), pp.11-15.

Hui Wu, H., (2018). Multidrug Resistance Transporters and Implications on Drug Development. *Molecular Enzymology and Drug Targets*, 4(1), pp.1.

Huwyler, J., (2008). Tumor targeting using liposomal antineoplastic drugs. *International Journal of Nanomedicine*, 3(1), pp.21-29.

Hwang, S. J. and Shroyer, K. R., (2012) Biomarkers of cervical dysplasia and carcinoma, *Journal of Oncology*, 2012, pp.1-9.

Ichwan, S., Al-Ani, I., Bilal, H., Suriyah, E., Taher, M. and Ikeda, M., (2014). Apoptotic Activities of Thymoquinone, an Active Ingredient of Black Seed (Nigella sativa), in Cervical Cancer Cell Lines. *The Chinese Journal of Physiology*, 57(5), pp.249-255.

Iftner, T., Eberle, S., Iftner, A., Holz, B., Banik, N., Quint, W. and Straube, A., (2010). Prevalence of low-risk and high-risk types of human papillomavirus and other risk factors for HPV infection in Germany within different age groups in women up to 30 years of age: An epidemiological observational study. *Journal of Medical Virology*, 82(11), pp.1928-1939.

Immordino, M., Dosio, F. and Cattel, L*.,* (2006) Stealth liposomes: Review of the basic science, rationale, and clinical applications, existing and potential, *International Journal of Nanomedicine*. Dove Press, 1(3), pp.297-315.

Insinga, R., Glass, A. and Rush, B., (2004). Diagnoses and outcomes in cervical cancer screening: A population-based study. *American Journal of Obstetrics and Gynecology*, 191(1), pp.105-113.

Jafri, S., Glass, J., Shi, R., Zhang, S., Prince, M. and Kleiner-Hancock, H., (2010). Thymoquinone and cisplatin as a therapeutic combination in lung cancer: In vitro and in vivo. *Journal of Experimental & Clinical Cancer Research*, 29(1), pp.1-11.

Jain, A., Pooladanda, V., Bulbake, U., Doppalapudi, S., Rafeeqi, T., Godugu, C. and Khan, W., (2017). Liposphere mediated topical delivery of thymoquinone in the treatment of psoriasis. *Nanomedicine: Nanotechnology, Biology and Medicine*, 13(7), pp.2251-2262.

Jang, M., Piao, X., Kim, J., Kwon, S. and Park, J., (2008). Inhibition of cholinesterase and amyloid-β aggregation by resveratrol oligomers from Vitis amurensis. *Phytotherapy Research*, 22(4), pp.544-549.

Jardim, G., Lima, D., Valença, W., Lima, D., Cavalcanti, B., Pessoa, C., Rafique, J., Braga, A., Jacob, C., da Silva Júnior, E. and da Cruz, E., (2017). Synthesis of Selenium-Quinone Hybrid Compounds with Potential Antitumor Activity via Rh-Catalyzed C-H Bond Activation and Click Reactions. *Molecules*, 23(1), pp.1-16.

Joura, E. A. and Pils, S., (2016) Vaccines against human papillomavirus infections: protection against cancer, genital warts or both?,*Clinical Microbiology and Infection*, 22(2016), pp.S125-S127.

Kalam, M., Raish, M., Ahmed, A., Alkharfy, K., Mohsin, K., Alshamsan, A., Al-Jenoobi, F., Al-Mohizea, A. and Shakeel, F., (2017). Oral bioavailability enhancement and hepatoprotective effects of thymoquinone by self-nanoemulsifying drug delivery system. *Materials Science and Engineering*, 76, pp.319-329.

Kaseb, A., Chinnakannu, K., Chen, D., Sivanandam, A., Tejwani, S., Menon, M., Dou, Q. and Reddy, G., (2007). Androgen Receptor– and E2F-1–Targeted Thymoquinone Therapy for Hormone-Refractory Prostate Cancer. *Cancer Research*, 67(16), pp.7782-7788.

Ke, X., Zhao, Y., Lu, X., Wang, Z., Liu, Y., Ren, M., Lu, G., Zhang, D., Sun, Z., Xu, Z., Song, J., Cheng, Y., Meltzer, S. and He, S., (2015. TQ inhibits hepatocellular carcinoma growth *in vitro* and *in vivo* via repression of Notch signaling. *Oncotarget*, 6(32), pp.32610-32621.

Khan, M. and Smith-McCune, K., (2014). Treatment of Cervical Precancers. *Obstetrics & Gynecology*, 123(6), pp.1339-1343.

KUNDU, J., CHOI, B., JEONG, C., KUNDU, J. and CHUN, K., (2014). Thymoquinone induces apoptosis in human colon cancer HCT116 cells through inactivation of STAT3 by blocking JAK2- and Src-mediated phosphorylation of EGF receptor tyrosine kinase. *Oncology Reports*, 32(2), pp.821-828.

Kuo, P., Hsu, Y. and Cho, C. (2006). Plumbagin induces G2-M arrest and autophagy by inhibiting the AKT/mammalian target of rapamycin pathway in breast cancer cells. *Molecular Cancer Therapeutics*, 5(12), pp.3209-3221.

Lammers, T., Kiessling, F., Hennink, W. and Storm, G., (2012). Drug targeting to tumors: Principles, pitfalls and (pre-) clinical progress. *Journal of Controlled Release*, 161(2), pp.175-187.

Ledermann, J., Canevari, S. and Thigpen, T., (2015). Targeting the folate receptor: diagnostic and therapeutic approaches to personalize cancer treatments. *Annals of Oncology*, 26(10), pp.2034-2043.

Li, F., Rajendran, P. and Sethi, G., (2010). Thymoquinone inhibits proliferation, induces apoptosis and chemosensitizes human multiple myeloma cells through suppression of signal transducer and activator of transcription 3 activation pathway. *British Journal of Pharmacology*, 161(3), pp.541-554.

Li, H., Wu, X. and Cheng, X., (2016). Advances in diagnosis and treatment of metastatic cervical cancer. *Journal of Gynecologic Oncology*, 27(4), pp.1-20.

LI, H., Zhang, S., Wang, Y., Liang, R., Li, J., An, P., Wang, Z., Yang, J. and Li, Z., (2012). Baicalein induces apoptosis via a mitochondrial-dependent caspase activation pathway in T24 bladder cancer cells. *Molecular Medicine Reports*, 7(1), pp.266-270.

Li, J., Khan, M., Wei, C., Cheng, J., Chen, H., Yang, L., Ijaz, I. and Fu, J., (2017). Thymoquinone Inhibits the Migration and Invasive Characteristics of Cervical Cancer

Cells SiHa and CaSki In Vitro by Targeting Epithelial to Mesenchymal Transition Associated Transcription Factors Twist1 and Zeb1. *Molecules*, 22(12), pp.1-12.

Li, L., Kou, X., Feng, X., Zhang, M., Chao, H. and Wang, L., (2015). Postoperative external beam irradiation with and without brachytherapy in pelvic node-positive IB1-IIA2 cervical cancer patients: a retrospective clinical study. *Radiation Oncology*, 10(1), pp.2-6.

Li, X., Stander, M., Van Kriekinge, G. and Demarteau, N., (2015). Cost-effectiveness analysis of human papillomavirus vaccination in South Africa accounting for human immunodeficiency virus prevalence. *BMC Infectious Diseases*, 15(1), pp.1-18.

Library, W. O. and Doorbar, J., (2016) Model systems of human papillomavirus-associated disease, *Journal of Pathology J Pathol*, 238(2), pp.166–179.

Lie, A. K. and Kristensen, G., (2008) Human papillomavirus E6/E7 mRNA testing as a predictive marker for cervical carcinoma, *Expert Review of Molecular Diagnostics*, 8(4), pp.405–415.

Liu, C., Ding, L., Bai, L., Chen, X., Kang, H., Hou, L. and Wang, J., (2017). Folate receptor alpha is associated with cervical carcinogenesis and regulates cervical cancer cells growth by activating ERK1/2/c-Fos/c-Jun. *Biochemical and Biophysical Research Communications*, 491(4), pp.1083-1091.

Liu, X., Dakic, A., Zhang, Y., Dai, Y., Chen, R. and Schlegel, R., (2009). HPV E6 protein interacts physically and functionally with the cellular telomerase complex. *Proceedings of the National Academy of Sciences*, 106(44), pp.18780-18785.

Liu, X., Disbrow, G., Yuan, H., Tomaić, V. and Schlegel, R., (2007). Myc and Human Papillomavirus Type 16 E7 Genes Cooperate To Immortalize Human Keratinocytes. *Journal of Virology*, 81(22), pp.12689-12695.

Longworth, M. S. and Laimins, L. A., (2004) Pathogenesis of Human Papillomaviruses in Differentiating Epithelia, *Microbiology and Molecular Biology Reviews*, 68(2), pp.362-372.

López-Ocejo, O., Viloria-Petit, A., Bequet-Romero, M., Mukhopadhyay, D., Rak, J. and Kerbel, R., (2000). Oncogenes and tumor angiogenesis: the HPV-16 E6 oncoprotein activates the vascular endothelial growth factor (VEGF) gene promoter in a p53 independent manner. *Oncogene*, 19(40), pp.4611-4620.

Lorenz, L., Rivera Cardona, J. and Lambert, P., (2013). Inactivation of p53 Rescues the Maintenance of High Risk HPV DNA Genomes Deficient in Expression of E6. *PLoS Pathogens*, 9(10), pp.1-14.

Low, P., Henne, W. and Doorneweerd, D., (2008). ChemInform Abstract: Discovery and Development of Folic-Acid-Based Receptor Targeting for Imaging and Therapy of Cancer and Inflammatory Diseases. *ChemInform*, 39(18), pp.120-129.

Lupidi, G., Scire, A., Camaioni, E., Khalife, K., De Sanctis, G., Tanfani, F. and Damiani, E., (2010). Thymoquinone, a potential therapeutic agent of Nigella sativa, binds to site I of human serum albumin. *Phytomedicine*, 17(10), pp.714-720.

Malam, Y., Loizidou, M. and Seifalian, A., (2009). Liposomes and nanoparticles: nanosized vehicles for drug delivery in cancer. *Trends in Pharmacological Sciences*, 30(11), pp.592-599.

Martin, C. M. and O'Leary, J. J., (2011) Histology of cervical intraepithelial neoplasia and the role of biomarkers, *Best Practice and Research: Clinical Obstetrics and Gynaecology*, 25(5), pp.605-615.

Martinez-Zapien, D., Ruiz, F., Poirson, J., Mitschler, A., Ramirez, J., Forster, A., Cousido-Siah, A., Masson, M., Pol, S., Podjarny, A., Travé, G. and Zanier, K., (2016). Structure of the E6/E6AP/p53 complex required for HPV-mediated degradation of p53. *Nature*, 529(7587), pp.541-545.

Masgras, I., Carrera, S., de Verdier, P., Brennan, P., Majid, A., Makhtar, W., Tulchinsky, E., Jones, G., Roninson, I. and Macip, S., (2012). Reactive Oxygen Species and Mitochondrial Sensitivity to Oxidative Stress Determine Induction of Cancer Cell Death by p21. *Journal of Biological Chemistry*, 287(13), pp.9845-9854.

McBride, A., (2013). The Papillomavirus E2 proteins. *Virology*, 445(1-2), pp.57-79.

McBride, A., Romanczuk, H. and Howley, P., (1991). The papillomavirus E2 regulatory proteins. *Journal of Biological Chemistry*, 266(28), pp.18411-18414.

McLaughlin-Drubin, M. E., Park, D. and Munger, K., (2013) Tumor suppressor p16INK4A is necessary for survival of cervical carcinoma cell lines, *Proceedings of the National Academy of Sciences of the United States of America*, 110(40), pp.16175-16180.

McNeil, S. E., (2005) Nanotechnology for the biologist, *Journal of Leukocyte Biology*, 78(3), pp.585-594.

Meissner, J. D., (1999) Nucleotide sequences and further characterization of human papillomavirus DNA present in the CaSki, SiHa and HeLa cervical carcinoma cell lines, *Journal of General Virology*, 80(7), pp.1725-1733.

Mello, C. F., (2013) Vaccination against human papillomavirus., *Einstein (São Paulo, Brazil)*, 11(4), pp.547-549.

Mendoza-Almanza, G., Ortiz-Sanchez, E., Rocha-Zavaleta, L., Rivas-Santiago, C., Esparza-Ibarra, E. and Olmos, J., (2019). Cervical cancer stem cells and other leading factors associated with cervical cancer development (Review). *Oncology Letters*, 18(4), pp.3423-3432.

Mephu, E. and Cril, N., (2004) The Global Transcriptional Effects of the Human Papillomavirus E6 Protein in Cervical Carcinoma Cell Lines Are Mediated by the E6AP Ubiquitin Ligase, *Machine Learning*, 79(6), pp.3737-3747.

Milla, P., Dosio, F. and Cattel, L., (2012). PEGylation of Proteins and Liposomes: a Powerful and Flexible Strategy to Improve the Drug Delivery. *Current Drug Metabolism*, 13(1), pp.105-119.

Mishra, G., Pimple, S. and Shastri, S., (2011). An overview of prevention and early detection of cervical cancers. *Indian Journal of Medical and Paediatric Oncology*, 32(03), pp.125-132.

Misra, R., Acharya, S. and Sahoo, S., (2010). Cancer nanotechnology: application of nanotechnology in cancer therapy. *Drug Discovery Today*, 15(19-20), pp.842-850.

Mognetti, B., Barberis, A., Marino, S., Berta, G., Francia, S., Trotta, F. and Cavalli, R., (2012). In vitro enhancement of anticancer activity of paclitaxel by a Cremophor free cyclodextrin-based nanosponge formulation. *Journal of Inclusion Phenomena and Macrocyclic Chemistry*, 74(1-4), pp.201-210.

Monie, A., Hung, C., Roden, R. and Wu, T., (2008) Cervarix™:A vaccine for the prevention of HPV 16, 18-associated cervical cancer, *Biologics: Targets and Therapy*, 2(1), pp.107-113.

Monteil, J., Maubon, A., Leobon, S., Roux, S., Marin, B., Renaudie, J., Genet, D., Fermeaux, V., Aubard, Y. and Tubiana-Matheiey, N., (2011) Lymph node assessment with 18F-FDG-PET and MRI in uterine cervical cancer, *Anticancer Research*, 31(11), pp.3865-3871.

Moore, D., Donnelly, J., McGuire, W., Almadrones, L., Cella, D., Herzog, T. and Waggoner, S., (2003). Limited Access Trial Using Amifostine for Protection Against Cisplatin- and Three-Hour Paclitaxel–Induced Neurotoxicity: A Phase II Study of the Gynecologic Oncology Group. *Journal of Clinical Oncology*, 21(22), pp.4207-4213.

Morrison, M., Morreale, R., Akunuru, S., Kofron, M., Zheng, Y. and Wells, S., (2011). Targeting the Human Papillomavirus E6 and E7 Oncogenes through Expression of the Bovine Papillomavirus Type 1 E2 Protein Stimulates Cellular Motility. *Journal of Virology*, 85(20), pp.10487-10498.

Mufamadi, M., Pillay, V., Choonara, Y., Du Toit, L., Modi, G., Naidoo, D. and Ndesendo, V., (2011). A Review on Composite Liposomal Technologies for Specialized Drug Delivery. *Journal of Drug Delivery*, 2011, pp.1-19.

Münger, K., Baldwin, A., Edwards, K., Hayakawa, H., Nguyen, C., Owens, M., Grace, M. and Huh, K., (2004). Mechanisms of Human Papillomavirus-Induced Oncogenesis. *Journal of Virology*, 78(21), pp.11451-11460.

Muñoz, N., Castellsagué, X., de González, A. and Gissmann, L., (2006). Chapter 1: HPV in the etiology of human cancer. *Vaccine*, 24, pp.S1-S10.

Nagata, Y., Takahashi, N., Davis, R. and Todokoro, K., (1998). Activation of p38 MAP Kinase and JNK But Not ERK Is Required for Erythropoietin-Induced Erythroid Differentiation. *Blood*, 92(6), pp.1859-1869.

Nam, E., Kim, J., Hong, J., Jang, H., Lee, S., Jang, S., Lee, D., Kim, S., Kim, J., Kim, Y., Kim, S. and Kim, J., (2008). Expression of the p16INK4a and Ki-67 in relation to the grade of cervical intraepithelial neoplasia and high-risk human papillomavirus infection. *Journal of Gynecologic Oncology*, 19(3), pp.162-168.

Narayana, A., (2014) Applications of Nanotechnology in Cancer: A Literature Review of Imaging and Treatment, *Journal of Nuclear Medicine & Radiation Therapy*, 05(04), pp.1-9.

Narisawa-Saito, M. and Kiyono, T., (2007) Basic mechanisms of high-risk human papillomavirus-induced carcinogenesis: Roles of E6 and E7 proteins, *Cancer Science*. Wiley/Blackwell (10.1111), pp.1505-1511.

Ng, W., Saiful Yazan, L., Yap, L., Wan Nor Hafiza, W., How, C. and Abdullah, R., (2015). Thymoquinone-Loaded Nanostructured Lipid Carrier Exhibited Cytotoxicity towards Breast Cancer Cell Lines (MDA-MB-231 and MCF-7) and Cervical Cancer Cell Lines (HeLa and SiHa). *BioMed Research International*, 2015, pp.1-10.

Ng, W., Yazan, L. and Ismail, M., (2011). Thymoquinone from Nigella sativa was more potent than cisplatin in eliminating of SiHa cells via apoptosis with down-regulation of Bcl-2 protein. *Toxicology in Vitro*, 25(7), pp.1392-1398.

Ngoma, M. and Autier, P., (2019) Cancer prevention: Cervical cancer, *Ecancermedicalscience*, 13(952), pp.1–6.

Nguyen, M., Song, S., Liem, A., Androphy, E., Liu, Y. and Lambert, P., (2002). A Mutant of Human Papillomavirus Type 16 E6 Deficient in Binding α-Helix Partners Displays Reduced Oncogenic Potential In Vivo. *Journal of Virology*, 76(24), pp.13039-13048.

Nguyen, V., Min, H., Kim, C., Han, J., Park, J. and Choi, E., (2019). Folate receptor-targeted liposomal nanocomplex for effective synergistic photothermal-chemotherapy of breast cancer in vivo. *Colloids and Surfaces B: Biointerfaces*, 173, pp.539-548.

Nicol, A., de Andrade, C., Gomes, S., Brusadelli, M., Lodin, H., Wells, S. and Nuovo, G., (2019). The distribution of novel biomarkers in carcinoma-in-situ, microinvasive, and squamous cell carcinoma of the uterine cervix. *Annals of Diagnostic Pathology*, 38, pp.115-122.

Nor Rashid, N., Yusof, R. and Watson, R., (2011). Disruption of repressive p130–DREAM complexes by human papillomavirus 16 E6/E7 oncoproteins is required for cell-cycle progression in cervical cancer cells. *Journal of General Virology*, 92(11), pp.2620-2627.

Odeh, F., Ismail, S., Abu-Dahab, R., Mahmoud, I. and Al Bawab, A., (2012). Thymoquinone in liposomes: a study of loading efficiency and biological activity towards breast cancer. *Drug Delivery*, 19(8), pp.371-377.

Ohlenschläger, O., Seiboth, T., Zengerling, H., Briese, L., Marchanka, A., Ramachandran, R., Baum, M., Korbas, M., Meyer-Klaucke, W., Dürst, M. and Görlach, M., (2006). Solution structure of the partially folded high-risk human papilloma virus 45 oncoprotein E7. *Oncogene*, 25(44), pp.5953-5959.

Ong, S., Ming, L., Lee, K. and Yuen, K., (2016). Influence of the Encapsulation Efficiency and Size of Liposome on the Oral Bioavailability of Griseofulvin-Loaded Liposomes. *Pharmaceutics*, 8(3), pp.2-17.

Ong, Y., Saiful Yazan, L., Ng, W., Abdullah, R., Mustapha, N., Sapuan, S., Foo, J., Tor, Y., How, C., Abd Rahman, N. and Zakarial Ansar, F., (2018). Thymoquinone loaded in nanostructured lipid carrier showed enhanced anticancer activity in 4T1 tumor-bearing mice. *Nanomedicine*, 13(13), pp.1567-1582.

Ozbun, M. A., (2002) Human Papillomavirus Type 31b Infection of Human Keratinocytes and the Onset of Early Transcription, *Journal of Virology*, 76(22), pp.11291-11300.

Padhye, S., Banerjee, S., Ahmad, A., Mohammad, R. and Sarkar, F, H., (2008) From here to eternity - the secret of Pharaohs: Therapeutic potential of black cumin seeds and beyond., *Cancer therapy*, 6(b), pp.495-510.

Pagola, S., Benavente, A., Raschi, A., Romano, E., Molina, M. and Stephens, P., (2004). Crystal structure determination of thymoquinone by high-resolution X-ray powder diffraction. *AAPS PharmSciTech*, 5(2), pp.24-31.

Pal, A. and Kundu, R., (2020) Human Papillomavirus E6 and E7: The Cervical Cancer Hallmarks and Targets for Therapy, *Frontiers in Microbiology*, 10, pp.3116-3030.

Pandey, H*.,* Rani, R. and Agarwal, V., (2016) Liposome and their applications in cancer therapy, *Brazilian Archives of Biology and Technology*, 59, pp.1-10.

Pérez-Herrero, E. and Fernández-Medarde, A., (2015). Advanced targeted therapies in cancer: Drug nanocarriers, the future of chemotherapy. *European Journal of Pharmaceutics and Biopharmaceutics*, 93, pp.52-79.

Petignat, P. and Roy, M., (2007) Diagnosis and management of cervical cancer, *BMJ*, 335(7623), pp.765-768.

Pettersson, F. and Silfversward, C., (1986) Diagnosis and management of cervical abnormalities., *IARC scientific publications*, 335(76), pp.221-237.

Pflaum, J., Schlosser, S. and Muller, M., (2014). p53 Family and Cellular Stress Responses in Cancer. *Frontiers in Oncology*, 4(285), pp.1-15.

Pise, H. N. and Padwal, S. L., (2017) Evaluation of anti-inflammatory activity of nigella sativa: An experimental study, *National Journal of Physiology, Pharmacy and Pharmacology*, 7(7), pp.707-711.

Porfire, A., Achim, M., Tefas, L. and Sylvester, B., (2017) Liposomal Nanoformulations as Current Tumor-Targeting Approach to Cancer Therapy, in *Liposomes*. InTech, pp.1-10.

Potente, M., Gerhardt, H. and Carmeliet, P., (2011). Basic and Therapeutic Aspects of Angiogenesis. *Cell*, 146(6), pp.873-887.

Puri, A., (2013). Phototriggerable Liposomes: Current Research and Future Perspectives. *Pharmaceutics*, 6(1), pp.1-25.

Qi, X., Zhao and Zhuang., (2011). Comparative study of the in vitro and in vivo characteristics of cationic and neutral liposomes. *International Journal of Nanomedicine*, 6, pp.3087-3098.

Raff, A., Woodham, A., Raff, L., Skeate, J., Yan, L., Da Silva, D., Schelhaas, M. and Kast, W., (2013). The Evolving Field of Human Papillomavirus Receptor Research: a Review of Binding and Entry. *Journal of Virology*, 87(11), pp.6062-6072.

Rajput, S., Kumar, B., Dey, K., Pal, I., Parekh, A. and Mandal, M., (2013). Molecular targeting of Akt by thymoquinone promotes G1 arrest through translation inhibition of cyclin D1 and induces apoptosis in breast cancer cells. *Life Sciences*, 93(21), pp.783-790.

Reindl, W., Yuan, J., Krämer, A., Strebhardt, K. and Berg, T., (2008). Inhibition of Polo-like Kinase 1 by Blocking Polo-Box Domain-Dependent Protein-Protein Interactions. *Chemistry & Biology*, 15(5), pp.459-466.

Ronco, G., Cuzick, J., Segnan, N., Brezzi, S., Carozzi, F., Folicaldi, S., Palma, P., Mistro, A., Gillio-Tos, A., Giubilato, P., Naldoni, C., Polla, E., Iossa, A., Zorzi, M., Confortini, M. and Giorgi-Rossi, P., (2007). HPV triage for low grade (L-SIL) cytology is appropriate for women over 35 in mass cervical cancer screening using liquid based cytology. *European Journal of Cancer*, 43(3), pp.476-480.

Rose, G, P., Bundy, N, B., Watkins, B, E., Thigpen, T., Deppe, G., Maiman, A, M., Clarke-Pearson, L, D. and Insalaco, S., (1999). Concurrent cisplatin-based radiotherapy and chemotherapy for locally advanced cervical cancer. 3(4), pp.345-347.

Rovira-Bru, M., Thompson, D. and Szleifer, I., (2002). Size and Structure of Spontaneously Forming Liposomes in Lipid/PEG-Lipid Mixtures. *Biophysical Journal*, 83(5), pp.2419-2439.

Ryu, Y., Kang, S., Cho, J., Yoon, J. and Park, M., (2018). Lymphovascular invasion can be better than pathologic complete response to predict prognosis in breast cancer treated with neoadjuvant chemotherapy. *Medicine*, 97(30), pp.1-7.

Saiful Yazan, L. and Wan Nor Hafiza., (2014). Potential implications of GRP58 expression and susceptibility of cervical cancer to cisplatin and thymoquinone-based therapy. *OncoTargets and Therapy*, 7, pp.1375-1387.

Sakalar, C., Yuruk, M., Kaya, T., Aytekin, M., Kuk, S. and Canatan, H., (2013). Pronounced transcriptional regulation of apoptotic and TNF–NF-kappa-B signaling genes during the course of thymoquinone mediated apoptosis in HeLa cells. *Molecular and Cellular Biochemistry*, 383(1-2), pp.243-251.

Salem, A., El Haty, I., Abdou, I. and Mu, Y., (2015). Interaction of human telomeric G-quadruplex DNA with thymoquinone: A possible mechanism for thymoquinone anticancer effect. *Biochimica et Biophysica Acta (BBA) - General Subjects*, 1850(2), pp.329-342.

Salem, M. L., (2005) Immunomodulatory and therapeutic properties of the Nigella sativa L. seed, *International Immunopharmacology*, 5(13–14), pp.1749-1770.

Salem, M., Alenzi, F. and Attia, W., (2011). Thymoquinone, the active ingredient of Nigella sativa seeds, enhances survival and activity of antigen-specific CD8-positive T cells *in vitro*. *British Journal of Biomedical Science*, 68(3), pp.131-137.

Sales, K. J., (2014) Human Papillomavirus and Cervical Cancer, in *Cancer and Inflammation Mechanisms: Chemical, Biological, and Clinical Aspects*. Elsevier, pp.165-180.

Salim, L., Mohan, S., Othman, R., Abdelwahab, S., Kamalidehghan, B., Sheikh, B. and Ibrahim, M., (2013). Thymoquinone Induces Mitochondria-Mediated Apoptosis in Acute Lymphoblastic Leukaemia in Vitro. *Molecules*, 18(9), pp.11219-11240.

Salmaso, S. and Caliceti, P., (2013) Stealth Properties to Improve Therapeutic Efficacy of Drug Nanocarriers, *Journal of Drug Delivery*, 2013, pp.1-19.

Sandanaraj, B., Gremlich, H., Kneuer, R., Dawson, J. and Wacha, S., (2009). Fluorescent Nanoprobes as a Biomarker for Increased Vascular Permeability: Implications in Diagnosis and Treatment of Cancer and Inflammation. *Bioconjugate Chemistry*, 21(1), pp.93-101.

Santos, S., (2015) The Use of Coating Agents to Enhance Liposomes Blood Circulation Time, *Journal of Molecular Pharmaceutics & Organic Process Research*, 03(1), pp.1-3.

Sarwath, H., Bansal, D., Husain, N., Mohamed, M., Sultan, A. and Bedri, S., (2017). Introduction of p16INK4a as a surrogate biomarker for HPV in women with invasive cervical cancer in Sudan. *Infectious Agents and Cancer*, 12(50), pp.1-8.

Saslow, D., Solomon, D., Lawson, W, H., Killackey, M., Kulasingam, L, S., Cain, J., Garcia, R, A, F,Moriarty, A., Waxman, G, A., Wilbur, C, D., Wentzensen, N., Downs, S, L., Spitzer, M., Moscicki, A, Franco, E., Stoler, H, M., Schiffman, M., Castle, E, P. and Myers, R, E., (2013). American Cancer Society, American Society for Colposcopy and Cervical Pathology, and American Society for Clinical Pathology Screening Guidelines for the Prevention and Early Detection of Cervical Cancer. *Yearbook of Pathology and Laboratory Medicine*, 62(3), pp.147-172.

Sauter, J., Mount, S., St. John, T., Wojewoda, C., Bryant, R. and Leiman, G., (2014). Testing of Integrated Human Papillomavirus mRNA Decreases Colposcopy Referrals: Could a Change in Human Papillomavirus Detection Methodology Lead to More Cost-Effective Patient Care?. *Acta Cytologica*, 58(2), pp.162-166.

Sawant, R. R. and Torchilin, V. P., (2012) Challenges in development of targeted liposomal therapeutics, *AAPS Journal*, 14(2), pp.303-315.

Scarinci, I., Garcia, F., Kobetz, E., Partridge, E., Brandt, H., Bell, M., Dignan, M., Ma, G., Daye, J. and Castle, P., (2010). Cervical cancer prevention. *Cancer*, 116(11), pp.2-17.

Scatchard, K., Forrest, J., Flubacher, M., Cornes, P. and Williams, C., (2012). Chemotherapy for metastatic and recurrent cervical cancer. *Cochrane Database of Systematic Reviews*, 2012(10), pp.1-61.

Schneider-Stock, R., Fakhoury, I., Zaki, A., El-Baba, C. and Gali-Muhtasib, H., (2014). Thymoquinone: fifty years of success in the battle against cancer models. *Drug Discovery Today*, 19(1), pp.18-30.

Schwendener, R. A. and Schott, H., (2017) Liposome Formulations of Hydrophobic Drugs, 15(9), pp.2-9.

Seitz, J., Vineberg, J., Herlihy, E., Park, B., Melief, E. and Ojima, I., (2015). Design, synthesis and biological evaluation of a highly-potent and cancer cell selective folate–taxoid conjugate. *Bioorganic & Medicinal Chemistry*, 23(9), pp.2187-2194.

Sercombe, L., Veerati, T., Moheimani, F., Wu, S., Sood, A. and Hua, S., (2015). Advances and Challenges of Liposome Assisted Drug Delivery. *Frontiers in Pharmacology*, 6(286), pp.1-13.

Serkies, K. and Jassem, J., (2018) Systemic therapy for cervical carcinoma – current status, *Chinese Journal of Cancer Research*, 30(2), pp.209-221.

Severina, I., Severin, F., Korshunova, G., Sumbatyan, N., Ilyasova, T., Simonyan, R., Rogov, A., Trendeleva, T., Zvyagilskaya, R., Dugina, V., Domnina, L., Fetisova, E., Lyamzaev, K., Vyssokikh, M., Chernyak, B., Skulachev, M., Skulachev, V. and Sadovnichii, V., (2013). In search of novel highly active mitochondria-targeted antioxidants: Thymoquinone and its cationic derivatives. *FEBS Letters*, 587(13), pp.2018-2024.

Shafiee G., Saidijan, M., Tavilani, H., Ghasemkhani, N. and Khodadadi, I., (2016) Genistein Induces Apoptosis and Inhibits Proliferation of HT29 Colon Cancer Cells. Int J Mol Cell Med, 5(3), pp.178-191.

Shankar, S., Prasad, D., Sanawar, R., Das, A. and Pillai, M., (2017). TALEN based HPV-E7 editing triggers necrotic cell death in cervical cancer cells. *Scientific Reports*, 7(1), pp.1-12.

Shanmugam, M., Ahn, K., Hsu, A., Woo, C., Yuan, Y., Tan, K., Chinnathambi, A., Alahmadi, T., Alharbi, S., Koh, A., Arfuso, F., Huang, R., Lim, L., Sethi, G. and Kumar, A., (2018). Thymoquinone Inhibits Bone Metastasis of Breast Cancer Cells Through Abrogation of the CXCR4 Signaling Axis. *Frontiers in Pharmacology*, 9(1294), pp.1-15.

Shao, F., Wang, S., Li, H., Chen, W., Wang, G., Ma, D., Wong, N., Xiao, H., Liu, Q., Zhou, G., Li, Y., Li, M., Wang, Y. and Liu, Z., (2016). EM23, a natural sesquiterpene lactone, targets thioredoxin reductase to activate JNK and cell death pathways in human cervical cancer cells. *Oncotarget*, 7(6), pp.6790-6808.

Sharma, A. and Sharma, U. S., (1997) Liposomes in drug delivery: progress and limitations, *International Journal of Pharmaceutics*, 154, pp.123-140.

Shaterzadeh-Yazdi, H., Noorbakhsh, M., Hayati, F., Samarghandian, S. and Farkhondeh, T., (2018). Immunomodulatory and Anti-inflammatory Effects of Thymoquinone. *Cardiovascular & Hematological Disorders-Drug Targets*, 18(1), pp.52-60.

Shi, W., Liu, H., Wu, D., Tang, Z., Shen, Y. and Guo, L., (2017). E6/E7 proteins are potential markers for the screening and diagnosis of cervical pre-cancerous lesions and cervical cancer in a Chinese population. *Oncology Letters*, 14(5), pp.6251-6258.

Shin, K., Kim, T., Cho, J., Kim, J., Park, S., Park, S., Kim, D., Chie, E., Pyo, H. and Cho, K., (2006). CT-guided intracavitary radiotherapy for cervical cancer: Comparison of conventional point A plan with clinical target volume-based three-dimensional plan

using dose–volume parameters. International Journal of Radiation Oncology*Biology*Physics, 64(1), pp.197-204.

Silva, D., Gonçalves, A., Cobucci, R., Mendonça, R., Lima, P. and Cavalcanti, G., (2017). Immunohistochemical expression of p16, Ki-67 and p53 in cervical lesions – A systematic review. Pathology - Research and Practice, 213(7), pp.723-729.

Singh, A., Ahmad, I., Akhter, S., Jain, G., Iqbal, Z., Talegaonkar, S. and Ahmad, F., (2013). Nanocarrier based formulation of Thymoquinone improves oral delivery: Stability assessment, in vitro and in vivo studies. Colloids and Surfaces B: Biointerfaces, 102, pp.822-832.

Singh, S., (2011). Nanoparticle based drug delivery system: Advantages and applications. *Indian Journal of Science and Technology*, 4(3), pp.177-184.

Spangle, J. M. and Munger, K., (2013) The HPV16 E6 Oncoprotein Causes Prolonged Receptor Protein Tyrosine Kinase Signaling and Enhances Internalization of Phosphorylated Receptor Species, *PLoS Pathogens*, 9(3), pp.2-12.

Srinivasarao, M., Galliford, C. and Low, P., (2015). Principles in the design of ligand-targeted cancer therapeutics and imaging agents. *Nature Reviews Drug Discovery*, 14(3), pp.203-219.

Stanley, M. A., (2012) Epithelial cell responses to infection with human papillomavirus, *Clinical Microbiology Reviews*. American Society for Microbiology Journals, pp.215-222.

Stern, S., Hall, J., Yu, L., Wood, L., Paciotti, G., Tamarkin, L., Long, S. and McNeil, S., (2010). Translational considerations for cancer nanomedicine. *Journal of Controlled Release*, 146(2), pp.164-174.

Strebhardt, K. and Ullrich, A., (2008) Paul Ehrlich's magic bullet concept: 100 Years of progress, *Nature Reviews Cancer*, 8(6), pp.473-480.

Sudhakar, A., (2009) History of Cancer, Ancient and Modern Treatment Methods., *Journal of cancer science & therapy*, 1(2), pp.1-4.

Sundar, S., Marconett, C., Doan, V., Willoughby, J. and Firestone, G., (2008). Artemisinin selectively decreases functional levels of estrogen receptor-alpha and ablates estrogen-induced proliferation in human breast cancer cells. *Carcinogenesis*, 29(12), pp.2252-2258.

Supoken, A., Kietpeerakool, C., Laopaiboon, M. and Lumbiganon, P., (2016). Simple versus radical hysterectomy with pelvic lymphadenectomy for women with stage IA2-IB1 cervical cancer. *Cochrane Database of Systematic Reviews*, pp.1-12.

Surekha, R. and Sumathi, T., (2016) An efficient encapsulation of thymoquinone using solid lipid nanoparticle for brain targeted drug delivery: Physicochemical characterization, pharmacokinetics and bio-distribution studies, *International Journal of Pharmaceutical and Clinical Research*, 8(12), pp.1616-1624.

Tabasi, N., Mahmoudi, M., Rastin, M., Sadeghnia, H., HosseinPour Mashhadi, M., Zamani Taghizade Rabe, S. and Khajavi Rad, A., (2014). Cytotoxic and apoptogenic properties ofNigella sativa and thymoquinone, its constituent, in human renal cell

carcinoma are comparable with cisplatin. *Food and Agricultural Immunology*, 26(1), pp.138-156.

Tamatani, T., Azuma, M., Motegi, K., Takamaru, N., Kawashima, Y. and Bando, T., (2007). Cepharanthin-enhanced radiosensitivity through the inhibition of radiation-induced nuclear factor-κB activity in human oral squamous cell carcinoma cells. *International Journal of Oncology*, 31, pp.761-768.

Tanaka, Y., (2016) Psoriatic arthritis in Japan: Difference in clinical features and approach to precision medicine, *Clinical and Experimental Rheumatology*, 34, pp.1-4.

Tavakoli, J., Miar, S., Zadezare, M, M. and Akbari, H., (2012) Evaluation of effectiveness of herbal medication in cancer care: A review study, *Iranian Journal of Cancer Prevention*. Kowsar Medical Institute, 5(3), pp.144-156.

Thigpen, J., (2006). Quality of Life Outcomes From a Randomized Phase III Trial of Cisplatin With or Without Topotecan in Advanced Carcinoma of the Cervix: A Gynecologic Oncology Group Study. *Yearbook of Oncology*, 2006, pp.136-137.

Tie, Y., Zheng, H., He, Z., Yang, J., Shao, B., Liu, L., Luo, M., Yuan, X., Liu, Y., Zhang, X., Li, H., Wu, M. and Wei, X., (2020). Targeting folate receptor β positive tumor-associated macrophages in lung cancer with a folate-modified liposomal complex. *Signal Transduction and Targeted Therapy*, 5(1), pp.1-15.

Tomaić, V., (2016) Functional roles of E6 and E7 oncoproteins in HPV-induced malignancies at diverse anatomical sites, *Cancers*, pp.8(95), pp.1-22.

Torchilin, V., (2011) Tumor delivery of macromolecular drugs based on the EPR effect, *Advanced Drug Delivery Reviews*, 63(3), pp. 131-135.

Torres, M., Ponnusamy, M., Chakraborty, S., Smith, L., Das, S., Arafat, H. and Batra, S., (2010). Effects of Thymoquinone in the Expression of Mucin 4 in Pancreatic Cancer Cells: Implications for the Development of Novel Cancer Therapies. *Molecular Cancer Therapeutics*, 9(5), pp.1419-1431.

Toussaint-Smith, E., Donner, D. and Roman, A., (2004). Expression of human papillomavirus type 16 E6 and E7 oncoproteins in primary foreskin keratinocytes is sufficient to alter the expression of angiogenic factors. *Oncogene*, 23(17), pp.2988-2995.

Tran, S., DeGiovanni, P., Piel, B. and Rai, P., (2017). Cancer nanomedicine: a review of recent success in drug delivery. *Clinical and Translational Medicine*, 6(44), pp.1-21.

Treasure, J., (2005) Herbal medicine and cancer: An introductory overview, *Seminars in Oncology Nursing*, 21(3), pp.177-183.

Tsikouras, P., Zervoudis, S., Manav, B., Tomara, E., Latrakis, G., Romanidis, C., Bothou, A. and Galazios, G., (2016) Cervical cancer: Screening, diagnosis and staging, *Journal of B.U.ON.*, 21(2), pp.320-325.

Tsu, V. and Jerónimo, J., (2016) Saving the World's Women from Cervical Cancer, *New England Journal of Medicine*, 374(26), pp.2509-2511.

Tsuda, N., Watari, H. and Ushijima, K., (2016). Chemotherapy and molecular targeting therapy for recurrent cervical cancer. *Chinese Journal of Cancer Research*, 28(2), pp.241-253.

Tubesha, Z., Imam, M., Mahmud, R. and Ismail, M., (2013). Study on the Potential Toxicity of a Thymoquinone-Rich Fraction Nanoemulsion in Sprague Dawley Rats. *Molecules*, 18(7), pp.7460-7472.

Turk, M. J., Waters, D. J. and Low, P. S., (2004) Folate-conjugated liposomes preferentially target macrophages associated with ovarian carcinoma, *Cancer Letters*, 213(2), pp.165-172.

Van Doorslaer, K., Li, Z., Xirasagar, S., Maes, P., Kaminsky, D., Liou, D., Sun, Q., Kaur, R., Huyen, Y. and McBride, A., (2016). The Papillomavirus Episteme: a major update to the papillomavirus sequence database. *Nucleic Acids Research*, 45(D1), pp.499-506.

Veldman, T., Liu, X., Yuan, H. and Schlegel, R., (2003). Human papillomavirus E6 and Myc proteins associate *in vivo* and bind to and cooperatively activate the telomerase reverse transcriptase promoter. *Proceedings of the National Academy of Sciences*, 100(14), pp.8211-8216.

Vineberg, J., Zuniga, E., Kamath, A., Chen, Y., Seitz, J. and Ojima, I., (2014). Design, Synthesis, and Biological Evaluations of Tumor-Targeting Dual-Warhead Conjugates for a Taxoid–Camptothecin Combination Chemotherapy. *Journal of Medicinal Chemistry*, 57(13), pp.5777-5791.

Vlahov, I. R. and Leamon, C. P., (2012) Engineering folate-drug conjugates to target cancer: From chemistry to clinic, *Bioconjugate Chemistry*, 23(7), pp.1357-1369.

Vlahov, I., Santhapuram, H., Kleindl, P., Howard, S., Stanford, K. and Leamon, C., (2006). Design and regioselective synthesis of a new generation of targeted chemotherapeutics. Part 1: EC145, a folic acid conjugate of desacetylvinblastine monohydrazide. *Bioorganic & Medicinal Chemistry Letters*, 16(19), pp.5093-5096.

Voinea, M. and Simionescu, M., (2002) Designing of 'intelligent' liposomes for efficient delivery of drugs, *Journal of Cellular and Molecular Medicine*, 6(4), pp.465-474.

Vora, C. and Gupta, S., (2019) Targeted therapy in cervical cancer, *ESMO Open Cancer Horizons*, 3, pp.1-8.

Wade, M., Li, Y. and Wahl, G., (2013). MDM2, MDMX and p53 in oncogenesis and cancer therapy. *Nature Reviews Cancer*, 13(2), pp.83-96.

Wang, C. C. and Palefsky, J. M., (2016) Human papillomavirus-related oropharyngeal cancer in the HIV-infected population, *Oral Diseases*, 22(1), pp.98-106.

Wang, L., Zhao, Y., Wu, Q., Guan, Y. and Wu, X., (2018). Therapeutic effects of β-elemene via attenuation of the Wnt/β-catenin signaling pathway in cervical cancer cells. *Molecular Medicine Reports*, 17, pp.4299-4306.

Wang, N., Zhan, T., Ke, T., Huang, X., Ke, D., Wang, Q. and Li, H., (2014). Increased expression of RRM2 by human papillomavirus E7 oncoprotein promotes angiogenesis in cervical cancer. *British Journal of Cancer*, 110(4), pp.1034-1044.

Wang, W. Y., Cao, X., Zhou, X. and Wei, B., (2019) Delivery of folic acid-modified liposomal curcumin for targeted cervical carcinoma therapy, *Drug Design, Development and Therapy*, 13, p.2205-2213.

Wang, X., Li, D., Ghali, L., Xia, R., Munoz, L., Garelick, H., Bell, C. and Wen, X., (2016). Therapeutic Potential of Delivering Arsenic Trioxide into HPV-Infected Cervical Cancer Cells Using Liposomal Nanotechnology. *Nanoscale Research Letters*, 11(94), pp.1-8.

Wang, X., Tian, X., Liu, F., Zhao, Y., Sun, M., Chen, D., Lu, C., Wang, Z., Shi, X., Zhang, Q., Zhang, D., Shen, Z., Li, F., Harris, C., Cai, H. and Ke, Y., (2010). Detection of HPV DNA in esophageal cancer specimens from different regions and ethnic groups: a descriptive study. *BMC Cancer*, 10(19), pp.1-8.

Wang, X., Wang, H., McCoy, J., Banerjee, N., Rader, J., Broker, T., Meyers, C., Chow, L. and Zheng, Z., (2009). Oncogenic HPV infection interrupts the expression of tumor-suppressive miR-34a through viral oncoprotein E6. *RNA*, 15(4), pp.637-647.

Ward, Z., Scott, A., Hricak, H. and Atun, R., (2021). Global costs, health benefits, and economic benefits of scaling up treatment and imaging modalities for survival of 11 cancers: a simulation-based analysis. *The Lancet Oncology*, 22(3), pp.341-350.

Wen, G., Deng, H., Bing, W. and Luo, S., (2007) Preliminarily experimental study on biological properties of 153Sm-citrate-nano-hydroxyapatite, *Journal of Sichuan University (Medical Science Edition)*, 38(6), pp.1017-1020.

Woo, C., Loo, S., Gee, V., Yap, C., Sethi, G., Kumar, A. and Benny Tan, K., (2011). Anticancer activity of thymoquinone in breast cancer cells: Possible involvement of PPAR-γ pathway. *Biochemical Pharmacology*, 82(5), pp.464-475.

Woodham, A., Da Silva, D., Skeate, J., Raff, A., Ambroso, M., Brand, H., Isas, J., Langen, R. and Kast, W., (2012). The S100A10 Subunit of the Annexin A2 Heterotetramer Facilitates L2-Mediated Human Papillomavirus Infection. *PLoS ONE*, 7(8), pp.1-15.

Wright, T., Massad, L., Dunton, C., Spitzer, M., Wilkinson, E. and Solomon, D., (2007). 2006 Consensus Guidelines for the Management of Women With Abnormal Cervical Screening Tests. *Journal of Lower Genital Tract Disease*, 11(4), pp.201-222.

Wu ZH., Chen Z., Shen Y., Huang LL. and Jiang P., (2011) Anti-metastasis effect of thymoquinone on human pancreatic cancer. Yao Xue Xue Bao, 46(8), pp.1-12.

Wu, H. C. and Chang, D. K., (2010) Peptide-mediated liposomal drug delivery system targeting tumor blood vessels in anticancer therapy, *Journal of Oncology*, 2010, pp.1-8.

Wu, M., Lin, C., Chiou, H., Yang, S., Lin, C., Liu, C. and Hsieh, Y., (2018). Praeruptorin A Inhibits Human Cervical Cancer Cell Growth and Invasion by Suppressing MMP-2 Expression and ERK1/2 Signaling. *International Journal of Molecular Sciences*, 19(1), pp.1-130.

Wu, S., Lee, A., Hou, S., Kemper, J., Erdjument-Bromage, H., Tempst, P. and Chiang, C., (2006). Brd4 links chromatin targeting to HPV transcriptional silencing. *Genes & Development*, 20(17), pp.2383-2396.

Xia, W., Hilgenbrink, A., Matteson, E., Lockwood, M., Cheng, J. and Low, P., (2009). A functional folate receptor is induced during macrophage activation and can be used to target drugs to activated macrophages. *Blood*, 113(2), pp.438-446.

Yamato, K., Yamada, T., Kizaki, M., Ui-Tei, K., Natori, Y., Fujino, M., Nishihara, T., Ikeda, Y., Nasu, Y., Saigo, K. and Yoshinouchi, M., (2008). New highly potent and specific E6 and E7 siRNAs for treatment of HPV16 positive cervical cancer. *Cancer Gene Therapy*, 15(3), pp.140-153.

Yamauchi, M., Tsutsumi, K., Abe, M., Uosaki, Y., Nakakura, M. and Aoki, N., (2007). Release of Drugs from Liposomes Varies with Particle Size. *Biological and Pharmaceutical Bulletin*, 30(5), pp.963-966.

Yang, P., Hu, D., Kao, Y., Lin, I. and Liu, F., (2018). Butein induces apoptotic cell death of human cervical cancer cells. *Oncology Letters*, 16, pp.6615-6623.

Yazan, L. S., Weikeat, N., Al-Naqeeb, G. and Ismail, M., (2009) Cytotoxicity of Thymoquinone (TQ) from Nigella sativa Towards Human Cervical Carcinoma Cells (HeLa), *Journal of Pharmacy Research*, 2(4), pp.585–589.

Ye, H., Zhang, Y., Wang, Y., Xia, J., Mao, X. and Yu, X., (2017). The restraining effect of baicalein and U0126 on human cervical cancer cell line HeLa. *Molecular Medicine Reports*, 16(1), pp.957-963.

Yi, T., Cho, S., Yi, Z., Pang, X., Rodriguez, M., Wang, Y., Sethi, G., Aggarwal, B. and Liu, M., (2009). Thymoquinone inhibits tumor angiogenesis and tumor growth through suppressing AKT and extracellular signal-regulated kinase signaling pathways. *Molecular Cancer Therapeutics*, 7(7), pp.1789-1796.

Yim, E, K. and Park, J, S., (2005) The role of HPV E6 and E7 oncoproteins in HPV-associated cervical carcinogenesis., *Cancer research and treatment : official journal of Korean Cancer Association*, 37(6), pp.319-324.

Yingchoncharoen, P., Kalinowski, D. and Richardson, D., (2016). Lipid-Based Drug Delivery Systems in Cancer Therapy: What Is Available and What Is Yet to Come. *Pharmacological Reviews*, 68(3), pp.701-787.

Zanier, K., ould M'hamed ould Sidi, A., Boulade-Ladame, C., Rybin, V., Chappelle, A., Atkinson, A., Kieffer, B. and Travé, G., (2012). Solution Structure Analysis of the HPV16 E6 Oncoprotein Reveals a Self-Association Mechanism Required for E6-Mediated Degradation of p53. *Structure*, 20(4), pp.604-617.

Zeferino, L. C. and Derchain, S. F., (2006) Cervical cancer in the developing world, *Best Practice and Research: Clinical Obstetrics and Gynaecology*, 20(3), pp.339-354.

Zhang, L., Casey, B., Galanakis, D., Marmorat, C., Skoog, S., Vorvolakos, K., Simon, M. and Rafailovich, M., (2017). The influence of surface chemistry on adsorbed fibrinogen conformation, orientation, fibre formation and platelet adhesion. *Acta Biomaterialia*, 54, pp.164-174.

Zhang, L., Kong, S., Zheng, Z., Meng, X., Feng, J., Tan, H., Lao, Y., Xiao, L. and Xu, H., (2016). Nujiangexathone A, a Novel Compound Derived from Garcinia nujiangensis, Induces Caspase-Dependent Apoptosis in Cervical Cancer through the ROS/JNK Pathway. *Molecules*, 21(10), pp.1-13.

Zhang, M., Du, H., Huang, Z., Zhang, P., Yue, Y., Wang, W., Liu, W., Zeng, J., Ma, J., Chen, G., Wang, X. and Fan, J., (2018). Thymoquinone induces apoptosis in bladder cancer cell via endoplasmic reticulum stress-dependent mitochondrial pathway. *Chemico-Biological Interactions*, 292, pp.65-75.

Zhang, W., Kazakov, T., Popa, A. and DiMaio, D., (2014). Vesicular Trafficking of Incoming Human Papillomavirus 16 to the Golgi Apparatus and Endoplasmic Reticulum Requires γ-Secretase Activity. *mBio*, 5(5), pp.1-11.

Zhang, Y., Zhai, M., Chen, Z., Han, X., Yu, F., Li, Z., Xie, X., Han, C., Yu, L., Yang, Y. and Mei, X., (2017). Dual-modified liposome codelivery of doxorubicin and vincristine improve targeting and therapeutic efficacy of glioma. *Drug Delivery*, 24(1), pp.1045-1055.

Zhao, C., Cheng, R., Yang, Z. and Tian, Z., (2018). Nanotechnology for Cancer Therapy Based on Chemotherapy. *Molecules*, 23(4), pp.1-29.

Zhou, X. and Münger, K., (2009) Expression of the human papillomavirus type 16 E7 oncoprotein induces an autophagy-related process and sensitizes normal human keratinocytes to cell death in response to growth factor deprivation, *Virology*, 385(1), pp.192-197.

Zhu, W., Wang, J., Guo, X., Liu, Z. and Dong, W., (2016). Thymoquinone inhibits proliferation in gastric cancer via the STAT3 pathway *in vivo* and *in vitro*. *World Journal of Gastroenterology*, 22(16), pp.4149-4159.

Zhu, X., Zhu, H., Luo, H., Zhang, W., Shen, Z. and Hu, X., (2016). Molecular mechanisms of cisplatin resistance in cervical cancer. *Drug Design, Development and Therapy*, 10, pp.1885-1895.